Electronic Thesis and Dissertation Repository

4-17-2018 10:30 AM

Hydrothermal liquefaction of microalgae for the production of bio-crude oil

Yulin Hu
The University of Western Ontario

Supervisor
Chunbao (Charles) Xu
The University of Western Ontario Joint Supervisor
Amarjeet Bassi
The University of Western Ontario

Graduate Program in Chemical and Biochemical Engineering
A thesis submitted in partial fulfillment of the requirements for the degree in Doctor of Philosophy
© Yulin Hu 2018

Recommended Citation

Abstract

Due to the depletion of fossil fuels and climate change, extensive research has performed towards renewable energy production from microalgal biomass. Microalgae have several inherent benefits, such as high photosynthetic efficiencies, fast growth rates, and high lipid contents. In addition, microalgae can be cultivated in the non-arable lands (e.g., saline and waste water), thereby no competition with food crops production.

Transesterification is the one of commonly used technologies for converting microalgae into liquid bio-fuels (i.e., biodiesel). Normally, an energy-intensive drying step is required in the transesterification treatment, which accounts for nearly half of the energy input. Hence, if "wet" microalgal biomass can be directly used as the feedstock for bio-fuel production without dewatering/drying, the overall economy of microalgae-to-fuel conversion can be greatly improved.

In this thesis work, an alternative pre-treatment by pre-cooled NaOH/urea solution was investigated for microalgae. Subsequently, the pre-treated microalgae were applied as the feedstock for producing bio-crude oil. In addition, hydrothermal liquefaction (HTL) of microalgae was carried out in water, alcohol or water-alcohol mixed solvents under various reaction conditions with aims to improve bio-crude oil yield and quality. More noteworthily, the feasibility of recycling aqueous by-product from HTL of microalgae as a reaction medium for bio-crude oil production was explored, which yields great significance for the large-scale HTL applications. Furthermore, the co-processing of microalgae with other lignocellulosic biomass (i.e., aspen sawdust) was performed in ethanol-water co-solvents, and this work demonstrated the synergistic interactions between microalgae/sawdust and ethanol/water in the co-liquefaction process.

Keywords

Co-Authorship Statement

Chapter 2 has been submitted to *Sustainable and Renewable Energy Review* and is co-authored by Dr. Mengyue Gong, Dr. Shanghuan Feng, Dr. Charles Xu, and Dr. Amarjeet Bassi.

Chapter 3 was published in *Fuel* and was co-authored by Dr. Mengyue Gong, Dr. Charles Xu, and Dr. Amarjeet Bassi.

Chapter 4 was published in *Fuel* and was co-authored by Dr. Shanghuan Feng, Dr. Charles Xu, and Dr. Amarjeet Bassi.

Chapter 5 was published in *Bioresource Technology* and was co-authored by Dr. Shanghuan Feng, Dr. Zhongshun Yuan, Dr. Charles Xu, and Dr. Amarjeet Bassi.

Chapter 6 has been submitted to *Applied Energy* and was co-authored by Dr. Shanghuan Feng, Dr. Charles Xu, and Dr. Amarjeet Bassi.

Chapter 7 has been submitted to *Energy Conversion and Management* and is co-authored by Dr. Shanghuan Feng, Dr. Charles Xu, and Dr. Amarjeet Bassi.

Acknowledgments

Table of Contents

List of Tables

List of Figures

List of Appendices

Chapter 1

1   Introduction

1.1   Background

Renewable energy has gained a great deal of attention over the past decades, owing to the exhaustion of fossil fuels and growing global population as well as the serious environmental problems (Marcilla et al., 2013). Therefore, extensive studies have focused on the production of bio-fuels from biomass. In general, bio-fuels can be categorized into first, second, and third generation according to their sources of biomass (Voloshin et al., 2016). First generation bio-fuels obtained from food crops such as corn, soybean, and sugarcane have been commercialized. To avoid competition with crop production, second generation bio-fuels from non-food crops such as wood chip, wheat straw, and rice husk have been widely investigated (Chen et al., 2015). Recently, third generation bio-fuels from microalgal biomass have attracted interests due to their inherent advantages, namely, (i) high biomass productivities; (ii) high lipid contents; (iii) the abilities to be cultivated in the brackish or waste water; and (iv) can be potentially used for carbon sequestration. (Guo et al., 2015; Barreiro et al., 2013).

In literature, there are two common conversion routes for producing liquid bio-fuels from microalgae, including (i) biodiesel via transesterification of the microalgal lipid and (ii) bio-crude oil via hydrothermal liquefaction (HTL) of the whole biomass (Tian et al., 2014). Drying as an energy-intensive pre-treatment is required prior to transesterification treatment (Guo et al., 2015). Therefore, some researches have used wet microalgal biomass as the feedstock for bio-crude oil production through HTL (Zou et al., 2010; Jena et al., 2011; Shakya et al., 2015). HTL of microalgae is usually carried out in water at 200-380 °C and 5-28 MPa with or without catalyst. At the end of HTL process, an energy-dense bio-crude oil is obtained as the main product, along with solid, aqueous, and gaseous by-product (Tian et al., 2014; Barreiro et al., 2013). Products distribution

and the bio-crude oil properties are primarily dependent on the feedstock characteristics and various operating conditions (e.g., temperature, residence time, microalgae/solvent ratio, catalyst, and solvent etc.) (Barreiro et al., 2013).

1.2   Objectives

The overall objective of this PhD project was to investigate the production of liquid bio-fuels from microalgae through HTL treatment. Specifically, this project aimed to: **(1)** develop an alternative pre-treatment method for maximizing energy recovery from microalgae; **(2)** investigate a two-step HTL coupled with a pre-treatment in order to produce a high-quality bio-crude oil; **(3)** recycle aqueous by-product from HTL of microalgae with an aim to improve the overall economy of HTL treatment; **(4)** examine the effects of operational parameters on the direct liquefaction of microalgae in terms of products distribution and bio-crude oil properties; and **(5)** explore co-liquefaction of microalgae and lignocellulosic biomass in ethanol-water co-solvents for improving bio-crude oil yield and quality.

1.3   Research approaches and methodology

This research study can be divided into two main phases. The first phase involved the establishment of an alternative pre-treatment approach for microalgae and its effect on the bio-crude oil recovery, and the second on investigating the effects of aqueous phase recycling and various operating parameters on the liquefaction of microalgal biomass.

In the first phase, a pre-treatment using a pre-cooled NaOH/urea solution was developed for microalgae and compared with existing pre-treatment approaches. Following this, the pre-treated microalgae was employed as the feedstock for producing bio-crude oil.

In the second phase, the effects of operating conditions such as reaction temperature, residence time, biomass/solvent mass ratio, catalyst, and solvent on the liquefaction yields and bio-crude oil properties were examined. In addition, the feasibility of recycling

water phase as a reaction medium was evaluated. Finally, the co-conversion of microalgae and lignocellulosic biomass (i.e., aspen sawdust) was carried out in ethanol-water mixed solvents.

1.4   Thesis overview

The thesis consists of eight chapters organized in the following sequence:

- **Chapter 1** provides a general introduction to the importance of production of microalgae-derived liquid bio-fuels through HTL. The research objectives, approaches and methodology, and thesis structure are also outlined.

- **Chapter 2** summarizes the available literature on the pre-treatment approaches (mechanical and non-mechanical techniques) for various microalgae strains. The underlying reaction mechanisms of microalgal biomacromolecules in the HTL and the effects of operational parameters on the microalgal HTL are reviewed. Finally, the physical and chemical properties of four different liquefaction products are also discussed.

- **Chapter 3** investigates an alternative pre-treatment with a low-temperature NaOH/urea solvent for microalgae and compared with current pre-treatment approaches (i.e., acid and ultrasonication-assisted approach).

- **Chapter 4** presents the results of a two-step HTL process combining with a pre-treatment for producing a high-quality bio-crude oil.

- **Chapter 5** explores the feasibility of recycling aqueous phase from microalgal HTL as a reaction medium for improving bio-crude oil production. The effects of catalyst and water phase recycling on the HTL of microalgae were studied. The roles of recycled aqueous by-product in the HTL of microalgae were also investigated.

- **Chapter 6** conducts a study of direct liquefaction of microalgal biomass in methanol with an aim for maximizing bio-crude oil yield under mild reaction conditions. Various operating parameters including residence time, biomass/solvent mass ratio, reaction temperature, and methanol-water mixed solvents composition were examined.

- **Chapter 7** reports the results from co-liquefaction of microalgae and lignocellulosic biomass (i.e., aspen sawdust) in ethanol-water mixed solvents under various reaction conditions in order to obtain higher quantity and quality of bio-crude oil products.

- **Chapter 8** summarizes the main conclusions from this present work and suggests future research directions.

1.5   Contributions and novelties

The main contributions and novelties of this research are summarized as follows:

- Development of an alternative pre-treatment approach for microalgae in order to improve energy recovery.

- Establishment of a two-step HTL process coupled with a pre-treatment for efficient bio-crude oil production.

- Demonstration of the effectiveness of reusing the water phase from HTL of microalgae as a liquefaction medium for bio-crude oil production, which plays a crucial role in the industrial-scale HTL applications.

- Comprehensive studies on the effects of various operational factors including temperature, residence time, biomass/solvent ratio, and methanol-water co-solvents composition on the direct liquefaction of microalgal biomass.

- Discovering the synergistic interactions between microalgae and lignocellulosic biomass in the co-liquefaction for improving the yield and properties of bio-crude oil products.

1.6   References

Barreiro DL, Prins W, Ronsse F, Brilman W. Hydrothermal liquefaction (HTL) of microalgae for biofuel production: state of the art review and future prospects. Biomass Bioenergy 2013; 53:113-127.

Chen WH, Lin BJ, Huang MY, Chang JS. Thermochemical conversion of microalgal biomass into biofuels: a review. Bioresour Technol 2015; 184: 314-327.

Guo Y, Yeh T, Song WH, Xu DH, Wang SZ. A review of bio-oil production from hydrothermal liquefaction of algae. Renew Sust Energy Rev 2015; 48: 776-790.

Jena U, Das KC, Kastner JR. Effect of operating conditions of thermochemical liquefaction on biocrude production from *Spirulina platensis*. Bioresour Technol 2011; 102: 6221-6229.

Marcilla A, Catala L, Garcia-Quesada G, Valdes FJ, Hernandez MR. A review of thermochemical conversion of microalgae. Renew Sust Energy Rev 2013; 27: 11-19.

Shakya R, Whelen J, Adhikari S, Mahadevan R, Neupane S. Effect of temperature and Na_2CO_3 catalyst on hydrothermal liquefaction of algae. Algal Res 2015; 12: 80-90.

Tian CY, Li BM, Liu ZD, Zhang YH, Lu HF. Hydrothermal liquefaction for algal biorefinery: a critical review. Renew Sustainable Energy Rev 2014; 38:933-950.

Voloshin RA, Rodionova MV, Zharmukhamedov SK, Veziroglu T, Allakhverdiev SI. Review: Biofuel production from plant and algal biomass. Int J Hydrog Energy 2016; 41: 17257-17273.

Zou SP, Wu YL, Yang MD, Imdad K, Li C, Tong JM. Production and characterization of bio-oil from hydrothermal liquefaction of microalgae *Dunaliella tertiolecta* cake. Energy 2010; 35: 5406-5411.

Chapter 2

2   Literature review

The information presented in this Chapter is based on the paper "Bio-crude oil production from microalgae using hydrothermal liquefaction: a review of recent developments", which has been submitted to *Sustainable and Renewable Energy Review*.

2.1   Abstract

Microalgae have been widely considered as the potential sources for bio-fuel production without affecting the environment. Hydrothermal liquefaction (HTL) is a suitable technology for converting high water-containing feedstock (e.g., microalgae) into liquid fuels. The structural diversity and rigidity of microalgal cell-wall remains as one of the major techno-economic bottlenecks for the recovery of intramolecular compounds from microalgae. In this section, recent developments in the pre-treatments and HTL for various microalgae strains are reviewed. The discussed pre-treatment approaches are mechanical (bead milling, high pressure homogenization, ultrasonication, microwave, and pulsed electric field) and non-mechanical (acid, alkali, osmotic shock, ionic liquid, and enzymatic cell-lysis) methods. In addition, the available literature investigating the effects of feedstock characteristics and operating conditions on the HTL of microalgae are presented. The reaction pathways of microalgal macromolecules (lipid, protein, and carbohydrates) and their corresponding model compounds in the HTL are reviewed, followed by a discussion on the physiochemical properties of liquefaction products (bio-crude oil, aqueous phase, solid residue, and gas).

2.2   Introduction

Due to their high lipid contents and fast growth rates, microalgae have been broadly regarded as the promising resources for the production of renewable energy (Garcia Alba

et al., 2012). In addition, microalgae can be applied for wastewater treatment by consuming NH_4^+, NO_3^-, and PO_4^{3-} in the waste streams from industries (Chen et al., 2017). Except that, microalgae have the potentials to be used as food supplements (Kwan et al., 2017), animal feeds (Madeira et al., 2017), cosmetics (Wang et al., 2015), and pharmaceuticals (Borowitzka et al., 1995). However, there remain several challenges for the industrial-scale microalgae-based biorefinement. Among them, one of the most critical problems cited in the literature is the low recovery efficiencies of intracellular components from microalgae, owing to their highly resilient and complex cell-wall structures (Günerken et al., 2015). Therefore, a wide range of cell disruption techniques such as bead milling (Zheng et al., 2011), high pressure homogenization (Shene et al., 2016), ultrasonication (Garoma et al., 2016), microwave (Heo et al., 2017), pulsed electric field (Carullo et al., 2018), acid treatment (Hu et al., 2017a), alkali treatment (Mahdy et al., 2014), osmotic shock (Rakesh et al., 2015), ionic liquid extraction (Pan et al., 2016), and enzymatic cell lysis (Wu et al., 2017), have been investigated.

One of the most common technologies for converting microalgae into liquid bio-fuels is the transesterification treatment, which requires dewater/drying stage of the feedstock (Brown et al., 2010). Compared to transesterification, HTL has several benefits, namely, (i) non-requirement for drying the biomass (Yu et al., 2011); (ii) not only lipid but also protein and carbohydrates can be processed (Li et al., 2014); (iii) the desirable properties of water under hydrothermal conditions, such as low dielectric constant, high ionic product, and low viscosity (Toor et al., 2011); and (iv) can separate and recycle nutrients (e.g., N, P, Mg, and K) for microalgal cultivation (Guo et al., 2015). Commonly, HTL of microalgae is performed in water at 200-380 °C and 5-28 MPa for 5-120 min with or without catalyst (Tian et al., 2014; Peterson et al., 2008; Toor et al., 2011). Despite the advantages mentioned above, the bio-crude oil obtained from microalgal HTL usually contains higher concentrations of N and O than those of petroleum crude oil, and this represents as a crucial barrier to the commercialization of microalgae-derived bio-crude oil (Barreiro et al., 2013a).

There are several comprehensive review papers discussing bio-fuels production from algae (including microalgae and macroalgae) (Tian et al., 2014, Guo et al., 2015), while, the focus of this chapter is to review the pre-treatment methods and bio-crude oil production specifically from microalgae. This is due to the fact that macroalgae typically contain higher ash contents than microalgae, which could negatively affect the bio-crude oil yield and cause slagging and fouling problems. In section 2.3, the fundamental principles of various pre-treatment technologies and the relating case studies are discussed in detail; followed by Section 2.4 where covers the reaction mechanisms and crucial factors in the HTL of microalgae with the focus on the feedstock characteristics, operating conditions, and products distribution.

2.3   Pre-treatment of microalgae

Microalgal cells are protected by a resistant cell wall, and the target products are often located inside the globules or bounded to the cell membrane, which makes the extraction of intra-molecules from microalgae by conventional solvent extraction very challenging. Thus, disrupting the microalgal cell wall is necessary before conducting solvent extraction (Maffei et al., 2018). An overview of recent studies on the cell disruption for microalgae is summarized in Table 2.1.

Table 2-1: An overview of recent studies investigating the cell disruption of microalgae.

Disruption approach	Microalgae strain	Operating conditions	Reference
Bead milling			
	C. vulgaris	0.4-0.6 mm glass beads, 67% beads filling, 20 min	Zheng et al. (2011)
	Schizochytrium S31	0.4-0.6 mm, 0.8-1.0 mm ZrO_2 beads, 54% beads filling, 1-7/100 g/mL cell concentration	Byreddy et al. (2016)
	C.vulgari, N. Oleoabundans, T. suecica	0.3-1 mm ZrO_2 beads, 65% beads filling	Postma et al. (2017)
	N. oculata, P. cruentum	0.375-2.15 mm glass beads, 0.2-1.25 mm ZrO_2 beads, 8-14 m/s rotational speed, 35-85% beads filling, 48-200 mL/min flow rate	Montalescot et al. (2015)
High-pressure homogenization			
	N. oculata	75-350 MPa, 1.6 wt.% cell dry weight	Shene et al. (2016)
	C. vulgaris	2700 bar, 2 wt.% cell dry weight	Carullo et al. (2018)
	Nannochloropsis sp.	30-150 Mpa, 3 h, 20-25 wt.% cell dry weight	Yap et al. (2015)
	T. suecica, Chlorococcum sp.	517 and 862 bar, 2,503-10,720 cells/mm^3 cell concentration	Halim et al. (2013)
	Chlorococcum sp.	500 and 850 bar, 15 min, 9,559 and 65,476 cells/mm3 cell concentration	Halim et al. (2012)
Ultrasonication			

C. vulgaris	20 kHz frequency, 55 W power, 20 min,	Garoma et al. (2016)
C. vulgaris	40 kHz frequency, 700 W power, 15 min	Heo et al. (2017)
C. vulgaris	40 kHz frequency, 80 W power, 10-30 min	Hu et al. (2017a)
T. suecica	40 kHz frequency, 32.5 and 130 W power, 25 min, 1,824-22,784 cells/mm^3 cell concentration	Halim et al. (2013)
Chlorococcum sp.	40 kHz frequency, 65 and 130 W power, 25 min, 9,559 and 65,476 cells/mm^3 cell concentration	Halim et al. (2012)
Nannochloropsis sp.	20 kHz frequency, 10 W power, 10 min, 10^7 cells/mL cell concentration	Kurokawa et al. (2016)
C. reinhardtii	20 kHz frequency, 64-144 μm_{p-p} amplitude, 5 s	Gerde et al. (2012)
Botryococcus sp., C. vulgaris, Scenedesmus sp., N. oculata	10 kHz frequency, 5 min	Lee et al. (2010)
Microwave		
Botryococcus sp., C. vulgaris, Scenedesmus sp.	100 ℃, 2450 MHz, 5 min	Lee et al. (2010)
N. oculata	1025 W, 20 min	McMilan et al. (2013)
Bortyococcus sp., C. sorokiniana,	2450 MHz, 100 ℃, 2-6 min	Rakesh et al. (2015)

Pulsed electric field

C. reinhardtii	0.5-15 kV/cm electric field strength, 1-15 number of pulses, 0.05-0.2 ms pulses length	't Lam et al. (2017)
A. protothecoides	20-50 kV/cm electric field strength, 52-211 kJ/kg$_{sus}$ specific energy	Goettel et al. (2013)
C. vulgaris	27-35 kV/cm electric field strength, 50-150 kJ/kg$_{sus}$ specific energy, 10.8 and 14 kV, 5 µs pulse length	Pataro et al. (2017)

Acid and alkali

C. vulgaris	120 ℃, 1-4% v/v H_2SO_4, 30 min	Hu et al. (2107a)
Chlorococcum sp.	120 and 160 ℃, 3 and 8 vol.% H_2SO_4, 15 and 45 min, 9,559 and 65,476 cells/mm3 cell concentration	Halim et al. (2012)
S. obliquus	58 -120 ℃, 30 min, 0.05-10 N H_2SO_4	Miranda et al. (2012)
C. vulgaris, Scenedesmus sp.	50 ℃, 24 and 48 h, 0.05-5 wt/wt NaOH	Mahdy et al. (2014)

Osmotic shock

C. vulgaris	10% w/v NaCl, 48 h	Heo et al. (2017)
Botryococcus sp., C. vulgaris, Scenedesmus sp.	10% NaCl, 48 h	Lee et al. (2010)
Bortyococcus sp., C. sorokiniana,	5-15% NaCl, 48 h	Rakesh et al. (2015)

Ionic liquid

C. vulgaris	1-ethyl-3-methyl imidazolium diethylphosphate, 120 ℃, 2 h, 5 wt.% loading	Choi et al. (2014)
C. vulgaris, N. oculata	(hydroxymethyl(phophonium chloride, 100 ℃, 24 h, 10 cm^3/1 g$_{biomass}$ loading	Olkiewicz et al. (2015)

Enzymatic cell lysis

Chlorella sp., Nannochloropsis sp., Scenedesmus sp.	pH=7 for lysozyme, pH=5 for cellulase, 37 ℃, 2-16 h	Al-Zuhair et al. (2017)
C. vulgaris	Cellulase, lysozyme, pH=4.8, 37 ℃, 2h	Zheng et al. (2011)

2.3.1   Mechanical methods

2.3.1.1   Bead milling

Bead milling has been demonstrated to be an effective disruption technique for the release of intracellular components from microalgae under mild operating conditions. The cell disruption is believed to achieve through sudden compaction or shear force, resulting from the high-speed solid beads (Lee et al., 2017). The optimal efficiency of cell disruption is dependent on the bead diameter, bead density, agitator speed (i.e., tip speed of agitator), bead filling ratio, biomass concentration, and suspension flow rate. Byreddy et al. (2016) found that the degree of cell disintegration increased with increasing agitator tip speed, while, in contrast, an opposite trend was observed for biomass concentration. Postma et al. (2017) observed that a bead size in the range of 0.3-0.4 mm resulted in the highest disruption rate for *C. vulgaris* and *N. oleoabundans*. Montalescot et al. (2015) investigated the cell disintegration of *N. oculate* and *P. cruentum* by bead milling and reported that the degree of cell disruption was proportional to bead filling ratio.

Although bead milling has advantages of high efficiency and scalability, the high energy demand and unavoidable heat generation represent as crucial barriers to its practical application (Günerken et al., 2015).

2.3.1.2   High pressure homogenization

High pressure homogenization (HPH) is an effective cell disruption technique, particular for microalgae with resilient cell wall like *Nannochloropsis* (Yap et al., 2015). In an HPH unit, cell paste is forced to flow through a narrow nozzle under a high pressure, followed by colliding to an impact ring, and then released into a low-pressure chamber. Cell disruption by HPH is thus to be achieved by high shear force and cavitation from the sudden pressure drop (Günerken et al., 2015). The degree of cell disintegration in HPH is mainly determined by loading pressure and cell dry weight. Halim et al. (2013) investigated the effects of loading pressure and cell dry weight on the cell disruption efficiency of *T. suecica* and *Chlorococcum sp*. The authors reported that the disruption rate was inversely proportional to cell dry weight but positively correlated to loading pressure. Similarly, Halim et al. (2012) pre-treated microalgae *Chlorococcum sp.* via HPH-assisted treatment and found that a higher loading pressure was beneficial for improving cell disintegration efficiency.

Together with bead milling, HPH is the most favorable cell disruption method for microalgae. Nevertheless, the high energy requirement and relatively expensive disruption equipment make HPH less favorable for industrial-scale implementations (Lee et al., 2017).

2.3.1.3   Ultrasonication

Ultrasonication has been extensively studied for the extraction of lipid, protein, and sugars from microalgae. In general, two main working principles exist for ultrasonication-based treatment, including (i) radiation force and acoustic stream and (ii) cavitation effects (e.g., free radical reactions, shock waves, shear stress, and microjet)

(Kurokawa et al., 2016). The first phenomenon occurs at low ultrasonic powers and is confirmed by the bio-effects on the cell cytoplasm (Miller et al., 1986). The latter phenomenon is caused by the formation of micro-bubbles when ultrasound is applied to the liquid. As the micro-bubbles continue to grow till a critical size, the cavitation phenomenon can be created and then imparts shock waves to break the surrounding cells (Gerde et al., 2012). Besides, the cavitation promotes the thermolysis of water into highly reactive free radicals like H· and OH·. In literature, the cell disruption efficiency of ultrasonication is primarily affected by ultrasound frequency and acoustic power (Kurokawa et al., 2016). Gerde et al. (2012) evaluated the cell disruption efficiency of *S. limacinum* from ultrasonication-assisted treatment. It was observed that the degree of disruption increased with increasing sonication energy, whereas further increase above 789 J/10 mL exhibited no significant effect.

The main benefits of ultrasonication include high disruption efficiency, short treatment time, negligible toxicity, and simple handing. However, the requirement of temperature control and relatively low disruption efficiencies for some microalgae species (e.g., *Chlorococcum sp.*) are considered as the main challenges for the large-scale implementation of ultrasonication treatment (Halim et al., 2012).

2.3.1.4   Microwave

Microwave is a non-contact disruption technique for microalgae. The working principle of microwave is as followed, heat can be generated from inter- and intra-molecular movements when microwave irradiation is applied to a dielectric polar material (e.g., water). Within a short time, water can reach its boiling point and causes cell expansion, followed by an increase in the internal pressure. Thus, the disruption of microalgal cells by microwave is caused by the local heat and internal pressure (Lee et al., 2012). Depending on the microalgae strains, a higher disruption efficiency can be achieved by microwave treatment, when compared with other mechanical methods. For instance, Lee et al. (2010) compared bead milling, autoclave, ultrasonication, and microwave for lipid recovery from *Botryococcus sp.*, *C. vulgaris*, and *Scenedesmus sp*. They reported that the

microwave treatment was the most effective disruption technique for improving lipid extraction. In another study, McMilan et al. (2013) observed that the highest disruption efficiency of 94.92% was achieved by microwave-assisted treatment, along with a relatively lower energy consumption.

Even though microwave treatment is highly effective and easily scale-up, some constrains still ahead, (i) it is not suitable for non-polar solvents (Wang et al., 2006) and (ii) it may lead to the formation of unstable bonds in the carbon-chain structure, thereby affecting the properties of target compounds (Lee et al., 2017).

2.3.1.5   Pulsed electric field

Pulsed electric field (PEF) has gained much attention as a low-cost and mild technique for cell disruption ('t Lam et al., 2017). Cell disruption by PEF is obtained by a reverse transmembrane potential (TMP), inducing pore formation in the cell wall. Literature indicated that the cell disintegration efficiency of PEF treatment is correlated to the specific energy input and electric field strength (Goettel et al., 2013). Pataro et al. (2017) examined the extraction of protein and carbohydrates from *C. vulgaris* using PEF treatment at electric field strength of 27-35 kV/cm and specific energy input of 50-150 kJ/kg. They reported that the carbohydrate-extracted yield increased ~2.7 times at 27 kV/cm and ~2.6 times at 35 kV/cm compared to that obtained without PEF treatment. Additionally, the effect of the electric field strength on the carbohydrate recovery was observed to be less important than that of energy input. In the case of protein extraction, the electric field strength had no significant effect on the protein-extracted yield. On the contrary, the protein recovery efficiency sharply increased with increasing energy input from 50 kJ/kg to 100 kJ/kg, and further increase in the energy input led to a lower protein-extracted yield.

Even though PEF-assisted extraction can be easily scale-up and combine with other disruption techniques, the requirement for additional pre-washing and deionization for

marine microalgae and the high energy requirement make PEF treatment undesirable for large-scale applications (Günerken et al., 2015).

2.3.2   Non-mechanical methods

2.3.2.1   Acid and alkali

Acid-based treatment has been widely employed for disrupting microalgal cell wall. During acid treatment, sugar polymers in the cell wall can be hydrolyzed, thereby facilitating recovery of intracellular components (Lee et al., 2017). Sulfuric acid (H_2SO_4) is reported to be the most commonly used acid. Miranda et al. (2012) observed that the extraction efficiency of carbohydrates from *S. obliquus* was as high as 95.6% in 2 N H_2SO_4 solution at 120 ℃ for 30 min.

Cell disruption by alkaline treatment is achieved through saponification of membrane lipid. Sodium hydroxide (NaOH) is the commonly utilized chemical in the alkali-assisted disruption. Mahdy et al. (2014) studied the effect of alkali pre-treatment on the *C. vulgaris* and *Scenedesmus sp.* for improving biogas production, and the cell disruption efficiency was found to increase with increasing NaOH dosage.

The main advantages of acid and alkaline pre-treatment are low energy demand, modest capital cost, and scalability (Gong and Bassi, 2016). However, the use of acid/alkali may damage target compounds, like degradation of pigment by acid and denaturation of protein by alkali, thereby limiting the practical applications of acid and alkali pre-treatment for microalgae.

2.3.2.2   Osmotic shock

Osmotic shock, a rarely used disruption technique, lowers the movement or concentration of water across the cell membrane by the addition of salts, which may facilitate the recovery of intracellular molecules (Mercer et al., 2011). Rakesh et al. (2015) applied

osmotic shock treatment for *Bortyococcus sp* and observed that the osmotic shock by 15% NaCl led to a higher disruption rate than microwave-assisted treatment.

The major drawbacks of osmotic shock include low disruption efficiency, high cost of salts, prolonged processing time, and can only be used for certain microalgal species.

2.3.2.3　Ionic liquid

Ionic liquid (ILs), also known as "green designer solvents", are molten salts consisting of relatively large asymmetric organic cations and smaller inorganic or organic anions (Lee et al., 2017). Owing to their non-volatile, thermal stability, and non-flammability characteristics, ILs have been broadly utilized for cell disruption and lipid recovery from various microalgae species (Choi et al., 2014; Olkiewicz et al., 2015). For example, Choi et al. (2014) investigated the lipid extraction from *C. vulgaris* using 1-ethyl-3-methyl imidazolium diethylphosphate ([Emim]DEP) and conventional organic solvents (hexane and hexane/methanol). The authors reported that the IL-assisted treatment can extract almost all fatty acids present in the raw material and observed to be more effective than hexane or hexane/methanol extraction. Olkiewicz et al. (2015) used (hydroxymethyl)phosphonium chloride $[P(CH_2OH)_4]Cl$ to extract lipid from *C. vulgaris*, and compared with Soxhlet and B&D extraction method. The results showed that IL-based extraction resulted in the highest recovery efficiency, which was ~2.3 times higher than Soxhlet extraction and ~1.2 times higher than B&D extraction.

ILs-assisted treatment could offer high extraction efficiencies of intracellular compounds; however, the environmental concerns, recyclability, and process scale-up must be addressed.

2.3.2.4　Enzymatic lysis

Enzymatic cell disruption is a promising technology for microalgae due to its biological specificity, mild operating conditions, and low energy demand (Demuez et al., 2015). Its basic working principle is that enzyme can selectively bond to specific molecules in the

cell wall, thereby causing breakage of bonds and degradation of cell wall (Günerken et al., 2015). Al-Zuhair et al. (2017) used lysozyme and cellulase for improving protein extraction from *Chlorella*, and the resultant protein-extracted yield was higher than that from ultrasonication-assisted extraction. Zheng et al. (2011) carried out a comparative study on varying cell disruption techniques for lipid recovery from *C. vulgaris*. The tested disruption methods included ultrasonication, bead milling, enzymatic lysis with cellulase/lysozyme, and microwave. The authors found that the enzymatic treatment caused distortion and collapse of most microalgal cells; however, ultrasonication, bead milling, and microwave only partially altered the morphologies of microalgal cells.

However, there are several weaknesses of enzyme-assisted treatment, such as (i) high cost of enzymes; (ii) long processing time; and (iii) requirement for maintaining stable operational conditions (Gong and Bassi, 2016).

2.4   Hydrothermal liquefaction of microalgae

Hydrothermal liquefaction (HTL) is a biomass-to-liquid fuel conversion route that can use a feedstock containing ~80 wt.% moisture content (Marcilla et al., 2013). During HTL treatment, all microalgal macromolecules (lipid, protein, and carbohydrate) can break down to form a bio-crude oil product with a comparable energy density to petroleum crude. However, the subsequent upgrading process (e.g., hydrotreatment) is needed before microalgae-derived bio-crude oil can be used as transportation fuel. A schematic diagram of the microalgae-based biorefinery is depicted in Fig. 2.1.

In this section, the effects of feedstock characteristics and various operational parameters on the products distribution and bio-crude oil properties are reviewed. The discussed operating factors include temperature, residence time, microalgae/solvent ratio, solvent, and catalyst (homogenous and heterogenous catalyst). In addition, the reaction mechanisms of major components of microalgae (lipid, protein, and carbohydrates) under hydrothermal conditions are presented. In addition, the physiochemical properties of four

liquefaction products (bio-crude oil, aqueous phase, solid residue, and gas) are discussed. Recent studies on the HTL of microalgae are summarized in Table 2.2.
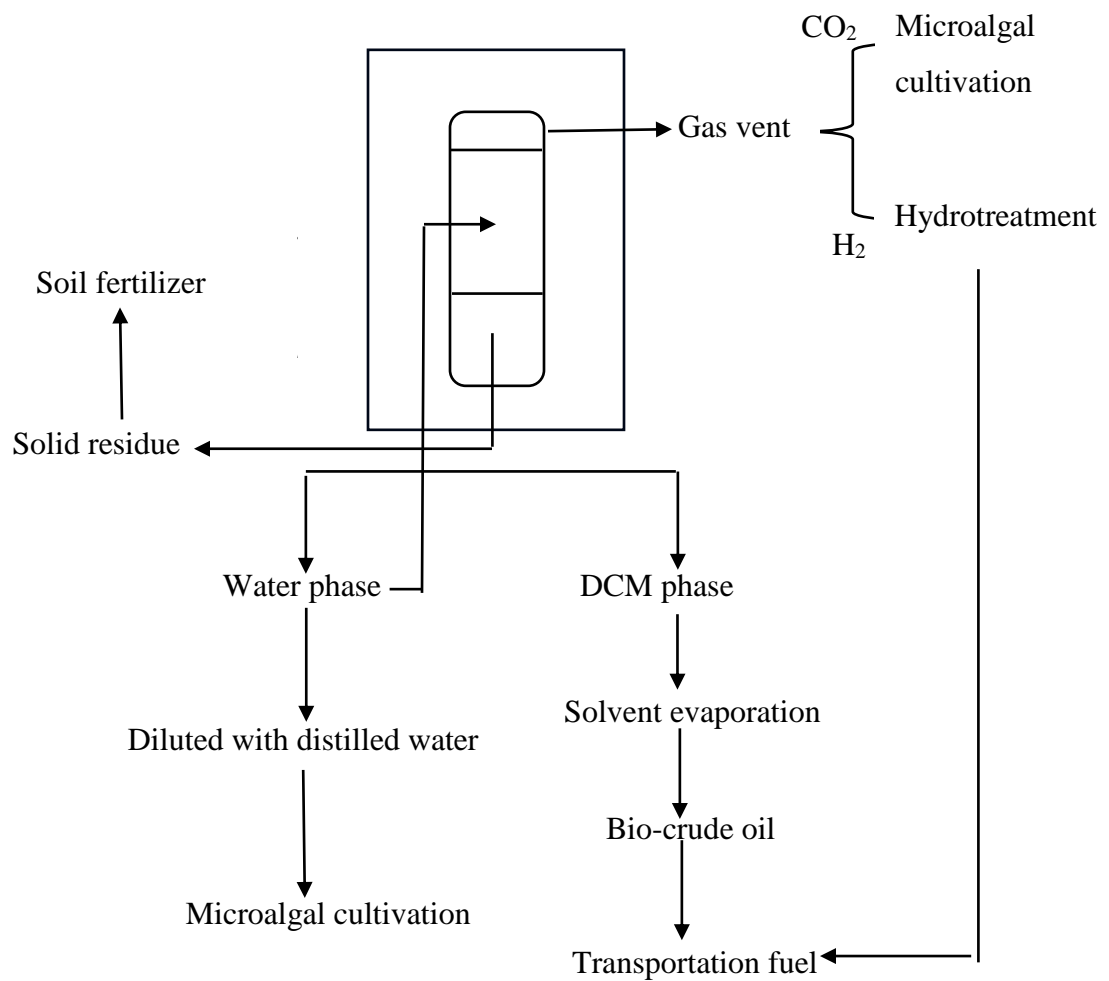
Figure 2-1: A schematic diagram of microalgae-based biorefinery.

Table 2-2: An overview of recent studies investigating the hydrothermal liquefaction of microalgae.

Microalgae strain	Reaction conditions	Reference
Desmodesmus sp.	175-450 °C, 5-60 min, 7-8 wt.% solids	Garcia Alba et al. (2012)
C. vulgaris, N. occulta, P. creuntum	350 °C, 1 h, 3/27 g/mL biomass/solvent, 1 M Na_2CO_3, HCOOH	Biller and Ross (2011)
C. pyrenoidosa	300 °C, 1 h, 25 wt.% solids	Chen et al. (2017)
Nannochloropsis sp.	200-500 °C, 60 min, 20 wt.% solids	Brown et al. (2010)
C. pyrenoidosa	100-300 °C, 0-120 min, 20 wt.% solids	Yu et al. (2011)
Nannochloropsis sp., Chlorella sp.	220-300 °C, 30-90 min, 15-25 wt.% solids	Li et al. (2014)
S. obliquus, N. gaditana, T. Suecica, C. vulgaris	250 and 375 °C, 5 min, 5-7 wt.% solids	Barreiro et al. (2013b)
N. gaditana, Chlorella sp.	180-350 °C, 30 min, 10% w/v solids	Reddy et al. (2016)
C. pyrenoidosa	170-370 °C, 5-120 min, 2.5/2-16 g/mL biomass/solvent, pure ethanol	Duan et al. (2013)
Tetraselmis sp.	310-370 °C, 5-60 min, 16 wt.% solids	Eboibi et al. (2014)
C. pyrenoidosa	220-300 °C, 0-120 min, 6.3-50/75 g/mL biomass/solvent, 0-100	Peng et al.

	vol.% ethanol content	(2016)
C. pyrenoidosa	170-350°C, 5-120 min, 2.5/2-16 g/mL biomass/solvent, pure acetone	Jin et al. (2014)
C. pyrenoidosa	200-300 °C, 30 min, 20 wt.% solids, 5 wt.% HZSM-5, Raney-Ni	Zhang et al. (2013)
C. pyrenoidosa	280 °C, 120 min, 30 wt.% solids, ethanol/water (0/7, 2/5, 1/1, 5/2, 7/2, v/v)	Zhang and Zhang (2014)
D. tertiolecta	250-340 °C, 30 min, 0-100 vol.% ethanol	Chen et al. (2012)
C. vulgaris	225-275 °C, 10-50 min, 5/25 g/mL biomass/solvent, 5 wt.% Na_2CO_3, HCOOH	Hu et al. (2017b)
Nannochloropsis sp.	250-350 °C, 1 h, 14 wt.% solids, 5 wt.% Na_2CO_3	Shakya et al. (2015)
C. vulgaris	300 and 350 °C, 1 h, 3/27 g/mL biomass/solvent, 1 M Na_2CO_3, KOH, CH_3COOH, HCOOH	Ross et al. (2010)
Nannochloropsis sp.	350°C, 1 h, 70 kPa He, 3500 kPa H_2, 50 wt.% Pd/C, Pt/C, Ru/C, Ni/SiO_2-Al_2O_3, $CoMo/γ$-Al_2O_3 (sulfided), zeolite	Duan and Savage (2010)
C. vulgaris, N. occulta	350 °C, 1 h, 3/27 g/mL biomass/solvent, 20 wt.% Pt/Al_2O_3, Ni/Al_2O_3, $Co/Mo/Al_2O_3$	Biller et al. (2011)

2.4.1 Effects of feedstock characteristics and reaction conditions on HTL of microalgae

2.4.1.1 Feedstock characteristics

Microalgae mainly consist of lipid, protein, carbohydrates, along with a small amount of ash. In general, high lipid-containing microalgae result in a higher yield of bio-crude oil.

Biller and Ross (2011) carried out HTL of three microalgae strains with different biochemical compositions (*C. vulgaris*, *N. occulta*, and *P. creuntum*) at 350 °C for 1 h, and reported that the contribution to bio-crude oil yield followed by, lipid > protein > carbohydrates. In another study, Barreiro et al. (2013b) investigated the effect of cell wall structure of microalgae on the products distribution from HTL of eight different microalgae species at 250 °C or 375 °C. At 250 °C, it was observed that a higher bio-crude oil yield was produced from HTL of microalgae without a very resistant and thick cell wall structure While, the influence of cell wall structure on the bio-crude oil yield was found to be minor at 375 °C.

Furthermore, the ash content in the original feedstock plays an important role in the liquefaction yields. High ash content in the biomass is believed to have a negative effect on the bio-crude oil yield, which can be explained as follows, (i) high ash content means less organic materials that can be converted into bio-crude oil, water-solubles, or gases in the HTL process and (ii) more ash may cover the surface of organic materials and thus prevents the interactions between organics and reaction medium (Tian et al., 2014).

2.4.1.2   Temperature

Temperature is regarded as the most important operating parameter in the HTL of microalgae. The competition reactions involve hydrolysis and re-polymerization define the role of temperature on HTL. Initially, the hydrolysis is a dominant reaction at temperatures below 220 °C. Gasification becomes active at later stage (T > 375 °C), which promotes the formation of gaseous products. Intermediate temperature range (250-375 °C) usually results in the highest yield of bio-crude oil (Garcia Alba et al., 2012). As demonstrated in Fig. 2.2, the bio-crude oil yield first increases with increasing temperature, whereas further increase in the temperature lowers the bio-crude oil yield.

Garcia Alba et al. (2012) found that the bio-crude oil yield from HTL of *Desmodesmus sp*. increased with increasing temperature up to 375 °C, and then dropped with further increase in the temperature. In a similar study, Brown et al. (2010) investigated the effect

of reaction temperature on the products distribution obtained from HTL of *Nannochloropsis s*p. at 200-500 °C for 60 min. The bio-crude oil yield was reported to increase with temperature, reaching the maximum level at 350 °C. Further increase in temperature decreased oil yield, accompanied by a dramatical increase in the gas yield. They speculated that the reduced oil yield may be attributed to the following reasons, (i) the secondary decomposition and gas formation appear to be predominant at higher temperatures and (ii) the enhanced repolymerization of free radical into high molecular-weight compounds like char that retained in the solid residue.

Besides, the properties of bio-crude oil are dependent on the liquefaction temperature. For instance, Reddy et al. (2016) performed HTL of *Nannochloropsis sp.* in water at 180-330 °C for 30 min. Higher heating value (HHV) of bio-crude oil increased with increasing temperature till 300 °C and thereafter decreased. In another study, Garcia Alba et al. (2012) reported that increasing temperature from 175 °C to 450 °C led to an increase in the C content of bio-crude oil, along with increased heating value of oil product. It was also reported that H content remained constant over the temperature range, while N content significantly increased with increasing temperature and then kept constant when temperature above 275 °C.
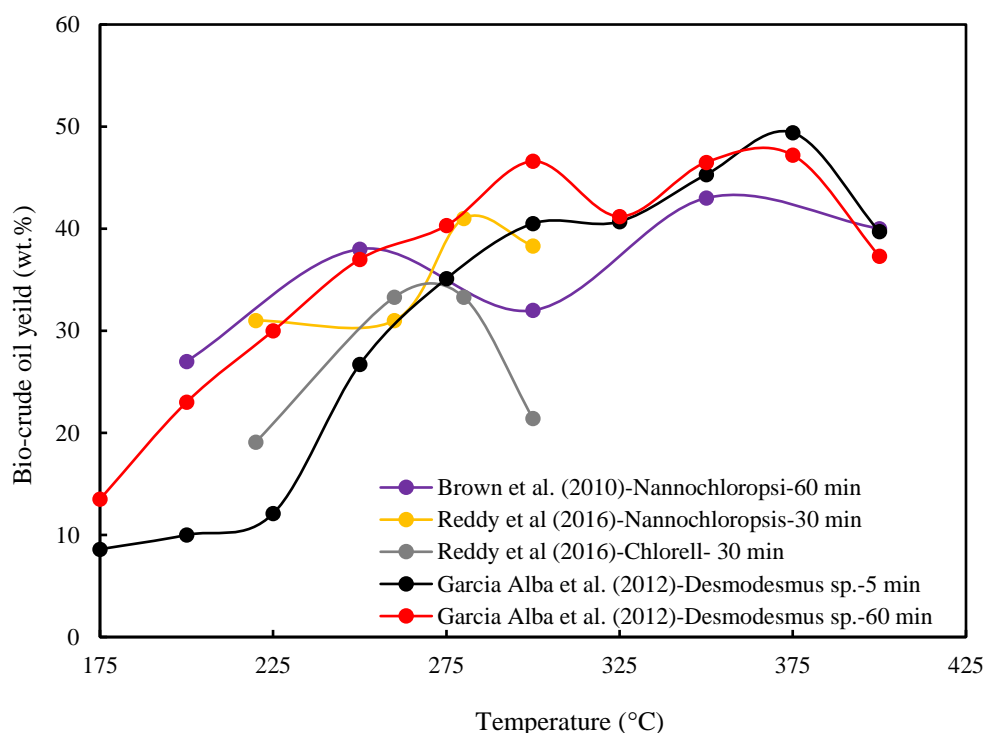
Figure 2-2: Effect of temperature on the bio-crude oil yield reported in the literature.

2.4.1.3   Residence time

Residence time is defined as the duration, in which the pre-designated temperature is maintained for the whole liquefaction process without heating and cooling time (Barreiro et al., 2013a). Many researchers have investigated the effects of residence time on the HTL of microalgae in terms of products distribution and bio-crude oil properties. In general, the effect of residence time on the HTL of microalgae is conjugated with the reaction temperature. Fig. 2.3 shows the bio-crude oil yield from microalgal HTL as a function of residence time. Duan et al. (2013) studied the effects of residence time on the HTL of *C. pyrenoidosa* at 350 °C for 5-120 min, and found that the yield of bio-crude oil increased from 56.8 wt.% at 5 min to 65.1 wt.% at 70 min and then sharply decreased as residence time extended till 120 min. Eboibi et al. (2014) carried out HTL experiment of *Tetraselmis sp.* at 310 °C for 5-60 min. The results showed that a large increase in the bio-crude oil yield occurred as residence time increased from 5 min to 15 min.

Afterwards, a minor increase in the oil yield was observed with the extension in the residence time till 30 min. Besides, the bio-crude oil obtained at 5 min contained a higher content of O than that obtained at 60 min, suggesting the promoted deoxygenation at longer residence times. Garcia Alba et al. (2012) reported that the residence time did not exert a significant effect on the products distribution at 300 ℃; however, a two-fold increase was found in the bio-crude oil yield at 200 ℃ when residence time extended from 5 min to 60 min.
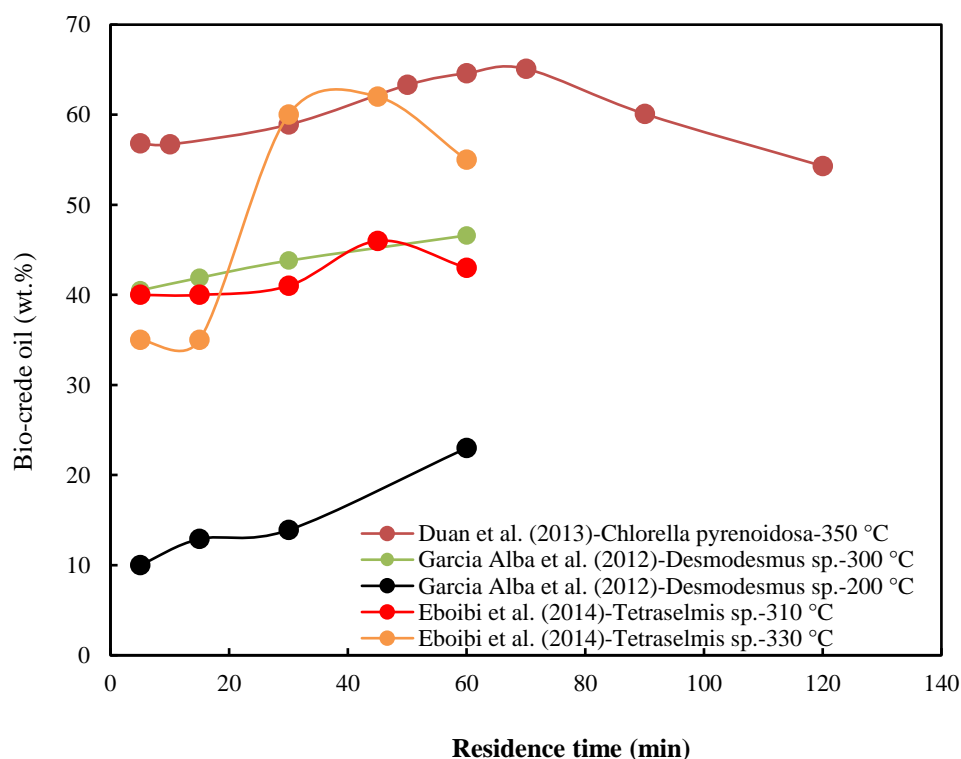
Figure 2-3: Effect of residence time on the bio-crude oil yield reported in the literature.

2.4.1.4   Microalgae/solvent ratio

Microalgae/solvent ratio can be defined as the ratio of mass of dried microalgae (g) to the volume of the solvent (mL) loaded into the reactor (Peng et al., 2016). According to previous studies, microalgae/solvent ratio has demonstrated as an important role in the HTL. Peng et al. (2016) found that the bio-crude oil yield obtained from HTL of *C.*

pyrenoidosa gradually increased from 30.7 wt.% at 6.3/75 g/mL to 39.8 wt.% at 18.8/75 g/mL, and then markedly dropped. A similar trend was also reported by Jin et al. (2014) in which microalgae was liquefied in acetone at 290 °C for 60 min with microalgae/solvent ratio ranging from 2.5/2 g/mL to 2.5/16 g/mL. At a lower solvent loading, microalgae cannot form a well-mixed suspension inside the reactor, causing undesirable mass and heat transfer conditions (Duan et al., 2013). On the other hand, introducing a higher amount of solvent into the liquefaction system could considerably increase the overall cost (Jin et al., 2014). To achieve a better economy, the solids concentration should be maintained at ~15-20 wt.% in the HTL of microalgae (Guo et al., 2015).

2.4.1.5   Solvent

Liquid water is the most common reaction medium in the microalgal HTL (Garcia Alba et al., 2012; Biller and Ross, 2011; Chen et al., 2017). As assessed by Yu et al. (2011), ~40% of carbon and ~70% of nitrogen in the original feedstock were migrated into water phase during HTL treatment rather than into oily phase. To solve this problem, numerous organic solvents have been employed as a reaction medium, including methanol, ethanol, acetone, ethylene glycol, n-propanol, and 1,4-dioxane (Duan et al., 2013; Jin et al., 2014; Zhang et al., 2013). The main advantages of organic solvent over water include: (i) the dielectric constant of organic solvent is lower than water under same conditions and (ii) can be operate under mild reaction conditions without sacrificing bio-crude oil yield (Duan et al., 2013).

In the recent years, several researchers have reported the existence of synergetic effects of ethanol-water co-solvents in the liquefaction process (Peng et al., 2016; Zhang and Zhang, 2014; Chen et al., 2012). Chen et al. (2012) liquified *D. tertiolecta* in ethanol-water mixed solvents at 320 °C for 30 min, and found that the yield of bio-crude oil peaked when using 40 vol.% ethanol-60 vol.% water mixed solvents as the reaction medium. Similarly, Zhang and Zhang (2014) reported that the highest bio-crude oil yield

from *C. pyrenoidosa* was obtained from liquefaction in ethanol-water mixed solvents (5:2, v/v).

2.4.1.6   Catalyst

Catalyst plays an important role in the HTL of microalgae. In general, the catalysts employed in the HTL system can be categorized into homogeneous and heterogenous catalysts.

2.4.1.6.1   Homogeneous catalyst

The most common homogenous catalyst employed for HTL of microalgae is Na_2CO_3. Shakya et al. (2015) observed that Na_2CO_3 enhanced the yield of bio-crude oil obtained from HTL of *Nannochloropsis* at 250 ℃. In contrast, Hu et al. (2017b) found that the catalytic HTL with Na_2CO_3 resulted in a much lower bio-crude oil compared to that obtained without catalyst. This contradicting phenomenon may be attributed to the differences in the biochemical compositions of microalgae, especially carbohydrate content. Previously, Zhou et al. (2010) found that the bio-crude oil yield from *E. prolifera* (a high carbohydrate-containing macroalgae) was improved when using Na_2CO_3 as a catalyst. Biller and Ross (2011) also observed that the high carbohydrate-containing microalgae strain was efficiently liquefied in the presence of Na_2CO_3, however, Na_2CO_3 had no or even negative influence on the high lipid or protein-containing microalgae. Previously, Dote et al. (1996) investigated the degradation behavior of protein in the presence of Na_2CO_3, and it was observed that Na_2CO_3 deterred the migration of N into oily phase. In addition, the addition of Na_2CO_3 may promote the saponification of lipid, thereby affecting bio-crude oil yield (Biller and Ross, 2011). Apart from alkaline catalysts, both organic (e.g., HCOOH and CH_3COOH) and inorganic acid (e.g., H_2SO_4) catalysts have been used in the microalgal liquefaction (Hu et al., 2017b; Zou et al., 2009; Ross et al., 2010). Zou et al. (2009) observed that the use of H_2SO_4 exhibited a positive effect on the bio-crude oil production from HTL of *D. tertiolecta*, meanwhile, N content of bio-crude oil was considerably reduced to 0.96 wt.%. Ross et al. (2010) applied both

acid and alkaline catalysts for HTL of *C. vulgaris*. The results showed that the acid catalysts (HCOOH and CH_3COOH) not only produced a higher bio-crude oil yield but also a better flowability of oil product, when compared with alkaline catalysts (Na_2CO_3 and KOH).

2.4.1.6.2   Heterogenous catalyst

Heterogenous catalyst (i.e., water-insoluble catalyst) typically exist in the different phases with liquefaction medium. The major benefits of heterogenous catalysts include: (i) can be used at severe reaction conditions that often damage homogeneous catalysts and (ii) recyclability (Galadima and Muraza, 2018). Duan and Savage (2010) performed catalytic HTL of *Nannochloropsis sp.* using Pd/C, Pt/C, Ru/C, $Ni/SiO_2-Al_2O_3$, $CoMo/\Upsilon$-Al_2O_3 (sulfide), or zeolite under inert and reducing conditions. When under inert condition, the bio-crude oil yields from all catalytic HTL experiments were generally higher than that obtained from non-catalytic liquefaction; however, the presence of $Ni/SiO_2-Al_2O_3$ or zeolite had a negative effect on the bio-crude oil yield under reducing condition. The work of Zhang et al. (2013) examined the catalytic effects of HZSM-5 and Raney-Ni on the direct liquefaction of *C. pyrenoidosa* in ethanol at 240-300 ℃ for 30 min. It was observed that catalysts exhibited a minor effect on the bio-crude oil yield under both inert and reducing conditions. Besides, a slight increase in the HHV was found in the bio-crude oil obtained using HZSM-5 as a catalyst. Nevertheless, Biller et al. (2011) observed that the presence of Pt/Al_2O_3, Ni/Al_2O_3, or $Co/Mo/Al_2O_3$ in the HTL of *C. vulgaris* and *N. occulta* had positive influences on the yield and quantity of bio-crude oil. More researches are still required to further elucidate the underlying mechanism of heterogenous catalyst in the HTL of microalgae.

2.4.2 Major components of microalgae in HTL process

2.4.2.1 Lipid

Microalgal lipid often exist in the form of triglyceride (TAG) consisting of a glycerol backbone bounded to three free fatty acids. In common, lipid content in the microalgae ranges from ~1 wt.% to ~70 wt.% on a dry weight but some species (e.g., *Botryococcus*) can contain ~90 wt.% of lipid content on a dry weight (Metting, 1996). A proposed reaction pathway of lipid in the hydrothermal medium is presented in Fig. 2.4.
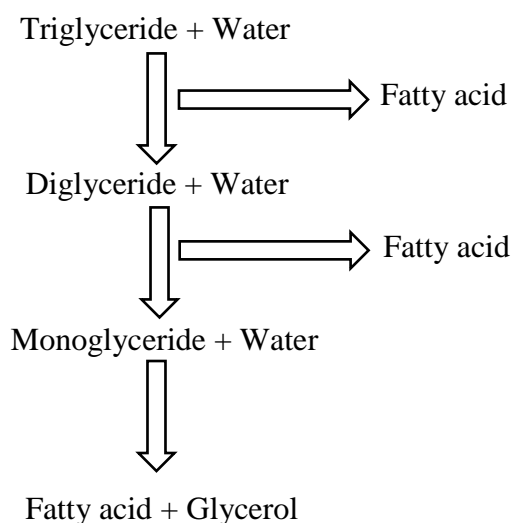
Figure 2-4: A predicted reaction network of triglyceride in the hydrothermal medium (adapted from Changi et al., 2015).

2.4.2.1.1 Glycerol

Glycerol is one of the main intermediate products from the hydrolysis of lipid. Under hydrothermal conditions, glycerol preferentially converts into water phase rather than into oily phase (Toor et al., 2011). Bühler et al. (2002) observed that the main decomposed products from glycerol in the near-critical water were methanol, ethanol, allyl alcohol, formaldehyde, acetaldehyde, propionaldehyde, acrolein, and gases (CO$_2$,

CO, and H_2). Lehr et al. (2007) examined the hydrothermal degradation behavior of glycerol in the subcritical water, and the results indicated that the acrolein was the main degradation product.

2.4.2.1.2   Fatty acids

Even though fatty acids are very stable in the subcritical water, they still can be partially decomposed into long-chained hydrocarbons (Toor et al., 2011). Fu et al. (2010) studied the degradation behavior of palmitic acid (16:0) in the near-critical water, and only ~0.7% molar yield of pentadecane was observed at 370 °C for 17 h. Watanable et al. (2006) reported that stearic acid (18:0) was highly stable in the supercritical water, and an approx. 2% conversion rate was obtained. In another study, Fu et al. (2011) compared the decarboxylation behavior of four different fatty acids [stearic (18:0), palmitic (16:0), oleic (18:1), and linoleic (18:2) acids] over Pt/C. The yields of corresponding n-alkanes from saturated fatty acids were not affected by the carbon number of fatty acids. Moreover, the decarboxylation product yield (i.e., heptadecane) from unsaturated fatty acids (oleic acid and linoleic acid) was significantly lower compared to that from stearic acid (18:0), indicating the decarboxylation rate of unsaturated fatty acids was dependent on the degree of unsaturation.

2.4.2.2   Protein

Protein is a polymer of amino acids linked by one or several peptide-chains. Protein content of microalgae is typically in the range of 6-71 wt.% on a dry weight basis (Changi et al., 2015). Previous literature suggested that the protein fraction of microalgae is the major contributor to the N element in the bio-crude oil, causing NO_x emission upon combustion and deactivation of catalyst in the existing refinery system (Jazrawi et al., 2015).

2.4.2.2.1   Protein depolymerization

When subjected to hydrothermal conditions, protein will be readily decomposed to simpler amino acids. The distribution of amino acids is dependent on the operating conditions and protein material. Rogalinski et al. (2005) conducted the hydro-thermolysis of bovine serum albumin (BSA) at 200-300 °C and 15-27 MPa for 4-180 s. The authors observed that BSA first hydrolyzed into 18 different amino acids and then further decomposed into carboxylic acids (e.g., acetic acid, propanoic acid, n-butyric acid, and iso-butyric acid), gases (e.g., CO_2, CO, H_2, and CH_4), and alcohols. Besides, pressure was observed to be less important on the recovery yield of amino acids, when compared with temperature and residence time. Quitain et al. (2001) investigated the amino acid production from shrimp shells in the sub/super-critical water. The yields of amino acids (glycine and alanine) sharply increased with increasing temperature till 250 °C and dropped thereafter.

2.4.2.2.2   Amino acids

Despite the heterogeneities of amino acids, they always undergo similar decarboxylation and deamination reactions. The decarboxylation and deamination occur simultaneously in the hydrothermal medium, and the ratio of decarboxylation/deamination is affected by the type of amino acid, pH of reaction medium, and composition of side chain, etc. (Changi et al., 2015). For instance, Li and Brill (2003) studied the hydrothermal degradation behavior of six amino acids (phenylalanine, serine, threonine, proline, histidine, and methionine) over varying pH values of reaction medium. It was found that the decarboxylation rates of phenylalanine, serine, threonine proline, and methionine increased in the pH range of 1.5-3, while further increase in the pH of reaction medium did not affect the decarboxylation rates. Additionally, the decarboxylation rate of histidine reached its minimum level at pH of 7.44 but it was improved under both acid and alkaline conditions. Sato et al. (2004) found that deamination was the predominant reaction for aspartic acid in the subcritical water at 200-340 °C and 20 MPa. The

proposed reaction pathways of glycine and alanine under hydrothermal conditions are shown in Fig. 2.5 (a) and (b), respectively.
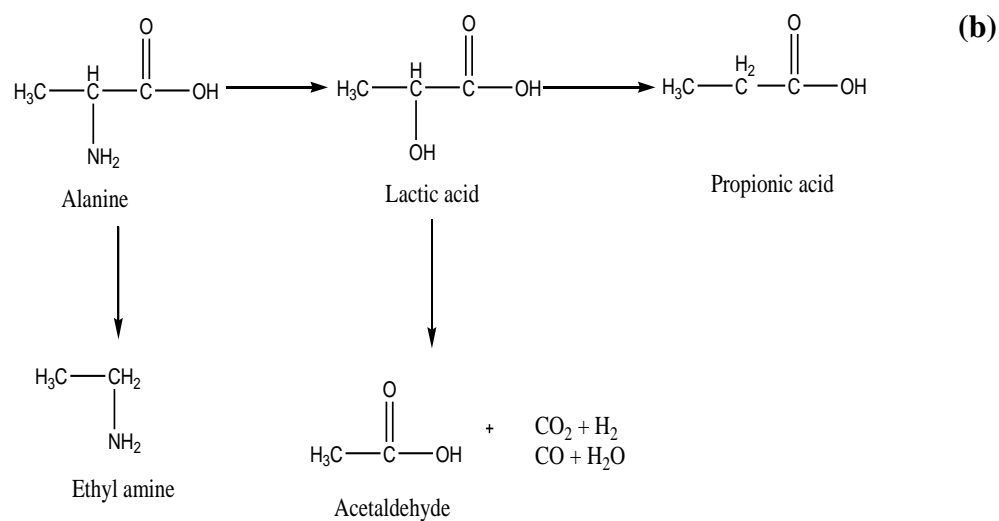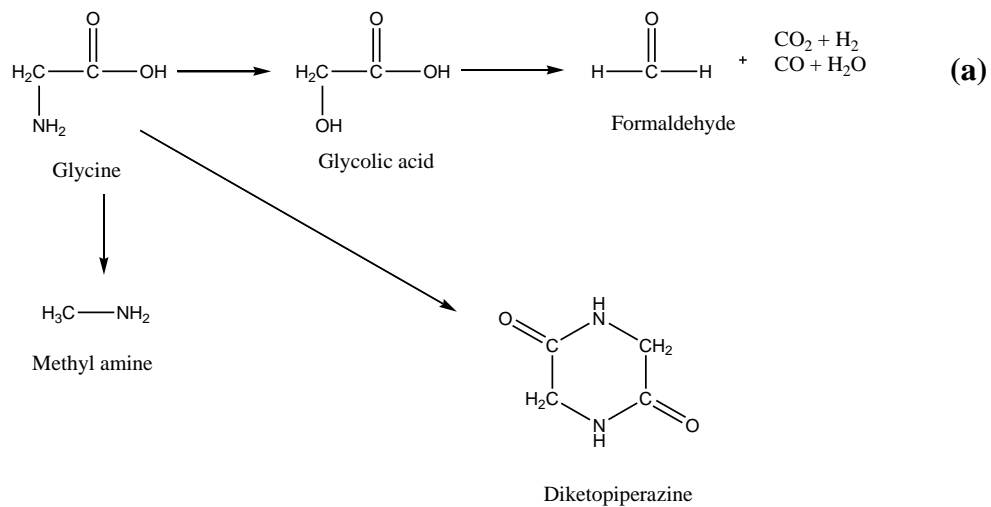
Figure 2-5: A predicted reaction network of glycine (a) and alanine (b) in the hydrothermal medium (adapted from Klingler et al., 2007).

2.4.2.3   Carbohydrates

Typically, microalgal carbohydrates exist in the form of cellulose, starch, and other polysaccharides (e.g., hemicellulose). Glucose is the most dominant simple sugar, along with small amounts of ribose, xylose, rhamnose, fructose, arabinose, mannose, and galactose (Changi et al., 2015).

2.4.2.3.1   Cellulose

Cellulose is one of the main structural components in the cell wall of microalgae. It is composed of glucose monomers linked by β-1,4--glycosidic bonds, which allows the formation of strong intra- and inter-molecular hydrogen bonds. Owing to its high crystallinity, cellulose is insoluble in the water at room temperature, whereas, it can be readily hydrolyzed to glucose monomers in the near-critical water (Toor et al., 2011). However, the hydrolysis yield of glucose is very low, which can be explained by the following two reasons: (i) glucose itself is readily subject to decomposition in the hydrothermal medium and (ii) some of the oligomers from cellulose degradation cannot be hydrolyzed to glucose (Peterson et al., 2008). The possible reaction pathway for the degradation of cellulose under hydrothermal conditions is shown in Fig. 2.6.
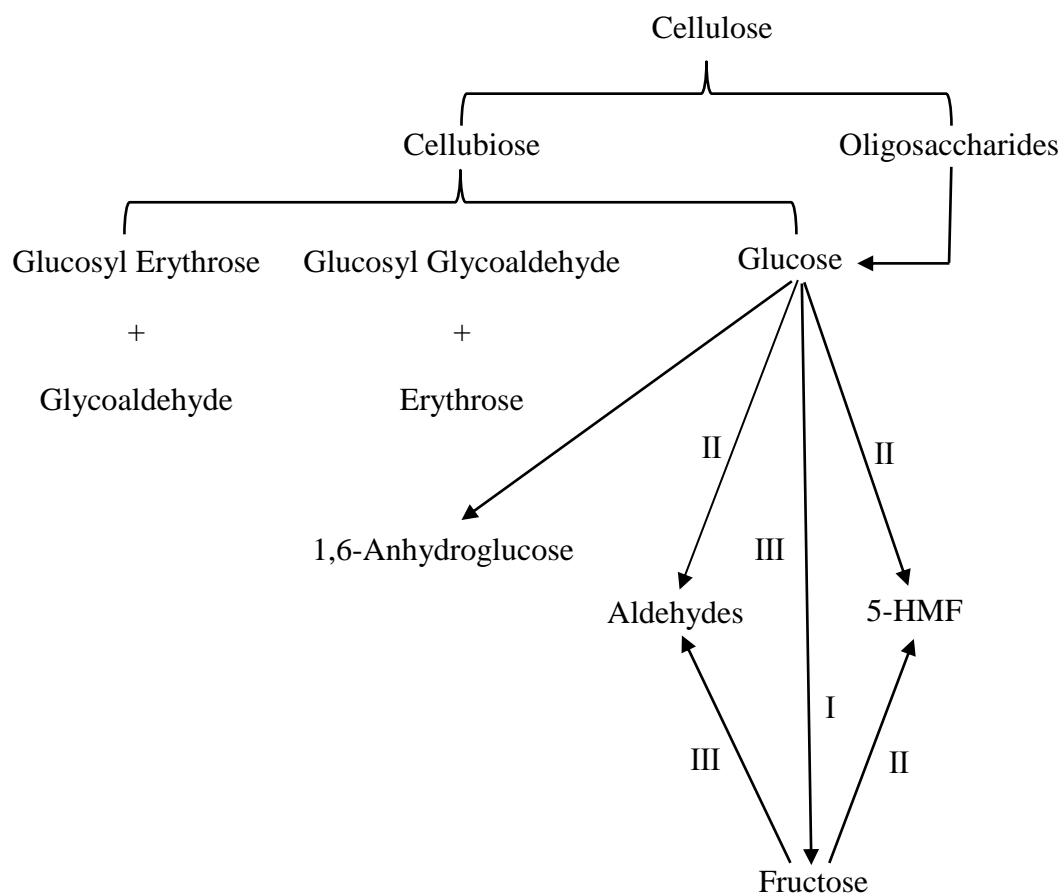
Figure 2-6: A predicted reaction network of cellulose in the hydrothermal medium (adapted from Cantero et al., 2013 and Yu and Wu, 2011). (Notes: I: Isomerization; II: Dehydration; III: Condensation).

2.4.2.3.2   Hemicellulose

Hemicellulose is a heterogenous polymer consisting of C_5 (D-xylose and L-arabinose) and C_6 (D-mannose, D-galactose, and D-glucose) sugars (Dhepe and Sahu, 2010). Due to the absence of β-(1→4)-glycosidic bonds and less uniform structure, hemicellulose appears to be less resistant to hydrothermal degradation (Peterson et al., 2008). Hashaikeh et al. (2007) found that the hemicellulose fraction in the willow began to decompose at 200 °C, whereas, in contrast, cellulose was fragmented and dissolved at 280-320 °C.

Xylose is the major hydrolysis product from hemicellulose (Changi et al., 2015). Aida et al. (2010) investigated the degradation behavior of $_D$-xylose in the sub and super-critical water at 350-400 °C and 40-100 MPa. The major decomposed products from $_D$-xylose were furfural, $_D$-xylulose, glyceraldehyde, glycolaldehyde, dihydroxyacetone, pyruvaldehyde, lactic acid, and formaldehyde.

2.4.2.3.3 Starch

Starch is a polysaccharide that consists of glucose monomers linked by β-1,6-glycosidic bonds (Changi et al., 2015). In general, it can be broadly categorized into two groups: (i) amylose with a linear structure and (ii) amylopectin with a more branched structure. In literature, starch can be readily decomposed in the hydrothermal medium. Nagamori and Funazukuri (2004) converted starch into glucose by hydrothermal hydrolysis at 180-240 °C in a batch reactor. The authors observed that the optimal glucose yield of 632 g/kg (on the carbon basis) was obtained at 200 °C for 30 min. In addition, the effect of residence time on the starch degradation was investigated at 220 °C for 0-20 min. The yield of glucose was found to reach its optimal yield at 10 min and then sharply decreased with further increase in the residence time. They speculated that the reduced glucose yield at prolonged residence time was mainly attributed to the formation of 5-HMF. Similarly, Miyazawa et al. (2006) investigated the hydrothermal degradation of starch at 180-290 °C and 10 MPa. The authors observed that the degradation of glucose into 5-HMF was not pronounced until 220 °C, while reached its optimal yield at 290 °C.

2.4.2.4 Multicomponent system

2.4.2.4.1 Binary mixtures of protein and carbohydrates

Two of the main decomposed components from protein and carbohydrates are amino acid and simple sugar (i.e., glucose, fructose, and xylose), which can react with each other to produce N&O-containing compounds via Maillard reaction (Gai et al., 2015). These compounds include pyrrole, pyrrolidinedione, thiazole, and imidazole, which can act as free radical scavengers in the sub-/super-critical water conditions (Toor et al., 2011). A

predicted reaction pathway between glycine and glucose has been proposed by Peterson et al. (2010), as shown in Fig. 2.7.
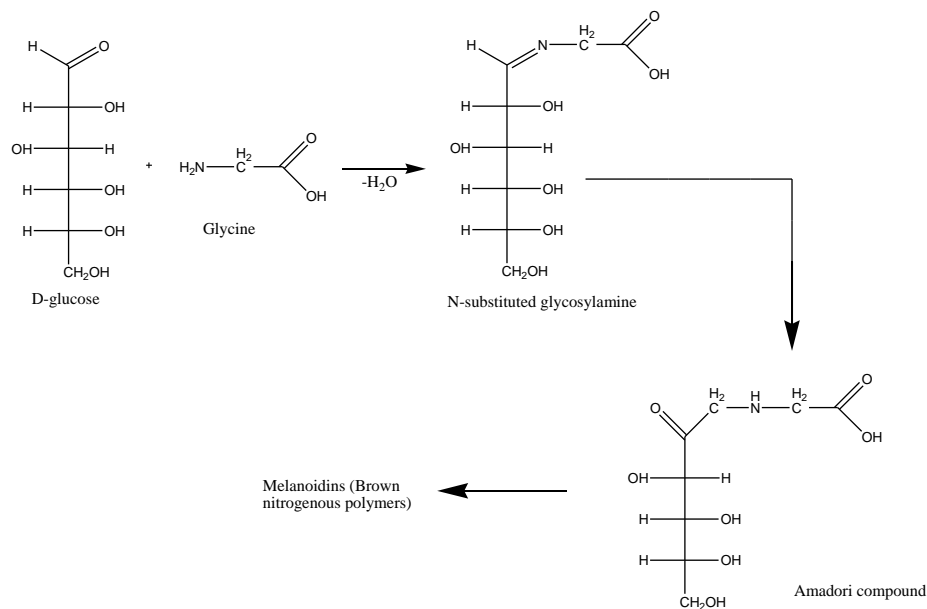
Figure 2-7: A simplified reaction pathway between glycine and glycose (Adapted from Peterson et al., 2010).

2.4.2.4.2 Ternary mixtures of lipid, protein, and carbohydrates

In a recent study, Sheng et al. (2018) investigated the hydrothermal interaction among lipid, protein, and carbohydrates fraction of microalgae by using different model compounds, including castor oil, soya protein, glucose, and their binary mixture at 280 °C for 60 min. The yield of bio-crude oil resulted from the mixture of glucose and soya protein was higher than that resulted from individual feedstock, which can be attributed to the interaction between protein and carbohydrates to form N-containing compounds via Maillard reaction. Besides, a similar result trend was observed in the binary mixture

of castor oil and glucose. Based on the liquefaction results, a proposed model for bio-crude oil yield from HTL of microalgae has been developed, as shown below:

$$Bio - crude\ oil\ yield\ (wt.\%) = 0.9(\pm0.043)X_L + 0.385(\pm0.039)X_P +$$
$$0.025(\pm0.064)X_C + 0.052(\pm0.022)\frac{X_L X_P}{|X_L - X_P|} + 0.093(\pm0.054)\frac{X_L X_C}{|X_L - X_C|} +$$
$$0.003(\pm0.005)\frac{X_P X_C}{|X_P - X_C|} \tag{2-1}$$

Where, X_L, X_P, and X_C represent lipid, protein, and carbohydrates content in the feedstock, respectively.

In a similar study, Teri et al. (2014) studied the interaction among protein, carbohydrates, and lipid at 300-350 °C for 10-90 min. A model for predicting the bio-crude oil yield produced from HTL of model compounds mixture has been indicated below:

$$Bio - crude\ oil\ yield\ (wt.\%) = 0.95X_L + 0.33X_P + 0.058X_C - 0.016X_L X_C +$$
$$0.271X_L X_P - 0.019X_P X_C \tag{2-2}$$

Where, X_L, X_P, and X_C represent lipid, protein, and carbohydrates content in the feedstock, respectively.

2.4.3   Products from HTL of microalgae

2.4.3.1   Bio-crude oil

Bio-crude oil is a dark and viscous liquid from microalgal HTL and contains an energy content of 70-95% of that of petroleum crude based on HHV (Barreiro et al., 2013a). The physical and chemical properties of bio-crude oil are determined by the feedstock properties and operating conditions. It is a complex mixture with a great number of compounds and a broad distribution of molecular weights (Tian et al., 2014). Commonly, the characterization of bio-crude oil is performed via Gas Chromatography-Mass Spectrometry (GC-MS) analysis. It should be noted that some low molecular-weight oil compounds might be lost in the solvent evaporation stage, and most of the heavy

compounds cannot be eluted into the column (Brown et al., 2010). According to their functional groups, the main chemical compounds in the microalgae-derived bio-crude oil can be categorized into aromatics (e.g., phenols and phenolic derivatives), organic acids (e.g., fatty acids), nitrogenated compounds, hydrocarbons, and other oxygenated compounds (e.g., alcohols, ketones, esters, and aldehydes) (Guo et al., 2015).

Previous studies have also determined the physical properties of bio-crude oil obtained from HTL of microalgae. Zou et al. (2010) measured the moisture, ash, density, and acidity of bio-crude oil obtained from HTL of *D. tertiolecta* at 360 °C and 50 min with the use of Na$_2$CO$_3$. The ash content of bio-crude oil was 0.2-0.5 wt.%, accompanied by a water content as high as ~ 9 wt.%. This high-water content may exhibit negative effects on the energy density and stability of bio-crude oil. In addition, the pH of oil product was 3.5-4.2, which results from the formation of organic acids during HTL.

2.4.3.2   Aqueous phase

Recirculation of aqueous by-product from HTL is considered as an essential element in the practical implementation of HTL applications (Biller et al., 2016). The water phase obtained from HTL of microalgae is composed of PO_4^{3-}, NH_4^+, CH_3COO^-, as well as some minerals (e.g., K^+, Na^+, and Mg^{2+}) (Ross et al., 2010). Since microalgae can assimilate nitrogen from a wide range of sources, HTL water phase has the potential to be recycled as the growth medium for microalgae (Biller et al., 2012; Jena et al., 2011; Du et al., 2012). Biller et al. (2012) cultivated *C. vulgaris* in a series of dilutions of recycled aqueous phase and compared to a standard growth medium. It was found that a higher biomass productivity was achieved in a diluted HTL process water (200 ×). Alternatively, water phase can be reused as a liquefaction medium for bio-crude oil production (Hu et al., 2017b; Ramos-Tercero et al., 2015). Hu et al. (2017b) for example found that the bio-crude oil yield from *C. vulgaris* gradually increased from 29.4 wt.% to 38.9 wt.% upon recycling of water phase for three rounds. The work by Ramos-Tercero et al., (2015) extended the number of recycling to a total of six and an increase in the bio-crude oil yield from *C. vulgaris* was also observed.

2.4.3.3 Gas

Gaseous fraction as a co-product from HTL usually accounts for ~10-20 wt.% of the original organics in the feedstock (Tian et al., 2014). It mainly consists of CO_2, and small amounts of CH_4, H_2, C_2H_4, and C_2H_6. Caporgno et al. (2016) found that CO_2 was the major gaseous product in the HTL of *N. oceanica* at 240-300 ℃. Brown et al. (2010) observed that the contents of H_2 and CH_4 were relatively low at 200-300 ℃, but their formation considerably promoted in the temperature range of 300-500 ℃. Besides, very little or no CO was observed in the HTL of *Nannochloropsis sp.* at 200-500 °C, which was probably consumed in the water-gas shift and/or methanation reactions. From a biorefinery point of view, CO_2 generated from HTL can be fed back for microalgal cultivation, and H_2 could be recycled for subsequent bio-crude oil upgrading (e.g., hydrotreatment) (Barreiro et al., 2013a). However, the relevant literature on the recirculation of gaseous products is still lacking.

2.4.3.4 Solid residue

HTL of microalgae results in a solid residue product mainly consisting of inorganics and a trace of organics. The yield of solid residue is strongly dependent on the ash content of original feedstock. Considering the low ash content in the microalgae strains, the solid residue yield from HTL is normally observed to be lower than 10 wt.%. An elemental analysis of solid residue obtained from HTL of *Nannochloropsis* at 350 ℃ for 60 min was conducted by Shakya et al. (2015) as followed, 50.2% C, 7.0% H, 2.2% N, 0.3% C, and 1.9% O. Owing to the presence of essential nutrients (e.g., N, S, K, and P), the solid residue is possible to be reused as a soil fertilizer.

2.5 Conclusions

In this review, the working principles and relating case studies of various pre-treatment approaches for microalgae are discussed. Mechanical methods are the most common pre-treatment techniques but are energy-intensive and non-selective release of intracellular

compounds. Hence, a number of energy-sufficient chemical and biological methods have been investigated. However, the high cost of chemicals/enzyme and potentially environmental hazards remain as the critical issues to their practical applications. Alternatively, a novel pre-treatment by pre-cooled NaOH/urea has been reported to be effective for removing cellulose (one of main structural components in microalgae) from lignocellulosic biomass. However, few studies have applied low-temperature NaOH/urea as a pre-treatment for microalgal biomass. In summary, energy-saving and eco-friendly pre-treatment methods are still needed to be established in the consideration of microalgal cell wall characteristics, overall cost, mildness, energy demand, and scalability.

Hydrothermal liquefaction (HTL) is a suitable processing technology for converting microalgae into liquid bio-fuels without dewatering the feedstock. HTL can convert not only lipid in the microalgae but also protein and carbohydrate into bio-crude oil. Previous studies have investigated the effects of feedstock characteristics and various operational parameters on the HTL of microalgae in terms of products distribution and bio-crude oil properties. In addition, previous studies have investigated the hydrothermal degradation behavior of microalgae macromolecules (lipid, protein, and carbohydrates) and their corresponding model compounds in the sub/super-critical water. However, HTL is still at the developmental stage and many issues remain unclear.

2.6   References

Aida TM, Shiraishi N, Kubo M, Watanabe M, Smith Jr RL. Reaction kinetics of D-xylose in sub- and supercritical water. J Supercrit Fluids 2010; 55:208-216.

Al-Zuhair S, Ashraf S, Hisaindee S, Al Darmaki N, Battah S, Svistunenko D, Reeder B, Stanway G, Chaudhary A. Enzymatic pre-treatment of microalgae cells for enhanced extraction of proteins. Eng Life Sci 2017; 17: 175-185.

Borowitzka MA. Microalgae as sources of pharmaceuticals and other biologically active compounds. J Appl Phycol 1995; 7: 3-15.

Barreiro DL, Prins W, Ronsse F, Brilman W. Hydrothermal liquefaction (HTL) of microalgae for biofuel production: state of the art review and future prospects. Biomass Bioenergy 2013a; 53:113-127.

Brown TM, Duan PG, Savage PE. Hydrothermal liquefaction and gasification of *Nannochloropsis sp*. Energy Fuels 2010; 34:3639-3646.

Byreddy AR, Barrow CJ, Puri M. Bead milling for lipid recovery from thraustochytrid cells and selective hydrolysis of *Schizochytrium* DT3 oil using lipase. Bioresour Technol 2016; 200: 464-469.

Barreiro DL, Zamalloa C, Boon N, Vyverman W, Ronsse F, Brilman W, Prins W. Influence of strain-specific parameters on hydrothermal liquefaction of microalgae. Bioresour Technol 2013b; 146:463-471.

Biller P, Ross AB. Potential yields and properties of oil from the hydrothermal liquefaction of microalgae with different biochemical content. Bioresour Technol 2011; 102:215-225.

Biller P, Riley R, Ross AB. Catalytic hydrothermal processing of microalgae: decomposition and upgrading of lipids. Bioresour Technol 2011; 102: 4841-4848.

Bühler W, Dinjus E, Ederer HJ, Kruse A, Mas C. Ionic reactions and pyrolysis of glycerol as competing reaction pathways in near- and supercritical water. J Supercrit Fluids 2002; 22:37-53.

Biller P, Madsen RB, Klemmer M, Becker J, Iversen BB, Glasius M. Effect of hydrothermal liquefaction aqueous phase recycling on bio-crude yields and composition. Bioresour Technol 2016; 220:190-199.

Biller P, Ross AB, Skill SC, Lea-Langton A, Balasundaram B, Hall C, Riley R, Llewellyn CA. Nutrient recycling of aqueous phase for microalgae cultivation from the hydrothermal liquefaction process. Algal Res 2012; 1:70-76.

Chen WT, Qian WY, Zhang YH, Mazur Z, Kuo CT, Scheppe K, Schideman LC, Sharma BK. Effect of ash on hydrothermal liquefaction of high-ash content algal biomass. Algal Res 2017; 25:297-306.

Carullo D, Abera BD, Casazza AA, Donsi F, Perego P, Ferrari G, Pataro G. Effect of pulsed electric fields and high pressure homogenization on the aqueous extraction of intracellular compounds from the microalgae *Chlorella vulgaris*. Algal Res 2018; 31: 60-69.

Choi SA, Oh YK, Jeong MJ, Kim SW, Lee JS, Park JY. Effects of ionic liquid mixture on lipid extraction from *Chlorella vulgaris*. Renew Energ 2014; 65: 169-174.

Chen Y, Wu YL, Zhang PL, Hua DR, Yang MD, Li C, Chen Z, Liu J. Direct liquefaction of *Dunaliella tertiolecta* for bio-oil in sub/supercritical ethanol-water. Bioresour Technol 2012; 124: 190-198.

Changi SM, Faeth JL, Mo N, Savage PE. Hydrothermal reactions of biomolecules relevant for microalgae liquefaction. Ind Eng Chem Res 2015; 54:11733-11758.

Cantero DA, Bermejo MD, Cocero MJ. Kinetics analysis of cellulose depolymerization reactions in near critical water. J Supercrit Fluids 2013; 75:48-57.

Caporgno MP, Pruvost J, Legrand J, Lepine O, Tazerout M, Bengoa C. Hydrothermal liquefaction of *Nannochloropsis oceanica* in different solvents. Bioresour Technol 2016; 214:404-410.

Cai J, Zhang L. Unique gelation behavior of cellulose in NaOH/urea aqueous solution. Biomacromolecules 2006; 7: 183-189.

Chen XM, Burger C, Wan F, Zhang J, Rong LX, Hsiao BS, Chu B, Cai J, Zhang L. Structure study of cellulose fibers wet-spun from environmentally friendly NaOH/urea aqueous solutions. Biomacromolecules 2007; 8: 1918-1926.

Demuez M, Mahdy A, Tomás-Pejó E, González-Fernández C, Ballesteros M. Enzymatic cell disruption of microalgae biomass in biorefinery processes. Biotechnol Bioeng 2015; 112: 1955-1966.

Duan PG, Jin BB, Xu YP, Yang Y, Bai XJ, Wang F, Zhang L, Miao J. Thermo-chemical conversion of *Chlorella pyrenoidosa* to liquid biofuels. Bioresour Technol 2013; 133:197-205.

Dote Y, Inoue S, Ogi T, Yokoyama S-y. Studies on the direct liquefaction of protein-contained biomass: the distribution of nitrogen in the products. Biomass Bioenergy 1996; 11: 491-498.

Duan P, Savage PE. Hydrothermal liquefaction of a microalga with heterogeneous catalysts. Ind Eng Chem Res 2010; 52:52-61.

Dhepe PL, Sahu R. A solid-acid-based process for the conversion of hemicellulose. Green Chem 2011; 12:2153-2156.

Du ZY, Shi AM, Ma XC, Cheng YL, Chen P, Liu YH, Lin XY, Ruan R. Cultivation of a microalga *Chlorella vulgaris* using recycled aqueous phase nutrients from hydrothermal carbonization process. Bioresour Technol 2012; 126:354-357.

Dai YZ, Si MY, Chen YH, Zhang NL, Zhou M, Liao Q, Shi DQ, Liu YN. Combination of biological pretreatment with NaOH/urea pretreatment at cold temperature to enhance enzymatic hydrolysis of rice straw. Bioresour Technol 2015; 198: 725-731.

Eboibi BE, Lewis DM, Ashman PJ, Chinnasamy S. Effect of operating conditions on yield and quality of biocrude during hydrothermal liquefaction of halophytic microalga *Tetraselmis sp*. Bioresour Technol 2014; 170:20-29.

Fu J, Lu XY, Savage PE. Catalytic hydrothermal deoxygenation of palmitic acid. Energy Environ Sci 2010; 3:311-317.

Fu J, Lu XY, Savage PE. Hydrothermal decarboxylation and hydrogenation of fatty acids over Pt/C. ChemSusChem 2011; 4:481-486.

Garcia Alba L, Torri C, Samorì C, van der Spek J, Fabbri D, Kersten SRA, Brilman DWF. Hydrothermal treatment (HTT) of microalgae: evaluation of the process as

conversion method in an algae biorefinery concept. Energy Fuels 2012; 26:642-657.

Gong MY, Bassi A. Carotenoids from microalgae: a review of recent developments. Biotechnol Adv 2016; 34: 1396-1412.

Günerken E, D'Hondt E, Eppink MHM, Garcia-Gonzalez LG, Elst K, Wijffels RH. Cell disruption for microalgae biorefineries. Biotechnol Adv 2015; 33:243-260.

Garoma T, Janda D. Investigation of the effects of microalgal cell concentration and electroporation, microwave, and ultrasonication on lipid extraction efficiency. Renew Energy 2016; 86: 117-123.

Guo Y, Yeh T, Song WH, Xu DH, Wang SZ. A review of bio-oil production from hydrothermal liquefaction of algae. Renew Sustainable Energy Rev 2015; 48:776-790.

Gerde JA, Montalbo-Lomboy M, Yao LX, Grewell D, Wang T. Evaluation of microalgae cell disruption by ultrasonic treatment. Bioresour Technol 2012; 125:175-181.

Goettel M, Eing C, Gusbeth C, Straessner R, Frey W. Pulsed electric field assisted extraction of intracellular valuables from microalgae. Algal Res 2013; 2:401-408.

Galadima A, Muraza O. Hydrothermal liquefaction of algae and bio-oil upgrading into liquid fuels: role of heterogenous catalysts. Renew Sustainable Energy Rev 2018; 81:1037-1048.

Gai C, Zhang YH, Chen WT, Zhang P, Dong YP. An investigation of reaction pathways of hydrothermal liquefaction using *Chlorella pyrenoidosa* and *Spirulina platensis*. Energy Convers Manag 2015; 96: 330-339.

Heo YM, Lee H, Lee C, Kang J, Ahn JW, Lee YM, Kang KY, Choi YE, Kim JJ. An integrative process for obtaining lipids and glucose from Chlorella vulgaris biomass with a single treatment of cell disruption. Algal Res 2017; 27: 286-294.

Hu YL, Gong MY, Xu CB, Bassi A. Investigation of an alternative cell disruption approach for improving hydrothermal liquefaction of microalgae. Fuel 2017a; 179: 138-144.

Halim R, Rupasinghe TWT, Tull DL, Webley RA. Mechanical cell disruption for lipid extraction from microalgal biomass. Bioresour Technol 2013; 140:53-63.

Halim R, Harun R, Danquah MK, Webley PA. Microalgal cell disruption for biofuel development. Appl Energy 2012; 91:116-121.

Hu YL, Feng SH, Yuan ZS, Xu CB, Bassi A. Investigation of aqueous phase recycling for improving bio-crude oil yield in hydrothermal liquefaction of algae. Bioresour Technol 2017b; 239:151-159.

Hashaikeh R, Fang Z, Butler IS, Hawari J, Kozinski JA. Hydrothermal dissolution of willow in hot compressed water as a model for biomass conversion. Fuel 2007; 86:1614-1622.

Jin BB, Duan PG, Zhang CC, Xu YP, Zhang L, Wang F. Non-catalytic liquefaction of microalgae in sub- and supercritical acetone. Chem Eng J 2014; 254: 384-392.

Jazrawi C, Biller P, He YY, Montoya A, Ross AB, Maschmeyer T, Haynes BS. Two-stage hydrothermal liquefaction of a high-protein microalga. Algal Res 2015; 8:15-22.

Jena U, Vaidyanathan N, Chinnasamy S, Das KC. Evaluation of microalgae cultivation using recovered aqueous co-product from thermochemical liquefaction of algal biomass. Bioresour Technol 2011; 102:3380-3387.

Kwan BKY, Chan AKY, Cheung SG, Shin PKS. Marine microalgae as dietary supplements in the culture of juvenile Chinese horseshoe crabs, *Tachypleus tridentatus* (*Xiphosura*). Aquac Res 2017; 48: 3910-3924.

Kim DY, Vijayan D, Praveenkumar R, Han JI, Lee K, Park JY, Chang WS, Lee JS, Oh YK. Cell-wall disruption and lipid/astaxanthin extraction from microalgae: *Chlorella* and *Haematococcus*. Bioresour Technol 2016; s199: 300-310.

Kurokawa M, King PM, Wu XG, Joyce EM, Mason TJ, Yamamoto K. Effect of sonication frequency on the disruption of algae. Ultrason Sonochem 2016; 31:157-162.

Klingler D, Berg J, Vogel H. Hydrothermal reactions of alanine and glycine in sub- and supercritical water. J Supercrit Fluids 2007; 43:112-119.

Li H, Liu ZD, Zhang YH, Li BM, Lu HF, Duan N, Liu MS, Zhu ZB, Si BC. Conversion efficiency and oil quality of low-lipid high-protein and high-lipid low-protein via hydrothermal liquefaction. Bioresour Technol 2014; 154: 322-329.

Lee SY, Cho JM, Chang YK, Oh YK. Cell disruption and lipid extraction for microalgal biorefineries: A review. Bioresour Technol 2017; 244:1317-1328.

Lee AK, Lewis DM, Ashman PJ. Disruption of microalgal cells for the extraction of lipids for biofuels: processes and specific energy requirements. Biomass Bioenergy 2012; 46: 89-101.

Lee JY, Yoo C, Jun SY, Ahn CY, Oh HM. Comparison of several methods for effective lipid extraction from microalgae. Bioresour Technol 2010; 101: S75-S77.

Lehr V, Sarles M, Ott L, Vogel H. Catalytic dehydration of biomass-derived polyols in sub- and supercritical water. Catal Today 2007; 121:121-129.

Li J, Brill TB. Spectroscopy of hydrothermal reactions 25: kinetics of the decarboxylation of protein amino acids and the effect of side chains on hydrothermal stability. J Phys Chem A 2003; 107:5987-5992.

Li MF, Fan YM, Xu F, Sun RC, Zhang XL. Cold sodium hydroxide/urea based pretreatment of bamboo for bioethanol production: characterization of the cellulose rich fraction. Ind Crops Prod 2010; 32: 551-559.

Madeira MS, Cardoso C, Lopes PA, Coelho D, Afonso C, Bandarra NM, Prates JAM. Microalgae as feed ingredients for livestock production and meat quality: a review. Livest Sci 2017; 205: 111-121.

Mahdy A, Mendez L, Ballesteros M, González-Fernández C. Autohydrolysis and alkaline pretreatment effect on *Chlorella vulgaris* and *Scenedesmus sp.* methane production. Energy 2014; 78: 48-52.

Montalescot V, Rinaldi T, Touchard R, Jubeau S, Frappart M, Jaouen P, Bourseau P, Marchal L. Optimization of bead milling parameters for the cell disruption of microalgae: process modeling and application to *Porphyridium cruentum* and *Nannochloropsis oculata*. Bioresour Technol 2015; 196: 339-346.

Miller DL. Effects of a high-amplitude 1-MHz standing ultrasonic field on the algae hydrodictyon. IEEE Trans Ultrason Ferroelectr Freq Control 1986; 33: 165-171.

McMillan JR, Watson IA, Ali M, Jaafar W. Evaluation and comparison of algal cell disruption methods: microwave, waterbath, blender, ultrasonic and laser treatment. Appl Energy 2013; 103: 128-134.

Miranda JR, Passarinho PC, Gouveia L. Pre-treatment optimization of *Scenedesmus obliquus* microalga for bioethanol production. Bioresour Technol 2012; 104:342-348.

Mercer P, Armenta RE. Developments in oil extraction from microalgae. Eur J Lipid Sci Technol 2011; 113: 539-547.

Marcilla A, Catala L, Garcia-Quesada JC, Valdes FJ, Hernandez MR. A review of thermochemical conversion of microalgae. Renew Sustainable Energy Rev 2013; 27: 11-19.

Metting FB. Biodiversity and application of microalgae. J Ind Microbiol 1996; 17:477-489.

Miyazawa T, Ohtsu S, Nakagawa Y, Funazukuri T. Solvothermal treatment of starch for the production of glucose and maltooligosaccharides. J Mater Sci 2006; 41:1489-1494.

Nagamori M, Funazukuri T. Glucose sproduction by hydrolysis of starch under hydrothermal conditions. J Chem Technol Biotechnol 2004; 79:229-233.

Olkiewicz M, Caporgno MP, Font J, Legrand J, Lepine O, Plechkova NV, Pruvost J, Seddon KR, Bengoa C. A novel recovery process for lipids from microalgae for biodiesel production using a hydrated phosphonium ionic liquid. Green Chem 2015; 17: 2813-2824.

Peterson AA, Vogel F, Lachance RP, Fröling m, Antal Jr MJ, Tester JW. Thermochemical biofuel production in hydrothermal media: a review of sub- and supercritical water technologies. Energy Environ Sci 2008; 1:32-65.

Postma PR, Suarez-Garcia E, Safi C, Yonathan K, Olivieri G, Barbosa MJ, Wijffels RH, Eppink MHM. Energy efficient bead milling on microalgae: effect of bed size on disintegration and release of proteins and carbohydrates. Bioresour Technol 2017; 224:670-679.

Pataro G, Goettel M, Straessner R, Gusbeth C, Ferrari G, Frey W. Effect of PEF treatment on extraction of valuable compounds from microalgae *C. vulgaris*. Chem Eng Trans 2017; 57: 57-72.

Peng XW, Ma XQ, Lin YS, Wang XS, Zhang XS, Yang C. Effect of process parameters on solvolysis liquefaction of *Chlorella pyrenoidosa* in ethanol-water system and energy evaluation. Energy Convers Manag 2016; 117:43-53.

Peterson AA, Lachance RP, Tester JW. Kinetic evidence of the Maillard reaction in hydrothermal biomass processing: glucose-glycine interactions in high-temperature, high-pressure water. Ind Eng Chem Res 2010; 49: 2107-2117.

Quitain AT, Sato N, Daimon H, Fujie K. Production of valuable materials by hydrothermal treatment of shrimp shells. Ind Eng Chem Res 2001; 40:5885-5888.

Rakesh S, Dhar DW, Prasanna R, Saxena AK, Saha S, Shukla M, Sharma K. Cell disruption methods for improving lipid extraction efficiency in unicellular microalgae. Eng Life Sci 2015;15: 443-447.

Reddy HK, Muppaneni T, Ponnusamy S, Sudasinghe N, Pegallapati A, Selvaratnam T, Seger M, Dungan B, Nirmalakhandan N, Schaub T, Holguin FO, Lammers P, Voorhies W, Deng SG. Temperature effect on hydrothermal liquefaction of *Nannochloropsis gaditana* and *Chlorella sp*. Appl Energy 2016; 165:943-951.

Ross AB, Biller P, Kubacki ML, Li H, Lea-Langton A, Jones JM. Hydrothermal processing of microalgae using alkali and organic acids. Fuel 2010; 89:2234-2243.

Rogalinski T, Hermann S, Brunner G. Production of amino acids from bovine serum albumin by continuous sub-critical water hydrolysis. J Supercrit Fluids 2005; 36:49-58.

Ramos-Tercero EA, Bertucco A, Brilman DWF. Process water recycle in hydrothermal liquefaction of microalgae to enhance bio-oil yield. Energy Fuels 2015; 29: 2422-2430.

Shene C, Monsalve MT, Vergara D, Lienqueo ME, Rubilar M. High pressure homogenization of *Nannochloropsis oculate* for the extraction of intracellular components: effect of process conditions and culture age. Eur J Lipid Sci Technol 2016; 118: 631-639.

Shakya R, Whelen J, Adhikari S, Mahadevan R, Neupane S. Effect of temperature and Na_2CO_3 catalyst on hydrothermal liquefaction of algae. Algal Res 2015; 12:80-90.

Sato N, Quitain AT, Kang K, Daimon H, Fujie K. Reaction kinetics of amino acid decomposition in high-temperature and high-pressure water. Ind Eng Chem Res 2004; 43:3217-3222.

Sasaki M, Fang Z, Fukushima Y, Adschiri T, Arai K. Dissolution and hydrolysis of cellulose in subcritical and supercritical water. Ind Eng Chem Res 2000; 39:2883-2890.

Sheng LL, Wang X, Yang XY. Prediction model of biocrude yield and nitrogen heterocyclic compounds analysis by hydrothermal liquefaction of microalgae with modlel compounds. Bioresour Technol. 2018; 247: 14-20.

Tian CY, Li BM, Liu ZD, Zhang YH, Lu HF. Hydrothermal liquefaction for algal biorefinery: a critical review. Renew Sustainable Energy Rev 2014; 38:933-950.

Toor SS, Rosendahl L, Rudolf A. Hydrothermal liquefaction of biomass: a review of subcritical water technologies. Energy 2011; 36:2328-2342.

't Lam GP, van der Kolk JA, Chordia A, Vermuë MH, Olivieri G, Eppink MHM, Wijffles RH. Mild and selective protein release of cell wall deficient microalgae with pulsed electric field. ACS Sustainable Chem Eng 2017; 5: 6046-6053.

Teri G, Luo LG, Savage PE. Hydrothermal treatment of protein, polysaccharide, and lipids alone and in mixtures. Energy Fuels 2014; 28: 7501-7509.

Wang HMD, Chen CC, Huynh P, Chang JS. Exploring the potential of using algae in cosmetics. Bioresour Technol 2015; 184: 355-362.

Wang L, Weller CL. Recent advances in extraction of nutraceuticals from plants. Trends Food Sci Technol 2006; 17: 300-312.

Wu CC, Xiao Y, Lin WG, Li JQ, Zhang SS, Zhu JY, Rong JF. Aqueous enzymatic process for cell wall degradation and lipid extraction from *Nannochloropsis sp*. Bioresour Technol 2017; 223: 312-316.

Watanabe M, Iida T, Inomata H. Decomposition of a long chain saturated fatty acid with some additives in hot compressed water. Energy Convers Manag 2006; 47:3344-3350.

Wang J, Li Y, Wang ZJ, Li YJ, Liu N. Cell wall disruption in low temperature NaOH/urea solution and its potential application in lignocellulose pretreatment. Cellulose 2015; 22: 3559-3568.

Yu G, Zhang YH, Schideman L, Funk T, Wang ZC. Distributions of carbon and nitrogen in the products from hydrothermal liquefaction of low-lipid microalgae. Energy Environ Sci 2011; 4:4587-4595.

Yap BHJ, Dumsday GJ, Scales PJ, Martin GJO. Energy evaluation of algal cell disruption by high pressure homogenisation. Bioresour Technol 2015; 184: 280-285.

Yu G, Zhang YH, Schideman L, Funk T, Wang ZC. Distributions of carbon and nitrogen in the products from hydrothermal liquefaction of low-lipid microalgae. Energy Environ Sci 2011; 4:4587-4595.

Yu Y, Wu HW. Kinetics and mechanism of glucose decomposition in hot-compressed water: effect of initial glucose concentration. Ind Eng Chem Res 2011; 50: 10500-10508.

Zheng HL, Yin JL, Gao Z, Huang H, Ji XJ, Dou C. Disruption of Chlorella vulgaris cells for the release of biodiesel-producing lipids: a comparison of grinding, ultrasonication, bead milling, enzymatic lysis, and microwaves. Appl Biochem Biotechnol 2011; 164: 1215-1224.

Zhang JX, Chen WT, Zhang P, Luo ZY, Zhang YH. Hydrothermal liquefaction of *Chlorella pyrenoidosa* in sub- and supercritical ethanol with heterogenous catalyst. Bioresour Technol 2013; 133: 389-397.

Zhang JX, Zhang YH. Hydrothermal liquefaction of microalgae in an ethanol-water co-solvent to produce biocrude oil. Energy Fuels 2014; 28:5178-5183.

Zhou D, Zhang L, Zhang SC, Fu HB, Chen JM. Hydrothermal liquefaction of macroalgae *Enteromorpha prolifera* to bio-oil. Energy Fuels 2010; 24:4054-4061.

Zou SP, Wu YL, Yang MD, Li C, Tong JM. Thermochemical catalytic liquefaction of the marine microalgae *Dunaliella tertiolecta* and characterization of bio-oils. Energy Fuels 2009; 23: 3753-3758.

Zou SP, Wu YL, Yang MD, Imdad K, Li C, Tong JM. Production and characterization of bio-oil from hydrothermal liquefaction of microalgae *Dunaliella tertiolecta* cake. Energy 2010; 35: 5406-5411.

Zhang RL, Chen J, Zhang XW. Extraction of intracellular protein from *Chlorella pyrenoidosa* using a combination of ethanol soaking, enzyme digest, ultrasonication and homogenization techniques. Bioresour Technol 2018; 247: 267-272.

Chapter 3

3 Investigation of an alternative pre-treatment for microalgae

The information presented in this Chapter is based on the paper "Investigation of an alternative cell disruption approach for improving hydrothermal liquefaction of microalgae", which was published in Fuel, 2017, Vol. 197, pages 138-144. The sections in Chapter 3 present the results towards the completion of objective 1 of this PhD project (see Section 1.2).

3.1 Abstract

High-energy and cost-intensive cell disruption processes represent one of the major techno-economic bottlenecks in the microalgae-based bio-refineries. Therefore, a feasible disruption method is required to ensure low energy input and operating cost, as well as high target-product (e.g., lipid) recovery. In this study, several different pre-treatment strategies for the pre-treatment of *Chlorella vulgaris* were investigated, including NaOH/urea, sulfuric acid and ultra-sonication. Experimental results showed that the pre-treatment by NaOH/urea solution resulted in an average mass loss of 33.7 wt.% and resulted in the removal of 77.2 % of carbohydrates and 46.3 % of protein (as N) from the original biomass. While these results were comparable to those obtained from the other pre-treatment methods, the NaOH/urea method is believed to be more advantageous in terms of energy-efficiency and cost. Afterwards, all pre-treated microalgae samples were subjected to the liquefaction process towards bio-crude oil production. The bio-crude oils obtained from NaOH/urea solvent pre-treated microalgae resulted in higher yields and demonstrated better flow properties and demonstrated better flow properties.

3.2   Introduction

In recent years, microalgae have been regarded as a potential source for the sustainable production of various products ranging from biofuels to nutraceuticals due to their high biomass productivities and abilities to be cultured in different environmental conditions and climates (Liang et al., 2012). Moreover, microalgae can be used as an option for both CO_2 mitigation and capture and biofuel production. Despite these advantages, microalgal technologies also have a number of limitations. One of the main techno-economic challenges is attributed to the rigid micro-algal cell walls, which can be a complex assembly of carbohydrates and glycoproteins (Hammed et al., 2013). However, the target intracellular bio-products (e.g., lipid) are usually located in intra-cellulose globule bodies or bound within cell membranes (Kim et al., 2016). Algaenans, which are insoluble and highly aliphatic structure have also been detected in the cell walls of certain microalgae, making the extraction of intracellular products more difficult. To-date, numerous cell disruption methods, including acid/alkaline hydrolysis, ultra-sonication, bead beating, grinding, and enzymatic lysis, have been reported. Zheng et al. (2011) investigated the cell disruption efficiency from *C. vulgaris* via ultra-sonication, bead milling, grinding, and enzymatic lysis. The grinding in liquid nitrogen was found to be the most effective method. Another study by Hernández et al. (2015) observed that the acid pre-treatment was the most efficient method to disrupt the cell walls and remove carbohydrates from *C. sorokiniana*. However, none of them are desired for microalgal biomass. For example, the acid/alkali pre-treatment usually preforms at temperature above 120 ℃, making these methods less favorable for mild microalgae-based biorefinery system (Günerken et al., 2015). Besides, although the current mechanical pre-treatments (e.g., bead milling, high pressure homogenization, and ultra-sonication) are highly effective in the cell disintegration, the high energy demand and the unavoidable heat generation represent barrier for their practical implementation (Lee et al., 2017).

According to previous studies, the low temperature NaOH/urea solvent has been regarded as an effective approach to remove cellulose through hydrolyzing inter-molecular bonds

and destroying crystalline structures. Kuo and Lee (2009) observed that the low-temperature NaOH/urea solvent greatly improved the cellulose dissolution for defatted cotton. Wang et al. (2015) investigated the pre-treatment of wheat straw by NaOH/urea solvent as low temperature (-20 ℃) and found that this approach could break down the hydrogen bonds in cellulose and simultaneously solubilize hemicellulose. However, to the best of our knowledge, the effect of low-temperature NaOH/urea solvent pre-treatment on microalgal cell disruption has not been investigated, in particular as a pre-treatment for biofuel production.

Microalgae-derived biofuels have been extensively investigated due to the depletion of fossil fuels and climate change (Biller and Ross, 2011). Recently, various technologies have been developed to convert microalgae into liquid fuels, including pyrolysis, gasification, and hydrothermal liquefaction. Among these techniques, hydrothermal liquefaction (HTL) is more suitable for feedstock with high moisture content (e.g., microalgae) due to its inherent advantage of being a wet processing technique without the requirement of drying the feedstock (Ross et al., 2010). Furthermore, oil products obtained from HTL have much lower oxygen content and moisture, as compared to pyrolysis oils (Peterson et al., 2008). The lower oxygen content is related to a higher heating value of bio-crude oil. In addition, the thermal and chemical stability of bio-crude oils is determined by oxygen and water content (Lee et al., 2016). However, microalgae-derived bio-crude oil (i.e., 5-7%) usually contains a much higher nitrogen content than that of petroleum crude oil (0.1-1.5%), which could result in the NO_x emissions upon combustion (Saber et al., 2016). Apart from the subsequent upgrading, the protein removal from the starting biomass might be an alternative way to produce a bio-crude oil containing a low nitrogen content.

In this research, the cell disruption efficiency of NaOH/urea solvent pre-treatment for C. vulgaris was investigated and compared with conventional approaches, like dilute acid and ultrasonication. The degree of microalgae disruption was quantified by measuring the release of cellular metabolites, such as carbohydrates and protein. Furthermore,

hydrothermal liquefaction studies for both crude and pre-treated microalgae were performed to illustrate the effect of pre-treatment method on quantity and quality of bio-crude oil.

3.3   Materials and methods

3.3.1   Materials

Microalgal biomass, *C. vulgaris*, was purchased from a health-food store (Pure Bulk, Inc., Roseburg, USA) as fine powder. Reagent grade sulfuric acid was purchased from Caledon Laboratories Ltd (Georgetown, Canada). Sodium hydroxide and urea were supplied by Sigma Aldrich (Oakville, Canada). The contents of lipid and carbohydrates were determined by the Bligh & Dyer method (Bligh and Dyer, 1956) and the phenol-sulfuric acid method (DuBois et al., 1956), respectively. The content of protein was estimated as % $N \times 6.25$ (Rebolloso-Fuentes et al., 2001).

3.3.2   Pre-treatment methods

3.3.2.1   NaOH/urea solvent

Pre-treatment studies by low-temperature NaOH/urea solvent were carried out according to Kuo et al. (2009) and Wang et al. (2015). In each experiment run, 50 g of NaOH/urea aqueous solution was first prepared by mixing NaOH powder, urea, and distilled water (7:12:81 by weight) and this mixture was stored in a freezer for 12 h at -5 to -10 ℃. An amount of 5.0 g of dry microalgae was thoroughly mixed with 50 g of the cold NaOH/urea solvent in a shaker at 200 rpm for 2 min.

3.3.2.2   Dilute acid

An aliquot of 5.0 g of dry algal biomass was thoroughly mixed with 50 mL of distilled water. The H_2SO_4 concentration of the mixture was adjusted to 1%, 2%, and 4% (v/v), respectively. The resultant mixture was then heated to 120 °C for 30 min in a

thermostatic oil bath with constant agitation at 60 rpm. After the selected processing time was elapsed, the mixture was cooled down to 22 °C.

3.3.2.3   Ultrasonication

An amount of 5.0 g of dry microalgae was mixed with 50 mL of distilled water. The mixture was placed into an ultrasonication apparatus (1510 Branson, Branson Ultrasonics, Danbury, USA) at frequency of 40 kHz and power of 80 W. The ultrasonication pre-treatment was carried out continuously at room temperature for 10 min, 20 min, and 30 min.

After pre-treatment, all samples were filtered and washed with distilled water till neutralization and then vacuum-dried at 50 °C for three days. The dried samples were thereafter ground in a mortal and kept in sealed plastic bags until further analysis. It should be mentioned that the particle size distribution of biomass is considered to be a secondary parameter in HTL. This is due to the fact that sub/supercritical water can both serve as a heat transfer medium and as an effective extractant during liquefaction (Akhtar and Amin, 2011). As a result, thermal gradients within the biomass particles (due to size distribution) themselves can be neglected. The ash content was determined by heating the dry biomass at 575 °C in a muffle furnace for 3 h to constant weight according to ASTM E1755 standard. The C, H, and N contents were analyzed using an elemental analyzer (Vario EL Cube, Elementar, Hanau, Germany), and the O content was estimated by difference (O%=100%-C%-H%-N%-Ash%).   TGA analysis of crude and pre-treated microalgae was performed on a TGA analyzer (PerkinElmer Thermogravimetric analyzer Pyris 1 TGA, Massachusetts, USA) from 50 °C to 800 °C in 20 mL/min N2 at a heating rate of 10°C/min. FT-IR spectra of the crude and pre-treated microalgae were recorded on a Nicolet 6700 Fourier Transform Infrared Spectroscopy (Thermo Fischer Scientific, Massachusetts, USA) in the region from 4000 to 550 cm^{-1}.

3.3.3   Hydrothermal liquefaction studies

Hydrothermal liquefaction experiments were carried out in a 100 mL batch autoclave (Parr 4590, Illinois, USA). In the case of crude microalgae, 5.0 g of dried sample was mixed with 25.0 g of fresh water and loaded into the reactor. For pre-treated sample, the pre-treated microalgae sludge as described in Section 3.3.2 (without drying) was mixed with additional fresh water to make a total of 30 g and then charged into the reactor as a slurry. The reactor was sealed and purged with N_2 for three times to remove air inside the system. After that, pure nitrogen at 0.69 MPa was purged into the reactor to prevent water from boiling during the experiments. Following this, the reactor was heated to a set-point temperature (250 °C) at a heating rate of ~ 5 ºC/min and then the temperature was maintained for 30 min. During the liquefaction process, the temperature was measured by a thermocouple inside the reactor, and the pressure was monitored by a pressure gauge connected to the reactor. After the process, the reactor was cooled to room temperature using tap water. The resulting gaseous products were then released through a control valve. Dichloromethane (DCM) was added to the reaction mixture to extract the bio-crude oil. The liquid and solid product were separated by filtration. The insoluble fraction remaining on the filter paper was dried in an oven at 105 °C overnight to obtain a solid residue. The remaining reaction mixture was transferred to a separatory funnel. The bio-crude oil phase (lower phase) was recovered by vacuum evaporation at 45 °C under reduced pressure to remove DCM. The upper phase was defined as aqueous phase, which was composed of large amounts of dissolved organics. Liquefaction yields were expressed in wt.%, and calculated as follows:

Bio-crude oil yield = (Mass bio-crude / Mass feedstock) × 100%   (3-1)

Solid residue yield = (Mass solid residue / Mass feedstock) × 100%   (3-2)

Aqueous phase & gas yield = 100% – Bio-crude oil yield – Solid residue yield   (3-3)

3.3.4   Analytical approach

The major compounds in the bio-crude were analyzed by an Agilent 7890 GC/5975 MS equipped with a HP-5MS nonpolar capillary column (30 m × 0.25 mm × 0.25 µm). The bio-crude oil was dissolved in DCM prior to GC-MS analysis. The injection temperature was set at 280 ℃. The oven temperature was set at 60 ℃ and held for 2 min, followed by a ramp at 20 ℃/min to 280 ℃ and then held for 10 min. The functional groups were characterized by a FT-IR Spectrometer (Nicolet 6700 Fourier Transform Infrared Spectroscopy, Thermo Fisher Scientific, Massachusetts, USA) with an attenuated total reflectance (ATR) mode between 4000 and 550 cm^{-1}.

3.4   Results and discussion

The *C. vulgaris* powder was characterized as described in Materials and Methods and found to be as follows (in wt.%): ash 7.13, lipid 12.99, protein 61.13, and carbohydrates 16.10 respectively. Various pre-treatment strategies were applied to the microalgae samples and these are further discussed below.

3.4.1　　Effects of NaOH/urea solvent pre-treatment

The mass loss from NaOH/urea pre-treatment was about 33.7 wt.%, as shown in Fig. 3.1.
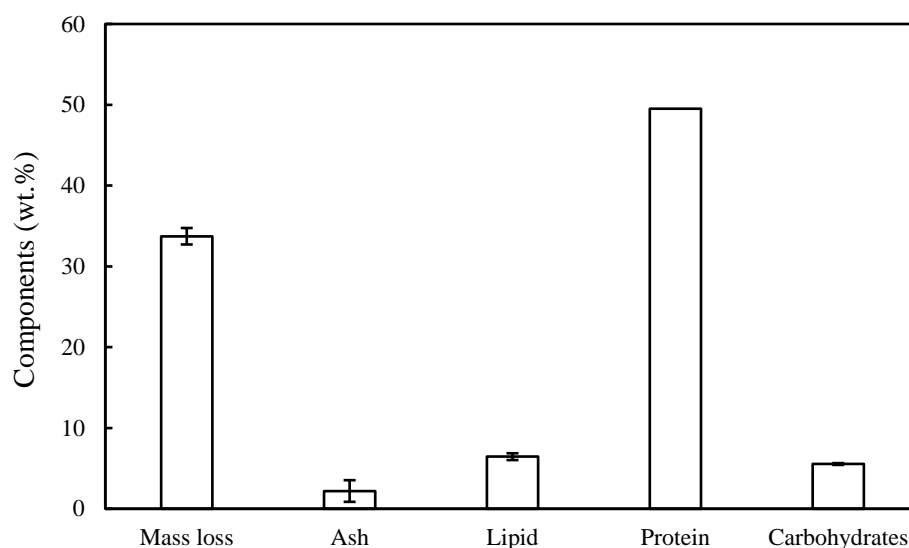
Figure 3-1: Mass loss of the microalgae in NaOH/urea solution pre-treatment and the contents of main components of the pre-treated sample.

This could be potentially due to the high extractive content of microalgae. Fig. 3.1 also shows the contents of main components of the pre-treated sample. For example, the carbohydrates content dropped to as low as ~5.54 wt.%, compared with 16.10 wt.% carbohydrates in the crude sample. The carbohydrates removal efficiency can then be calculated taking 100 g of dry crude sample as the calculation base: [(16.10% × 100 g) - (5.54% × 100 g × (1-33.7 wt.%))] / (16.10% × 100 g) = 77.20 %. That is, around 77.20% of carbohydrates in the original biomass were removed during pre-treatment, suggesting the NaOH/urea solvent was an effective approach for carbohydrates dissolution. Similar results were reported by Wang et al. (2015). As shown in Fig. 3.1, the protein content dropped to as low as 49.50 wt.%, compared with 61.13 wt.% protein in the crude sample, corresponding to 46.33% protein removal by NaOH/urea pre-treatment. The ash content in the pre-treated microalgae was much lower than that in the original biomass. The possible reason for large ash removal could be the "wash out" effect of water on the

minerals. The lowered ash content in the feedstock is be beneficial to the downstream HTL treatment because the high ash content in feedstock might potentially lead to slagging and fouling problems. However, it should be noticed that some lipid presented in the crude microalgae was removed by NaOH/urea solvent pre-treatment. This may be due to the removal of glycolipid and phospholipid (structural components) and some intercellular lipid during pre-treatment.

The mass loss (TG) and curves of crude and pre-treated microalgae are depicted in Fig. 3.2. As shown in Fig. 3.2, there are more volatile materials (T: 30-600 °C) present in the pre-treated microalgae than that in the crude feedstock. This suggests that more volatiles can be converted into liquid/gases in the HTL treatment. In addition, there were still approximately 30 wt.% of crude microalgae and 10 wt.% of pre-treated microalgae remaining as the solid products. These solid products are primarily bio-char and ash. The ash contents of the two microalgae samples were 7.13 wt.% (Table 3.1) and 2.20 wt.% (Fig. 3.1), respectively. This indicated that around 23 wt.% of crude microalgae cannot be processed during the thermal treatment, which was significantly higher than that of pre-treated microalgae (around 8 wt.%). As is known, a high ash content could seriously affect heat transfer during thermochemical conversion. Therefore, the pre-treated microalgae obtained from NaOH/urea solvent pre-treatment were found to be more suitable than untreated microalgae during the thermal-chemical processing since more organic materials can be converted into target products in terms of bio-crude oil for subsequent hydrothermal liquefaction.
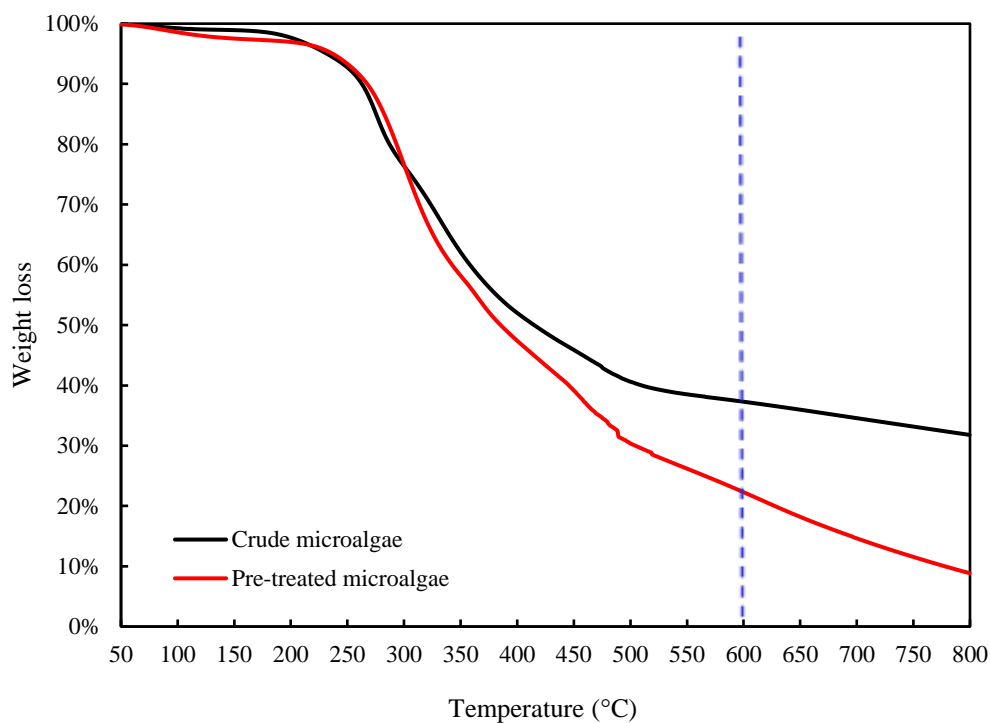
Figure 3-2: TG curves of pre-treated and crude microalgae.

The FT-IR spectra of crude and pre-treated microalgae were shown in Fig. 3.3. It was observed that the spectra of two microalgae samples were similar, and no new peaks were identified. The results were consistent with those reported by Wang et al. (2016). This showed that potentially no new chemical compounds were generated during pre-treatment by NaOH/urea solvent. Thus, it can be concluded that the NaOH/urea solvent pre-treatment is a suitable approach for microalgal biomass.
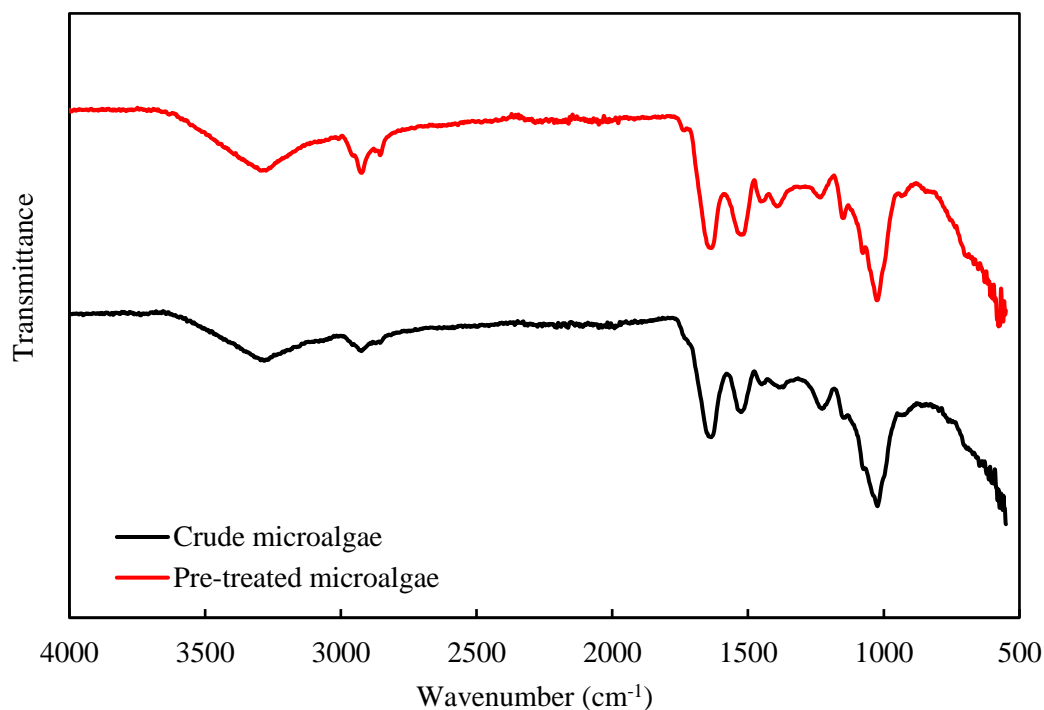
Figure 3-3: Functional groups of crude and pre-treated (NaOH/urea solvent pre-treatment) microalgae.

3.4.2 Effects of NaOH/urea solvent pre-treatment on liquefaction yields

The major volatile chemical compounds (i.e., relative peak area > 1%) detected in the bio-crude oil obtained from pre-treated microalgae at 250 °C for 30 min are summarized in Appendix-A. The major compounds can be categorized into four groups, including hydrocarbons [e.g., 1,11-Tridecadiene (RT. 10.12) and 1,4-Eicosadiene (RT. 10.39)], N-containing compounds [e.g., pyrazine (RT. 2.66) and indole (RT. 8.40)], O-containing compounds [e.g., cyclohexanol, 2,6-dimethyl (RT. 10.86)], and aromatics [e.g., 3-ethoxy-4-methoxyphenol (RT. 11.53)]. Surprisingly, no fatty acids were observed in the oil samples. It was possibly due to the conversion of fatty acids into hydrocarbons via decarboxylation (Watanabe et al., 2006). Fatty acid methyl ester (FAME) analysis will be carried out in future studies to investigate that the conversion of fatty acids to hydrocarbons is from decarboxylation. Fatty acid methyl ester (FAME) analysis will be

carried out in future studies to investigate that the conversion of fatty acids to hydrocarbons is from decarboxylation. As is known, the presence of these long-chain fatty acid can result in a high viscosity of bio-crude oil, which negatively affects its flowability (Guo et al., 2015). A high percentage of N-containing compounds were detected in the bio-crude oils due to a higher protein content of *C. vulgaris*. The results were consistent with those obtained by Gai et al. (2014) and Biller and Ross (2011). The bio-crude oil also contained some phenolic compounds, like phenol, 2,2'-methylenebis[6-(1,1-dimethylethyl)-4-ethyl- (RT. 14.55) and phenol, 3,5-dimethoxy- (RT. 12.07), which were possibly derived from the decomposition of carbohydrates during liquefaction process (Guo et al., 2015). Due to the complexity of bio-crude oil, a single technique cannot provide a fully understanding of its chemical composition. In addition, some fractions of non-volatile compounds in the oil cannot be detected by GC-MS analysis without derivatization (Michailof et al., 2016). Therefore, some other techniques, such as the HPLC and HPLC-MS, will be conducted in the future work to achieve a better understanding of HTL bio-crude oil.

It should be noted that the GC-MS results only represented a fraction of the bio-crude oil with boiling points lower than 280 °C; thereby FT-IR analysis was conducted to thoroughly elucidate its chemical properties. Fig. 3.4 shows the FT-IR spectrum of the bio-crude oil obtained from pre-treated microalgae at 250 °C for 30 min. A prominent stretching vibration absorption observed between 3700 and 3200 cm^{-1} can be ascribed to O-H or N-H group (Gai et al., 2014). The C-H stretching appeared at 3000-2800 cm^{-1} was observed in the oil, suggesting the existence of methylic or methylene alkanes. As expected, the heteroatom functionality and N-H bending (1667 cm^{-1}) was observed in the bio-crude oil samples, resulting from N-containing compounds (e.g., pyrazine, methyl- and indole) (Patel et al., 2015). The peak at 1452 cm^{-1} was related to the C-H bending vibration in methyl groups. The absorption bands from 1400 to 1199 cm^{-1} were attributed to the polysaccharide derivatives, which could result in the formation of undesired nitrogenous compounds via Maillard reaction. The spectrum indicated C-O stretching at

1260-1000 cm^{-1} may be assigned to C-O vibration stretching from alcohol. The region of 950-700 cm^{-1} confirmed the presence of aromatic C-H in the bio-crude oil.
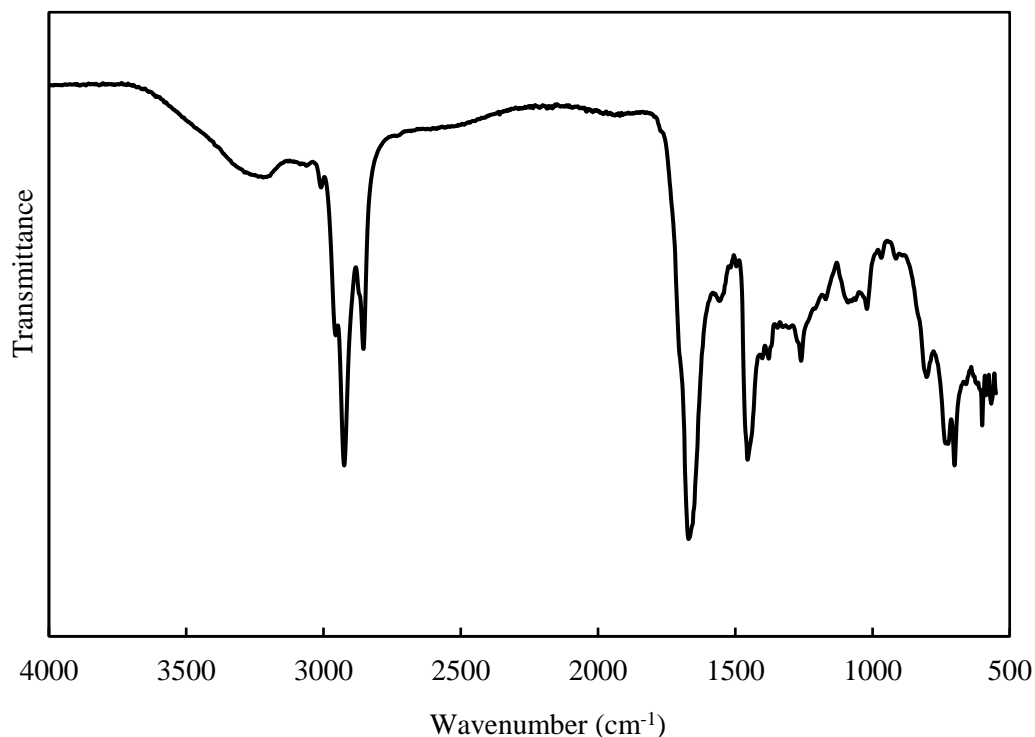
Figure 3-4: Functional groups of bio-crude oil obtained from pre-treated (NaOH/urea solvent pre-treatment) microalgae.

3.4.3   Comparison of various pre-treatment methods

3.4.3.1   Pre-treatment performance

The mass loss (ML) of microalgae during pre-treatment was one of the most important indicators for expressing a change in the quality of pre-treated biomass. As summarized in Table 3.1, the mass loss obtained from NaOH/urea solvent pre-treatment was much higher than that from ultrasonication and the acid pre-treatments at the lowest concentration (1% v/v). In addition to mass loss during the pre-treatments, contents of carbohydrates and protein of the pre-treated samples are also presented in Table 3.2, in

comparison with crude microalgae (Data represents average value of oven dry weight ± standard deviations).

Table 3-1: Mass loss of the microalgae and content of carbohydrates and protein due to various pre-treatment approaches, for crude and pre-treated microalgae (Data represents average value of oven dry weight ± standard deviations).

Samples	Mass loss (wt.%)	Carbohydrates (wt.%)	Protein (wt.%)[a]
Crude microalgae	-	16.10	61.13
Sample A	33.73 ± 1.02	5.54 ± 0.11	49.50
Sample B	15.31 ± 0.11	2.88 ± 0.59	45.88
Sample C	40.72 ± 1.97	1.48 ± 0.75	46.88
Sample D	42.94 ± 3.30	1.46 ± 1.24	43.69
Sample E	15.24 ± 3.15	4.85 ± 0.02	46.44
Sample F	19.23 ± 0.42	4.29 ± 0.95	46.81
Sample G	20.50 ± 4.67	4.00 ± 0.79	47.19

[a] Estimated by %N × 6.25; Sample A represents pre-treated microalgae obtained from NaOH/urea solvent pre-treatment; Sample B, Sample C, Sample D represents pre-treated microalgae obtained from sulfuric acid pre-treatment at 1%, 2%, and 4%, respectively; Sample E, Sample F, and Sample G represents pre-treated microalgae obtained from ultrasonication pre-treatment at 10 min, 20 min, and 30 min, respectively.

As explained previously in Section of 3.4.1 and Fig. 3.1, 77.20% of carbohydrates and 46.33% of protein in the original biomass were removed during the pre-treatment by NaOH/urea solution. The pre-treatment by sulfuric acid at concentration of 4 % (v/v) obtained the NaOH/urea solvent highest mass loss (42.94 wt.%). However, it should be noted that high temperatures (> 120 °C) are necessary to acid treatment, thereby making this approach less desirable for mild microalgae-based biorefinery. Moreover, the destructive effect of acid on cell components (e.g., pigments) is an issue that should be overcome before applying acid for microalgae pre-treatment (Günerken et al., 2015).

Based on the similar calculations as described previously in Section 3.4.1, around 84.85 %, 94.55%, and 94.83% of carbohydrates, and 36.44%, 54.54%, and 59.22% of protein in the feedstock were removed in the pre-treatment with 1%, 2%, and 4% (v/v) H_2SO_4, respectively. The removal efficiency can be positively related to the acid concentration, which is in agreement with the results reported by Hernández et al. (2015). The ultrasonication method was shown to obtain the lowest mass loss from *C. vulgaris* (15.24 – 20.50 wt.%). According to Sheng et al. (2011), the major drawback of ultrasonication could be related to the temperature control during treatment, which might seriously affect pre-treatment performance. Therefore, with respect of low energy input and short processing time, the pre-treatment by NaOH/urea solvent at low temperature was preferable for microalgal pre-treatment when compared with current approaches, including sulfuric acid and ultrasonication.

3.4.3.2 Liquefaction yields

Liquefaction processes require mixing (solid) biomass with water. A low solids concentration requires more energy input for pre-heating the water and potentially increases costs for downstream wastewater treatment (Guo et al., 2015). On the other hand, a high concentration of solids may negatively impact the yield of bio-crude oil. The study by Jena et al. (2011) observed that the HTL of microalgae at a solids concentration of 20% produced the highest bio-crude oil yield but further increase in solid concentration showed no effect on the oil yield. Therefore, in this study, a biomass to water ratio of 1:5 (g/mL) was selected. The products distribution obtained from crude and various pre-treated microalgae samples are shown in Fig. 3.5.
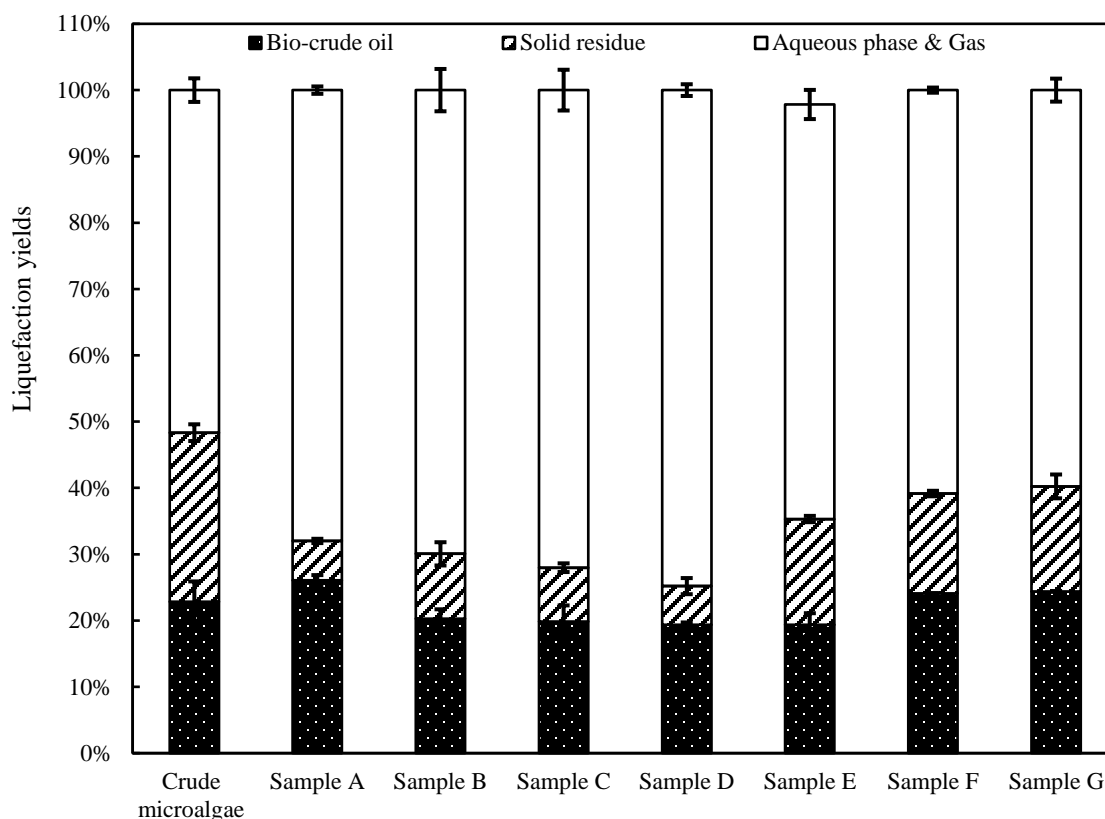
Figure 3-5: Liquefaction yields obtained from various pre-treated microalgae at 250 °C for 30 min. (Notes: Sample A represents pre-treated microalgae obtained from NaOH/urea solvent pre-treatment; Sample B, Sample C, and Sample D represents pre-treated microalgae obtained from sulfuric acid pre-treatment at 1%, 2%, and 4%, respectively; Sample E, Sample F, and Sample G represents pre-treated microalgae obtained from ultrasonication pre-treatment for 10 min, 20 min, and 30 min, respectively).

The maximum bio-crude oil yield of 26.06 wt.% was obtained from NaOH/urea solvent pre-treated microalgae. This might be due to the NaOH/urea solvent pre-treatment could change the structure of biomass and help excrete the intracellular compounds such as lipids and thus benefiting the subsequent liquefaction process towards oil formation. The oil yield obtained from sulfuric acid pre-treatment was decreased from 20.26 wt.% to 19.38 wt.% as the acid concentration increased from 1% to 4% (v/v). Contrarily, in the case of ultrasonication pre-treatment, the bio-crude oil yield was increased from 19.38 wt.% to 24.39 wt.% when the processing time extended from 10 min to 30 min.

Compared with HTL of crude microalgae (22.86 wt.%), the oil yields after sulfuric acid pre-treatment were unchanged, ~20 wt.% by weight. As expected, the solid residue yields obtained from all pre-treated microalgae were significantly lower than that obtained from crude microalgae. It was surprising to notice that the yields of solid residues obtained from NaOH/urea solvent pre-treated microalgae were smallest (5.9 wt.%), which could suggest that an almost complete liquefaction of microalgal biomass at subcritical water condition. Overall, the first pre-treatment step with NaOH/urea solvent likely changed the microalgae structure, and so an increased accessibility to water during the following HTL step. Therefore, the performance of the following HTL step can be improved in terms of increasing the bio-crude oil yield.

3.5　Conclusions

In this study, a novel cell disruption technique using low-temperature NaOH/urea solvent was applied to pre-treat microalgal biomass. Two current cell disruption approaches, namely sulfuric acid and ultrasonication, were investigated and compared with NaOH/urea solvent pre-treatment. The results indicated that this new technique was effective for releasing carbohydrates and protein into aqueous solution. Although a fraction of lipid was removed during pre-treatment, the pre-treatment with NaOH/urea solvent was preferable for microalgal biomass in terms of low energy input and short processing time. TGA analysis indicated the pre-treated microalgae obtained from NaOH/urea solvent pre-treatment was more suitable for subsequent hydrothermal liquefaction towards bio-crude oil production, when compared with crude microalgae. Moreover, the hydrothermal liquefaction studies showed that a higher yield of bio-crude oil with a better flow property was obtained with the NaOH/urea solvent pre-treated microalgae, compared with that of the crude microalgae.

3.6   References

Akhtar, J., Amin, N.A.S., 2011. A review on process conditions for optimum bio-oil yield in hydrothermal liquefaction of biomass. Renew. Sustainable. Energy. Rev. 15, 1615-1624.

Biller P, Ross AB. Potential yields and properties of oil from the hydrothermal liquefaction of microalgae with different biochemical content. Bioresour Technol 2011; 102: 215-25.

Bligh EG, Dyer WJ. A rapid method of total lipid extraction and purification. Canadian Journal of Biochemistry and Physiology. 1956; 37: 911-917.

Chen W, Maa J, Zhang Y, Gai C, Qian W. Physical pretreatments of wastewater algae to reduce ash content and improve thermal decomposition characteristics. Bioresour Technol 2014; 169: 816-20.

DuBois M, Gilles KA, Hamilton JK, Rebers PA, Smith F. Colorimetric method for determination of sugars and related substances. Analytical Chemistry. 1956; 28: 350-356.

Guo Y, Yeh T, Song, WH, Xu DH, Wang SZ. A review of bio-oil production from hydrothermal liquefaction of algae. Renewable and Sustainable Energy Reviews. 2015, 48: 776-790.

Günerken E, D'Hondt E, Eppink MHM, Garcia-Gonzalez L, Elst K, Wijffels RH. Cell disruption for microalgae biorefineries. Biotechnol Adv 2015; 33:243-60.

Guo Y, Song WH, Lu JM, Ma QR, Xu DH, Wang SZ. Hydrothermal liquefaction of *cyanophyta*: evaluation of potential bio-crude oil production and component analysis. Algal research 2015; 11: 242-7.

Gai C, Zhang Y, Chen W, Zhang P, Dong Y. Energy and nutrient recovery efficiencies in biocrude oil produced via hydrothermal liquefaction of *chlorella pyrenoidosa*. RSC Advances 2014; 4: 16958-67.

Hammed AM, Jaswir I, Amid A, Alam Z, Asiyanbi HTT, Ramli N. Enzymatic hydrolysis of plants and algae for extraction of bioactive compounds. Food Rev Int 2013; 29: 352-70.

Hernández D, Riano B, Coca M, Garcia-Gonzalez M. Saccharification of carbohydrates in microalgal biomass by physical, chemical and enzymatic pre-treatments as a previous step for bioethanol production. Chem Eng J 2015; 262: 939-45.

Jazrawi C, Biller P, He Y, Montoya A, Ross AB, Maschmeyer T, Haynes BS. Two-stage hydrothermal liquefaction of a high-protein microalgae. Algal research. 2015; 8: 15-22.

Jena U, Das KC, Kastner JR. Effect of operating conditions of thermochemical liquefaction on biocrude production from *Spirulina platensis*. Bioresource Technology. 2011, 102: 6221-6229.

Kuo C, Lee C. Enhancement of enzymatic scarification of cellulose by cellulose disruption pretreatments. Carbohydr Polym 2009; 77: 41-6.

Kim DY, Vijayan D, Praveenkumar R, Han JI, Lee K, Park JY, Chang WS, Lee JS, Oh YK. Cell-wall disruption and lipid/astaxanthin extraction from microalgae: *Chlorella* and *Haematococcus*. Bioresour Technol 2016; 199: 300-310.

Liang K, Zhang Q, Cong W. Enzyme-assisted aqueous extraction of lipid from microalgae. J Agric Food Chem 2012; 60: 11771-16.

Lee HJ, Kim YM, Lee IG, Jeon JK, Jung SC, Chung JD, Choi WG, Park YK. Recent advances in the catalytic hydrodeoxygenation of bio-oil. Korean Journal of Chemical Engineering. 2016; 33: 3299-3315.

Michailof CM, Kalogiannis KG, Sfetsas T, Patiaka DT, Lappas AA. Advanced analytical techniques for bio-oil characterization. Advanced Review. 2016; 5: 614-639.

Peterson AA, Vogel F, Lachance RP, Fröling M, Antal Jr MJ, Tester JW. Thermochemical biofuel production in hydrothermal media: A review of sub- and supercritical water technologies. Energy Enviorn Sci 2008; 1: 32-65.

Patel B, Hellgardt K. Hydrothermal upgrading of algae paste in a continuous flow reactor, Bioresour Technol 2015; 191: 460-8.

Ross AB, Biller P, Kubacki ML, Li H, Lea-Langton A, Jones JM. Hydrothermal processing of microalgae using alkali and organic acids. Fuel 2010; 89: 2234-43.

Rebolloso-Fuentes MM, Navarro-Pérez N, Garcia-Camacho F, Ramos-Miras JJ, Guil-Guerrero JL. Biomass nutrient profiles of the miroalga *Nannochloropsis*. Journal of Agricultural and Food Chemistry. 2001; 49: 2966-2972.

Sheng J, Vannela R, Rittmann BE. Evaluation of cell-disruption effects of pulsed-electric-filed treatment of *Synechocystis* PCC 6803. Environ Sci Technol 2011; 45: 3795-3802.

Saber M, Nakhshiniev B, Yoshikawa K. A review of production and upgrading of algal bio-oil. Renew Sust Energ Rev 2016; 58: 918-930.

Wang Q, Wei W, Kingori GP, Sun J. Cell wall disruption in low temperature NaOH/urea solution and its potential application in lignocellulose pretreatment. Cellulose 2015; 22: 3559-68.

Watanabe M, Lida T, Inomata H. Decomposition of a long chain saturated fatty acid with some additives in hot compressed water. Energy Convers Manag 2006; 47: 3344-50.

Wang J, Li Y, Wang ZJ, Li YJ, Liu N. Influence of pretreatment on properties of cotton fiber in aqueous NaOH/urea solution. Cellulose. 2016; 23: 2173-83.

Zheng HL, Yin JL, Gao Z, Huang H, Ji XJ, Dou C. Disruption of *Chlorella vulgaris* cells for the release of biodiesel-producing lipids: a comparison of grinding, ultrasonication, bead milling, enzymatic lysis, and microwaves. Appl Biochem Biotechnol 2011; 164: 1215-24.

Zhou JP, Qin Y, Liu SL, Zhang L. Homogenous synthesis of hydroxyethylcellulose in NaOH/urea aqueous solution. Macromol Biosci 2006; 6: 84-89.

Chapter 4

4 Production of high-quality bio-crude oils from microalgae pre-treated with pre-cooled NaOH/urea solution

The information presented in this Chapter is based on the paper "Production of low nitrogen of bio-crude oils from microalgae with pre-treated with pre-cooled NaOH/urea solution", which is published in Fuel, 2017, Vol 206, pages 300-306. The sections in Chapter 4 present the results towards the completion of objective 2 of this PhD project (see Section 1.2).

4.1 Abstract

In this study, a two-stage hydrothermal liquefaction (HTL) process was employed to produce low-nitrogen bio-crude oils from microalgae, involving pre-treatment of the microalgae with a pre-cooled NaOH/urea solution or a dilute acid and HTL of the pre-treated algal feedstock at 250 °C for 10-50 min. The results indicated that the pre-treatment with a pre-cooled NaOH/urea solution effectively removed carbohydrates and protein from the raw microalgae, leading to a decrease in carbohydrates and protein content by 12 wt.% and 10 wt.% (both absolute values), respectively, while retaining 70 wt.% of the solid mass, corresponding to as high as 82% carbohydrates removal efficiency and 40% protein removal efficiency. The two-stage HTL process slightly increased the overall bio-crude oil yields relative to the conventional single-stage HTL process, and the bio-crude oils obtained from the two–stage HTL process have a better quality than those obtained from the single-stage HTL, in terms of lower nitrogen and oxygen level and higher energy content.

4.2   Introduction

Due to the global shortage of fossil fuels and concerns about greenhouse gas (GHG) emissions, it has become important to develop economical and sustainable pathways for the production of bio-renewable liquid fuels. Recently, microalgae have been intensively investigated as alternative sources for bio-fuels production owing to their inherent advantages i.e., (i) high photosynthetic efficiencies; (ii) high lipid productivities; (iii) ease of cultivation on marginal and non-arable land; (iv) potential recyclability of stationary emissions of carbon dioxide (CO_2); and (v) adaptabilities to seawater or waste water (Peng et al., 2016). Various techniques (e.g., hydrothermal liquefaction and pyrolysis) have been employed to convert biomass into liquid bio-fuels. Compared to pyrolysis, hydrothermal liquefaction (HTL) is regarded as a more suitable method for feedstock with high moisture content since it requires no dewatering of the feedstock, thereby avoiding enthalpy energy loss (Jena et al., 2011). In general, the yield and property of bio-crude oils obtained from HTL are dependent on the operating conditions, including reaction temperature, retention time, ratio of biomass to water, and catalyst (Peng et al., 2016; Jena et al., 2011; Garcia Alba et al., 2012; Anastasakis and Ross, 2011; Gai et al., 2014). Among them, reaction temperature has been commonly identified as the most important parameter for microalgal HTL. The appropriate reaction temperatures reported in the literature for maximizing bio-crude oil yield are in the range of 250-375 ºC (Guo et al., 2015). Although a higher reaction temperature results in an increase in the oil yield, the nitrogen content in the bio-crude oil can be simultaneously increased. Yu et al. (2012) observed that the nitrogen content in the bio-crude oil from *Chlorella* increased from 3.06 wt.% to 7.46 wt.% with reaction temperature rising from 200 ºC to 280 ºC with a constant residence time of 10 min. Garcia Alba et al. (2012) investigated the effect of reaction temperature on the distribution of nitrogen in the bio-crude oil, and found that nitrogen tended to accumulate in the oil at higher temperatures. In addition, it should be noticed that a higher operational temperature is less energy efficient, thereby conducting microalgae HTL at a relatively lower temperature is a more economical option.

As well known, microalgae-derived bio-crude oils commonly contain a high nitrogen content which could lead to undesirable NO_x emission in combustion. Therefore, further upgrading is necessary to improve bio-crude oil quality by reducing the heteroatoms (e.g., nitrogen and sulfur) contents. Up to now, numerous upgrading strategies have been reported in the literature, such as supercritical fluid and hydroprocessing. Duan and Savage (2011) processed the bio-crude oil from HTL of *Nannochloropsis sp.* in the supercritical water (400 ºC) with the presence of Pt/C. Guo et al. (2014) hydroprocessed bio-crude oils over bimetallic Ni-Cu/ZrO$_2$ catalyst to improve the algal bio-crude oils properties. Alternatively, a two-stage process could be employed to produce low-nitrogen bio-crude oils from microalgae. The two-stage process mainly consists of pre-treating raw microalgae at a low temperature (100 ºC – 200 ºC), followed by a high-temperature liquefaction (250 ºC – 375 ºC). For example, Jazrawi et al. (2015) reported up to a 55 wt.% nitrogen removal via HTL coupled with a mild acid pre-treatment (< 200 ºC), when compared with the single-stage liquefaction.

In recent years, biomass pre-treatment approach using a pre-cooled NaOH/urea solution was developed (Mao et al., 2008; Zhou et al., 2006). Compared to other conventional biomass pre-treatment methods (e.g., dilute acid), NaOH/urea solution pre-treatment is more environmental friendly. The dilute acid pre-treatment could cause corrosion and generates "toxic" intermediates, leading to an increase in the downstream wastewater treatment cost (Zhao et al., 2008). In contrast, the process water produced from the pre-treatment with NaOH/urea solution can be recycled or used as a good catalyst for biomass hydrothermal liquefaction to improve the yield and quality of bio-crude oil products. For instance, NaOH has been commonly demonstrated to be an active catalyst for microalgae HTL (Yu et al., 2014). Thus, the novel pre-treatment method with a pre-cooled NaOH/urea solution may provide a great potential to improve the HTL efficiency for microalgae.

To the best of our knowledge, the pre-treatment method using pre-cooled NaOH/urea solution has not well studied for microalgae. Therefore, in this present work, the

feasibility of using pre-cooled NaOH/urea solution for microalgae conversion was studied. The effects of the pre-treatment on the yield and quality of microalgal bio-crude oil products were further investigated by HTL of raw and pre-treated microalgae at 250 ℃ for 10-50 min.

4.3   Materials and methods

4.3.1   Materials

Food-grade powder *C. vulgaris* was purchased from a health-food store (Pure Bulk, Inc., Roseburg, USA). The obtained microalgae sample has a moisture and ash content of 4.3 wt.%. and 7.1 wt.%, respectively. The ultimate analyses on a dry basis are as follows: 51.5 wt.% carbon, 7.7 wt.% hydrogen, 9.8 wt.% nitrogen, 0.5 wt.% sulfur, and 23.4 wt.% oxygen (calculated by %O = 100% - %C - %H - %N - %S - %Ash). The major chemical components of C. vulgaris are lipid, protein, and carbohydrates with 13.0 wt.%, 61.3 wt.%, and 16.1 wt.%, respectively. Reagent grade dichloromethane (DCM) was purchased from Caledon Laboratories Ltd (Georgetown, Canada). The sodium hydroxide and urea used in the pre-treatment tests were obtained from Sigma-Aldrich (Oakville, Canada).

4.3.2   Pre-treatment studies

4.3.2.1   Pre-cooled NaOH/urea solution method

Microalgae pre-treatment studies with pre-cooled NaOH/urea solution was performed using a procedure modified from that previously reported by Cai and Zhang (2005), as briefly described below. An amount of 35.0 g of NaOH/urea solution was prepared by mixing NaOH, urea, and distilled water (7:12:81 by weight) and stored in a freezer (-5 to -10 ℃) overnight. An aliquot of 7.0 g of *C. vulgaris* was thoroughly mixed with the de-frozen NaOH/urea solution for 5 min at room temperature. The mixture was then neutralized with 1.0 M HCl solution, followed by centrifugation. After that, the solid fraction was separated from the aqueous phase by vacuum filtration, and directly used as the feedstock for HTL experiments.

4.3.2.2   Dilute acid method

An amount of 7.0 g of dry microalgae and 35 mL of 2% (v/v) sulfuric acid were mixed thoroughly and placed in an oil bath at 120 ℃ for 20 min with constant agitation at 60 rpm. The mixture was thereafter cooled to room temperature and then neutralized with 1.0 M NaOH solution. The solid fraction was separated via centrifugation, and subsequently filtrated to recover the solid fraction, which was directly used for HTL studies.

4.3.3   Hydrothermal liquefaction process

A 100 mL bench-top autoclave reactor equipped with a magnetic drive stirrer, was used for the HTL tests (Parr 4590, Illinois, USA). In a single-stage HTL run, 7.0 g of crude biomass with 35.0 mL of distilled water were loaded into the reactor. In a two-stage HTL experimental run, the pre-treated microalgae slurry sample as described earlier was mixed with additional distilled water to make a total of 42.0 g and then charged into the reactor. The reactor was then sealed and flushed with nitrogen for 3 times to remove residual air inside the reactor. After that, pure nitrogen at 0.69 MPa was purged into the reactor to prevent water from boiling during the experiments. The reactor was then heated from room temperature to the pre-set temperature of 250 °C at a heating rate of 5 °C/min for ~45 min. This temperature was maintained for 10 min, 30 min, and 50 min. Throughout the reaction process, the pressure was monitored by a pressure gauge attached to the reactor head. The final pressure was ~45 bar at 250 °C. At the end of the reaction, the reactor was rapidly quenched to room temperature using a water bath to stop the reaction. After the pre-set residence time elapsed, the reactor was immediately quenched in a water bath to stop further reactions. After the system cooled to room temperature, the gaseous products were released via the fume hood (in this work gas samples were not collected and analyzed, as our preliminary tests showed that the total yield of gases at 250 ℃ was negligibly low, less than 5 wt.% and CO_2 was the main gas species formed in the process). The reactor contents were then completely rinsed into a beaker using DCM. This reaction mixture was then filtered, and the filter residue was further washed with

DCM. The residue was then dried for 12 h at 105 °C to obtain a dry solid residue fraction. The two-phase mixture was transferred to a separation funnel to isolate the aqueous phase (upper layer) from the bio-crude oil phase (lower layer). The bio-crude oil phase was transferred to a pre-weighed 500 mL Erlenmeyer flask to remove DCM by rotary evaporation at 45 ℃ under reduced pressure and to obtain bio-crude oil product. Liquefaction yields are expressed in wt.% and were calculated as follows:

$$\text{Bio-crude oil yield} = \frac{Mass_{bio-crude\ oil}}{Mass_{dry\ microalgae}} \times 100\% \qquad (4\text{-}1)$$

$$\text{Solid residue (SR) yield} = \frac{Mass_{solid\ residue}}{Mass_{dry\ microalgae}} \times 100\% \qquad (4\text{-}2)$$

$$\text{Aqueous phase \& Gas yield} = 100\%\text{-Bio-crude oil yield-Solid residue yield} \qquad (4\text{-}3)$$

All HTL experiments were performed in triplicate and the repeatability of liquefaction yields was typically $\pm$ 5 wt.%. The bio-crude oil recovery and extraction procedure is shown in Fig. 4.1.

Microalgae

Pre-treatment

Pre-cooled NaOH/urea   Dilute acid

Pre-treated slurry

HTL

Gas ◄────── Reaction mixture

Solid residue ◄──── Filtration

Separatory funnel

Evaporation
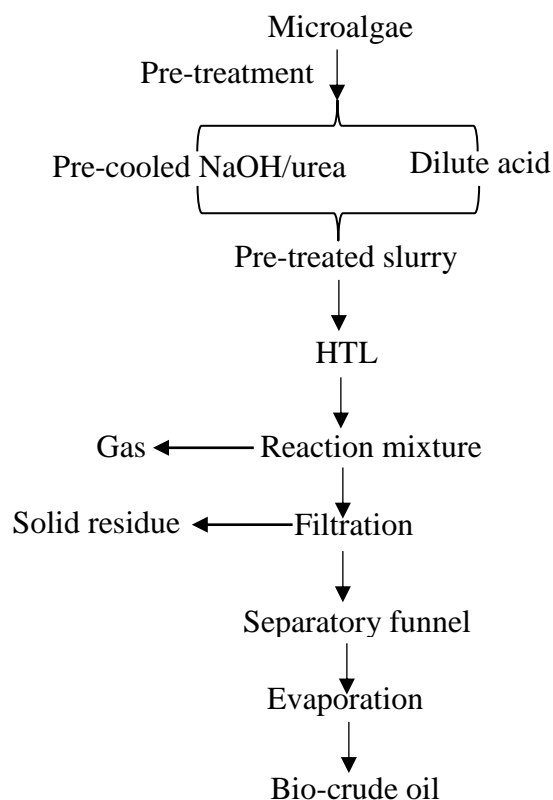
Bio-crude oil

Figure 4-1: Flow diagram of bio-crude oil recovery and product separation procedure.

4.3.4   Analytical approach

4.3.4.1   Raw and pre-treated microalgae

The pre-treated microalgae slurry obtained from previously described pre-treatment studies were oven dried at 50 ℃ for 3 days to obtained pre-treated samples for the following analyses. The ash contents of raw and pre-treated microalgae were measured gravimetrically with a muffle furnace at 550 ℃ for 3 h based on the ASTM E 1755 standard. Elemental compositions were determined by using an elemental analyzer (Vario EL Cube, Elementar, Hanau, Germany). The lipid and carbohydrates contents of raw and pre-treated biomass were measured by the Bligh and Dyer (B&D) method and DuBois method, respectively (Bligh and Dyer, 1956; DuBois et al., 1956). The protein contents of

raw and pre-treated samples were estimated by multiplying N (wt.%) by 6.25 (Becker et al., 1994).

4.3.4.2   Bio-crude oils

The volatile compositions of the bio-crude oils were analyzed by a gas chromatograph (GC, Agilent 7890B) equipped with a mass spectrometric detector (MS, 5977A) and a HP-5MS nonpolar capillary column (30 m × 0.25 mm × 0.25 µm), with temperature programming from an initial temperature hold of 2 min at 50 °C followed by a ramp at 10 °C/min to a final temperature of 280 °C with a 2 min hold. Compounds were identified with the use of the National Institute of Standards and Technology (NIST) mass spectral data library. FT-IR analysis of bio-crude oils was performed using a Nicolet 6700 Fourier Transform Infrared Spectroscopy over a range of 550−4000 cm^{-1}. Elemental compositions of bio-crude oils and solid residues were determined with the same method as described previously for the raw and pre-treated microalgae. The higher heating value (HHV) of bio-crude oils and solid residues was calculated using the DuLong's equation as widely adopted in literature (Channiwala and Parikh, 2002):

$$HHV\ (MJ/kg) = 0.338 \times C + 1.428 \times (H - O/8) \tag{4-4}$$

4.4   Results and discussion

4.4.1   Characterizations of pre-treated microalgae

The main characteristics of pre-treated microalgae samples obtained from pre-cooled NaOH/urea and dilute acid pre-treatments were summarized in Fig. 4.2. First of all, two pre-treatment methods resulted in an average mass loss of the feedstock, by ~30 wt.% (NaOH/urea) and ~41 wt.% (dilute acid). It should be noted that the dilute acid pre-treatment approach is essentially unselective as its economic benefits could be significantly outweighed by the reduction in the bio-crude oil yield (Jazrawi et al.,2015). The ash contents in two pre-treated microalgae samples were much lower than the raw microalgae, and the % of ash reduction was ~81.3 (NaOH/urea) and ~82.0 (dilute acid). The reduction in ash content might be partially due to the "wash out" effects of water on

minerals. Microalgae are reported to contain 5-20 wt.% of ash content (Changi et al., 2015). Its main components can either serve as catalysts or inhibitor for intra-macromolecules (lipid, protein, and carbohydrates) degradation when subjected to hydrothermal condition (Changi et al., 2015).
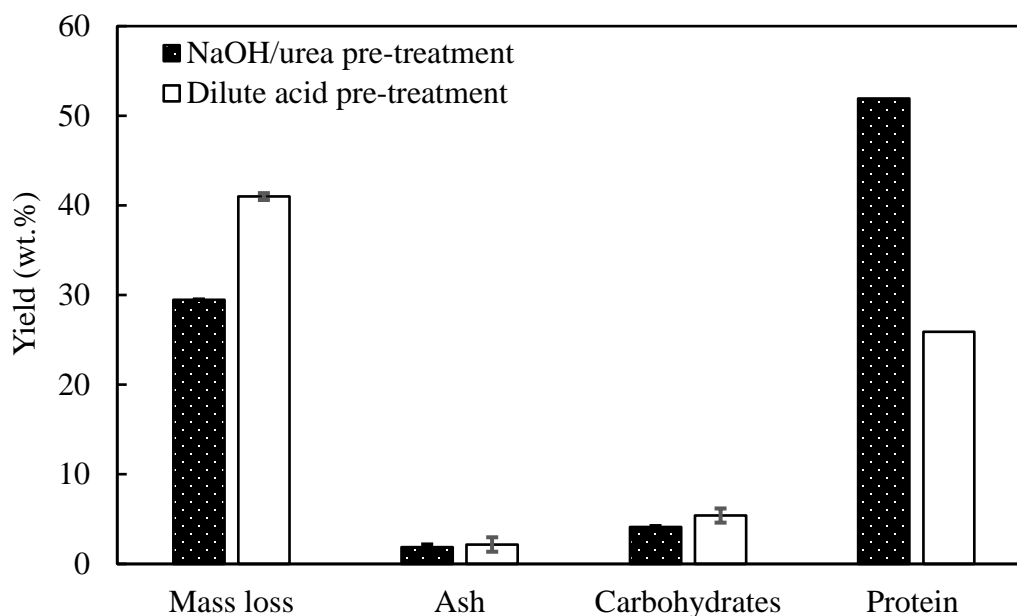
Figure 4-2: Characterizations of the microalgae after different pre-treatments.

Besides, approx. 12 wt.% of carbohydrates and 9 wt.% of protein (both absolute amounts) in raw biomass were removed by pre-cooled NaOH/urea solution pre-treatment, corresponding to as high as ~82% carbohydrates removal efficiency and ~40% protein removal efficiency. It should be noted that it is significant to handle the remaining process water after pre-treatment to reduce pollution. Due to the high contents of carbon and nitrogen, the process water might be employed as the growth medium for heterotrophic algae strains. Some algae species have showed their abilities to consume municipal and industrial wastewater as carbon source. In addition, algae could assimilate a wide range of nitrogen sources, including organics and inorganics (Barreiro et al., 2013). Another solution is to recycle the process water as reaction medium for HTL to improve bio-crude oil production and more efficient utilization of NaOH. These above

two options will be investigated in the future study. In the case of dilute acid pre-treatment, a similar amount of carbohydrates (~11 wt.%, absolute value) and around ~35 wt.% (absolute value) of protein were removed.

However, it should be mentioned that the amounts of chemicals used for NaOH/urea solution pre-treatment could be very high for the actual industrial application. Therefore, to address this problem, a number of methods, such as NaOH recovery and partially substitution of NaOH with CaO or $Ca(OH)_2$, can be utilized. Another crucial practical problem related to this pre-treatment approach is that it is energy costly to pre-cooling the NaOH/urea solution at $-10\sim12$ ℃ in the perspective of large-scale operation. A previous study performed by Zhao et al. (2008) found that the winter temperature, especially in the northern region (Madison, Wisconsin, USA), was low enough to cool the system to the required processing temperature without any extra energy input for cooling the pre-treatment system.

4.4.2   Liquefaction yields

Due to its advantage of high efficiency, low energy demand, and short processing time, the pre-treatment by pre-cooled NaOH/urea solution was chosen to explore the effects of pre-treatment and residence time on the products distribution from HTL of microalgae. Residence time is one of the key operating parameters that determine the liquefaction efficiency and product distributions. Generally, an insufficient residence time leads to an incomplete conversion process; whereas, in contrast, an excessive residence time could cause the secondary reactions of desirable products, such as decomposition or re-polymerization of bio-crude oils (Guo et al., 2015). Effect of residence time on the liquefaction yields was studied with the raw and pre-treated (the pre-cooled NaOH/urea solution) microalgae at 250 ℃ for 10-50 min, and the results are illustrated in Fig. 4.3. In general, the bio-crude oil yields from the raw and pre-treated biomass increased with prolonging reaction time. This tendency is consistent with the results reported in some previous studies (Peng et al., 2016; Garcia Alba et al., 2012). In addition, at any given reaction time, the oil yields from the two-stage HTL process with the pre-treated

feedstock were higher than those obtained from the single-stage HTL process with raw microalgae. This might be attributable to the changes in the cell structure in the pre-treatment, which may facilitate the extraction of intra-macromolecules, like lipid, from microalgal cells and their conversion into oil products. The solid residue yields from both raw and pre-treated microalgae decreased slightly by increasing retention time, as similarly reported in literature (Guo et al., 2015).
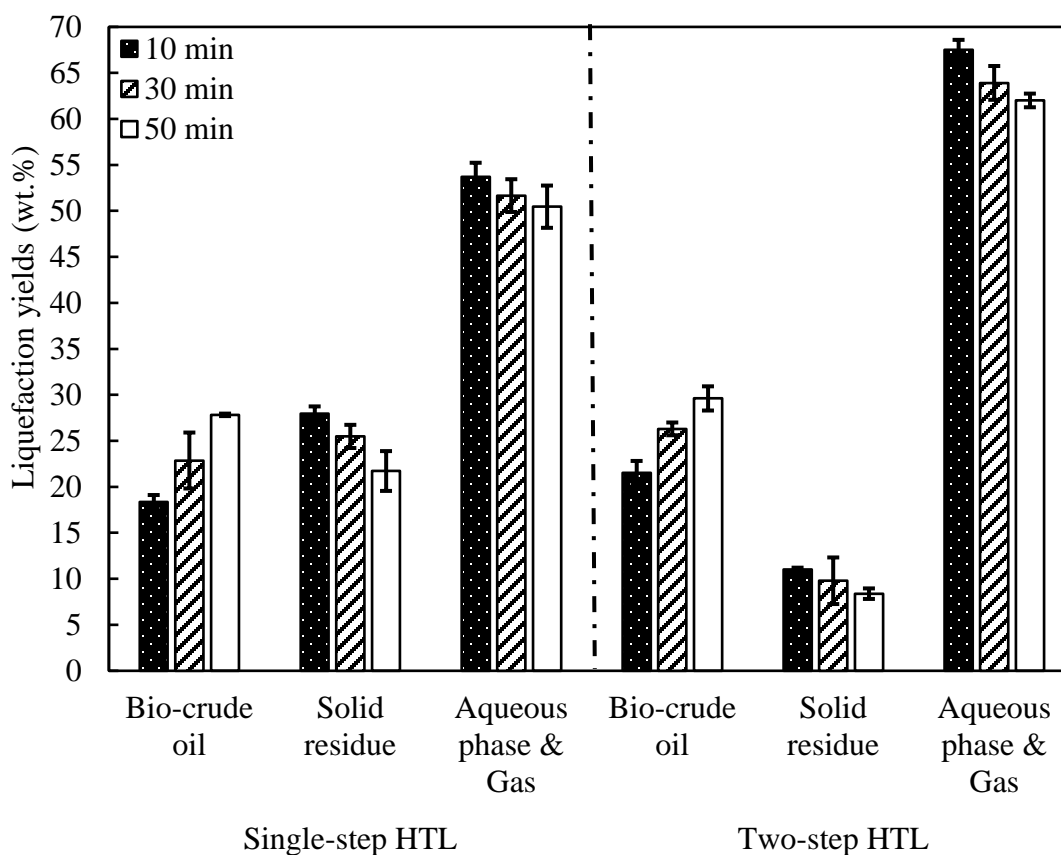
Figure 4-3: Liquefaction yields obtained from HTL of microalgae at 250 ℃ for 10 min, 30 min, and 50 min.

4.4.3　Characterization of liquefaction products

Elemental compositions of bio-crude oils obtained from raw/pre-treated (with pre-cooled NaOH/urea solution) microalgae at 250 ℃ for 10 min are summarized in Table 4.1. HHV of the bio-crude oil from the pretreated microalgae (~ 36 MJ/kg) is higher than that of the

bio-crude oil from raw microalgae (~ 31 MJ/kg). The carbon content in the bio-crude oil obtained from two-stage process was higher compared to that of the oil obtained from single-stage HTL process, so is the hydrogen content in the bio-crude oils. As expected, the nitrogen and sulfur contents in the oil derived from pre-treated microalgae (6.39 wt.% N and 0.19 wt.% S) are lower than those of the oil derived from raw biomass (7.49 wt.% N and 0.32 wt.% S), which was likely due to the removal of protein and other sulfur-containing components in the pre-treatment. Although the pre-treatment could remove a fraction of protein from crude biomass, the oil products still contain significant quantities of nitrogen. Accordingly, further upgrading via deoxygenation or denitrogenation is required, so as to make the microalgae-based bio-crude oils liquid bio-fuels comparable to petroleum-based fuels. In this work, energy recovery ratio was calculated with the following equation (Biller and Ross, 2011):

$$\text{Energy Recovery ratio (\%)} = \frac{HHV_{bio-crude\ oil} \times Mass_{bio-crude\ oil}}{HHV_{biomass} \times Mass_{bio-crude\ oil}} \times 100\% \qquad (4\text{-}5)$$

As shown in Table 4.1, the two-stage HTL process (HTL coupled with the NaOH/urea solution pre-treatment) had a higher recovery ratio (~ 32%) than single-stage process (24 %), which was mainly resulted from the higher energy content and yield of bio-crude oil products in the two-stage HTL process.

Table 4-1: Ultimate analysis of bio-crude oils obtained from HTL of the raw and pretreated microalgae at 250 °C for 10 min.

Elemental composition (wt.%)	Oil from the pre-treated microalgae	Oil from raw microalgae
C	70.14	62.42
H	10.22	9.45
O[a]	13.06	20.32
N	6.39	7.49
S	0.19	0.32
HHV (MJ/kg)[b]	35.97	30.97
Energy recovery ratio (%)[c]	31.97	23.50

[a] Oxygen content determined by difference; [b] HHV (MJ/kg) calculated by Dulong equation Eq.4-4); [c] Energy recovery ratio (%) calculated by Eq. 4-5.

Similarly, an energy recovery ratio of ~32% was reported in a previous study by Biller and Ross (2011), in which the *Chlorella vulgaris* was liquefied at 350 °C for 1 h with the addition of HCOOH as a catalyst.

Major volatile chemical compounds in the bio-crude oils obtained from the raw and pre-treated microalgae (with pre-cooled NaOH/urea solution) were analyzed by GC-MS, and the results with the oils at 250 °C for 10 min are shown in Fig. 4.4. The compounds detected in the oil samples can be categorized into five groups: (1) hydrocarbons; (2) fatty acids; (3) amides; (4) oxygen-containing compounds (including aldehydes, alcohols, esters, ethers, and ketones); (5) cyclic oxygenates or aromatics (including phenols, phenol derivatives, and benzenes); and (6) nitrogen-containing compounds.
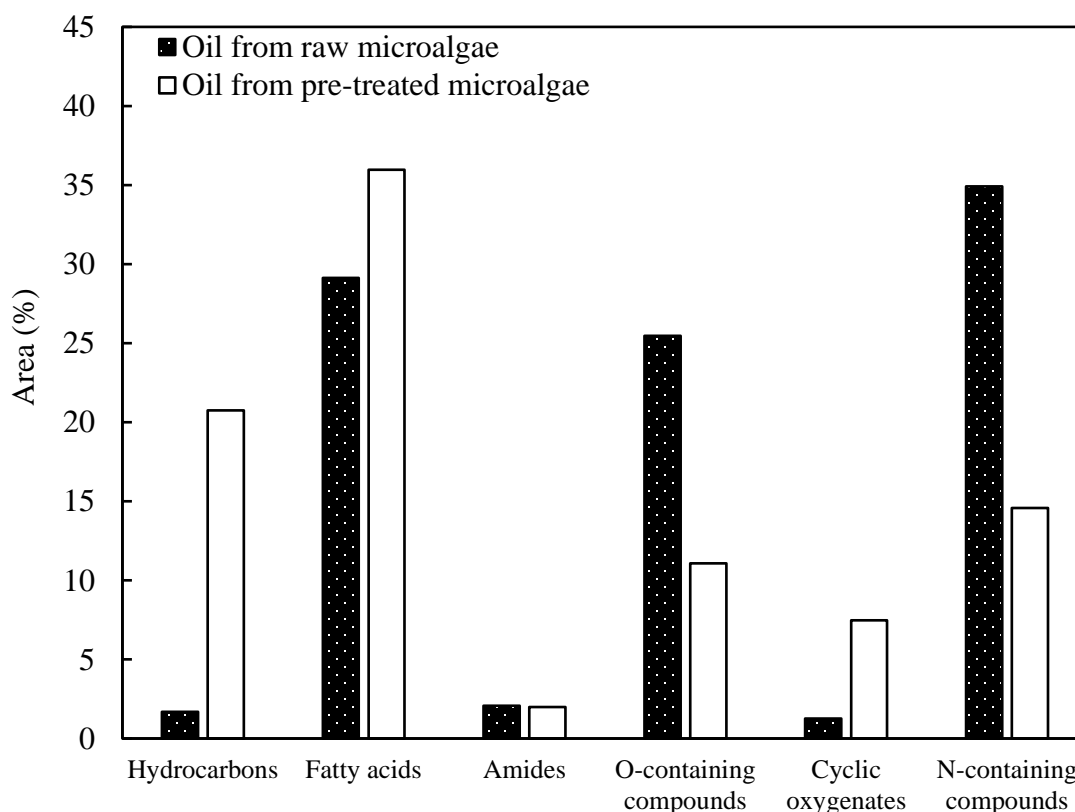
Figure 4-4: Major compounds detected by GC-MS in the bio-crude oils obtained from HTL of microalgae at 250 °C for 10 min.

The detailed compounds in the bio-crude oils were summarized in Appendix-B. As shown in Fig. 4.4, the bio-crude oil from the pre-treated microalgae contained a higher content of hydrocarbons, which could be directly produced from decarboxylation of fatty acids (Gai et al.,2014). Hydrocarbons were identified as the major compounds for two oil samples, such as 1,3,5-hexatriene, (E)- and 3-eicosyne. Compared with the oil samples from the single-stage HTL with raw microalgae, the oils from the two-stage HTL process have a higher content of fatty acid. This might be due to the fact that the lipid in pre-treated microalgae was easier to be extracted, thereby improving the bio-crude oil yield as well (Fig. 4.3). Large amounts of nitrogen-containing compounds were also detected in all oil samples, such as cyclo(valylvalyl) (RT. 9.17) and 2,5-Piperazinedione, 3-methyl-6-(phenylmethyl)- (RT. 11.09), as similarly reported by Ross et al. (2010) and Gai et al. (2014). The bio-crude oils from the pre-treated microalgae contain a lower concentration of nitrogen-containing compounds than that in the oils obtained from raw microalgae, which is in a good agreement with the results of elemental analysis (Table 4.1). Besides, the amides were identified in the bio-crude oils, which could result from the substitution reactions among fatty acids and ammonia (Garcia Alba et al., 2015). Fig. 4.4 indicates that the oil products from the two-stage HTL process with the pre-treated microalgae had a relatively higher fraction of cyclic oxygenates or aromatics (e.g. biphenyl). In contrast, bio-crude oils from the single-stage HTL with raw microalgae contained a much higher content of oxygen-containing compounds (e.g., aldehydes, alcohols, esters, ethers, and ketones).

FT-IR spectra of bio-crude oils derived from both raw and pre-treated microalgae (with pre-cooled NaOH/urea solution) at 250°C for 10 min are displayed in Fig. 4.5. FT-IR analysis of the functional groups in the bio-crude oils may supplement the results obtained by GC-MS analysis (valid only for volatile chemical components). As can be seen in Fig. 4.5, the spectra of the two bio-crude oil samples are very similar. An absorption peak at 3200 cm^{-1} can be assigned to O-H or N-H stretching bonds (Peng et al., 2016). The peaks at 2924 cm^{-1} and 2856 cm^{-1} are ascribed to the C-H stretching vibration, suggesting the existence of alkyl C-H (Guo et al., 2015). A strong absorbance

at 1670 cm^{-1} can be attributed to the C=O stretching band in carbonyl groups, which is consistent with the ketones, aldehydes and fatty acids detected in the bio-crude oil via GC-MS analysis (Table 4.2) (Gai et al., 2014). Another peak at 1450 cm^{-1} could indicate the presence of C-H bending in the oils. The peak at 736 cm^{-1} can be related to the C-H bending from aromatics and their derivatives, some of which were identified by GC-MS (Table 4.2), such as biphenyl and phenol, 2,2'-methylenebis[6-(1,1-dimethylethyl)-4-ethyl- (RT. 11.65).
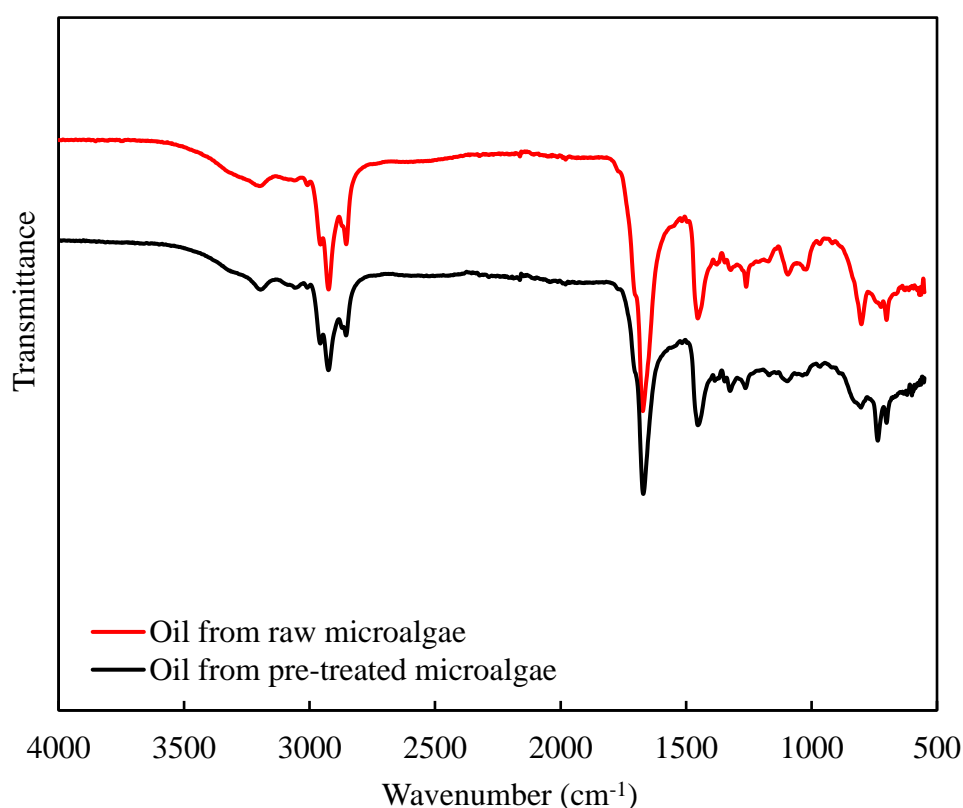
Figure 4-5: FT-IR spectra of bio-crude oils obtained from HTL of microalgae at 250 °C for 10 min.

On the other hand, the solid residues (or bio-chars) obtained from the pyrolysis or HTL of microalgae could be used as soil fertilizers for soil amelioration or solid fuels as they contain alkali ash, carbon and nitrogen (Bird et al.,2011). The proximate and ultimate analyses of the solid residue derived from raw and the pre-treated microalgae (with pre-

cooled NaOH/urea solution) at 250 °C for 10 min are displayed in Table 4.2. Owing to the reduced ash content in the microalgae pre-treatment the two-stage HTL process resulted in a solid residue with an ash content much lower than that of the single-stage HTL process. In general, the solid residues from microalgae HTL contain significant amounts of carbon, hydrogen, and nitrogen, as well as a high energy content (HHVs 28 ~30 MJ/kg), making them a potential solid fuel for energy production or a soil conditioner.

Table 4-2: Properties of solid residue (SR) derived from the raw and pretreated microalgae at 250 °C for 10 min.

	SR from the pre-treated microalgae	SR from raw microalgae
Ash (wt.%, dry basis)	1.34	4.09
Ultimate analysis (wt.%, dry basis)		
C	61.89	59.90
H	8.58	7.96
O[a]	20.16	19.98
N	7.85	7.96
S	0.18	0.11
HHV (MJ/kg)[b]	29.57	28.05

[a] Determined by difference; [b] Calculated by Dulong equation (Eq. 4-4).

4.5   Conclusions

In this study, a two-stage HTL process involving pre-treatment of the feedstock with a pre-cooled NaOH/urea solution was investigated for microalgae liquefaction. The pre-treated microalgae resulted in higher yields of bio-crude oils with a better quality with respect to higher energy contents and reduced nitrogen and oxygen contents, when compared with those obtained from the single-stage HTL process. The solid residues from microalgae HTL contain significant amounts of carbon, hydrogen, and nitrogen, as

well as a high energy content (HHVs 28 ~30 MJ/kg), making them a potential solid fuel for energy production or a soil conditioner.

4.6   References

Anastasakis K, Ross AB. Hydrothermal liquefaction of the brown macro-alga Laminaria Saccharina: Effect of reaction conditions on product distribution and composition. Bioresour Technol 2011; 102: 4876-4883.

Bird MI, Wurster CM, de Paula Silva PH, Bass AM, de Nys R. Algal biochar – production and properties. Bioresour Technol 2011; 102: 1886-1891.

Biller P, Ross AB. Potential yields and properties of oil from the hydrothermal liquefaction of microalgae with different biochemical content. Bioresour Technol 2011; 102: 215-225.

Bligh EG, Dyer WJ. A rapid method of total lipid extraction and purification. Can J Biochem Physiol 1956; 37: 911-917.

Becker EW. Microalgae: Biotechnology and Microbiology. Cambridge: Cambridge University Press; 1994.

Barreiro DL, Prins W, Ronsse F, Brilman W. Hydrothermal liquefaction (HTL) of microalgae for biofuel production: state of the art review and future prospects. Biomass Bioenergy 2013; 53: 113-127.

Changi SM, Faeth JL, Mo N, Savage PE. Hydrothermal reactions of biomolecules relevant for microalgae liquefaction. Ind Eng Chem Res 2015; 54: 11733-11758.

Cai J, Zhang L. Rapid dissolution of cellulose in LiOH/urea and NaOH/urea aqueous solutions. Macromol Biosci 2005; 5: 539-548.

Channiwala SA, Parikh PP. A unified correlation for estimating HHV of solid, liquid, and gaseous fuels. Fuel 2002; 81: 1051-1063.

Duan P, Savage PE. Upgrading of crude algal bio-oil in supercritical water. Bioresour Technol 2011; 102: 1899-1906.

DuBois M, Gilles KA, Hamilton JK, Rebers PA, Smith F. Colorimetric method for determination of sugars and related substances. Anal Chem 1956; 28: 350-356.

Garcia Alba L, Torri C, Samori C, Spek vd JJ, Fabbri D, Kersten SRA, Brilman DWF. Hydrothermal treatment (HTT) of microalgae: evaluation of the process as

conversion method in an algae biorefinery concept. Energy Fuels 2012; 26: 642-657.

Gai C, Zhang YH, Chen WT, Zhang P, Dong YP. Energy and nutrient recovery efficiencies in biocrude oil produced via hydrothermal liquefaction of *Chlorella pyrenoidosa*. RSC Adv 2014; 4: 16958-16967.

Guo QJ, Wu M, Wang K, Zhang L, Xu XF. Catalytic hydrodeoxygenation of algae bio-oil over bimetallic Ni-Cu/ZrO$_2$ catalysts. Ind Eng Chem Res 2014; 54: 890-899.

Guo Y, Yeh T, Song WH, Xu DH, Wang SZ. A review of bio-oil production from hydrothermal liquefaction of algae. Renew Sustainable Energy Rev 2015; 48: 776-790.

Guo Y, Song WH, Lu JM, Ma QR, Xu DH, Wang SZ. Hydrothermal liquefaction of cyanophyta: Evaluation of potential bio-crude oil production and component analysis. Algal Res 2015; 11: 242-247.

Jena U, Das KC, Kastner JR. Effect of operation conditions of thermochemical liquefaction on biocrude production from *Spirulina platensis*. Bioresour Technol 2011; 102: 6221-6229.

Jazrawi C, Biller P, He Y, Montoya A, Ross AB, Maschmeyer T, Haynes BS. Two-stage hydrothermal liquefaction of a high-protein microalgae. Algal Res 2015; 8: 15-22.

Liu HM, Wang FY, Liu YL. Alkaline pretreatment and hydrothermal liquefaction of cypress for high yield of bio-oil production. J Anal Appl Pyrolysis 2014; 108: 136-142.

Mao Y, Zhang L, Cai J, Zhou JP, Kondo T. Effects of coagulation conditions on properties of multifilament fibers based on dissolution of cellulose in NaOH/Urea aqueous solution. Ind Eng Chem Res. 2008; 47: 8676-8683.

Peng XW, Ma XQ, Lin YS, Wang XS, Zhang XS, Yang C. Effect of process parameters on solvolysis liquefaction of *Chlorella pyrenoidosa* in ethanol – water system and energy evaluation. Energy Convers Manag 2016; 117: 43-53.

Ross AB, Biller P, Kubacki ML, Li H, Lea-Langton A, Jones JM. Hydrothermal processing of microalgae using alkali and organics acids. Fuel 2010; 89: 2234-2243.

Yu G. Hydrothermal liquefaction of low-lipid microalgae to produce bio-crude oil. PhD Dissertation. Department of Agriculture and Biological Engineering. University of Illinois at Urban-Champaign 2012.

Yu G, Zhang YH, Guo B, Funk T, Schideman L. Nutrient flows and quality of bio-crude oil produced via catalytic hydrothermal liquefaction of low-lipid microalgae. Bioenergy Res 2014; 7: 1317-1328.

Zhou JP, Qin Y, Liu SL, Zhang L. Homogenous synthesis of hydroxyethylcellulose in NaOH/urea aqueous solution. Macromol Biosci 2006; 6: 84-89.

Zhao YL, Wang Y, Zhu JY, Ragauskas A, Deng YL. Enhanced enzymatic hydrolysis of spruce by alkaline pretreatment at low temperature. Biotechnol Bioeng 2008; 99: 1320-1328.

Chapter 5

5 Investigation of aqueous phase recycling for improving bio-crude oil yield in hydrothermal liquefaction of algae

The information presented in this Chapter is based on the paper "Investigation of aqueous phase recycling for improving bio-crude oil yield in hydrothermal liquefaction of algae", which is published in Bioresource Technology, 2017, Vol. 239, pages 151-159. The sections in Chapter 5 present the results towards the completion of objective 3 of this PhD project (see Section 1.2).

5.1 Abstract

In this study, the aqueous phase obtained from catalytic/non-catalytic hydrothermal liquefaction (HTL) of *Chlorella vulgaris* was recycled as the reaction medium with an aim to reduce water consumption and increase bio-crude oil yield. Although both Na_2CO_3 and HCOOH catalysts have been reported to be effective for promoting biomass conversion, the bio-crude oil yield obtained from HTL with Na_2CO_3 (11.5 wt.%) was lower than that obtained from non-catalytic HTL in pure water at 275 ºC for 50 min. While, the HCOOH led to almost the same bio-crude yield from HTL (29.4 wt.%). Interestingly, the bio-crude oil yield obtained from non-catalytic or catalytic HTL in recycled aqueous phase was much higher than that obtained from HTL in pure water. Recycling aqueous phase obtained from catalytic HTL experiments resulted in a sharp increase in the bio-crude oil yield by 32.6 wt.% (Na_2CO_3-HTL) and 16.1wt.% (HCOOH-HTL), respectively.

5.2 Introduction

Algal biomass has been considered as promising feedstocks for the production of renewable and environmentally friendly transport fuels (Yang et al., 2014). The advantages of algal biomass over conventional lignocellulosic biomass such as agro-forest residues include fast growth rates (Zou et al., 2010) and high photosynthetic

efficiencies (Biller and Ross, 2011). Furthermore, algal biomass can be cultivated in either waste water or sea without competing with food production (Peng et al., 2016). Pyrolysis and hydrothermal liquefaction (HTL) are two dominant techniques converting biomass into liquid biofuels (Jena et al., 2012). In comparison, HTL is more suitable for biomass with high moisture content due to the elimination of the feedstock drying step (Biller and Ross, 2011). Moreover, the oil products produced from HTL generally have higher energy content and better stability properties than pyrolysis oil (Barreiro et al., 2013).

To date, extensive research on HTL has been conducted in the water at 200-350 ℃ for 5-60 min with or without the presence of a catalyst (Brown et al., 2010). It has been found that when temperature elevates from 25 °C to 350 °C, the ionic product (K_w) of water increases from 10^{-14} to 10^{-12} (Toor et al., 2011). The resulting high levels of H^+ and OH^- could promote the acid and base-catalyzed hydrolysis reactions (Gai et al., 2014). Meanwhile, the dielectric constant of water decreases, rendering the water molecular more affinitive to organic compounds (Peng et al., 2016). However, two major challenges for algal HTL still exist ahead: (i) large amounts of processing water as a co-product that requires additional treatments before discharging into the environment (Zhu et al., 2015); (ii) algae-based bio-crude oil requires further upgrading due to the higher contents of heteroatoms (e.g., N, O, and S) (Guo et al., 2015).

To address the problems above, several studies have been carried out with recycled aqueous phase as the growth medium for algae cultivation due to its high content of C, N, and P. For instance, Jena et al. (2011a) found that microalgae can grow in the recycled aqueous phase from HTL of *Spirulina*, but heavy dilution was necessary to reduce the inhibitory effects of phenol and nickel. Alternatively, the recycled aqueous phase can be introduced back into the HTL system for improving bio-crude oil yield. Zhu et al. (2015) found that the bio-crude oil yield from HTL of barley straw slightly increased from 34.9 wt.% to 38.4 wt.% after three rounds of aqueous phase recycle. In another study, the bio-

crude oil yield from HTL of dried distillers grains with solubles (DDGS) was increased by recycling aqueous phase for up to nine cycles (Biller et al., 2016).

Apart from aqueous phase recycling, numerous homogenous catalysts (including alkali and organic acids) have been used to improve algal HTL process in terms of bio-crude oil yield and quality. By far, the most employed catalyst for HTL is Na_2CO_3 (Jena et al., 2012; Ross et al., 2010; Shakya et al., 2015; Zhou et al., 2010), and the catalytic mechanism involves a series of reactions (Fang et al., 2004). One of its important catalytic effects on HTL is the formation of reducing gas, H_2, which could promote biomass liquefaction by stabilizing the fragmented intermediates and preventing condensation, cyclization, and repolymerization of the free radicals, leading to a higher yield of oil and reduced char formation (Akhtar and Amin, 2011). Also, some studies showed that organic acids have demonstrated positive roles on algal HTL. Ross et al. (2010) found that the use of organic acids (including HCOOH and CH_3COOH) resulted in a higher yield of bio-crude oil with an improved flow property, compared to the use of alkali catalysts (including Na_2CO_3 and KOH). The mechanism of organic acids in biomass liquefaction involves the decomposition of HCOOH and CH_3COOH to form in-situ H_2 and CO, the in-situ H_2 can serve as a hydrogen donor to enhance oil yield and quality. The oxygen content present in the biomass can be removed by water formation (Guo et al., 2015). However, to the best of our knowledge, there was a limited extent of literature relating to algal liquefaction using organic acid catalysts (Yang et al., 2014). Although most homogenous catalysts have positive effects on algal HTL, the processes can only be economically viable if the aqueous phase and the catalysts can be reused (Guo et al., 2015). Moreover, the aqueous phase recycling has been regarded as a necessity for industrial applications of HTL technology (Biller et al., 2016).

In this present work, the aqueous phases obtained from both catalytic and non-catalytic HTL were recycled as the reaction medium with an aim to improve oil yield and reduce water consumption. Effects of aqueous phase recycling on products distribution and bio-crude oil properties were investigated. As indicated in the literature, glycerol and acetic

acid were commonly identified in the aqueous phase from algal HTL (Yang et al., 2014; Zhou et al., 2010). Several studies have demonstrated that the glycerol could be used as a co-solvent to facilitate liquefaction process for lignocellulosic biomass (Cao et al., 2016; Pedersen et al., 2015). Therefore, effects of glycerol and acetic acid on products distribution and bio-crude oil properties were also investigated in order to elucidate the possible roles of the recycled aqueous phase in the algal HTL.

5.3   Materials and methods

5.3.1.1   Materials

C. vulgaris was obtained from a health-food store (PureBulk, Inc, Roseburg, USA) and received as fine powder. The reagent grade dichloromethane (DCM), HCOOH, CH_3COOH, and glycerol were purchased from Caledon Laboratories Ltd (Georgetown, Canada), and the Na_2CO_3 was purchased from EMD Millipore (Massachusetts, USA). All chemicals were used as received.

5.3.2   HTL process and products separation

5.3.2.1   HTL in pure water

HTL was performed in a 100 mL stainless steel autoclave reactor (Parr 4590, Parr Instrument Co, Illinois, USA). Temperature inside the reactor was measured by a Type J thermocouple, and pressure in the reactor was monitored with a pressure gage installed on the top of the reactor. In a typical non-catalytic HTL run, the reactor was loaded with ~5.0 g of microalgae (on a dry basis) and ~25.0 g of water at a solid/water ratio of 1:5 (w/w). In the case of catalytic HTL process, the reactor was charged with ~5.0 g of microalgae and ~25.0 g of water containing either 5 wt.% Na_2CO_3 or HCOOH. After the loading, the reactor was sealed and flushed with nitrogen for three times to remove the residual air inside. After that, pure nitrogen at 0.69 MPa was purged into the reactor to prevent the mixed reaction medium from boiling during the heating process. The stirring speed was set at ~300 rpm throughout the liquefaction process. The reactor was then heated up to the pre-set temperature of 225-275 ºC with a heating rate of ~5 ºC/min, and

maintained at the pre-set temperature for 10-50 min. At the end of the reaction, the reactor was rapidly cooled to room temperature in a water bath.

5.3.2.2   Products separation

After the reactor was cooled to room temperature, gases in the reactor were vented through a control valve into a fume hood. Since gaseous products (mainly CO_2) yield was very low (3~5 wt.%) according to our preliminary tests, gas fraction was thus not collected and analyzed in this study. Afterward, the reactor was opened and the reaction mixture was washed out with DCM and carefully transferred to a 500 mL beaker, followed by rinsing the reactor walls and the stirrer with DCM twice. The solid residue in the mixture was then separated by vacuum filtration. The solids recovered on the filter paper were dried in an oven at 105 °C for 24 h. After that, the filtrate was transferred to a separatory funnel and allow to stand for 30 min for phase separation. The DCM soluble fraction (bottom phase) was transferred into a 500 mL round bottle flask and evaporated at 45 ℃ under reduced pressure to remove DCM, resulting in bio-crude oil products. The aqueous phase fraction (top phase) was filtered to remove undissolved materials and stored in a fridge for the subsequent recycling studies. Meanwhile, approximately 1 mL of the aqueous phase was sampled for GC-MS analysis. All HTL experiments either in recycled aqueous phase or in pure water were performed in triplicate to demonstrate the acceptable reproducibility. As explained above, the aqueous phase and gas products were lumped together and their yield was simply calculated by mass balance. The product yields of bio-crude oil and solid residue were calculated using Eq. (5-1).

Yield bio-crude oil/solid residue = (Weight of products (dry basis))/(Weight of biomass (dry basis)) ×100%   (5-1)

5.3.2.3   HTL in recycled aqueous phase

The maximum bio-crude oil yield from non-catalytic HTL in pure water was selected as the baseline experiment for aqueous phase recycling studies. As indicated later in the Section 5.3, the maximum bio-crude oil yield was obtained at 275 °C for 50 min, with a

solid/liquid ratio of 1:5 (w/w). These reaction parameters were applied for the HTL in recycled aqueous phase. For non-catalytic HTL recycling studies, the aqueous phase obtained from the baseline experiment (non-catalytic HTL in pure water) was used as the reaction medium for the first recycling experiment (Recycle-1), and so on for the subsequent recycling tests (Recycle-2 and Recycle-3). No more than three recycling runs were carried out because the aqueous phase almost reaches saturation point at end of the third round, which is explained later in the Section 5.4.2.2. In the case of catalytic HTL recycling studies, a similar procedure was employed expect for using the aqueous phase produced from catalytic HTL with Na_2CO_3 or HCOOH. Since this present study aims to determine the feasibility for reusing aqueous phase as the reaction medium, only one round of recycle was performed in the catalytic HTL recycling studies. Besides, no additional catalysts were used.

5.3.3   Analysis

5.3.3.1   Feedstock

The moisture content was determined by drying the sample in an oven at 105 ºC for 24 h. The ash content was determined by combusting the dry sample in a muffle furnace at 550 ºC in air for at least 3 h until reaching a constant weight. The lipid content was determined by the Bligh and Dyer method (Bligh and Dyer, 1956). The protein content was estimated by $6.25 \times$ wt.% N (Rebolloso-Fuentes et al., 2001). The carbohydrates content was determined by the phenol-sulfuric acid method (DuBois et al., 1956). From the above analysis, content of moisture, ash, lipid, protein and carbohydrates was 4.30 wt.%, 7.13 wt.%, 12.99 wt.%, 61.13 wt.%, and 16.10 wt.%, respectively. The mass balance cannot reach 100% here due to the experimental errors and unavoidable mass loss during sample transfer. The ultimate analysis of feedstock was performed by Chemistry Department of Lakehead University (Ontario, Canada), and the reported values are an average of three measurements. The elemental composition on a dry basis was as follows: 51.50 wt.% C, 7.67 wt.% H, 9.78 wt.% N, 0.50 wt.% S, and 23.42 wt.% O (calculated by difference, %O = 100% - %C - %H - %N -%S - %Ash). The higher

heating value (HHV) was calculated according to the Dulong equation (Eq. 5-2) (Channiwala and Parikh, 2002):

$$HHV \text{ (MJ/kg)} = 0.338 \times C + 1.428 \times (H - O/8) \qquad (5\text{-}2)$$

Where, C, H, and O were the weight percentages of carbon, hydrogen, and oxygen in the feedstock, respectively.

5.3.3.2 Liquefaction products

The functionality of bio-crude oil was determined by FT-IR analysis. A FT-IR Spectrometer (PerkinElmer, Massachusetts, USA) was employed to scan bio-crude oil samples over the wavelength range of 4000-550 cm^{-1} at the resolution of 4 cm^{-1}. The elemental composition and HHV of bio-crude oil were determined using similar methods as adopted for feedstock. The energy recovery (%) from feedstock into the bio-crude oil was calculated by Eq. 5-3 (Biller and Ross, 2011):

$$\text{Energy recovery (\%)} = \frac{HHV_{bio-crude\,oil} \times Weight_{bio-crude\,oil}}{HHV_{microalgae} \times Weight_{microalgae}} \times 100\% \qquad (5\text{-}3)$$

The chemical composition of bio-crude oil and aqueous phase was analyzed using an Agilent 7890 GC/5975 MS equipped with a HP-5MS capillary column (30 m $\times$ 0.25 mm id., 0.25 µm film thickness) (Agilent Technologies, California, USA). For each GC-MS run, 1 µL of sample was injected at 280 ℃ with a split ratio of 20:1. Helium was used as a carrier gas with a flow rate of 2.64 mL/min. The GC oven temperature was programed as follows: held at 60 ℃ for 2 min, then ramped to 280 ℃ with a heating rate of 20 ℃/ min, and held for 10 min. The volatile chemical compounds in the samples were identified using NIST (National Institute of Standards and Technology) database and reported qualitatively by % peak area.

5.4   Results and discussion

The non-catalytic HTL in pure water were conducted in the subcritical water at 225-275 ℃ for 10-50 min, with a solid/water ratio of 1:5 (w/w), and the resulting liquefaction

yields were summarized in Table 5.1. The bio-crude oil yield increased with the increased reaction severity (a higher temperature or longer residence time), but solid residue yield decreased. This trend was consistent with the previous studies (Brown et al., 2010; Shakya et al., 2015). A maximum bio-crude oil yield of 29.39 wt.% was obtained from non-catalytic HTL at 275 ºC for 50 min. Thus, temperature of 275 ºC and 50 min residence time were applied for the subsequent studies on catalytic HTL in pure water and aqueous phase recycling studies.

Table 5-1: Liquefaction yields (average value ± standard deviation) obtained from HTL of *C. vulgaris* in pure water without catalyst.

Reaction conditions		Liquefaction yields (wt.%)	
Temperature (ºC)	Residence time (min)	Bio-crude oil	Solid residue
	10	10.50 ± 0.49	32.63 ± 1.53
225	30	13.21 ± 0.52	26.97 ± 2.42
	50	13.82 ± 1.79	30.07 ± 4.71
	10	18.36 ± 0.75	27.95 ± 0.79
250	30	22.86 ± 3.04	25.48 ± 1.26
	50	27.83 ± 0.13	21.72 ± 2.16
	10	22.48 ± 3.41	16.98 ± 0.38
275	30	29.21 ± 0.94	16.23 ± 1.03
	50	29.39 ± 3.80	17.60 ± 3.07

5.4.1   Effects of catalysts

5.4.1.1   Products distribution

Effects of catalysts on products distribution from HTL of *C. vulgaris* in pure water at 275 ºC for 50 min are displayed in Fig. 5.1. The yield of bio-crude oil obtained with Na_2CO_3 was much lower that obtained from non-catalytic HTL, which was in a good agreement with the results previously reported by Biller and Ross (2011). This was due to the fact that carbohydrates tend to decompose into C_2-C_5 carboxylic acids (e.g., acetic and lactic acids) under alkaline conditions. These water-solubles acids are preferable to partition into the water phase and therefore do not contribute to bio-crude oil formation. Meanwhile, the use of Na_2CO_3 during HTL reduced solid residue yield from 17.60 wt.% to 6.41 wt.%.
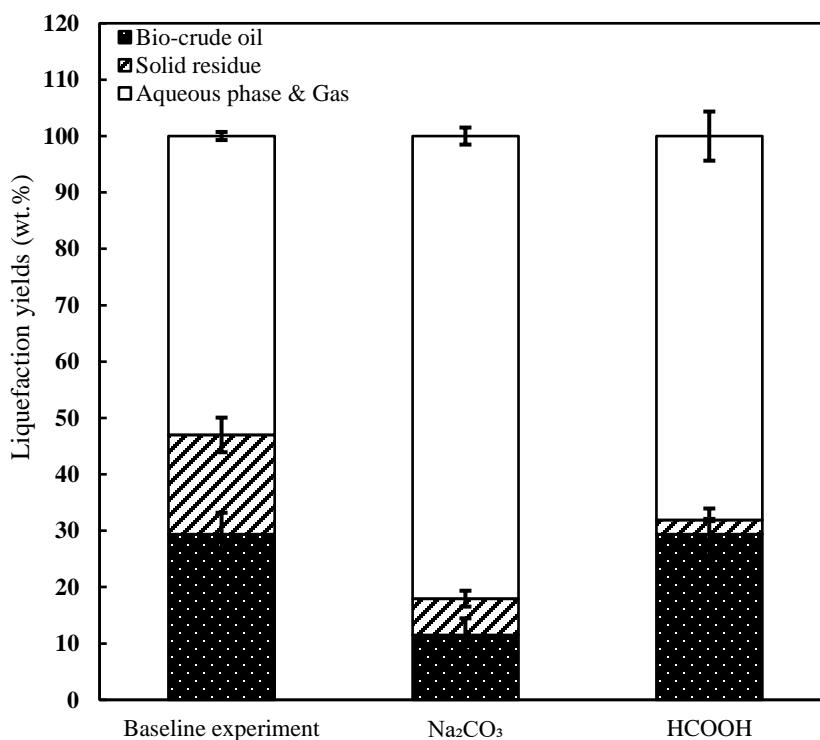
Figure 5-1: Effects of catalysts on products distribution at 275 °C for 50 min.

As for the effect of HCOOH on product distribution from HTL, the bio-crude oil yield was almost the same as that from baseline experiment. In contrast, the solid residue yield decreased markedly from 17.60 wt.% to 2.52 wt.% after adding HCOOH to HTL system. As indicated in the literature, the carbohydrates under acidic conditions could form 5-hydroxymethylfurfural (5-HMF) and levulinic acid, which are considered as the precursors of bio-crude oil (Yin and Tan, 2012). On the other side, the organic acid could facilitate the protein decomposition into amino acids, and the amino acids can be further converted into aqueous ammonia and other water-soluble compounds (Abdelmoez et al., 2007). Since feedstock applied in this study contains more than 60 wt.% of protein but only approx. 16 wt.% of carbohydrates, the positive effect of HCOOH on bio-crude oil production from carbohydrates could be outweighed by its negative impact on oil formation from protein. From the liquefaction results above it can be concluded that neither alkaline catalysts nor organic acids are favorable for liquefying high-protein containing biomass.

5.4.1.2   Elemental composition of bio-crude oil

The elemental composition of bio-crude oil obtained from catalytic/non-catalytic HTL at 275 °C for 50 min is presented in Table 5.2. The bio-crude oil obtained with HCCOH had slightly higher carbon and hydrogen contents, but lower oxygen content, when compared with non-catalytic HTL. This was likely due to the de-hydration/hydro-de-oxygenation effects of HCOOH as a hydrogen donor solvent on removing oxygen via water formation (Akhtar and Amin, 2011). In contrast, the bio-crude oil obtained with Na_2CO_3 had lower carbon and hydrogen contents, but higher oxygen content. This increase in the oxygen content could be due to the alkaline-promoted Maillard reaction between reducing sugars and amino acids to form oxygenated oil compounds. Besides, the nitrogen content in all bio-crude oils obtained from catalytic HTL was lower compared to that obtained from non-catalytic HTL. However, it should be noted that the nitrogen content in the bio-crude oil was still much higher than that of petroleum crude oil (0-0.8 wt.%) (Shakya et al., 2015). Thus, the subsequent upgrading (e.g., hydro-treatment and cracking) is necessary for the applications of algal bio-crude oils for drop-in fuels. The sulfur content in all bio-crude oil samples was lower than 1 wt.%, lower than that of petroleum crude oils (0-3 wt.%) (Shakya et al., 2015). As also shown in Table 5.2, HHVs of the bio-crude oils obtained from HTL with HCOOH was 36.03 MJ/kg, higher than that of the bio-crude oil obtained from non-catalytic HTL (HHV 33.87 MJ/kg) or that from Na_2CO_3 catalyzed HTL (HHV 31.80 MJ/kg).

Table 5-2: Elemental composition of bio-crude oils obtained from HTL of *C. vulgaris* in pure water at 275 ºC for 50 min with or without catalyst.

Elemental compositions (wt.%)	Baseline experiment [a]	Na_2CO_3	HCOOH
C	69.61	68.21	71.47
H	8.89	8.34	9.73
O [b]	13.20	17.71	11.31
N	8.20	5.62	7.49
S	0.10	0.12	0
HHV (MJ/kg) [c]	33.87	31.80	36.03

[a] The baseline experiment was performed in pure water at 275 °C for 50 min without catalyst; [b] The amount of oxygen was determined by difference (%O = 100% - %C - %H - %N -%S); [c] The HHV was calculated by Dulong equation given in Eqn. (5-2).

5.4.2   Effect of aqueous phase recycling

5.4.2.1   Products distribution

The liquefaction yields obtained from catalytic and non-catalytic HTL of *C. vulgaris* with and without recycled aqueous phase are displayed in Fig. 5.2. In general, HTL in recycled aqueous phase resulted in a higher bio-crude oil yield, which might be attributed to the transformation of some reactive compounds in the aqueous phase into the oily phase. The possible roles of the recycled aqueous phase in promoting bio-crude oil formation during HTL process was discussed later in the Section 5.3 and 5.4. As for non-catalytic HTL in recycled aqueous phase, the bio-crude oil yield gradually increased from 29.39 wt.% (baseline experiment in pure water) to 38.87 wt.% upon recycling of aqueous phase for three times. At the same time, the solid residue yield increased from 17.60 wt.% to 22.59 wt.% after using two cycles of aqueous phase, while, in contrast, the solid residue decreased to 17.01 wt.% from HTL in the third recycled aqueous phase. As also shown in Fig. 5.2, HTL in recycled aqueous phase obtained from Na_2CO_3-catalyzed HTL led to a sharp increase in the bio-crude oil yield from 11.54 wt.% (algal HTL with Na_2CO_3) to 44.10 wt.% (Recycle-Na_2CO_3), whereas, the solid residue yield was almost constant. Similarly, the bio-crude oil yield obtained with recycled aqueous phase from HCOOH-catalyzed HTL increased from 29.39 wt.% (algal HTL with HCOOH) to 45.46 wt.% (Recycle-HCOOH), along with an increase in the solid residue yield from 2.52 wt.% to 8.43 wt.%.
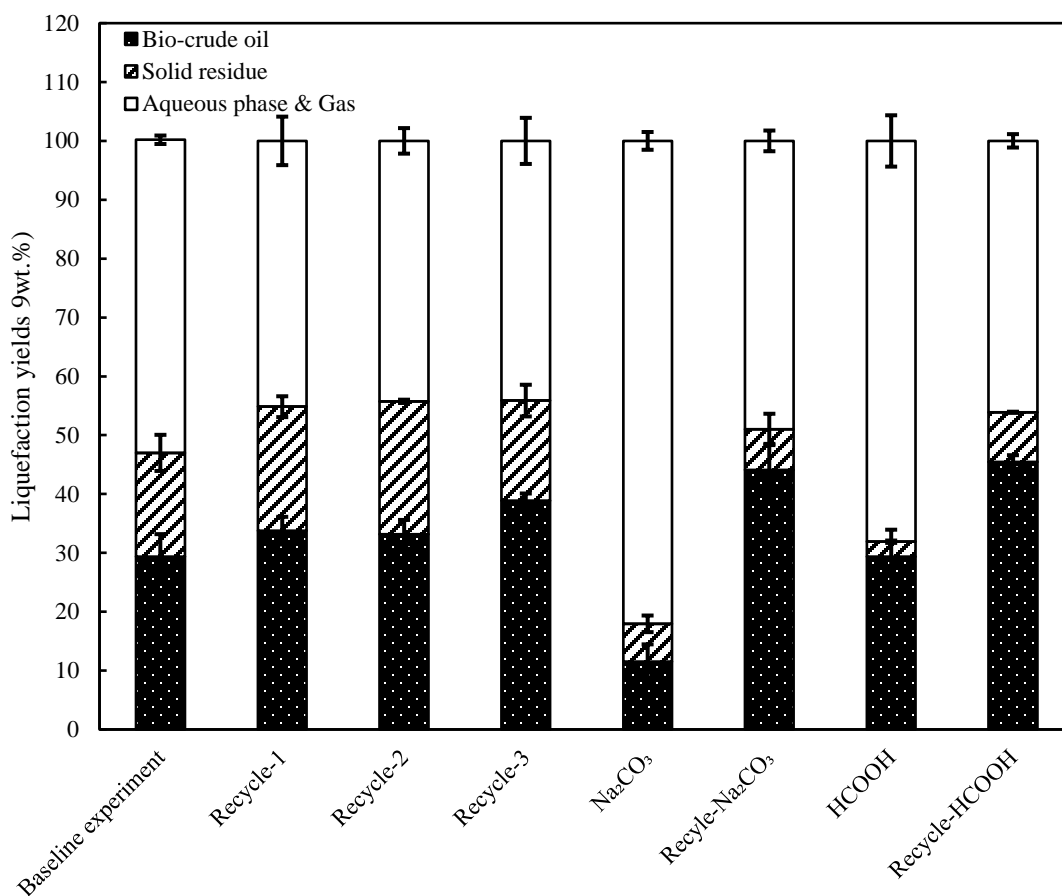
Figure 5-2: Liquefaction yields obtained from non-catalytic and catalytic HTL experiments with and without recycled aqueous phase at 275 ºC for 50 min.

5.4.2.2 Elemental composition of bio-crude oils

Effects of aqueous phase recycling on the elemental composition and energy content of the bio-crude oil along with its energy recovery are shown in Table 5.3. The aqueous phase recycling exerted a little effect on the elemental composition as well as energy content of the resulting bio-crude oil products. Besides, the HHVs of bio-crude oils obtained from algal HTL in recycled aqueous phase ranged from 31.37 MJ/kg to 35.61 MJ/kg, which was comparable to that of the baseline HTL in pure water (33.87 MJ/kg). As also shown in Table 5.3, the aqueous phase recycling could lead to a much higher

energy recovery compared to the baseline HTL, which was probably due to the markedly increased bio-crude oil yield.

Table 5-3: Effects of aqueous phase recycling on the elemental composition and energy content of the bio-crude oils and the energy recovery in the oil products.

	C	H	O[b]	N	S	HHV (MJ/kg)[c]	Energy recovery (%)[d]
Baseline experiment [a]	69.61	8.89	13.20	8.20	0.10	33.87	41.13
Recyle-1	67.06	8.77	16.36	7.59	0.22	32.27	45.05
Recyle-2	65.57	8.68	17.85	7.66	0.24	31.37	42.99
Recycle-3	68.45	9.05	14.54	7.69	0.27	33.46	53.75
Recycle-Na_2CO_3	71.90	9.37	11.63	7.10	0	35.61	64.89
Recycle-HCOOH	70.87	9.23	12.29	7.61	0	34.94	65.64

[a] The baseline experiment was performed in pure water at 275 °C for 50 min without catalyst; [b] The amount of oxygen was determined by difference (% O = 100% - % C - % H - % N - % S); [c] The HHV (MJ/kg) of bio-crude oil was calculated by Dulong equation given in Eqn. (5-2); [d] The energy recovery (%) into the oil products was calculated by Eqn. (5-3).

5.4.3   Analysis of aqueous phase

5.4.3.1   Non-catalytic HTL

The major chemical compounds in the aqueous phase obtained from non-catalytic HTL before and after water phase recycling experiments are summarized in Appendix-C. The chemical compounds identified in the aqueous phase were categorized into organic acids, straight & branched amides, cyclic oxygenates, N-containing compounds, and other oxygenates (including esters, ketones, and alcohols), as displayed in Fig. 5.3. Numerous N-containing compounds can be observed in aqueous phase, which was due to the hydrolytic decomposition of protein (Zhou et al., 2010). Besides, some organic acids were also observed, which was in accordance with the results reported by Gai et al. (2015). Acetic acid has previously been reported to be an effective catalyst for algal HTL

leading to a higher bio-crude oil yield and better quality (Ross et al., 2010). As a result, the presence of acetic acid in the recycled aqueous phase may contribute to an increase in the bio-crude oil from water phase recycling studies. Glycerol that originates from triglyceride (the algal lipid) via hydrolysis (Toor et al., 2011) was also detected in the aqueous phase. Effects of acetic acid and glycerol on algal HTL were later discussed.
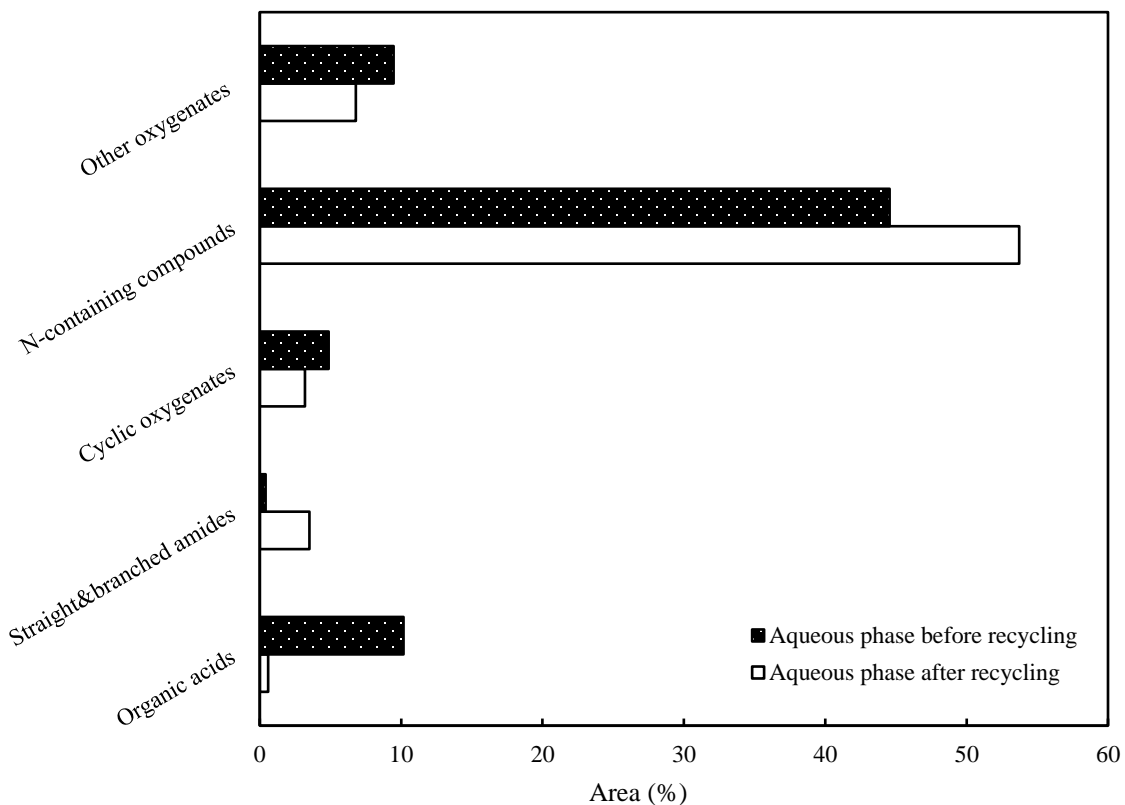
Figure 5-3: The major compounds in the aqueous phase obtained before and after recycling at 275 °C for 50 min.

The color of aqueous phase became darker as a result of increased recycling times, as shown in Appendix-D. This could indicate the enrichment of the organic compounds in the aqueous phase. Although we did not quantify the compounds using internal/external standards, some changes in the relative peak areas to the total area were still visible. As shown in Fig. 5.3, some reductions in the relative peak areas (e.g., organic acids) can be observed, indicating the reduced concentration of some organic components in aqueous phase. This could be resulted from the fact that after several recycles, the concentration of

organic solutes increases, which could decrease the solubility of organic acids in the aqueous phase and thus contributes to oil formation. Meanwhile, the relative peak areas of N-containing compounds in bio-crude oil increase after HTL in recycled aqueous phase, which can be attributed to the Maillard reaction between amino acids and reducing sugars in the recycled aqueous phase. According to the study by Déniel et al. (2016), the Maillard products can act as scavengers of reactive intermediates, deterring the degradation of bio-crude oil into char and/or gas. This could be the reason for the slight decrease in the solid residue yield after three cycles (as shown in Fig. 5.2).

5.4.3.2   Catalytic HTL

The major chemical compounds in the aqueous phase obtained from HTL with Na_2CO_3 or HCOOH are presented in Table 5.4. Phytol (a long carbon-chain alcohol, $C_{20}H_{40}O$) was detected in the aqueous phase obtained from HTL with Na_2CO_3. The presence of phytol in the recycled aqueous phase may lead to the formation of bio-crude oil products (e.g., isophytol, phytene, and phytane) (Changi et al., 2012), when employing this aqueous phase as the reaction medium for algal HTL. Another possible role of the recycled aqueous phase from algal HTL with Na_2CO_3 can be related to the decreased solubility of organic chemicals due to the "salting out" effect, and the organic chemicals flow into bio-crude oil stream and thus bio-crude oil yield increases (Fig. 5.2). In general, some compounds of environmental concerns can be detected in all aqueous phase samples above, such as 2-pyrrolidinone and 3-pyridinol, 6-methyl-. Thus, the downstream wastewater treatments are required before the aqueous phase can be safely discharged into the environment (Gai et al., 2015).

Table 5-4: The major compounds in the aqueous phase obtained with Na_2CO_3 or HCOOH at 275 °C for 50 min.

RT (min)[a]	Compounds in aqueous phase	Area (%)	
		Na_2CO_3	HCOOH
3.52	1,5-Pentanediol		2.93
6.78	7H-Dibenzo[b,g]carbazole, 7-methyl	7.53	
9.04	Acetic acid		2.42
9.22	Pyridine, 5-ethyl-2-methyl-	4.10	
9.89	Glycerol		27.54
9.94	Threitol		4.97
10.04	Isovaleraldehyde		4.00
10.39	5H-1-Pyrindine, 6,7-dihydro-	1.40	
10.45	2-Cyclopenten-1-one, 3-ethyl-2-hydro-		3.69
10.61	2-Pyrrolidinone		5.44
10.83	N-methyl-1,3-Propanediamine		9.85
11.16	3-Pyridinol, 6-methyl-		2.87
11.73	1-[2-(2,5-dimethyl-1H-pyrrol-1-yl)ethyl]piperazine		2.84
11.96	2-Cyclopropylaniline	3.11	
12.13	4-(2-Oxiranyl)-1-butanol		2.07
12.97	Indole	8.72	2.73
13.79	3,4-Dimethyl-2-hexanol		3.43
13.96	Ethanone, 1-(3-cycloocten-1-yl)-		1.72
14.06	Isopropyl 6-(4-ethoxyphenyl)-3-methyl-4-oxo-4,5,6,7-tetrahydro-1H-indole-2-carboxylate		2.65
15.11	2,4-Dimethylbenzo[h]quinoline		1.77
15.35	N,N-Dimethyl-4-nitroaniline		1.48
15.52	3,3-Dimethyl-4-methylamino-butan-2-one	10.60	

15.6	1-Naphthalenamine		1.30
15.68	Bicyclo[3.1.1]heptane, 2,6,6-trimethyl-, (1α,2β,5α)-	2.83	
16.01	6,6-Dimethyl-2-azaspiro[4.4]non-1-ene	3.48	
16.09	5-Methyl-2,3-dihydroimidazo[1,2-c]quinazoline	3.75	
16.19	3-(1,5-Dimethyl-hex-4-enyl)-2,2-dimethyl-cyclopent-3-enol	3.57	
16.56	Isophytol	4.41	
17.07	2-Ethylacridine		1.74
17.08	dl-Alanyl-l-leucine	10.22	
17.63	Phytol	28.66	
18.08	Butanamide	6.77	

[a] Represents retention time (min).

5.4.4   Effects of glycerol and acetic acid on algal HTL

As indicated above, glycerol and acetic acid can be identified in the recycled aqueous phase. Their promotion effects on algal HTL were investigated at 275 ºC for 50 min, with a solid/liquid ratio of 1:5 (w/w). The baseline conditions for most of the HTL experiments in this study were discussed previously, and contents in Table 5.5 were some key results. Table 5.5 shows that the bio-crude oils yield was lower when glycerol was added in water as the reaction medium, compared to those obtained from HTL in pure water. It is speculated that this may be due to the conversion of glycerol into water-soluble compounds rather to an oily phase during HTL (Toor et al., 2011). The chemical composition of aqueous phase obtained from glycerol-water co-solvent was determined by GC-MS analysis. The results indicated that n-hexadecanoic acid (commonly identified in the bio-crude oil) can be observed in the aqueous phase. This was likely due to the less polarity of glycerol/water mixture than pure water, leading to more organic compounds partition into aqueous phase. On the other hand, the solid residue yield from HTL in recycled aqueous phase was lower than that obtained from baseline HTL in pure water. This was possibly due to the fact that glycerol could lead to the formation of formic acid

and ethanol by C-C bond cleavage when subjected to hydrothermal condition (Pedersen et al., 2015). Formic acid and ethanol can further serve as a hydrogen donor and radical scavenger, prohibiting char formation (Guo et al., 2015). In addition, the nitrogen content in the bio-crude oil obtained from HTL in water/glycerol co-solvent was lower than that obtained from HTL in pure water, indicating the addition of glycerol promotes the de-nitrogenation of bio-crude oil. This could be due to the migration of high polar N-containing compounds into water phase in the presence of polar glycerol (Lu et al., 2017).

Table 5-5: Effects of glycerol and acetic acid on products distribution (average yield ± standard deviation) and elemental composition of the bio-crude oils.

|	Baseline experiment [a]	Glycerol to water ratio		Acetic acid addition	
		1:2 (v/v)	1:1 (v/v)	3 % (w/w)	5 % (w/w)
Bio-crude oil yield (wt.%)	29.39 ± 3.80	21.79 ± 2.28	23.64 ± 4.39	31.45 ± 1.21	40.99 ± 0.85
Solid residue yield (wt.%)	17.60 ± 3.07	13.62 ± 1.92	8.37 ± 1.56	10.65 ± 1.01	7.69 ± 0.31
Elemental composition of bio-crude oils (wt.%)					
C	69.61	66.82	57.27	-	68.51
H	8.89	9.42	9.21	-	9.10
O [b]	13.20	18.73	29.91	-	15.11
N	8.20	5.00	3.61	-	7.28
S	0.10	0.03	0.00	-	0.00
HHV (MJ/kg) [c]	33.87	32.69	27.17	-	33.45

[a] The baseline experiment was performed in pure water at 275 °C for 50 min without catalyst; [b] The amount of oxygen was determined by difference (% O = 100% - % C - % H - % N -% S); [c] The HHV (MJ/kg) of bio-crude oil was calculated by Dulong equation given in Eqn. (5-2).

However, HTL in acetic acid-water mixture medium improved the algal conversion and bio-crude oil yield, when compared with the baseline HTL in pure water. This was consistent with the previous study on HTL of *E. prolifera* (Yang et al., 2014). The increase in the bio-crude oil yield might be attributed to the reactions between acetic acids and alcohols and amino compounds to form esters and amides and eventually flow into bio-crude oil. The chemical composition of aqueous phase obtained from HTL in acetic acid/water co-solvent was determined by GC-MS analysis. Compared to baseline experiment, a higher relative peak area of acetamide was observed in the aqueous phase from HTL in acetic acid/water co-solvents, confirming the formation of acetamide through reaction between acetic acid and ammonia.

5.4.5   Chemical analysis of bio-crude oils

5.4.5.1   GC-MS analysis

The chemical compounds in the bio-crude oils obtained from non-catalytic HTL with and without recycled aqueous phase (i.e., Baseline experiment, Recycle-1, Recycle-2, and Recycle-3) were characterized by GC-MS, as presented in Appendix-E. It should be noted that some low molecular weight components could be lost during the solvent evaporation process for bio-crude oil recovery, while the high molecular weight compounds could not elute from the GC column. Thus, only part of the components in bio-crude oil can be characterized through GC-MS. During the analysis process, only the components with identification probability > 60 % were selected and analyzed. To ease discussion, chemical components in the bio-crude oils were categorized into five groups based on their functional groups, namely aromatics (e.g., monoaromatics and polyaromatics), fatty acids (e.g., saturated and unsaturated fatty acids), hydrocarbons (e.g., straight and branched hydrocarbons), other oxygenates (e.g., esters and ketones), and nitrogenates (e.g., indoles, pyrazines, and amines).

As illustrated in Fig. 5.4, no obvious differences can be observed among all four bio-crude oil samples in terms of their chemical compositions. A high fraction of nitrogenated compounds was observed in all the bio-crude oils, which can be attributed to

the high protein content (61.13 wt.%) in the feedstock biomass. Similar results were reported in the previous studies on algal HTL (Gai et al., 2014; Ross et al., 2010). Besides, saturated and unsaturated fatty acids such as n-hexadecenoic acid and 9,12-octadecadienoic acid (Z,Z)- can be detected in the bio-crude oils. Fatty acids can be directly produced from lipid hydrolysis (Shakya et al., 2015). Some straight and branched hydrocarbons were also identified in the bio-crude oils and hydrocarbons can be formed through fatty acids decarboxylation (Gai et al., 2014). Moreover, some aromatics (e.g., phenols and phenol derivatives) were also found in the oil products, and these aromatics could be produced from carbohydrates (Gai et al., 2014). In addition, a small fraction of other oxygenates was also observed in the bio-crude oil. These oxygenates might be yielded from the degradation of polysaccharide in algal feedstock via hydrolysis, dehydration, and cyclization (Yang et al., 2014).
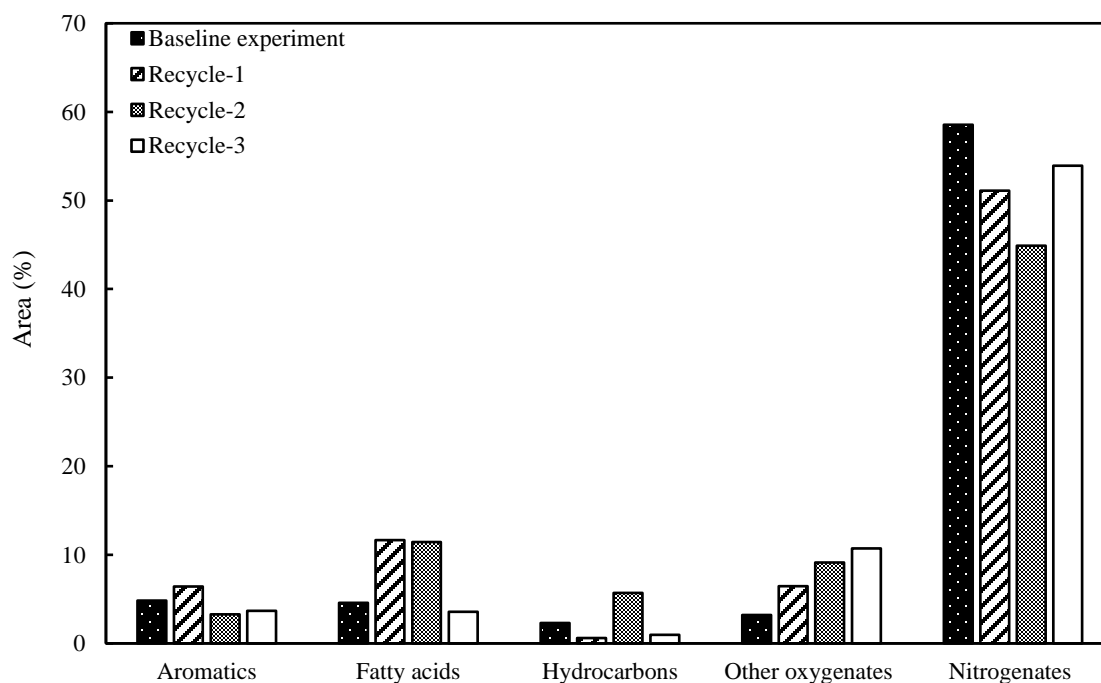
Figure 5-4: The major compounds in the bio-crude oils obtained from non-catalytic HTL with and without recycled aqueous phase at 275 °C for 50 min.

Although chemical components in all the bio-crude oils obtained from non-catalytic HTL with and without recycled aqueous phase, slight differences can be still identified. No fatty acid esters were detected in the bio-crude oils obtained from HTL in pure water, whereas fatty acid esters existed in the bio-crude oils obtained from non-catalytic algal HTL in recycled aqueous phase. Ammonia (weak base) is commonly observed in the aqueous phase, which may be attributed to the decomposition of protein (Shakya et al., 2015). Glycerol present in the aqueous phase can decompose into methanol during HTL (Bühler et al., 2002). As a result, the transesterification between fatty acids and methanol to form methyl ester like 8,11-octadecadienoic acid, methyl ester could take place.

5.4.5.2 FT-IR analysis

IR characteristics of bio-crude oils were consistent to the previous studies on algal HTL (Jena et al., 2011b; 2012; Zou et al., 2010). As shown in Fig. 5.5, all four bio-crude oil samples exhibited similar functionalities. The peak from 3600 cm^{-1} to 3100 cm^{-1} can be related to O-H or N-H stretching vibrations. The bands at 2940 cm^{-1}, 2924 cm^{-1}, and 2855 cm^{-1} were attributed to C-H stretching vibrations in methylene and methyl groups. A strong peak at 1670 cm^{-1} can be assigned to C=O stretching bands, which could exist in forms of ketones, aldehydes, or carboxylic acids in the bio-crude oils. The band at 1453 cm^{-1} may be attributed to C-H bending vibration from methyl groups. The peaks at 1262 cm^{-1}, 1169 cm^{-1}, 1070 cm^{-1}, and 968 cm^{-1} can be assigned to the presence of primary, secondary, and tertiary alcohols in the bio-crude oil samples. The peaks at 812 cm^{-1}, 734 cm^{-1}, and 701 cm^{-1} were ascribed to the C-H bending from aromatics and their derivatives.
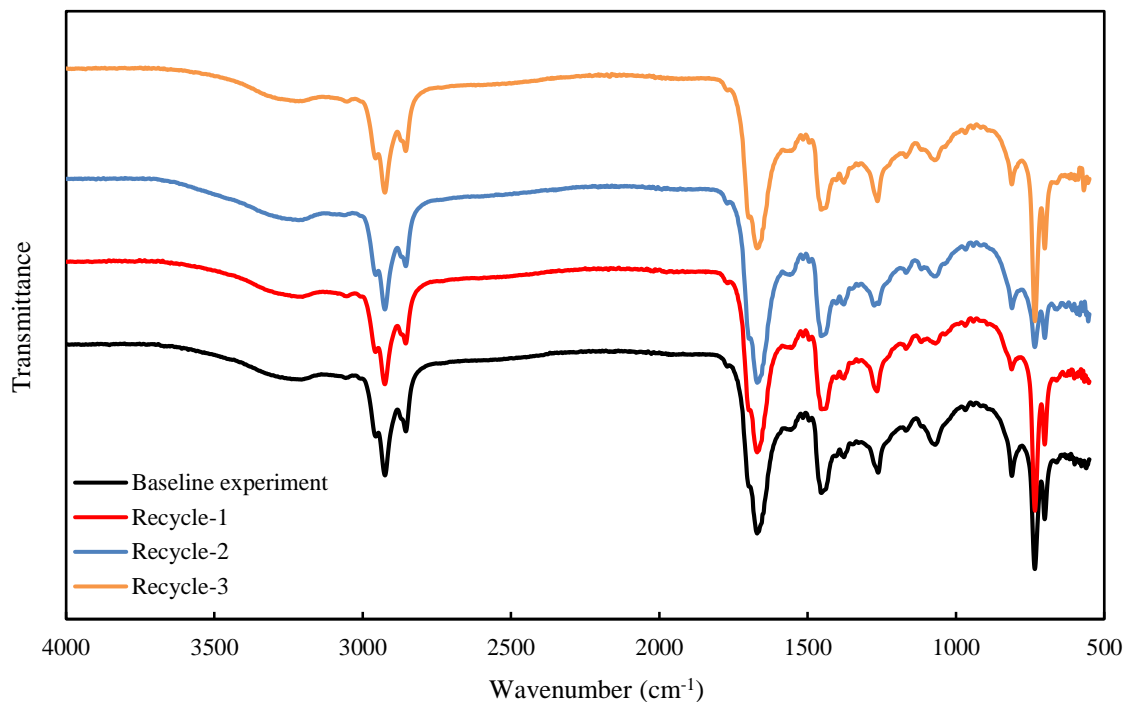
Figure 5-5: The FT-IR spectra of bio-crude oils obtained from non-catalytic HTL recycling studies.

5.5   Conclusions

HTL of *C. vulgaris* was performed with/without catalyst in this study. Although the two catalysts Na_2CO_3 and HCOOH did not exert positive effects on bio-crude oil yield, recycling the aqueous phase obtained from HTL especially from the catalytic algal HTL as the reaction medium in the subsequent HTL contributed to higher bio-crude oil yields. The bio-crude oil obtained from HTL in recycled aqueous phase had a comparable energy content with that obtained from HTL in pure water. Thus, the aqueous phase recycling not only improves the efficiency of biomass utilization without sacrificing oil quality, but also reduces waste generation.

5.6   References

Akhtar, J., Amin, N.A.S., 2011. A review on process conditions for optimum bio-oil yield in hydrothermal liquefaction of biomass. Renew. Sustainable. Energy. Rev. 15, 1615-1624.

Abdelmoez, W., Nakahasi, T., Yoshida, H., 2007. Amino acid transformation and decomposition in saturated subcritical water conditions. Ind. Eng. Chem. Res. 46, 5286-5294.

Barreiro, D.L., Prins, W., Ronsse, F., Brilman, W., 2013. Hydrothermal liquefaction (HTL) of microalgae for biofuel production: state of the art review and future prospects. Biomass. Bioenergy. 53. 113-127.

Biller, P., Ross, A.B., 2011. Potential yields and properties of oil from the hydrothermal liquefaction of microalgae with different biochemical content. Bioresour. Technol. 102, 215-225.

Biller, P., Madsen, R.B., Klemmer, M., Becker, J., Iversen, B.B., Glasius, M., 2016. Effect of hydrothermal liquefaction aqueous phase recycling on bio-crude yields and composition. Bioresour. Technol. 220, 190-199.

Bligh, E.G., Dyer, W.J., 1956. A rapid method of total lipid extraction and purification. Can. J. Biochem. Physiol. 37, 911-917.

Brown, T.M., Duan, P., Savage, P.E., 2010. Hydrothermal liquefaction and gasification of *Nannochloropsis sp*. Energy Fuels. 24, 3639-3646.

Bühler, W., Dinjus, E., Ederer, H.J., Kruse, A., Mas, C., 2002. Ionic reactions and pyrolysis of glycerol as competing reaction pathways in near- and supercritical water. J. Supercrit. Fluids. 22, 37-53.

Cao, L.C., Zhang, C., Hao, S.L., Luo, G., Zhang, S.C., Chen, J.M., 2016. Effect of glycerol as co-solvent on yields of bio-oil from rice straw through hydrothermal liquefaction. Bioresour. Technol. 220, 471-478.

Changi, S., Brown, T.M., Savage, P.E., 2012. Reaction kinetics and pathways for phytol in high-temperature water. Chem. Eng. J. 189-190, 336-345.

Channiwala, S.A., Parikh, P.P., 2002. A unified correlation for estimating HHV of solid, liquid, and gaseous fuels. Fuel. 81, 1051-1063.

Déniel, M., Haarlemmer, G., Roubaud, A., Weiss-Hortala, E., Fages, J., 2016. Bio-oil production from food processing residues: improving the bio-oil yield and quality by aqueous phase recycle in hydrothermal liquefaction of blackcurrant (Ribes nigrum L.) Pomace. Energy Fuels. 30, 4895-4904.

DuBois, M., Gilles, K.A., Hamilton, J.K., Rebers, P.A., Smith, F., 1956. Colorimetric method for determination of sugars and related substances. Anal. Chem. 28, 350-356.

Fang, Z., Minowa, T., Smith Jr, R.L., Ogi, T., Kozinski, J.A., 2004. Liquefaction and gasification of cellulose with Na_2CO_3 and Ni in subcritical water at 350 ºC. Ind. Eng. Chem. Res. 43, 2454-2463.

Guo, Y., Yeh, T., Song, W.H., Xu, D.H., Wang, S.Z., 2015. A review of bio-oil production from hydrothermal liquefaction of algae. Renew. Sustainable. Energy. Rev. 48, 776-790.

Gai, C., Zhang, Y.H., Chen, W.T., Zhou, Y., Schideman, L., Zhang, P., Tommaso, G., Kuo, C.T., Dong, Y.P., 2015. Characterization of aqueous phase from the hydrothermal liquefaction of *Chlorella pyrenoidosa*. Bioresour. Technol. 184, 328-335.

Gai C., Zhang Y.H., Chen W.T., Zhang P., Dong Y.P., 2014. Energy and nutrient recovery efficiencies in biocrude oil produced via hydrothermal liquefaction of *Chlorella pyrenoidosa*. Rsc. Adv. 4, 16958-16967.

Jena, U., Vaidyanathan, N., Chinnasamy, S., Das, K.C., 2011a. Evaluation of microalgae cultivation using recovered aqueous co-product from thermochemical liquefaction of algal biomass. Bioresour. Technol. 102, 3380-3387.

Jena, U., Das, K.C., Kastner, J.R., 2011b. Effect of operating conditions of thermochemical liquefaction on biocrude production from *Spirulina platensis*. Bioresour Technol. 102, 6221-6229.

Jena, U., Das, K.S., Kastner, J.R., 2012. Comparison of the effects of Na_2CO_3, $Ca_3(PO_4)_2$, and NiO catalysts on the thermochemical liquefaction of microalga *Spirulina platensis*. Appl. Energy. 98, 368-375.

Lu, J.W., Liu, Z.D., Zhang, Y.H., Li, B.M., Lu, Q., Ma, Y.Q., Shen, R.X., Zhu, Z.B., 2017. Improved production and quality of biocrude oil from low-lipid high-ash macroalgae *Enteromorpha prolifera* via addition of crude glycerol. J. Clean. Prod. 142, 749-757.

Peng, X.W., Ma, X.Q., Lin, Y.S., Wang, X.S., Zhang, X.S., Yang, C., 2016. Effect of process parameters on solvolysis liquefaction of *Chlorella pyrenoidosa* in ethanol-water system and energy evaluation. Energ. Convers. Manage. 117, 43-53.

Pedersen, T.H., Jasiūnas, L., Casamassima, L., Singh, S., Jensen, T., Rosendahl, L.A., 2015. Synergetic hydrothermal co-liquefaction of crude glycerol and aspen wood. Energ. Convers. Manage. 106, 886-891.

Ross, A.B., Biller, P., Kubacki, M.L., Li, H., Lea-Langton, A., Jones, J.M., 2010. Hydrothermal processing of microalgae using alkali and organic acids. Fuel. 89, 2234-2243.

Rebolloso-Fuentes, M.M., Navarro-Pérez, A., García-Camacho, F., Ramos-Miras, J.J., Guil-Guerrero, J.L., 2001. Biomass nutrient profiles of the microlaga *Nannochloropsis*. J. Agric. Food. Chem. 49, 2966-2972.

Shakya, R., Whelen, J., Adhikari, S., Mahadevan, R., Neupane, S., 2015. Effect of temperature and Na_2CO_3 catalyst on hydrothermal liquefaction of algae. Algal. Res. 12, 80-90.

Toor, S.S., Rosendahl, L., Rudolf., A., 2011. Hydrothermal liquefaction of biomass: a review of subcritical water technologies. Energy. 36, 2328-2342.

Yang, W.C., Li, X.G., Liu, S.S., Feng, L.J., 2014. Direct hydrothermal liquefaction of undried macroalgae *Enteromorpha prolifera* using acid catalysts. Energ. Convers. Manage. 87, 938-945.

Yin, S.D., Tan, Z.C., 2012. Hydrothermal liquefaction of cellulose to bio-oil under acidic, neutral and alkaline conditions. Appl. Energy. 92, 234-239.

Zou, S.P., Wu, Y.L., Yang, M.D., Imdad, K., Li, C., Tong, J.M., 2010. Production and characterization of bio-oil from hydrothermal liquefaction of microalgae *Dunaliella tertiolecta* cake. Energy. 35, 5406-5411.

Zhou, D., Zhang, L., Zhang, S.C., Fu, H.B., Chen, J.M., 2010. Hydrothermal liquefaction of macroalgae *Enteromorpha prolifera* to bio-oil. Energy. Fuels. 24, 4054-4061.

Zhu, Z., Rosendahl, L., Toor, S.S., Yu, D.H., Chen, G.Y., 2015. Hydrothermal liquefaction of barley straw to bio-crude oil: effects of reaction temperature and aqueous phase recirculation. Appl. Energy. 137, 183-192.

Chapter 6

6 Highly efficient conversion of algal biomass into bio-crude oil via direct liquefaction in methanol at mild reaction conditions

The information presented in this Chapter is based on the paper "Highly efficient conversion of algal biomass into bio-crude oil via direct liquefaction in methanol at mild reaction conditions", which has been submitted to *Applied Energy*. The sections in Chapter 6 present the results towards the completion of objective 4 of this PhD project (see Section 1.2).

6.1   Abstract

In this study, algal biomass, *Chlorella*, was applied as the feedstock for producing bio-crude oil via direct liquefaction (DL). Initially, the screening tests were carried out at 275 °C for 60 min by employing different reaction media including pure water, water with four acid catalysts (formic acid, acetic acid, sulfuric acid, and hydrochloride acid), and four different organic solvents (methanol, ethanol, ethyl acetate, and acetone) without acid catalyst. Based on the bio-crude oil yield from screening tests, methanol as the most effective reaction medium was chosen for the further investigation on the effects of residence time, biomass/solvent mass ratio, reaction temperature, and methanol-water composition on the products distribution. Liquefaction products (bio-crude oil, aqueous phase, and solid residue) were analyzed by elemental analysis, gas chromatogram-mass spectrometry (GC-MS), and Fourier transform infrared (FT-IR). The results showed that DL at 225 °C for 60 min with 1:5 biomass/solvent mass ratio produced the highest bio-crude oil yield of 85.5 wt.%. Higher heating values (HHVs) of bio-crude oils obtained were in the range of 30.6-34.1 MJ/kg. As indicated by GC-MS analysis, main components of bio-crude oils from DL in methanol were fatty acid esters, especially C_{17} and C_{19} fatty acid methyl esters, suggesting the existence of esterification in the DL process.

6.2   Introduction

Recently, algae have attracted much attention as sustainable sources for the 3rd generation bio-fuels production. Compared to the conventional lignocellulosic biomass (e.g., corn stalk, wheat straw, and wood chip, etc.), algae have unique advantages such as high lipid contents, non-arable land use, and substantial environmental benefits through the capture of atmospheric CO_2 (Yang et al., 2014; Barreiro et al., 2013).

A variety of techniques (e.g., pyrolysis and hydrothermal liquefaction) have been investigated for converting algae into liquid bio-fuels (Yang et al., 2014; Barreiro et al., 2013; Huang et al., 2014; Reddy et al., 2016; Xu et al., 2014). Among them, hydrothermal liquefaction (HTL) is regarded as a more suitable conversion route for wet biomass due to the non-requirement for feedstock drying/dewatering step (Brown et al., 2011). According to an assessment performed by Lardon et al. (2009), the drying step accounts for more than 75% of the total energy consumption in the thermochemical conversion of wet algal biomass. In addition, the bio-crude oils from pyrolysis contain higher oxygen contents compared to HTL bio-crude oils, which could negatively affect bio-crude oil properties (e.g., heating value) (Guo et al., 2015). However, there are several challenges of HTL still ahead, such as harsh reaction conditions, relatively lower oil yield, and poor bio-crude oil quality (Duan et al., 2013).

To address the above challenges, a number of catalysts have been applied for the HTL of algae, such as sodium carbonate (Shakya et al., 2015; Biller and Ross, 2011), potassium hydroxide (Ross et al., 2010; Anastasakis and Ross, 2011), formic acid (Ross et al., 2010; Hu et al., 2017), acetic acid (Yang et al., 2014; Ross et al., 2010), and sulfuric acid (Yang et al., 2014; Muppaneni et al., 2017). The advantages of using catalyst for algal liquefaction may be summarized as follows: (i) promoting decomposition of the macromolecules of biomass into smaller molecules; and (ii) improving bio-crude oil properties in terms of lower contents of heteroatoms (i.e., O, N, and S) and better flowability or lower viscosity (Yang et al., 2014; Guo et al., 2015). According to previous literatures, effects of catalyst on the quantity and quality of bio-crude oils are not only

dependent on the type and dosage of the catalyst but also on the feedstock characteristics (Shakya et al., 2015; Biller and Ross, 2011). For example, the use of sodium carbonate as a catalyst significantly promoted bio-crude oil production in the HTL of high carbohydrates-containing algae, while, in contrast, a negative effect was observed in the HTL of high protein-containing algae (Shakya et al., 2015). Additionally, the liquefaction behavior of amino acids (a building block for protein) with the addition of sodium carbonate was examined by Dote et al. (1998). The results showed that sodium carbonate promoted the distribution of N element in the amino acid to water phase in the form of ammonia, thereby negatively affecting bio-crude oil yield. To date, both organic and inorganic acids have been used as catalyst for the HTL of algae. Ross et al. (2010) observed that the yields of bio-crude oils from *C. vulgaris* (a high protein-containing algae) were higher using an acid catalyst (formic acid or acetic acid) than an alkaline catalyst (sodium carbonate or potassium hydroxide), along with an improved flow property. In another study, Yang et al. (2014) carried out a comparative study on HTL of algae with the addition of organic acid or inorganic acid as a catalyst. The results showed that the organic acid and inorganic acid exhibited different catalytic performances in terms of yields and properties of bio-crude oils. Considering the high protein content in algal biomass used in this study, various acid catalysts including organic and inorganic acids were adopted in the liquefaction treatment.

Previously, Yu et al. (2011) performed the mass balance analysis for the liquefaction process using water as a reaction medium (also denoted as HTL). The authors observed that more than one-third of carbon in the feedstock were preferentially transferred to water phase rather than oily phase. For this reason, a range of organic solvents (e.g., methanol, ethanol, ethyl acetate, and 1,4-dioxaen) have been used as the reaction medium (Duan et al., 2013; Zhou et al., 2012; Yuan et al., 2011; JI et al., 2017; Chen et al., 2012), and this process is commonly defined as direct liquefaction (DL). The main advantages of using organic solvent over water as a reaction medium are as follows: (i) higher bio-crude oil yield; and (ii) moderate reaction conditions (Duan et al., 2013). According to the previous studies, the type of solvent, particularly its polarity, plays a significant role

in the algal liquefaction with respect to the products distribution and properties of bio-crude oils (Duan et al., 2013; Yuan et al., 2011). Generally, a higher bio-crude oil yield was obtained using a solvent with strong polarity, such as an alcohol. More importantly, it was observed that the bio-crude oil from liquefaction in alcohol solvent primarily consisted of fatty acid alkyl esters resulted from esterification of the carboxylic acids in the liquefied product with the alcohol solvent, which was similar to biodiesel on the composition (Zhou et al., 2012). In addition, the alcohol solvents (e.g., methanol and ethanol) can be derived from renewable resources, thereby reducing the overall cost of the liquefaction treatment (Chen et al., 2012). Apart from solvent type, reaction conditions such as residence time, biomass/solvent mass ratio, reaction temperature, catalyst type and dosage, and solvent composition are significantly influence the quantity and quality of bio-crude oil during algal liquefaction (Ji et al., 2017).

In this present study, nine different reaction media including pure water, water with four different acid catalysts (formic acid, acetic acid, sulfuric acid, and hydrochloride acid), and various organic solvents (methanol, ethanol, ethyl acetate, and acetone) were investigated for the liquefaction of *Chlorella*. The most effective reaction medium identified was then selected to study the effects of residence time, biomass/solvent mass ratio, reaction temperature, and solvent composition on the products distribution. Furthermore, physical and chemical properties of liquefaction products (bio-crude oil, aqueous phase, and solid residue) were characterized by elemental analysis, gas chromatography-mass spectroscopy (GC-MS), and Fourier transform infrared (FT-IR).

6.3   Materials and methods

6.3.1   Materials

Algal biomass, *Chlorella* with cracked cell wall, was purchased as food-grade material and received as fine powder. The main characteristics, such as proximate analysis, ultimate analysis, and biochemical analysis (lipid, protein and carbohydrates) of the algal biomass sample are summarized in Table 6.1. All chemicals used in this study were purchased from Caledon Laboratories Ltd (Georgetown, Canada), and used as received.

Table 6-1: The main characteristics of algal used in this work as the biomass feedstock (Data represents average value ± standard deviation).

Proximate analysis (wt.%)

Moisture	Ash	Organic matters [a]		
3.48 ± 0.62	7.15 ± 0.10	89.37		

Elemental analysis (wt.%, d.b.) [b]

C	H	O [c]	N	S
46.54 ± 1.84	7.37 ± 0.30	29.86 ± 2.14	8.59 ± 0.25	0.48 ± 0.24

HHV (MJ/kg) [d]

20.97 ± 1.45

Biochemical analysis (wt.%)[b]

Lipid	Protein [e]	Carbohydrates [f]
6.10 ± 1.77	53.66 ± 1.55	33.09

[a] Determined by difference; [b] Determined on dry basis; [c] Calculated by %O = 100% -%C - %H - %N - %S - %Ash; [d] Calculated by the Dulong equation; [e] Estimated by %Protein = %N × 6.25 (Rebolloso-Fuentes et al., 2001); [f] Determined by %Carbohydrates = 100% - %Lipid- %Protein - %Ash.

6.3.2 Liquefaction experiments

Liquefaction experiments were carried out using a 100 mL Micro-Bench top reactor equipped with a magnetic stirrer (Parr 4590, Illinois, USA). Throughout the liquefaction processes, temperature and pressure were monitored by a Type J thermocouple and Alloy 400 Pressure Gaga, respectively. The baseline liquefaction run was performed by loading 5.0 g of dried algal biomass and 25.0 g of distilled water into the reactor without catalyst. For the catalytic HTL runs, the reactor was charged with 5.0 g of dried algal biomass and 25.0 g of distilled water containing 1.5 g of acid catalyst (5 wt.% of the total slurry). The tested acid catalysts in this work included formic acid, acetic acid, sulfuric acid, and hydrochloride acid. In the case of liquefaction experiments in organic solvent, 5.0 g of

dried algal biomass and 25.0 g of a specific organic solvent (methanol, ethanol, ethyl acetate or acetone) or an organic solvent-water mixed medium were loaded into the reactor without catalyst. Afterwards, the reactor was sealed and purged with pure nitrogen to displace the residual air inside the reactor. After that, pure nitrogen at 0.69 MPa was purged into the reactor to prevent the reaction medium from boiling during the heating process. The reactor was then heated to the desired reaction temperature at a heating rate of approx. 5 °C/min and then this temperature was held for a pre-set residence time. The liquefaction experiments were carried out under varying reaction temperatures (175 °C, 225 °C, 275 °C, and 300 °C), residence times (30 min, 60 min, 90 min, and 120 min), biomass/solvent mass ratios (1/2.5, 1/5, and 1/10), and organic solvent content in the mixed solvent (0 wt.%, 25 wt.%, 50 wt.%, 75 wt.%, and 100 wt.%).

6.3.3   Product separation

The procedure used for the baseline experiment and the catalytic HTL was fully described in our previous report (Hu et al., 2017). For the liquefaction in mixed solvents, a similar procedure as earlier adopted by Peng et al. (2016) was used. In addition, the procedure to separate different product fractions from the liquefaction in organic solvent is described below. Briefly, after the reactor was cooled to room temperature, the gases were released into the fume hood. It shall be noted that the gas formation, mainly CO_2, was found to be negligible due to the low liquefaction temperatures used in this work, thus the gas yield was not quantified. After that, the reaction mixture was then transferred into a 250 mL beaker. The reactor and stirrer were further washed using 100 mL of dichloromethane (DCM) for three times, followed by filtration through a pre-weighed filter paper. The filter paper was then oven-dried at 105 °C for 24 h and weighed to determine the solid residue yield. The DCM together with the reaction solvent (methanol, ethanol, acetone, or ethyl acetate) were transferred to a 500 mL pre-weighed round-bottom flask and evaporated at 65 °C under reduced pressure. The remaining dark material in the flask was weighed and denoted as bio-crude oil. The yields of bio-crude oil and solid residue were determined in wt.%, in relation to dried mass of the feedstock, and the balance was calculated as the yield of other products (gases + aqueous phase).

6.3.4   Analysis

6.3.4.1   Feedstock

The moisture content was determined by drying the sample in an oven at 105 °C for 24 h. The ash content was measured by ashing the dried algal biomass in a muffle furnace at 575 °C in air for 3 h until reaching a constant weight. The elemental compositions (C, H, N, and S) were analyzed using a CHNS [Cl] Elementar vario EL, while the O content was estimated by difference on dry basis (%O = 100% - %Ash - %C - %H - %N -%S). The higher heating value (HHV) was calculated by the Dulong equation [HHV (MJ/kg) = 0.338C + 1.428(H-O/8) + 0.095S]. The lipid content was determined by the Bligh & Dyer method (Bligh and Dyer, 1956). The protein content was estimated by %N × 6.25 (Rebolloso-Fuentes et al., 2001). The carbohydrates content was calculated by difference on dry basis (%Carbohydrates = 100% - %Ash - %Lipid - %Protein).

6.3.4.2   Liquefaction products

The elemental compositions and HHV of bio-crude oil and solid residue were analyzed using the same method as earlier described for feedstock. The key chemical components of bio-crude oil and aqueous products were determined by an Agilent 7890-5975 GC-MS equipped with a HP-5MS nonpolar capillary column (30 m × 0.25 mm × 0.25 µm). Pure helium was used as the carrier gas, with a flow rate of 2.64 mL/min. Prior to GC-MS analysis, the bio-crude oil or aqueous phase sample was diluted in acetone. In a typical test, 1 µL diluted sample was injected at 280 °C with a split ratio of 20:1. The GC oven temperature was programmed as follows: held at 60 °C for 2 min, followed by heating at 20 °C/min to 280 °C and held for 10 min. The major components were identified by NIST (National Institute of Standards and Technology) database. The functional groups of bio-crude oil were characterized with a Nicolet 6700 Fourier Transform Infrared Spectroscopy (Thermo Fischer Scientific, Massachusetts, USA) in the range of 4000-600 cm^{-1}, with a resolution of 4 cm^{-1}.

6.4   Results and discussion

6.4.1   HTL media screening

Initial studies were carried out at 275 °C for 60 min, with a biomass/solvent mass ratio of 1/5 for screening nine different reaction media including pure water, water with acid catalyst (formic acid, acetic acid, sulfuric acid, or hydrochloride acid), or organic solvent (methanol, ethanol, ethyl acetate, or acetone), with respect to the products distribution from liquefaction of algal biomass.

As shown in Fig. 6.1, the type of reaction medium considerably affected the products yield. For the organic acid-catalyzed HTL, the bio-crude oil yield was significantly higher (38.0 wt.% with formic acid and 32.6 wt.% with acetic acid) compared to that (20.3 wt.%) obtained from the baseline operation without catalyst. Additionally, the yield of solid residue drastically reduced from 21.0 wt.% (no catalyst) to 3.3 wt.% (formic acid) and 9.8 wt.% (acetic acid), respectively. This result was consistent with previous studies on the HTL catalyzed by organic acid (Ji et al., 2017; Bi et al., 2017). The increased oil yield may be attributed to the acid-catalyzed degradation of macromolecules (e.g., protein and carbohydrates) into small molecules in the liquefaction system. In the case of catalytic HTL with hydrochloride acid, only a slightly higher yield of bio-crude oil (22.1 wt.%) was observed compared to that (20.3 wt.%) obtained without catalyst. Surprisingly, the addition of sulfuric acid resulted in a decrease in bio-crude oil yield (12.6 wt.%) than that (20.3 wt.%) from baseline experiment. On the contrary, Zou et al. (2009) studied the effect of sulfuric acid on the HTL of *D. tertiolecta*, and the results showed an increase of bio-crude oil yield with the use of sulfuric acid. This opposite result could be attributed to the differences in feedstock characteristics and operating conditions. For instance, the reaction temperature (275 °C) tested in this study was much higher than those of the literature work (commonly < 200 °C). At a high temperature, the presence of a strong inorganic (mineral) acid like H_2SO_4 could catalyze dehydration or condensation of the oil products to yield more water by-product at the expense of bio-crude yield, as evidenced by markedly increased yield of others (gases + aqueous

products including water by-product) being 66.8 wt.% with H_2SO_4 vs. 58.8 wt.% without catalyst.
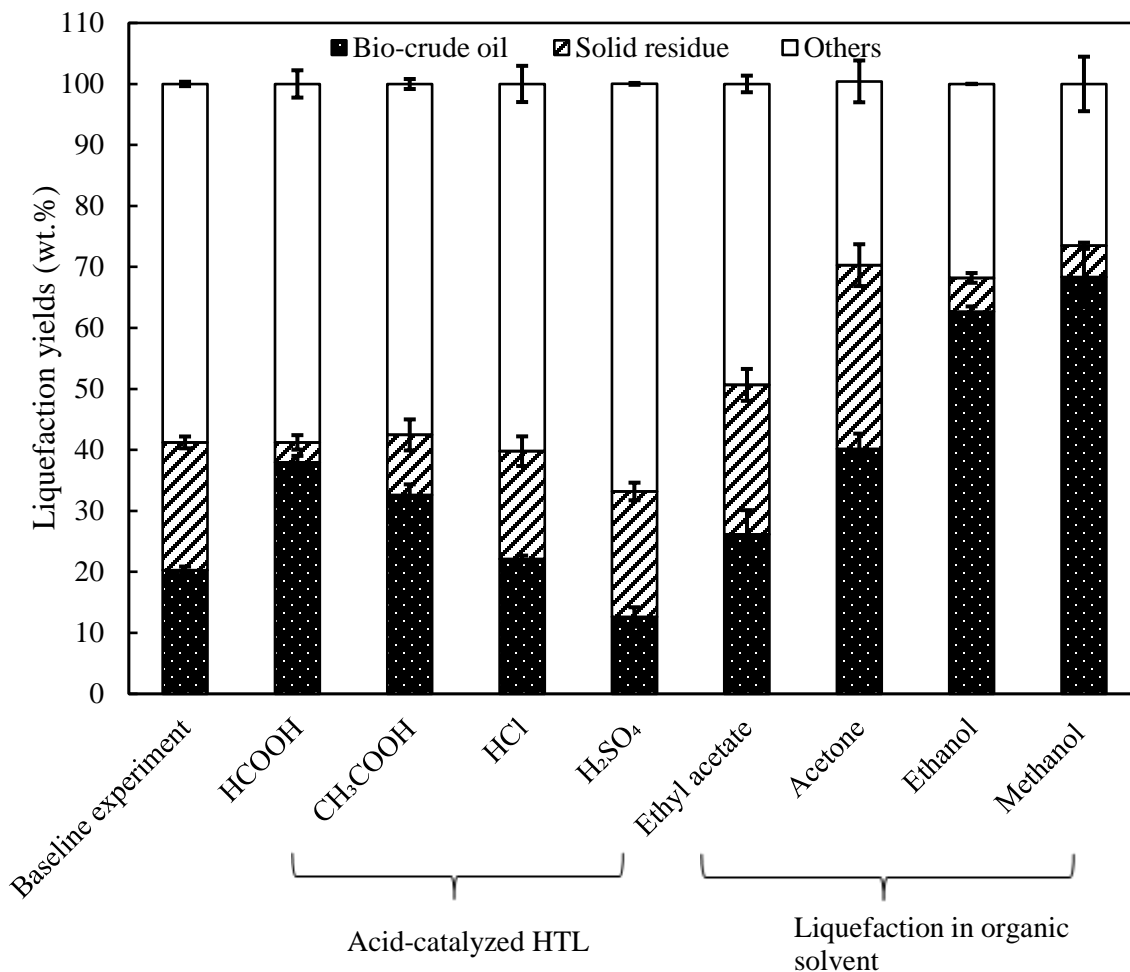
Figure 6-1: The products distribution obtained from nine different reaction media at 275 °C for 60 min, with a biomass/solvent mass ratio of 1/5 (Note: The baseline experiment and catalytic HTL were performed in pure water with or without catalyst).

On the other hand, as clearly shown in Fig. 6.1, the bio-crude oil yield was consistently higher when using organic solvent as the reaction medium (26.2 wt.%, 40.1 wt.%, 62.7 wt.%, and 68.3 wt.% with ethyl acetate, acetone, ethanol, and methanol, respectively) than that from liquefaction in water (20.3 wt.%). This result is in good agreement with the findings of many previous literature reports (Ji et al., 2017; Peng et al., 2016; Jin et al., 2014). Fig. 6.1 also shows that the type of organic solvent played an important role in

the products distribution. Specifically, the yield of bio-crude oil obtained using a polar protic solvent (methanol or ethanol) as the reaction medium was significantly higher than that obtained using a polar aprotic solvent (ethyl acetate or acetone). One possible reason could be that the hot-compressed methanol/ethanol can serve as a hydrogen donor solvent. The released hydrogen free radical (H·) could promote the hydrocracking of macromolecules to small molecules. Meanwhile, the fragments/intermediates from liquefaction process can be stabilized, thereby preventing char formation and improving bio-crude oil yield (Akhtar and Amin, 2011). This could be confirmed with the extremely low yield of solid residue (~5 wt.%) with these alcohols compared to that from baseline experiment (21.0 wt.%). In contrast, the solid residue yield obtained in ethyl acetate (25.4 wt.%) or acetone (30.1 wt.%) was observed to be higher than those obtained in an alcohol solvent (methanol or ethanol).

Based on the results as described above, methanol was identified as the most effective reaction medium for converting algal biomass to bio-crude oil via direct liquefaction. Following this, effects of residence time, solvent/biomass mass ratio, reaction temperature, methanol-water composition on the products distribution were investigated.

6.4.2   Effects of operating conditions on products distribution

6.4.2.1   Residence time

Effects of residence time on the products distribution were investigated under the conditions of 275 °C, biomass/solvent mass ratio of 1:5 and 100 wt.% methanol, for a residence time varying from 30 min to 120 min. As shown in Fig. 6.2, the bio-crude oil yield increased from 59.0 wt.% to 68.3 wt.% while prolonging residence time from 30 min to 60 min, and thereafter dropped to 41.1 wt.% at 120 min.
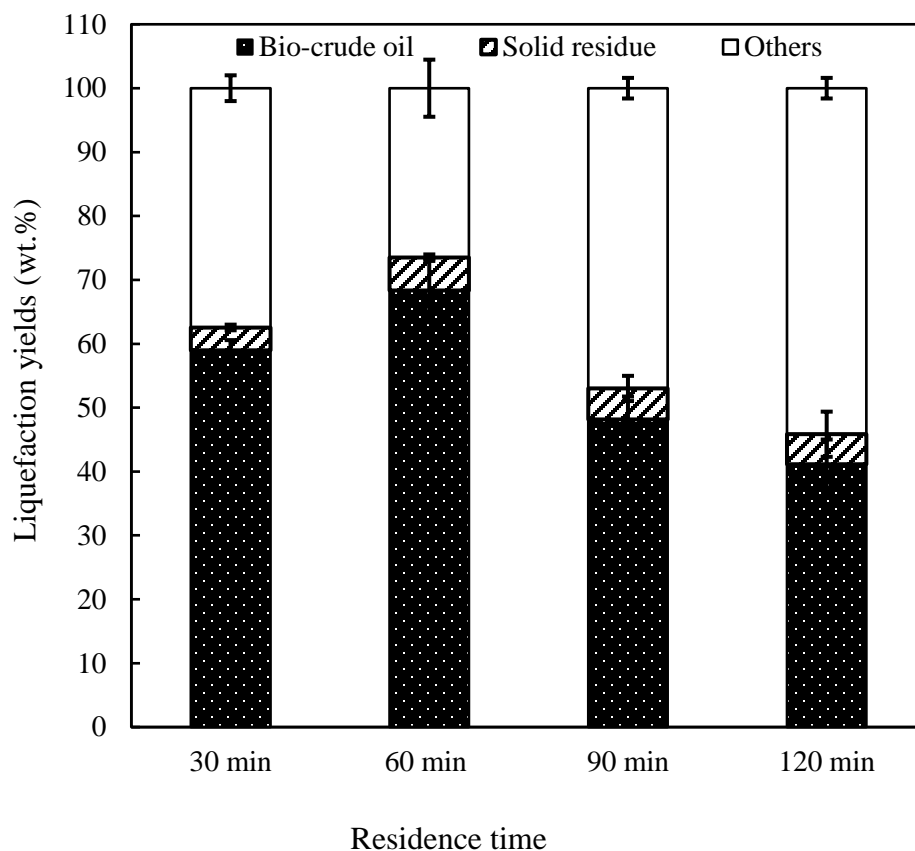
Figure 6-2: Effects of residence time on the products distribution (Other reaction conditions: 275 °C, biomass/solvent mass ratio of 1/5, and in 100 wt.% methanol).

A similar trend was reported by Ji et al. (2017) in the direct liquefaction of *Spirulina* in ethanol-water mixed solvents. The reduction of bio-crude oil yield at extended residence time may be due to the further decomposition of oil products to gaseous and/or aqueous products, as evidence by a sharp increase in the others yield (gases + aqueous products) from 26.5 wt.% at 60 min to 54.2 wt.% at 120 min. While, it was observed that the residence time had no significant effect on the solid residue yield. As mentioned early, methanol can act as a hydrogen donor solvent that could stabilize the fragments/intermediates from liquefaction and consequently prevent their re-polymerization to form char (Akhtar and Amin, 2011).

The best residence time for obtaining the highest bio-crude oil yield from algal biomass appeared to be 60 min for the given reaction conditions. This residence time was therefore chosen for investigating the effects of biomass/solvent mass ratio on the products distribution.

6.4.2.2 Biomass/solvent mass ratio

Fig. 6.3 demonstrates the effect of biomass/solvent mass ratio on the products distribution at 275 °C for 60 min in 100 wt.% methanol. Variations of biomass/solvent mass ratio were obtained by mixing a fixed feedstock loading (5.0 g on dry basis) with different solvent loading amounts from 12.5 g to 50 g, corresponding to a biomass/solvent mass ratio from 1:2.5, 1:5 to 1:10, respectively.
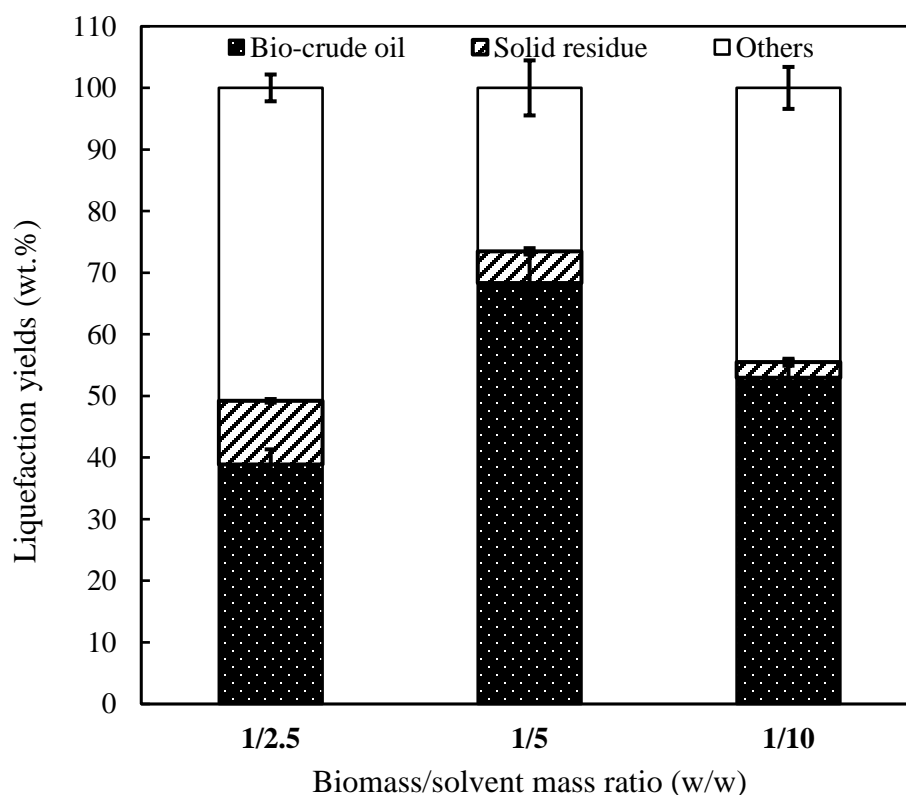
Figure 6-3: Effects of biomass/solvent mass ratio on the products distribution (Other reaction conditions: 275 °C, residence time of 60 min, and in 100% methanol).

As shown in Fig. 6.3, the bio-crude oil yield sharply increased from 38.9 wt.% to 68.3 wt.% when increasing the solvent/biomass mass ratio from 2.5/1 to 5/1. Whereas, further increasing the solvent loading decreased the bio-crude oil yield. This phenomenon is consistent with that reported in previous literature on liquefaction of algae (Duan et al., 2013; Ji et al., 2017). The increased oil yield at higher solvent loading was likely owing to the presence of a larger amount of solvent that could prevent re-polymerization of the fragments/intermediates from liquefaction to form char, or it could possibly be attributed to the enhanced mass and heat transfer during algal liquefaction (Jin et al., 2014). However, oil products could be partially cracked into aqueous and/or gaseous products as the solvent loading was too high (e.g., with the solvent/biomass mass ratio of 10/1), which can be confirmed with the markedly increased yield of (gas + aqueous phase). Besides, the yield of solid residue gradually decreased from 10.3 wt.% to 2.5 wt.% with increasing the solvent loading amount, suggesting the promoted conversion of biomass or the suppressed re-polymerization of bio-crude oil to form char with a higher solvent loading. It should however be noted that very low solid residue yield (approx. 3-5 wt.% on dry basis) was obtained at a higher solvent loading, even smaller than the ash content (7.2 wt.%) of the original feedstock. This was possibly caused by the dissolution of some inorganic salts of the ash fraction into the water phase during algal liquefaction, thereby reducing the yield of solid residue (Duan et al., 2013). With respect to bio-crude oil yield, the biomass/solvent mass ratio of 1:5 was selected for exploring the effects of reaction temperature and methanol-water mixed solvent composition on the products distribution.

6.4.2.3   Reaction temperature

Effects of reaction temperature on the products distribution are shown in Fig. 6.4, which presents the results obtained at 175-300 °C for 60 min in 100 wt.% methanol solvent with biomass/solvent mass ratio of 1:5. The critical temperature and pressure of methanol are 240 °C and 8.1 MPa. Hence, the liquefaction experiments were carried out in sub-/super-critical methanol. As indicated in Fig. 6.4, increasing reaction temperature increased bio-crude oil yield, but peaked at 225 °C where a maximum oil yield of 85.5 wt.% was obtained, and thereafter it drastically dropped to 17.5 wt.% at 300 °C.
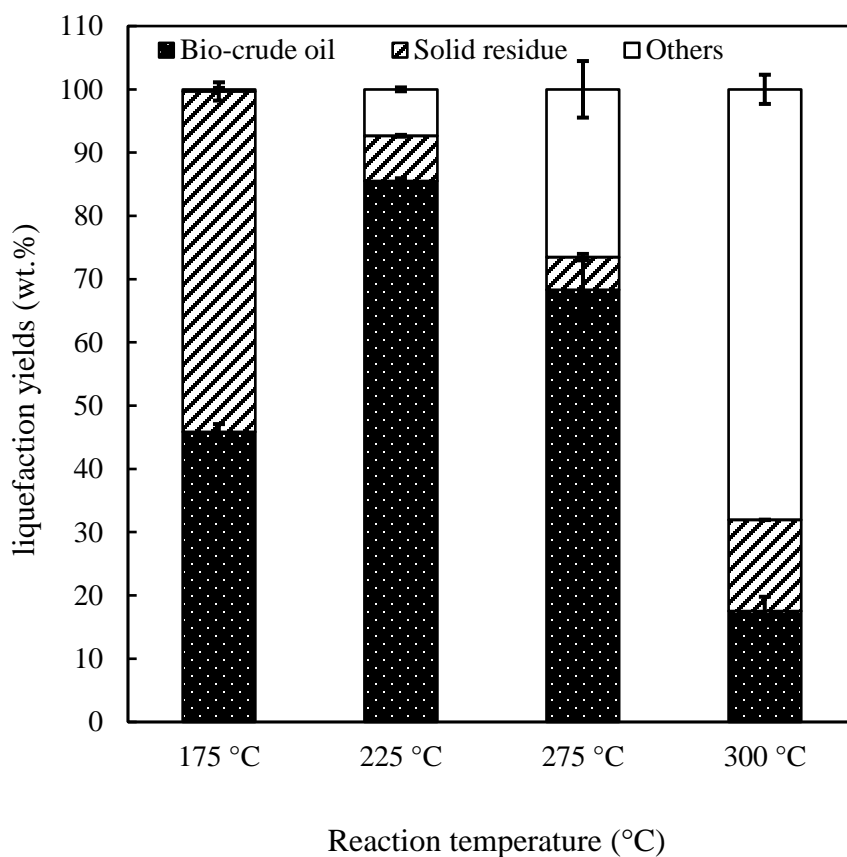
Figure 6-4: Effects of reaction temperature on the products distribution (Other reaction conditions: residence time of 60 min, biomass/solvent mass ratio of 1/5, and in 100% methanol).

Such strong dependency of bio-crude oil yield on reaction temperature was commonly reported previously in many literature work, e.g., by Biswas et al. (2017). Interestingly, the bio-crude oil yield was as high as 45.9 wt.% even at a low reaction temperature of 175 °C. This was probably owing to the feedstock characteristics. The algal biomass used was *Chlorella* with broken cell wall, as earlier mentioned in Section 6.2.1, which hence facilitate hydrolysis and depolymerization of biomass macromolecules to yield more liquefaction products (Lee et al., 2017). Another possible reason for such higher bio-crude oil yield could be the incorporation of methanol to oil products esterification reactions (Duan et al., 2013), which may be evidenced by the formation of methyl esters according to the GC-MS (Fig. 6.6 and Appendix-D) and FTIR (Fig. 6.7) results to be discussed later.

Moreover, the yield of solid residue drastically decreased from 53.8 wt.% at 175 °C to 5.1 wt.% at 275 °C, and thereafter increased to 14.4 wt.% at 300 °C. On one hand, due to the endothermic nature of the biomass macromolecules degradation, while increasing reaction temperature more fraction of biomass macromolecules could be liquefied and then converted into bio-crude oil, aqueous products, or gases. On the other hand, as further increased temperature (to above critical point) would favor cracking and gasification (such as decarboxylation and steam reforming reactions) of the oil/aqueous products (Guo et al., 2015), which would lead to significant formation of solids (char/coke) and gases, as shown in Fig. 6.4. Specifically, with the reaction temperature ramped from 275 °C to 300 °C, the bio-crude oil yield dramatically decreased from 68.3 wt.% to 17.5 wt.%, accompanied by an increase in the yield of solid residue from 5.1 wt.% to 14.4 wt.%. As described previously the highest bio-crude oil yield (85.5 wt.%) was achieved in this work employing methanol solvent at milder conditions (225 °C). The oil yield obtained is much higher than that reported in previous studies (Chen et al., 2012; Peng et al., 2016). In this study, 225 °C was selected as the reaction temperature for the rest of the experiments to investigate effect of methanol-water composition in mixed solvent on the products distribution.

6.4.2.4 Methanol-water mixed solvent composition

To investigate the effect of methanol-water mixed solvent composition on the products distribution, liquefaction experiments with various methanol contents (in methanol-water mixed solvents) were performed at reaction temperature of 225 °C, residence time of 60 min, and biomass/solvent mass ratio of 1:5. As can be seen in Fig. 6.6, the bio-crude oil yield gradually increased from 14.9 wt.% to 85.5 wt.% with methanol content in the reaction medium increased from 0 to 100 wt.%, as similarly reported by Jiang et al. (2017) in liquefaction of pine wood. This result suggests that 100% methanol performed the best in liquefaction of algal biomass for bio-crude production at 225 °C, which is different from the findings reported in many literature studies on direct liquefaction of algae (Ji et al., 2017; Chen et al., 2012; Peng et al., 2016) and woody biomass (Cheng et

al., 2010) where alcohol-water mixed solvents with 40-60% alcohol demonstrated synergistic effects.
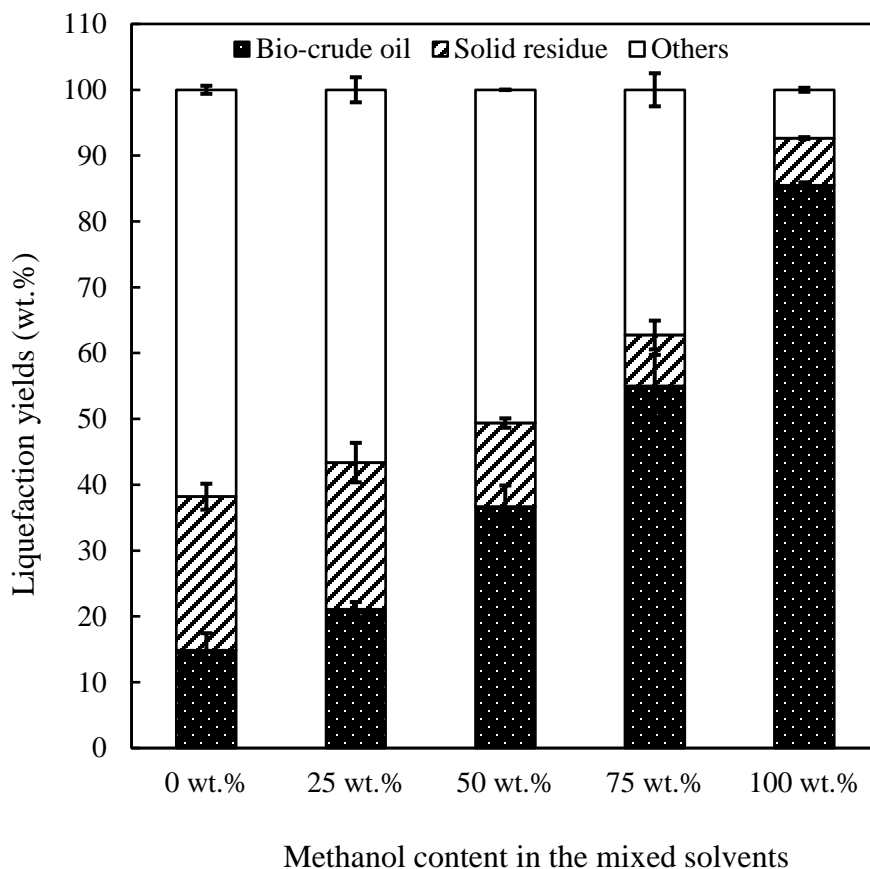
Figure 6-5: Effects of methanol content (in methanol-water mixed solvents) on the products distribution (Other reaction conditions: 225 °C, residence time of 60 min, and biomass/solvent mass ratio of 1/5).

For instance, the bio-crude oil yield from HTL of microalgae in ethanol-water mixed solvents at 300 °C was found to increase with increasing ethanol content, and peaked at 40% of ethanol (ethanol : water, v/v) (Chen et al., 2012; Peng et al., 2016). The above different results could mainly be due to the differences in the feedstock properties (structure) and reaction temperature. First of all, the pre-treated *Chlorella* with broken cell wall used in this work is believed to have cell wall structure less rigid than that of the untreated algae, and thus could be liquefied under mild conditions (225 °C) without the

need of hydrolytic reactions. In contrast, the original untreated algae whose degradation requires a higher reaction temperature (250-375 °C) and the hydrolysis reactions (Guo et al., 2015; Biswas et al., 2017; Cheng et al., 2010), which may explain the synergistic performance of alcohol-water mixed solvent. As such, the *Chlorella* with broken cell wall used in this work can be effectively liquefied at a mild temperature (225 °C) in absence of water by employing 100% methanol. Moreover, the yield of solid residue consistently decreased from 23.3 wt.% to 7.2 wt.% with increasing methanol content from 0 to 100 %, suggesting best biomass conversion with 100% methanol.

6.4.3   Bio-crude oil characterization

6.4.3.1   Elemental analysis

The elemental compositions and HHVs of bio-crude oils obtained in methanol-water mixed solvents with various methanol contents are summarized in Table 6.2. The algae derived bio-crude oils from all liquefaction runs have HHVs in the range of 30.6-34.1 MJ/kg, and the maximum HHV (34.1 MJ/kg) was obtained for the bio-crude oil from the liquefaction in methanol/water (50/50, wt/wt) co-solvents. As a comparison, the algal bio-crude oil contained around 71-79% energy content of that of petroleum crude oil. Besides, the HHVs of the obtained bio-crude oil products are much higher than the original biomass (21.0 MJ/kg), and comparable to those from earlier studies (Shakya et al., 2015; Biller and Ross, 2011; Ross et al., 2010; Zhou et al., 2012). In general, all bio-crude oil samples have higher carbon and hydrogen contents (62.4-69.1 wt.% and 8.7-9.3 wt.%, respectively), and relatively lower oxygen content (13.7-19.8 wt.%), compared to the feedstock material. As expected, a high nitrogen content (6.2-8.4 wt.%) was observed in all bio-crude oils, due to the higher protein content in the feedstock (approx. 54 wt.%, in Table 6.1), typical of algae-derived bio-crude oils (Jin et al., 2014). Thus, the subsequent hydrotreatment of microalgae-derived bio-crude oil is required for nitrogen removal in order to meet the requirement for transportation fuel. As also expected, the resultant bio-crude oils have a lower sulfur content between 0.3 wt.% and 0.6 wt.% owing to the low sulfur content in the feedstock (0.48 ± 0.24 wt%). This result was lower

than sulfur content of petroleum crude oil. Interestingly, nitrogen content of the bio-crude oils was observed to increase with increasing methanol content in the solvent as presented in Table 6.2, which might be resulted from the reduced water content while increasing the methanol content in the methanol-water mixed solvent. As previously reported by Dote et al. (1998), most of N in amino acids from hydrolysis of protein was preferentially transferred to water phase rather than oil phase in hydrothermal liquefaction of algal biomass. Hence, the presence of less water in the reaction medium would result in more N-containing compounds in the oil products (Table 6.2).

Table 6-2: The elemental compositions of bio-crude oils obtained in methanol-water mixed solvents with various methanol contents at 225 °C for 60 min, with a biomass/solvent mass ratio of 1/5.

Elemental composition (wt.%)	Methanol content in reaction medium (wt.%)					Petroleum crude[c]
	0	25	50	75	100	
C	65.09	69.05	68.81	64.46	62.41	83-87
H	8.69	9.08	9.25	8.83	9.12	10-14
O[a]	19.55	14.21	13.74	18.24	19.84	0.5-6.0
N	6.17	7.08	7.72	8.09	8.39	0.1-1.5
S	0.51	0.58	0.48	0.39	0.25	0.1-2.0
HHV (MJ/kg)[b]	30.97	33.82	34.06	31.18	30.60	42.90
Atomic ratio (mol/mol)						
H/C	1.60	1.58	1.61	1.64	1.75	
O/C	0.23	0.15	0.15	0.21	0.24	
N/C	0.08	0.09	0.10	0.11	0.12	

[a] Determined by difference; [b] Calculated by the Dulong equation.

6.4.3.2   GC-MS analysis

The chemical compounds in bio-crude oils obtained from direct liquefaction of algal biomass were determined by GC-MS analysis, although some compounds in the oils were not able to be detected by GC-MS analysis, due to (i) some light oil compounds might be lost during solvent evaporation; and (ii) the heavy compounds cannot be eluted through the GC column (Brown et al., 2011). The GC-MS analysis results for three bio-crude oil samples obtained at 225 °C for 60 min with a biomass/solvent mass ratio of 1:5 in methanol-water mixed solvents with different methanol contents (0, 50, and 100 wt.%) are presented in Fig. 6.7 and detailed in Appendix-F. The major compounds (i.e., the relative percentage of peak areas over than 1%) of three bio-crude oil samples are categorized into N-containing compounds, esters, other O-containing compounds (alcohols, ketones, and ethers), and cyclic oxygenates.

Some distinct differences can be observed in the relative concentrations of compounds (based on peak areas) among three bio-crude oil samples. The major compounds in bio-crude oil obtained with pure water are N-containing compounds (76.0%), while esters (66.3%) are the most abundant compounds in the bio-crude oil obtained with pure methanol. As given in Appendix-F, the bio-crude oil obtained with the methanol-water mixed solvent consists mainly of both N-containing compounds (20.7%) and ester compounds (47.3%). The content of hexadecenoic acid, methyl ester (RT. 12.87) increases from 2.4% in pure water to 19.6% in methanol-water mixed solvents, and to 27.0% in pure methanol, and 9,12-octadecadienoic acid (Z,Z)-, methyl ester (RT. 13.88) is also higher in the oil obtained with pure methanol or the methanol-water mixed solvent. Typically, C_{16} and C_{18} fatty acids with various degree of unsaturation such as hexadecenoic acid and ($C_{16:0}$) and 9,12-octadecadienoic acid (Z,Z)- ($C_{18:2}$) are the most common fatty acid in the algal lipid (Changi et al., 2015). The above results evidence that the esterification reactions between fatty acids from algal biomass and the alcohol. In fact, the most abundant compounds in the biodiesel are C_{16-20} fatty acid methyl/ethyl esters, similar to the esters detected in the bio-crude oil obtained from the liquefaction of an algal biomass in methanol (Zhou et al., 2012). Nevertheless, some nitrogen-containing

esters like DL-proline, 5-oxo-, methyl ester (RT. 10.89) were also observed in the bio-crude oils obtained in pure methanol or methanol-water mixed solvents, which was likely resulted from the reactions of amino acids with alcohols (Anastasakis and Ross, 2011). Based on the GC-MS results above, it may be inferred that liquefaction of algal biomass in methanol could improve bio-crude oil properties such as long-time stability (shelf time) and corrosivity. In previous studies, the biodiesel properties, including acid value, saponification value, iodine number, and cetane number, are determined by the fatty acid composition of oil (Srivastava et al., 2018; Knothe, 2005). Thus, in the future study, the acid value, saponification value, iodine number, and cetane number of biodiesel produced from this study will be measured.
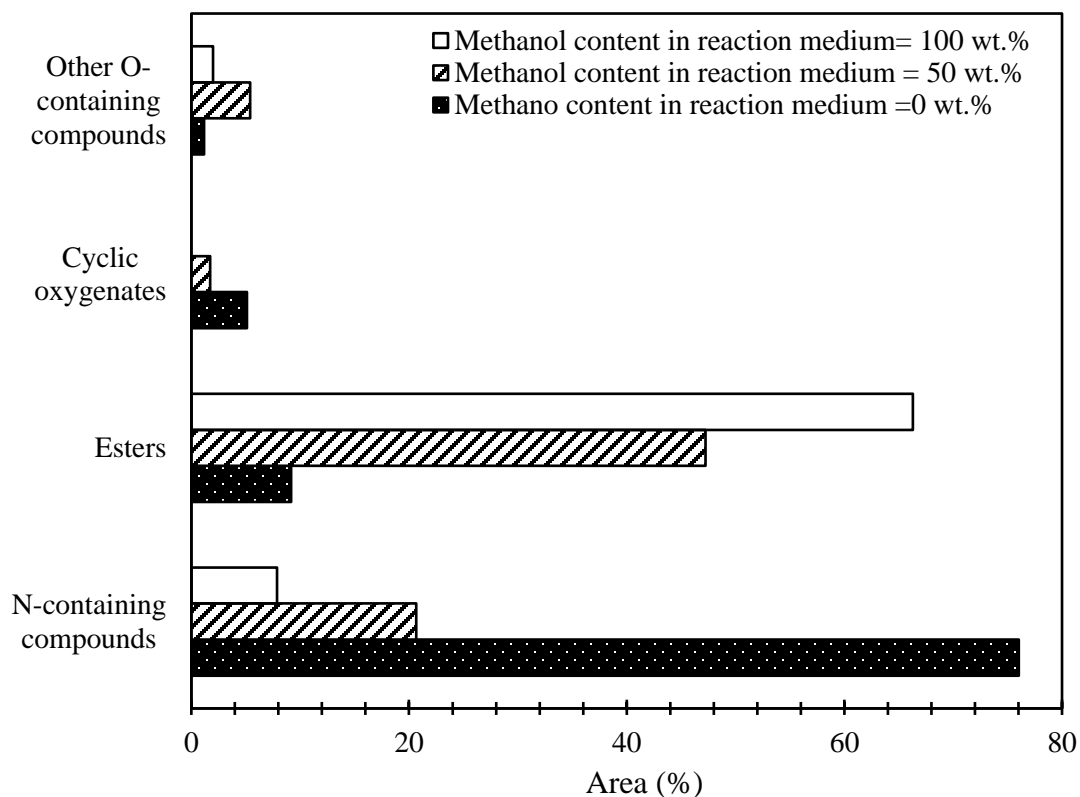
Figure 6-6: Major chemical compounds of bio-crude oils obtained from liquefaction of algal biomass in water-methanol mixed solvents with different methanol contents at 225 °C for 60 min, with a biomass/solvent mass ratio of 1/5.

6.4.3.3 FT-IR analysis

The FT-IR spectra of bio-crude oil samples obtained in different reaction media (water, methanol and water-methanol mixed solvent) at 225 °C for 60 min, with a biomass/solvent mass ratio of 1/5 are displayed in Fig. 6.8.
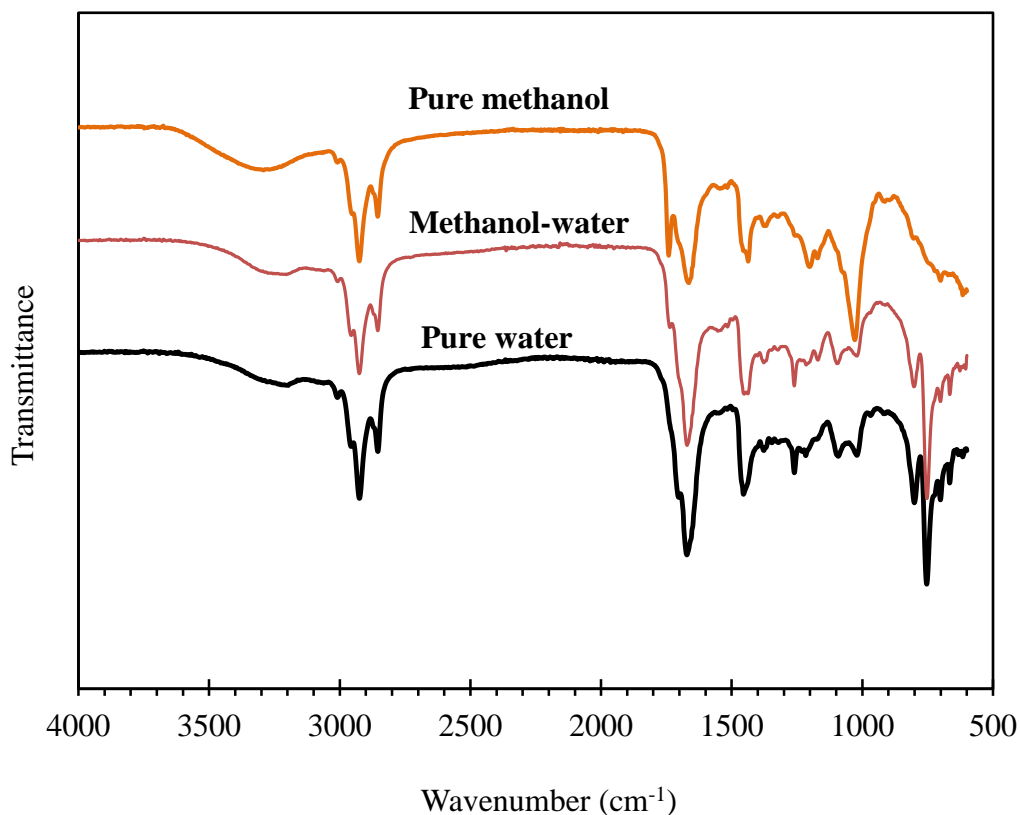
Figure 6-7: FT-IR spectra of bio-crude oils obtained in various liquefaction media at 225 °C for 60 min, with a biomass/solvent mass ratio of 1/5.

The interpretation of major peaks was performed according to Socrates (1994). A broad absorption band from 3700 to 3100 cm^{-1} can be assigned to O-H or N-H stretching vibration. The peaks at 2944, 2925, and 2853 cm^{-1} can be ascribed to C-H asymmetrical and symmetrical stretching vibration, indicating the presence of alkyl C-H in the bio-crude oils. Another peak at 1742 cm^{-1} could be related to C=O carbonyl group, which is consistent with the ketones and esters identified in the bio-crude oil (Appendix-D). The peak at 1666 cm^{-1} represents the C=O stretching vibration from primary amide

compounds. Besides, the peak at 1440 cm^{-1} could be attributed to C-H bending vibration in methyl groups. The peaks at 1199 and 1031 cm^{-1} can be related to the C-O stretching vibration. Finally, a strong peak at 753 cm^{-1} indicated the presence of aromatic C-H in the bio-crude oil.

Although the FT-IR spectra of three bio-crude oils obtained in different reaction media (water, methanol and water-methanol mixed solvent) show similar functionalities, some evident differences among oil samples can be observed in Fig. 6.7. Firstly, the stretching vibrations of carbonyl C=O at 1742 cm^{-1} and C-O at 1029 cm^{-1} were observed to be more intensive in the bio-crude oil obtained using pure methanol as the reaction medium, suggesting formation of esters between acid intermediates and alcohol (Ji et al., 2017), as evidenced by the contents of esters identified in the bio-crude oil by GC-MS (Appendix-F). Furthermore, the peak at 753 cm^{-1} representing aromatic C-H vibration is weaker in the bio-crude oil obtained in pure methanol, implying enhanced hydrogenation of the oil products attributed to the hydrogen donor property of near-critical methanol.

6.4.4   Aqueous phase characterization

In this work, major chemical components of aqueous phase samples obtained at 225 °C for 60 min, with a biomass/solvent mass ratio of 1/5 in methanol-water mixed solvents with various methanol contents were also determined by GC-MS analysis. As illustrated Fig. 6.9 and detailed in Appendix-G, the major compounds identified in the aqueous products are organic acids, alcohols, esters, N-containing compounds, and cyclic oxygenates. N-containing compounds were observed to be the most abundant compounds in the aqueous phase, which was expected as most of N in amino acids from protein tend to partition to water phase in the form of ammonium during algal liquefaction (Dote et al., 1998; Gai et al., 2015). Some compounds identified in the aqueous phase samples, such as 3-pyridinol and 3-pyridinol, 6-methyl-, as shown in Appendix-G could be toxic to the surrounding environment (Pham et al., 2013), as such the aqueous phase without treatments should not be discharged directly to the surrounding environment. To address the above challenge related to the aqueous phase, the authors have demonstrated

innovative solution by recycling aqueous phase as a reaction medium for improving bio-crude oil productivity in hydrothermal liquefaction of algae (Hu et al., 2017). Besides, it was observed that glycerol was identified in all aqueous phase samples. As also shown in Appendix-G, phenolic compounds were also identified in all aqueous phase samples, which are likely derived from carbohydrates.
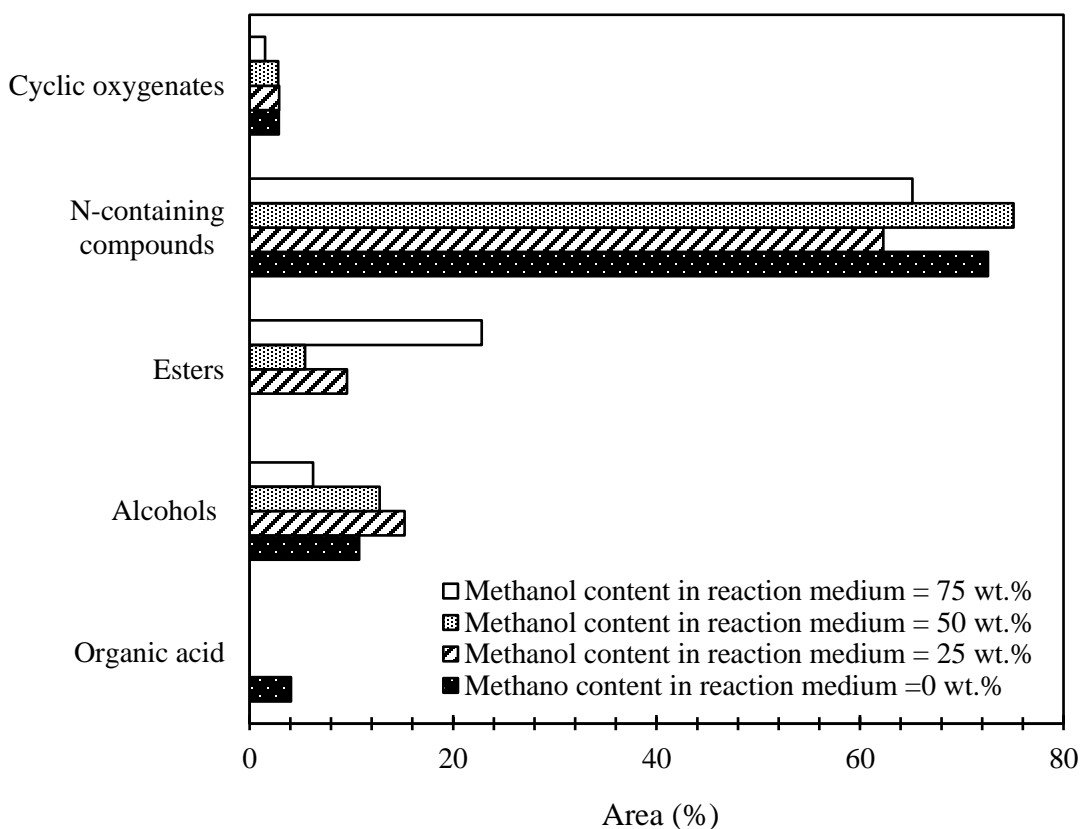
Figure 6-8: Major chemical compounds of aqueous phase samples obtained from liquefaction of algal biomass (pre-treated Chlorella with broken cell wall) in water-methanol mixed solvents with different methanol contents at 225 °C for 60 min, with a biomass/solvent.

Several distinct differences can be observed among three aqueous phase samples. Acetic acid is absent in the aqueous phase sample obtained in the methanol-containing media, which may be caused by esterification of acetic acid and methanol. However, no ester compound was detected in the aqueous phase sample obtained in pure water. This may be

due to no or negligible alcohols produced from HTL of algal biomass under the given conditions, although alcohol could be formed by reduction of organic acid from deamination of amino acids. In addition, decarboxylation reaction is another main decomposition pathway for amino acids under hydrothermal condition (Barreiro et al., 2013; Guo et al., 2015). Decarboxylation and deamination usually occur simultaneously, and the extent of decarboxylation/deamination could be affected by the type of amino acid, the pH of reaction medium, operating condition (Changi et al., 2015). Based on the chemical compositions analysis of both bio-crude oils and aqueous phase, a possible reaction pathway of liquefaction of algal biomass may be proposed and illustrated in Fig. 6.10.
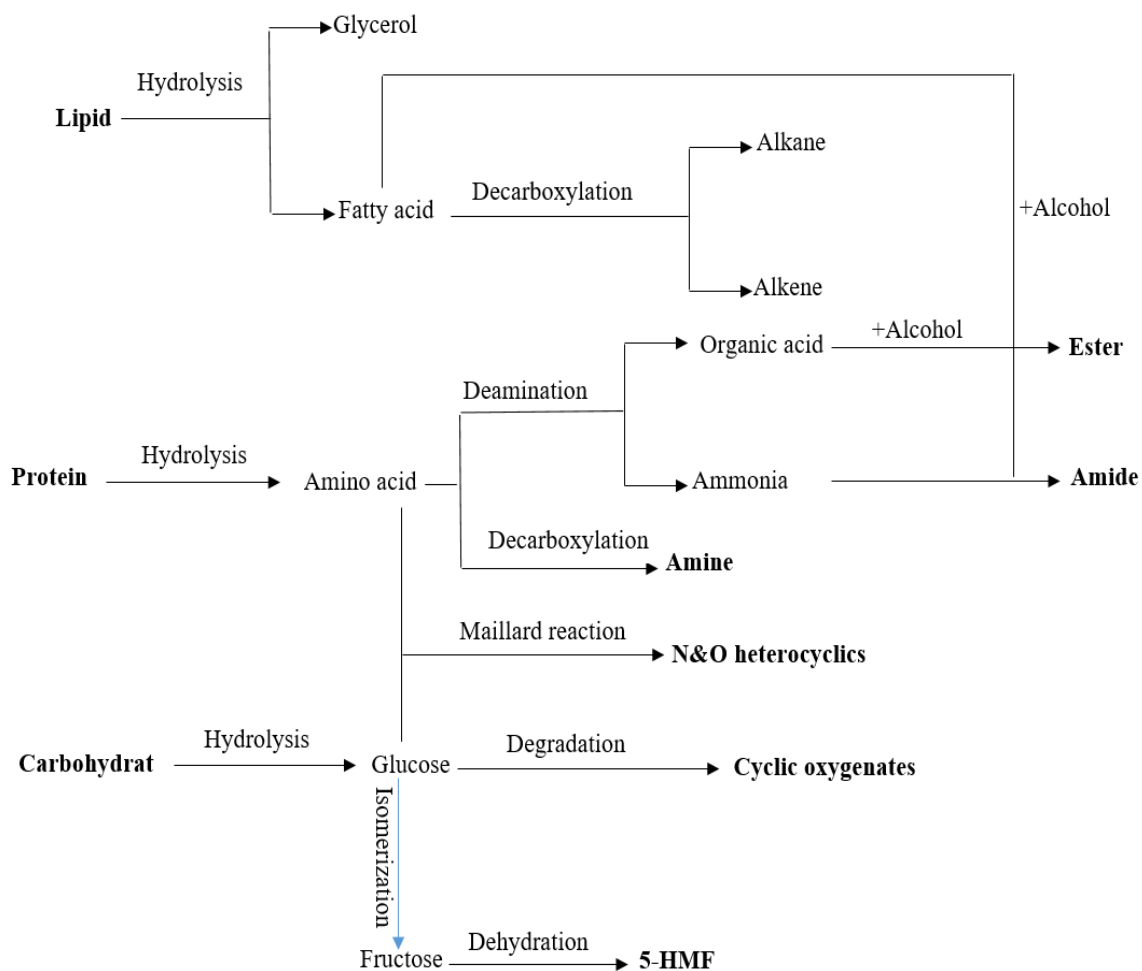
Figure 6-9: The proposed reaction pathway of liquefaction of algal biomass.

6.4.5 Solid residue characterization

Table 6.3 summarizes the elemental compositions and HHVs of solid residue samples obtained at 225 °C for 60 min, with a biomass/solvent mass ratio of 1/5 in methanol-water mixed solvents with various methanol contents. As clearly shown in the Table 6.3, increasing the methanol content in the reaction medium produced solid residues with lower carbon, hydrogen, and nitrogen contents but higher oxygen content, hence resulting in the reduced HHV (decreasing from 30.47 MJ/kg with pure water medium to 9.97 MJ/kg with pure methanol medium). Besides, the nitrogen contents of all solid residues were observed to be as high as 5.5-7.8 wt%, making them an attractive option for the application as a soil amendment (Shakya et al., 2015).

Table 6-3: The elemental compositions of solid residue samples obtained in methanol-water mixed solvents with various methanol contents at 225 °C for 60 min, with a biomass/solvent mass ratio of 1/5.

Elemental composition (wt.%)	Methanol content in reaction medium (wt.%)				
	0	25	50	75	100
C	65.05	63.73	55.91	40.29	37.85
H	8.38	8.08	6.96	5.56	4.49
O[a]	18.53	20.10	29.39	47.50	51.47
N	7.83	7.81	7.48	6.37	5.53
S	0.21	0.29	0.26	0.28	0.66
HHV (MJ/kg)[b]	30.67	29.52	23.62	13.11	10.08
Atomic ratio (mol/mol)					
H/C	1.55	1.52	1.49	1.66	1.42
O/C	0.21	0.24	0.39	0.88	1.02
N/C	0.10	0.11	0.11	0.14	0.13

[a] Determined by difference; [b] Calculated by the Dulong equation.

6.5   Conclusions

In this study, algal biomass, *Chlorella*, was converted into bio-crude oil products as potential advanced bio-fuels via direct liquefaction in water with/without catalyst, methanol or water-methanol mixed solvents. The screening tests showed that the methanol was the most effective reaction medium from the perspective of bio-crude oil yield. In addition, the effects of other reaction conditions (residence time, biomass/solvent mass ratio, reaction temperature, and methanol-water composition) on the products distribution were investigated. The highest bio-crude oil yield of 85.5 wt.% was obtained at 225 °C, for 60 min, with biomass/solvent mass ratio of 1/5, and in pure methanol. The HHVs of the obtained bio-crude oils are in the range of 30.4-33.9 MJ/kg. Both GC-MS and FTIR analyses evidenced that the bio-crude oils obtained in methanol primarily contained various fatty acid esters, suggesting the esterification reactions between fatty acids from algal biomass and the alcohol in the reaction medium during the liquefaction process.

6.6 References

Anastasakis K, Ross AB. Hydrothermal liquefaction of the brown macro-alga *Laminaria saccharina*: effect of reaction conditions on product distribution and composition. Bioresour Technol 2011; 102:4876-4883.

Akhtar J, Amin NAS. A review on process conditions for optimum bio-oil yield in hydrothermal liquefaction of biomass. Renew Sustainable Energy Rev; 2011; 15: 1615-1624.

Barreiro DL, Prins W, Ronsse F, Brilman W. Hydrothermal liquefaction (HTL) of microalgae for biofuel production: state of the art review and future prospects. Biomass Bioenergy; 2013; 53:113-127.

Brown TM, Duan PG, Savage PE. Hydrothermal liquefaction and gasification of *Nannochloropsis sp*. Energy Fuels; 2011; 24: 3639-3646.

Biller P, Ross AB. Potential yields and properties of oil from the hydrothermal liquefaction of microalgae with different biochemical content. Bioresource Technol; 2011; 102:215-225.

Bligh EG, Dyer WJ. A rapid method of total lipid extraction and purification. Can J Biochem Physiol; 1956; 37; 911-917.

Bi ZT, Zhang J, Peterson E, Zhu ZY, Xia CJ, Liang YN, Wiltowski T. Biocrude from pretreated sorghum bagasse through catalytic hydrothermal liquefaction. Fuel; 2017; 188; 112-120.

Biswas B, Kumar AA, Bisht Y, Singh R, Kumar J, Bhaskar T. Effects of temperature and solvent on hydrothermal liquefaction of *Sargassum tenerrimum* algae. Bioresour Technol; 2017; 242: 344-350.

Chen Y, Wu YL, Zhang PL, Hua D, Yang MD, Li C, Chen Z, Liu J. Direct of liquefaction of *Dunaliella tertiolecta* for bio-oil in sub/supercritical ethanol-water. Bioresource Technol; 2012; 124: 190-198.

Cheng S, Dcruz I, Wang_M, Leitch M, Xu C. Highly Efficient Liquefaction of Woody Biomass in Hot-compressed Alcohol-Water Co-solvents. Energy Fuels 2010; 24: 4659–4667.

Changi SM, Faeth JL, Mo N, Savage PE. Hydrothermal reactions of biomolecules relevant for microalgae liquefaction. Ind Eng Chem Res 2015; 54:11733-11758.

Duan PG, Jin BB, Xu YP, Yang Y, Bai XJ, Wang F, Zhang L, Miao J. Thermo-chemical conversion of *Chlorella pyrenoidosa* to liquid biofuels. Bioresource Technol; 2013; 133: 197-205.

Dote Y, Inoue S, Ogi T, Yokoyama SY. Distribution of nitrogen to oil products from liquefaction of amino acids. Bioresour Technol 1998; 64:157-160.

Guo Y, Yeh T, Song WH, Xu DH, Wang SZ. A review of bio-oil production from hydrothermal liquefaction of algae. Renew Sustainable Energy Rev; 2015; 48: 776-790.

Gai C, Zhang YH, Chen WT, Zhou Y, Schideman L, Zhang P, Tommaso G, Kuo CT, Dong YP. Characterization of aqueous phase from the hydrothermal liquefaction of *Chlorella pyrenoidosa*. Bioresour Technol; 2015; 184: 328-335.

Guo SQ, Dong XY, Zhu CX, Han YY, Wang ZZ. A simple modeling approach for characteristics analysis of hydrothermal liquefaction products from low-lipid aquatic plants. Appl Therm Eng 2017; 125: 394-400.

Guo S, Dong X, Wu T, Shi F, Zhu C. Characteristics evolution of hydrochar from hydrothermal carbonization of corn stalk. J Anal Appl Pyrolysis 2015; 116: 1-9.

Hu YL, Feng SH, Yuan ZS, Xu CB, Bassi A. Investigation of aqueous phase recycling for improving bio-crude oil yield in hydrothermal liquefaction of algae. Bioresour Technol; 2017; 239; 151-159.

Ji CH, He ZX, Wang Q, Xu GS, Wang S, Xu ZX, Ji HS. Effect of operating conditions on direct liquefaction of low-lipid microalgae in ethanol-water co-solvent for bio-oil production. Bioresource Technol; 2017; 141: 155-162.

Jin BB, Duan PG, Zhang CC, Xu YP, Zhang L, Wang F. Non-catalytic liquefaction of microalgae in sub- and supercritical acetone. Chem Eng J; 2014; 254: 384-392.

Jiang X, Zhao T, Shi Y, Wang J, Li J, Yang H. H_2SO_4 and NaOH pretreatment to enhance bio-oil yield of pine wood liquefaction in methanol. BioResources 2017; 12:3801-3815.

Kim DY, Vijayan D, Praveenkumar R, Han JI, Lee K, Park JY, Chang WS, Lee JS, Oh YW. Cell-wall disruption and lipid/astaxanthin extraction from microalgae. Bioresour Technol 2016; 199: 300-310.

Knothe G. Dependence of biodiesel fuel properties on the structure of fatty acid alkyl esters. Fuel Process Technol 2005; 86: 1059-1070.

Lardon L, Helias A, Sialve B, Stayer JP, Bernard O. Life-cycle assessment of biodiesel production from microalgae. Environ Sci Technol; 2009; 43: 6475-6481.

Lee SY, Cho JM, Chang YK, Oh YK. Cell disruption and lipid extraction for microalgal biorefineries: a review. Bioresour Technol 2017; 244:1317-1328.

Muppaneni T, Reddy HK, Selvaratnam T, Dandamudi KPR, Dungan B, Nirmalakhandan N, Schaub T, Holguin FO, Voorhies W, Lammers P, Deng SG. Hydrothermal liquefaction of *Cyanidioschyzon merolae* and the influence of catalyst on products. Bioresource Technol; 2017; 223: 91-97.

Overend RP, Chornet E. Fractionation of lignocellulosics by steam-aqueous pretreatment. Philos R Soc Lond Ser A 1987; 321: 523-536.

Peng XW, Ma XQ, Lin YS, Wang XS, Zhang XS, Yang C. Effect of process parameters on solvolysis liquefaction of *Chlorella pyrenoidosa* in ethanol-water system and energy evaluation. Energy Convers Manage. 2016; 117:43-53.

Pham M, Schideman L, Scott J, Rajagopalan N, Plewa MJ. Chemical and biological characterization of wastewater generated from hydrothermal liquefaction of *Spirulina*. Environ Sci Technol; 2013; 47: 2131-2138.

Reddy HK, Muppaneni T, Ponnusamy S, Sudasinghe N, Pegallapati A, Selvaratnam T, Seger M, Dungan B, Nirmalakhandan N, Schaub T, Holguin FO, Lammers P, Voorhies W, Deng SG. Temperature effect on hydrothermal liquefaction of *Nannochloropsis gaditane* and *Chlorella sp*. Appl Energy 2016; 165: 943-951.

Ross AB, Biller P, Kubacki ML, Li H, Lea-Langton A, Jones JM. Hydrothermal processing of microalgae using alkali and organic acids. Fuel; 2010; 89: 2234-2243.

Rebolloso-Fuentes MM, Navarro-Pérez A, García-Camacho F, Ramos-Miras JJ, Guil-Guerrero JL. Biomass nutrient profile of the microalga *Nannochloropsis*; 2001; 49; 2966-2972.

Shakya R, Whelen J, Adhikari S, Mahadevan R, Neupane S. Effect of temperature and Na$_2$CO$_3$ catalyst on hydrothermal liquefaction of algae. Algal Res; 2015; 12:80-90.

Socrates G. Infrared characteristic group frequencies. 2 nd ed. Hoboken, NJ: John Wiley and Sons; 1994.

Srivastava G, Paul AK, Goud VV. Optimization of non-catalytic transesterification of microalgae oil to biodiesel under supercritical methanol condition. Energy Convers Manag 2018; 156: 269-278.

Xu YF, Zhang XJ, Yu HQ, Hu XG. Hydrothermal liquefaction of *Chlorella pyrenoidosa* for bio-oil production over Ce/HZSM-5. Bioresour Technol 2014; 156: 1-5.

Yang WC, Li XG, Liu SS, Feng LJ. Direct hydrothermal liquefaction of undried macroalgae *Enteromorpha prolifera* using acid catalyst. Energy Convers Manage; 2014; 87: 938-945.

Yu G, Zhang YH, Schideman L, Funk T, Wang ZC. Distribution of carbon and nitrogen in the products from hydrothermal liquefaction of low-lipid microalgae. Energy Environ Sci; 2011; 4; 4587-4595.

Yuan XZ, Wang JY, Zeng GM, Huang H, Pei XK, Li H, Liu ZF, Cong MH. Comparative studies of thermochemical liquefaction characteristics of microalgae using different organic solvents. Energy; 2011; 6406-6412.

Zou SP, Wu YL, Yang MD, Li C, Tong JM. Thermochemical catalytic liquefaction of the marine microalgae *Dunaliella tertiolecta* and characterization of bio-oils. Energy Fuels; 2009; 23; 3753-3758.

Zhou D, Zhang SC, Fu HB, Chen JM. Liquefaction of macroalgae *Enteromorpha prolifera* in sub-/supercritical alcohols: direct production of ester compounds. Energy Fuels; 2012; 26; 2342-2351.

Chapter 7

7 Improvement in bio-crude production through co-liquefaction of algal biomass and sawdust in ethanol-water mixed solvents

The information presented in this Chapter is based on the paper "Improvement in bio-crude production through co-liquefaction of algal biomass and sawdust in ethanol-water mixed solvents", which has been submitted to *Energy Conversion and Management*. The sections in Chapter 7 present the results towards the completion of objective 5 of this PhD project (see Section 1.2).

7.1   Abstract

This study investigated co-liquefaction of algal biomass (AB) and sawdust (SD) in ethanol-water mixed solvent for bio-crude production. Effects of temperature (200-300 °C), residence time (30-120 min), ethanol-water mixed solvent composition (0/100-100/0 wt/wt), and AB/SD mass ratio (0/100-100/0) on the products distribution were explored. The results indicated that both AB/SD and ethanol/water exhibited positive synergistic effects on the co-liquefaction process. The highest bio-crude yield of 58 wt.% was obtained from co-liquefaction of AB and SD (50/50, wt/wt) in ethanol-water (75/25, wt/wt) mixed solvent at 250 °C for 60 min. In addition, the bio-crude from co-liquefaction contained a higher fraction of light oil components than that obtained using AB or SD as feedstock. Aqueous by-product from co-liquefaction was recycled and reused as reaction medium, which results in a bio-crude product at a comparable yield and a greater heating value (HHV of 34.8 MJ/kg).

7.2   Introduction

Due to the shortage of fossil fuels and severe environmental issues, bio-fuels from renewable resources have gained increasing attention. Generally, bio-fuels can be classified into first, second, and third generation categories. First and second-generation bio-fuels can be produced from food crops (e.g., corn, soybean, and sugarcane) and non-

food crops (e.g., rice husk and wood chip), respectively. While, the development of first and second-generation bio-fuels are limited owing to the land availability and competition with crop production (Duan et al., 2013). Recently, algae as third-generation biomass have been widely applied for the production of liquid fuels. Algae have several advantages, such as high growth rate, high lipid content, be able to sequester atmospheric CO_2, and can be cultivated in non-arable land (Guo et al., 2015).

Until now, numerous technologies have been developed for converting algal biomass into renewable fuels, including transesterification (López et al., 2016), pyrolysis (Andrade et al., 2018), and hydrothermal liquefaction (Jena et al., 2011). Compared to conventional technologies, hydrothermal liquefaction (HTL) has been identified as a more suitable conversion route for high water-containing feedstocks, due to the elimination of drying/dewatering the feedstock. Typically, HTL is carried out in sub- or near-critical water at 250-350 °C and 5-15 MPa for 5-120 min with or without catalyst (Peng et al., 2016). Recently, some researchers have co-liquefied algae and lignocellulosic biomass in subcritical water (Gai et al., 2015; Chen et al., 2014). For instance, Gai et al. (2015) investigated co-liquefaction of *C. pyrenoidosa* and rice husk at 200-350 °C for 10-90 min and found positive synergistic effects existed in the co-liquefaction of *C. pyrenoidosa* and rice husk in terms of higher quantity and quality of bio-crude.

Most previous studies have employed water as liquefaction medium, which is based on the unique properties of water under hydrothermal conditions. The ionic product (K_w) of water increases with increasing temperature and pressure, thereby promoting acid- or base-catalyzed reactions like biomass hydrolysis. Meanwhile, the dielectric constant of water decreases from 78 F m^{-1} at 25 °C and 0.1 MPa to 14.07 F m^{-1} at 350 °C and 20 MPa, making water molecules more affinitive to organic compounds (Toor et al., 2011). However, there remain several limitations regarding the use of water. Previously, Yang et al. (2004) reported that more than half of C and H in the feedstock was favorable to migrate into water phase rather than oily phase. For this reason, various organic solvents (e.g., ethanol, methanol, acetone, and 1,4-dioxane, etc.) have been applied for algal

liquefaction (Duan et al., 2013; Yuan et al., 2011; Jin et al., 2014). Among them, ethanol is reported to be the most desirable reaction medium, which can be explained as follows, (i) enhanced degradation of macromolecules due to a lower dielectric constant than water (Chen et al., 2012); (ii) can act as a hydrogen donor solvent (Akhtar and Amin, 2011); (iii) can achieve a high bio-crude yield at mild operating conditions (Duan et al., 2013); and (iv) can be derived from renewable sources (Chen et al., 2012). In literature, the ethanol-water mixed solvent has demonstrated positive effects on the liquefaction of microalgae with respect to bio-crude yield (Peng et al., 2016; Chen et al., 2012; Ji et al., 2017). Ji et al. (2017) studied the effect of ethanol-water mixed solvent composition on the products distribution from liquefaction of *Spirulina* at 300 °C for 45 min. It was reported that the bio-crude yield reached its maximum level when the liquefaction was conducted in ethanol-water (75/25, v/v) mixed solvent. Hence, in this study, the ethanol-water mixed solvent rather than pure ethanol was introduced into liquefaction system. As cited in the literature, water phase recycling plays a crucial role in the industrial-scale implementation of liquefaction treatment (Biller et al., 2016). In the previous studies, Ramos-Tercero et al. (2015) and Hu et al. (2017) demonstrated the feasibility of reusing water phase from HTL of algae as liquefaction medium for improving bio-crude production.

To fill the above knowledge gaps in the literature, co-liquefaction of algal biomass (AB) and sawdust (SD) was carried out in the ethanol-water mixed solvent. According to an assessment by Natural Resources Canada at 2013, around half of the landscape of Canada is covered by forests. Sawdust identified as a typical forestry residue appear to be good alternative resources for fuels production, since they are available in large quantities and at low price (Dimitriadis and Bezergianni, 2017). Initially, the effects of temperature, residence time, ethanol-water mixed solvent composition, and AB/SD mass ratio on the products distribution were investigated. Afterwards, the physiochemical properties of bio-crude and solid residue were characterized. Finally, the aqueous by-product was recycled and reused as reaction medium for bio-crude oil production.

7.3   Materials and methods

7.3.1   Materials

Algal biomass (AB), Chlorella with cracked cell wall in powder form (0.2 mm particle size), was purchased from PureBulk, Inc (Roseburg, USA). Aspen wood sawdust (SD) was supplied from a lumber mill (Thunder Bay, Canada), with the pre-treatment of crushing and sieving to 0.5 mm particle size. Dichloromethane (DCM) and ethanol were purchased from Caledon Laboratory Ltd (Georgetown, Canada). The characteristics of AB and SD were summarized in Table 7.1.

Table 7-1: Proximate and elemental analysis of algal biomass and sawdust.

	Algal biomass	Sawdust
Proximate analysis (wt.%)		
Moisture	3.48 ± 0.62	0.38 ± 0.05
Ash	7.15 ± 0.10	0.58 ± 0.10
Elemental analysis (%)[a]		
C	46.54	48.12
H	7.37	6.91
O^b	29.87	44.32
N	8.59	0.07
S	0.48	0.00
H/C	1.90	1.72
O/C	0.48	0.69
N/C	0.16	0.00
HHV (MJ/kg)[c]	20.97	18.22

[a] On dry basis; [b] Determined by difference; [c] Calculated by DuLong equation.

7.3.2   Experimental procedure

The co-liquefaction experiments were performed in a 100 mL benchtop autoclave reactor coupled with a magnetic stirrer (Parr 4590, Moline, USA). In a typical run, 3.0 g of the mixed feedstock (AB+SD) and 30.0 g of ethanol-water mixed solvent were loaded into the reactor. The reactor was tightly closed and flushed with pure nitrogen to remove residual air inside the reactor. After that, pure nitrogen at 0.69 MPa was purged into the reactor to prevent the mixed reaction medium from boiling during the heating process. The reactor was then heated up to the pre-set temperature at a heating rate of ~5 °C/min. This temperature was then kept for a designated residence time. The agitation speed was set at ~250 rpm throughout the whole co-liquefaction process. The reaction conditions investigated in this study were as follows: temperatures (200 °C, 225 °C, 250 °C, 275 °C, and 300 °C), residence times (30 min, 60 min,90 min, and 120 min), ethanol-water mixed solvent compositions (0/100, 25/75, 50/50, 75/25, and 100/0 w/w,), and AB/SD mass ratios (0/100, 25/75, 50/50, 75/25, and 100/0).

At end of the reaction, the reactor was quenched in a water bath. After the reactor was cooled to room temperature, the gaseous products inside the reactor were vented through a control valve into fume hood. The yield of gaseous products main consisting of CO_2 was found to be negligible under the conditions tested in our preliminary experiments, so the gases were not analyzed in this work. The reaction mixture was collected from the reactor by washing with a proper amount of ethanol, followed by filtration to separate the solid residue. The solid residue was then dried in an oven at 105 °C for 24 h. The filtrate was transferred to a 500 mL round bottom flask to remove ethanol via rotary evaporation at 45°C under reduced pressure. Afterwards, the remaining mixture was transferred into a separatory funnel, and 100 mL of dichloromethane (DCM) was added to extract bio-crude. Leaving the upper layer containing water and aqueous by-product, the bottom layer was transferred into a 500 mL pre-weighed round-bottom flask to remove DCM using a rotary evaporator at 40°C under reduced pressure, and the remaining dark material was denoted as bio-crude.

Furthermore, a series of co-liquefaction experiments were conducted using the upper water layer as liquefaction medium instead of ethanol-water mixed solvent. The water phase recycling runs were only carried out at the optimal reaction conditions determined from this work.

The bio-crude and solid residue yield were expressed in wt.% and calculated on a dry basis. The combined yield of gas and aqueous phase was defined as "others yield", and simply determined by the weight difference. The energy recovery (%) of co-liquefaction process was calculated by Eqn. (1).

$$\text{Energy recovery (\%)} = \frac{HHV_{bio-crude} \times Weight_{bio-crude}}{HHV_{AB} \times Weight_{AB} + HHV_{SD} \times Weight_{SD}} \tag{7-1}$$

7.3.3   Analytic approaches

The moisture content was measured by drying the feedstocks in an oven at 105 °C overnight. The ash content was determined by combusting the dried feedstocks in a muffle furnace at 575 °C for at least 3 h until the weight reached a constant level. The particle size was analyzed using a particle size analyzer (HELOS/BF, Sympatec GmbH). The elemental analysis (CHNS) of raw material, bio-crude, and solid residue was performed via an elemental analyzer (Vario EL Cube, Elementar, Germany). The higher heating values (HHVs) of original biomass, bio-crude, and solid residue was calculated by Dulong equation [HHV (MJ/kg) = 0.338C + 1.428(H-O/8) + 0.095S] (Jin et al., 2014). The thermal degradation characteristics of feedstocks were analyzed by a thermogravimetric analyzer (Pris 1 TGA, Massachusetts, USA). TGA analysis was carried out in a N_2 flow at 30 mL/min from 30 °C to 800 °C at the heating rate of 10 °C/min, using dried feedstock samples. The functionalities of bio-crude samples were characterized with a FT-IR spectrometer (PerkinElmer, Massachusetts, USA) in the range of 4000-600 cm^{-1} at a resolution of 4 cm^{-1}. The average molecular weight (M_w and M_n) and polydispersity index (PDI = M_w/M_n) of bio-crude samples were measured on a Waters Breeze GPC-UV equipped with a Waters Styragel HR1 column and calibrated with polystyrene standards. The boiling point distribution of the obtained bio-crude oils

was estimated by TGA analysis with the same Pris 1 TGA instrument and operating conditions as earlier described. The chemical composition of aqueous phase was determined by GC-MS analysis (Agilent 7890 GC/5975 MS) using a similar GC temperature program, as previously described (Hu et al., 2017).

7.4   Results and discussion

7.4.1   Thermal degradation characteristics

The thermogravimetric (TG) and differential thermogravimetric (DTG) curves of AB, SD, and AB+SD (50/50, wt/wt) are displayed in Fig. 7.1 (a) and (b), respectively. Clearly, TG and DTG curves of AB and SD are significantly different from each other owing to their great differences in the chemical composition.

As shown in Fig. 7.1 (a and b), all feedstock samples exhibited three stages during the thermal degradation process. The first weight loss stage (Stage-I) was observed from 30 °C to 150 °C, possibly caused by the dehydration of feedstocks and the removal of light volatile compounds (Azizi et al., 2017). The second weight loss stage (Stage-II) from 150-600 °C accounts for the majority of the weight loss, which can be attributed to the degradation of major biomass biomolecules. The third weight loss stage (Stage- III) starts from 600 °C and ends at 800 °C. This stage exhibits slight weight loss of feedstocks, resulting from the decomposition of carbonaceous materials retained in the solid residue. Surprisingly, DTG curve of AB+SD is very similar to that of SD, while much differing from that of AB, as indicated in Fig. 7.1 (b). This suggests that the presence of SD might play a predominant role over AB in the devolatilization and co-liquefaction process.
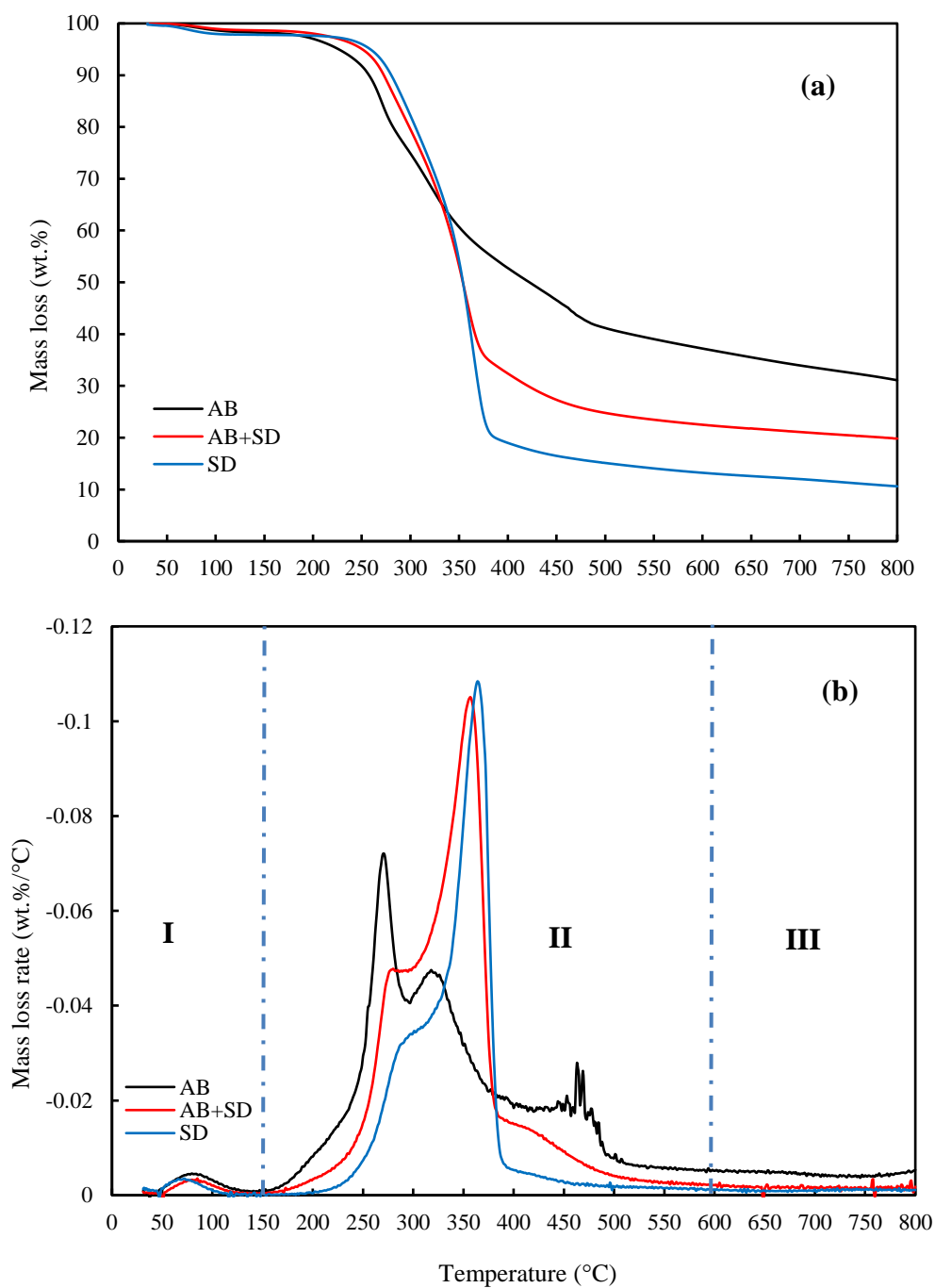
Figure 7-1: The thermogravimetric (TG) (a) and differential thermogravimetric (DTG) (b) curves for algal biomass (AB), sawdust (SD), and mixed feedstocks of AB+SD (50/50, wt/wt).

Specifically, in the case of AB, the first major weight loss began at 150 °C and ended at 295 °C, possibly caused by the degradation of carbohydrates (Ross et al., 2008). The second major weight loss representing the decomposition of protein ranged from 295 °C to 390 °C (Ross et al., 2008). The final weight loss stage occurred at 450 °C, which might be attributed to the degradation of lipid. On the other hand, hemicellulose decomposition occurs as a shoulder at 285 °C and the degradation of cellulose defined as a clear peak at 366 °C. This observance is consistent with the previous literature performing TGA analysis of woody biomass (Azizi et al., 2017). The peak of lignin (another main component of wood) decomposition cannot be seen in Fig. 7.1 (b). This is likely due to the fact that the lignin degradation usually appears on a wide temperature zone and thus may be not present (TranVan et al., 2014).

7.4.2 Effects of liquefaction conditions on the products distribution

7.4.2.1 Temperature

Effects of liquefaction temperature on the products distribution obtained from co-liquefaction of AB and SD (50/50, wt/wt) in ethanol-water (50/50, wt/wt) mixed solvent at 200-300 °C for 60 min were investigated. As illustrated in Fig. 7.2, the bio-crude yield increased from 32 wt.% to 51 wt.% as the reaction temperature increased from 200 °C to 250 °C, which is likely due to the enforced bond cessation and promoted hydrolysis of biomass macromolecules at higher temperatures (Akhtar and Amin, 2011). However, the bio-crude yield peaked at 250 °C, and a further increase in reaction temperature gradually decreased bio-crude yield from 47 wt.% at 275 °C to 27 wt.% at 300 °C. Such variation of bio-crude yield with HTL reaction temperature is in a good agreement with many earlier studies, e.g., by Jena et al. (2011). The reduced bio-crude yield at above 250 °C was likely caused by thermal cracking of oil compounds into gases and/or water-soluble products (Chen et al., 2012), as evidence by a sharp increase in the by-products yield (gases + aqueous solubles) from 39 wt.% at 275 °C to 55 wt.% at 300 °C. At a high temperature, thermal cracking of oil intermediates could also form lighter and more volatile oil compounds that however were unable to be recovered as they might be lost in

the solvent evaporation stage for bio-crude recovery. The yield of solid residue consistently decreased with increasing temperature from 200 °C until 275 °C, suggesting the promoted conversion of organics into liquefaction products (bio-crude, water-solubles, and gaseous products). In contrast, when the temperature further increased from 275 °C to 300 °C, the solid residue yield increased from 13 wt.% to 17 wt.%. This increased solid residue yield was probably attributed to the enhanced repolymerization of oil intermediates into solid products (Peng et al., 2016). According to the results above, it can be concluded that 250 °C appeared to be the best temperature for co-liquefaction of AB and SD in ethanol-water mixed solvents.
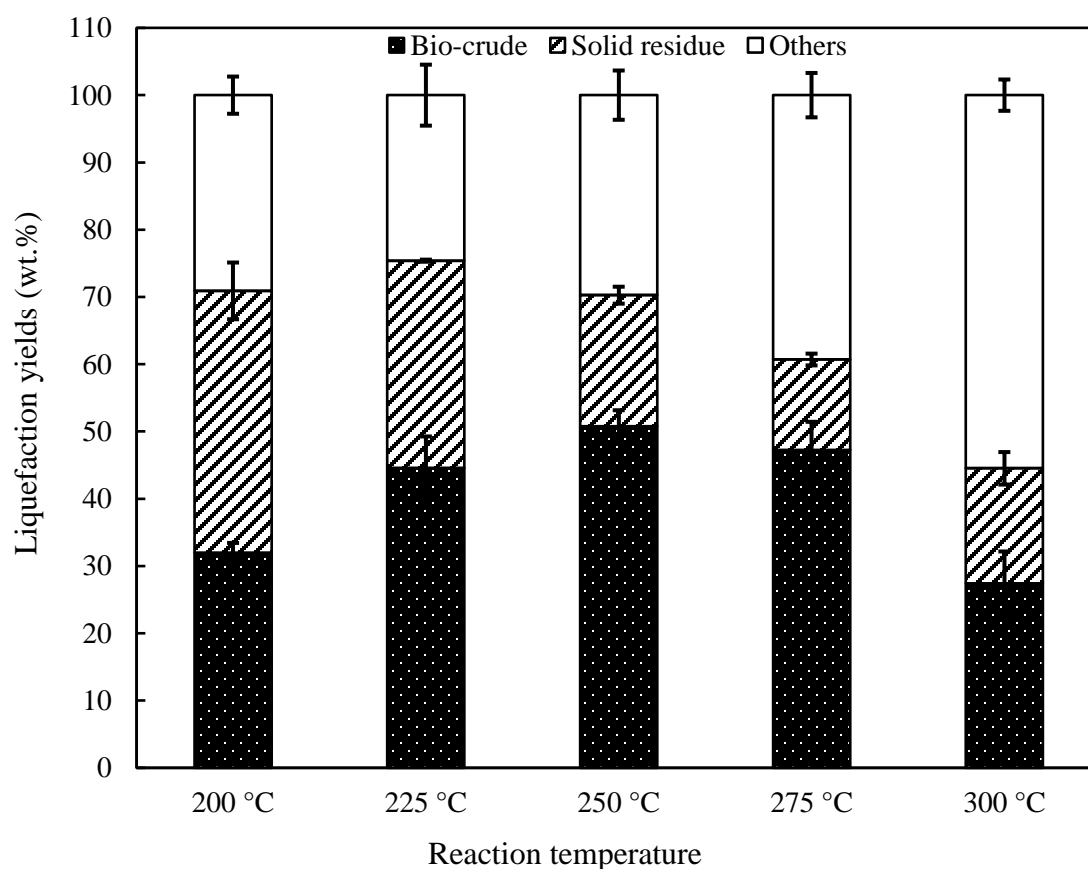
Figure 7-2: Effect of reaction temperature on the products distribution obtained from co-liquefaction of algal biomass (AB) and sawdust (SD) (50/50, wt/wt) in ethanol-water (50/50, wt/wt) mixed solvents at 200-300 °C for 60 min.

7.4.2.2   Residence time

Effects of residence time on the products distribution obtained from co-liquefaction of AB and SD (50/50, wt/wt) in ethanol-water (50/50, wt/wt) mixed solvent were explored at 250 °C for 30-120 min. As illustrated by Fig. 7.3, the bio-crude yield increased from 25 wt.% at 30 min to 51 wt.% at 60 min, but dropped to 30 wt.% when the residence time further increased till 120 min.
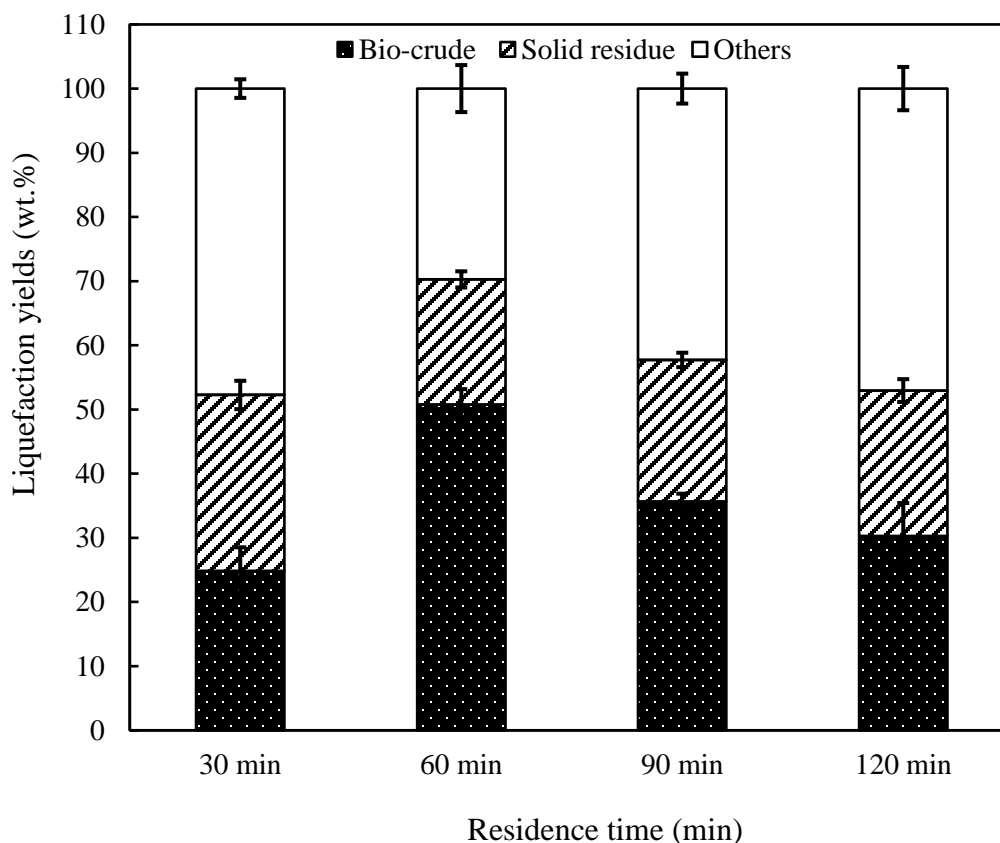
Figure 7-3: Effect of residence time on the products distribution obtained from co-liquefaction of algal biomass (AB) and sawdust (SD) (50/50, wt/wt) in ethanol-water (50/50, wt/wt) mixed solvents at 250 °C for 30-120 min.

This trend is consistent with those reported in previous investigations on the co-liquefaction (Gai et al., 2015; Jin et al., 2014). The reduced bio-crude yield at residence time might be attributed to the subsequent cracking (to form gaseous or light compounds)

and/or repolymerization (to form solid residues) of bio-crude at a prolonged residence time, as evidenced by the increasing of both yields of others (gaseous + aqueous products) and solid residues for a residence time longer than 60 min. For instance, the solid residue yield decreased from 27 wt.% at 30 min to 20 wt.% at 60 min, but increased to 23 wt.% at 120 min. Hence, 60 min was selected in further tests to investigate the effect of ethanol-water mixed solvent on the products distribution.

7.4.2.3   Ethanol-water mixed solvents composition

To determine the optimal ethanol-water mixed solvent composition, co-liquefaction experiments of AB and SD (50/50, wt/wt) were conducted at 250 °C for 60 min. As indicated in Fig. 7.4, it is clear that the bio-crude yields (20-58 wt.%) were higher with ethanol-water mixed solvent as reaction medium compared to that obtained in water (11 wt.%) or ethanol (29 wt.%) alone, and much higher than the predicted bio-crude yield based on the arithmetic average. This phenomenon may demonstrate the synergistic interaction between ethanol and water in the co-liquefaction process. Similar findings were also observed by Chen et al. (2012) and Ji et al. (2017). Specifically, the bio-crude yield increased from 11 wt.% to 58 wt.% with ethanol content in the mixture increased from 0 wt.% to 75 wt.%. This increase in bio-crude yield could be explained as follows: ethanol can readily dissolve relatively high molecular weight intermediates from biomass macromolecules due to its lower dielectric constant than water (Chen et al., 2012). On the other side, ethanol can act as a hydrogen donor solvent to stabilize the fragments and/or intermediates and deter the condensation, cyclization, and re-polymerization of free radicals to form char that retained in the solid residue (Akhtar and Amin, 2011). This can be confirmed with an apparent reduction in the solid residue yield from 31.3 wt.% to 20.1 wt.% when increasing the ethanol content in the mixed solvent from 0 wt.% to 75 wt.%. Whereas, further increase in ethanol content to 100 wt.% (pure ethanol) drastically reduced bio-crude yield to as low as 29 wt.%, accompanied by a sharp increase in the solid residue yield. This observance can be explained by the fact that ethanol is a weaker acid than water and thus the hydrolytic degradation of biomass might be limited in the liquefaction process with pure ethanol (Cheng et al., 2010). It is therefore concluded that

the ethanol-water (75/25, wt/wt) mixed solvent could be the most effective reaction medium in the co-liquefaction of AB and SD.
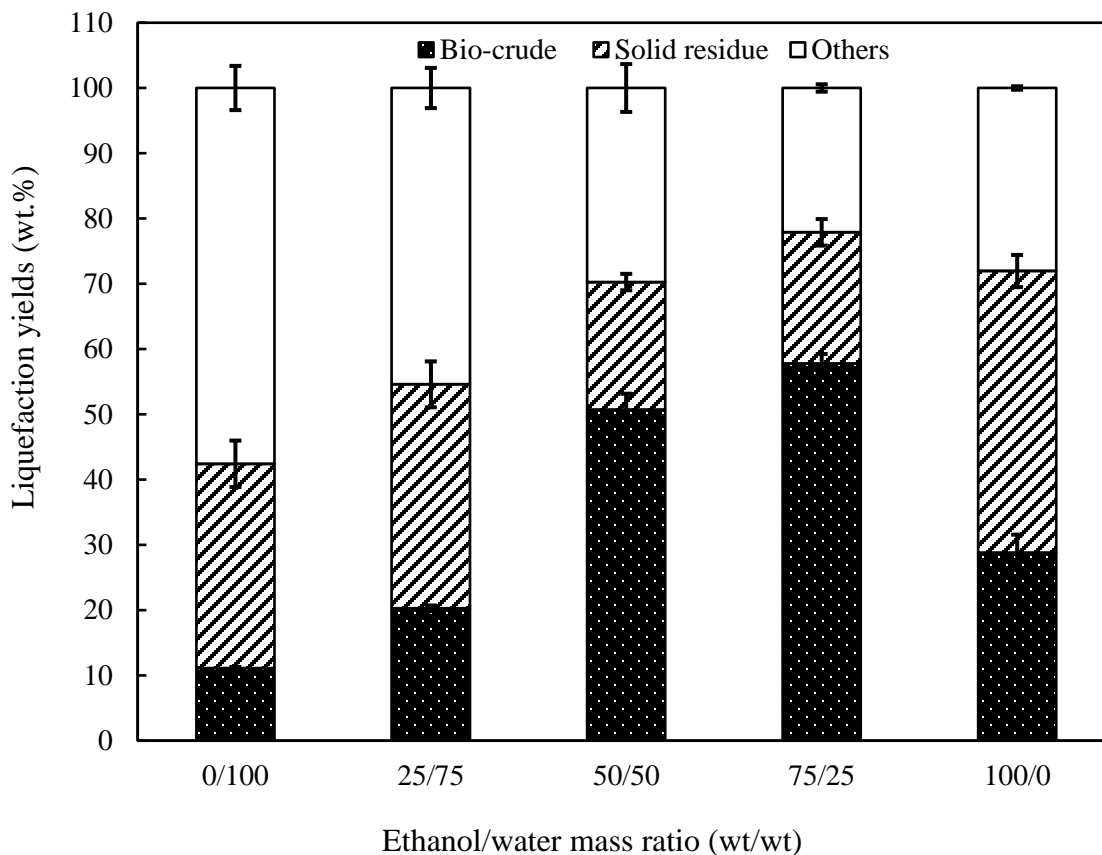
Figure 7-4: Effect of ethanol-water mixed solvents composition on the products distribution obtained from co-liquefaction of algal biomass (AB) and sawdust (SD) (50/50, wt/wt) at 250 °C for 60 min.

7.4.2.4   AB/SD mass ratio

Fig. 5 shows the effects of AB/SD mass ratio on the products distribution obtained from co-liquefaction of the mixture of AB and SD in ethanol/water mixed solvent (75/25, wt/wt) at 250 °C for 60 min. As clearly indicated in Fig. 7.5, the bio-crude yields (49-58 wt.%) were higher from co-liquefaction of AB and SD than those obtained from HTL of mono feedstock of either AB (46 wt.%) or SD (42 wt.%). Besides, the obtained oil yields from co-liquefaction process were higher than the predicted bio-crude yields based on the

arithmetic average. According to these results, it can be inferred that the synergistic interaction between AB and SD may be existed in the co-liquefaction process, which will be further discussed in the Section 3.3. Similar observances were reported in a previous study on the co-liquefaction of microalgae and rice husk (Gai et al., 2015). This could be due to the protein fraction of microalgae can be decomposed into acid compounds, which may facilitate the degradation of cellulose and hemicellulose fraction of sawdust. The bio-crude yield peaked at 58 wt.% with AB/SD mixture (50/50, wt/wt). On the other hand, the yield of solid residue continuously decreased from 31 wt.% (SD feedstock) to 7 wt.% (AB feedstock) when increasing mass percentage of AB in the mixed feedstocks from 0 wt.% to 100 wt.%.
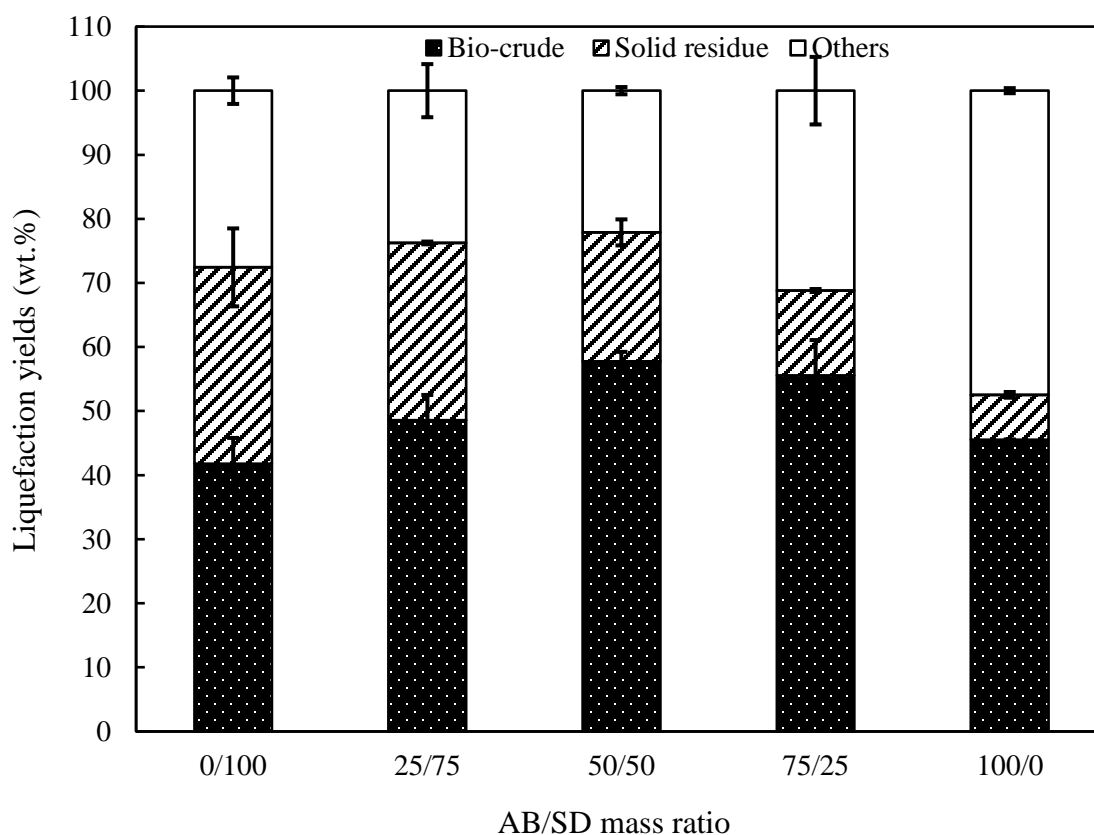
Figure 7-5: Effect of algal biomass (AB)/sawdust (SD) mass ratio on the products distribution obtained from co-liquefaction of AB and SD in ethanol-water (75/25, wt/wt) mixed solvents at 250 °C for 60 min.

7.4.3   Characterization of bio-crude

7.4.3.1   Elemental composition

The CHNS elemental compositions and HHVs of bio-crude oils obtained from co-liquefaction of AB and SD with various AB/SD mass ratios in ethanol/water (75/25, wt/wt) mixed solvent at 250 °C for 60 min are summarized in Table 7.2. In general, the C (62.6-66.8%) and H (7.2-9.4%) contents in all bio-crude oils are higher, accompanied by a lower O content (16.0-26.8%), than those in the feedstocks. As a result, all bio-crude oils have higher HHVs (27.7-33.2 MJ/kg) than the original feedstocks. In addition, the O/C atomic ratios of bio-crude samples were lower than two feedstocks, implying that partial deoxygenation appears in the liquefaction process. Oxygen can be removed as H_2O via dehydration or CO_2 via decarboxylation (Tian et al., 2014). As expected, the N/C ratios of bio-crude products were greater than the feedstock of SD but were lower than AB. During liquefaction process, the denitrogenation can proceed through deamination of amino acid (building block of protein) (Chen et al., 2014). In contrast, the H/C ratios of all bio-crude oils are lower than that of two feedstocks. Clearly, the N content of bio-crude oil was linearly proportional to the mass percentage of AB in the mixed feedstocks, along with an opposite trend for O content of the oils. This is expected due to the higher N content (8.6 wt.%) and lower O content (29.87 %) of AB than those of SD. The S contents in all bio-crude samples range from 0% to 0.2%, which is much lower than that of petroleum crude (0.1-2%) (Jena et al., 2011). Besides, HHVs of bio-crude produced from co-liquefaction are in the range of 28.3-32.1 MJ/kg, which are higher than those reported in a previous study where a mixture of swine manure and mixed-culture algae were co-liquefied (Chen et al., 2014). As also shown in Table 7.2, the highest energy recovery of 91.0% was obtained in the co-liquefaction of AB and SD (50/50, wt/wt), which is much greater than the average value calculated based on that of AB (72.0%) and SD (63.6%), again demonstrating the synergistic effects between AB and SD in the co-liquefaction process.

Table 7-2: Elemental compositions and HHVs of bio-crude oils obtained from co-liquefaction of algal biomass (AB) and sawdust (SD) with different mass ratios in ethanol-water (75/25, wt/wt) mixed solvents at 250 °C for 60 min.

Elemental composition (%)[a]	AB/SD mass ratio (w/w)				
	0/100	25/75	50/50	75/25	100/0
C	65.75	62.64	64.23	65.54	66.82
H	7.22	8.19	9.17	9.33	9.40
O[b]	26.84	25.87	22.10	18.69	16.02
N	0.19	3.30	4.50	6.43	7.61
S	0.00	0.00	0.00	0.01	0.15
H/C	1.32	1.57	1.71	1.71	1.69
O/C	0.31	0.31	0.26	0.21	0.18
N/C	0.00	0.05	0.08	0.08	0.10
HHV (MJ/kg)[c]	27.74	28.25	30.86	32.14	33.16
Energy recovery (%)[d]	63.63	72.60	91.00	88.08	72.01

[a] On dry basis; [b] Estimated by difference; [c] Calculated by DuLong equation; [d] Determined by Eqn. (7-1).

7.4.3.2　Boiling point distribution

The boiling point distributions of bio-crude oils obtained from co-liquefaction of algal biomass (AB) and sawdust (SD) with various mass ratios in ethanol-water (75/25, wt/wt) mixed solvent at 250 °C for 60 min are estimated from the TGA results and presented in Table 7.3. The bio-crude from SD contains the highest percentages of mild boiling point compounds (26 wt.%, bp 343-538 °C) and high boiling point compounds (31 wt.%, bp > 538 °C), along with the lowest percentage (~43 wt.%) of low boiling point compounds (bp < 343 °C). In general, the bio-crude oils from co-liquefaction had a higher percentage (51-73 wt.%) of low boiling point compounds than that from liquefaction of AB (58 wt.%) or SD (43 wt.%) alone, suggesting the co-liquefaction process promotes the

formation of light oil compounds. In addition, oil samples obtained from co-liquefaction of AB and SD were found to have the lowest percentage of high boiling point (15-30 wt.%) components. The distillable fraction (bp < 538 °C) of bio-crude from co-liquefaction is 70-85 wt.%, which is much higher that of conventional petroleum crude oil (e.g., 66 wt.% for Venezuelan crude, and 44-65 wt.% for North American tar sand bitumen) (Vardon et al., 2011).

Table 7-3: The boiling point distributions of bio-crude oils obtained using pure algal biomass (AB), AB/SD (50/50, wt/wt), or pure sawdust (SD) as feedstock in ethanol-water (75/25, wt/wt) mixed solvents at 250 °C for 60 min.

Distillate range (°C)[a]	AB/SD mass ratio				
	0/100	25/75	50/50	75/25	100/0
<193 (Heavy Naphtha)	18.88	16.97	20.70	16.75	13.59
193-271 (Kerosene)	10.77	16.37	35.72	20.95	26.94
271-343 (Gas Oil)	13.33	17.98	16.73	23.73	17.58
343-538 (Vac Gas Oil)	26.26	18.29	12.21	20.05	22.24
>538 (Residues)	30.76	30.39	14.64	18.51	19.66

[a] From Vardon et al. (2011).

7.4.3.3   Average molecular weight

The average molecular weights (M_w: weight average; M_n: number average) and polydispersity index (PDI = M_w/M_n) of bio-crude oils obtained from co-liquefaction of AB/SD with various mass ratios in ethanol-water (75/25 wt/wt) mixed solvent at 250 °C for 60 min were determined via GPC-UV. Fig. 7.6 presents the GPC curves of bio-crude oils.
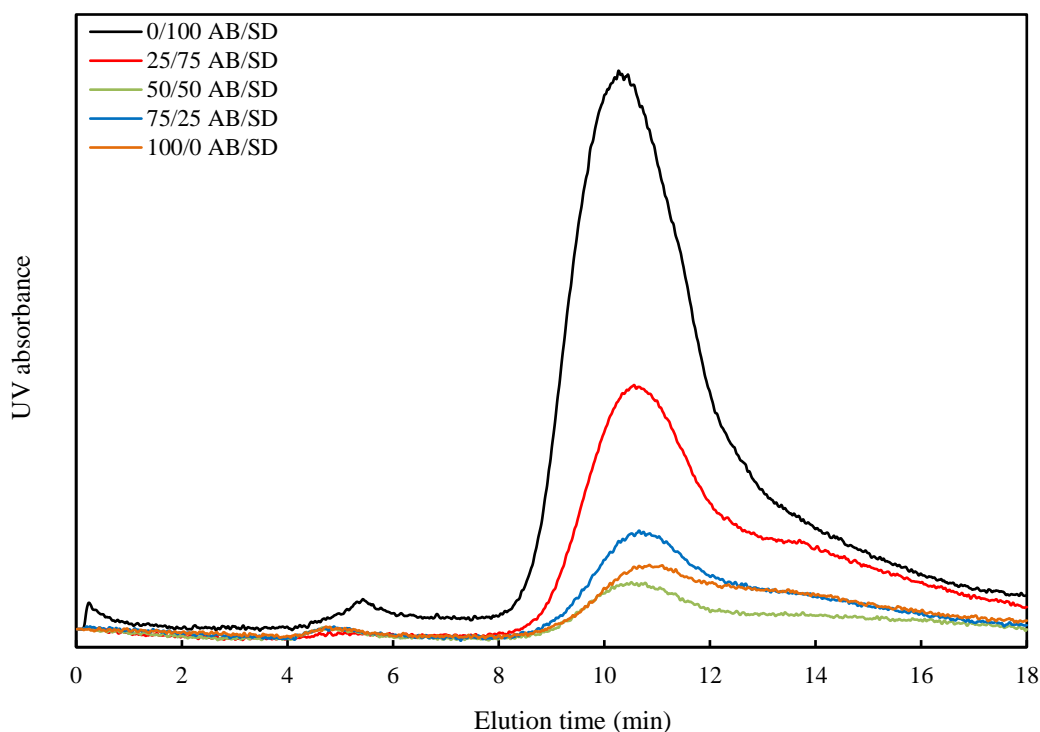
Figure 7-6: The average molecular weight of bio-crude oils obtained using pure algal biomass (AB), AB/SD (50/50, wt/wt), or pure sawdust (SD) as feedstock in ethanol-water (75/25 wt/wt) mixed solvents at 250 °C for 60 min.

As shown in Table 7.4, the bio-crude from AB has the smallest M_n (253 g/mol) and M_w (536 g/mol), and the oil from SD has the highest M_n (468 g/mol) and M_w value (957 g/mol), while the bio-crude obtained from co-liquefaction of AB and SD has average molecular weights falling in between (M_n: 299-325 g/mol and M_w: 671-723 g/mol). Although a high M_w of bio-crude could be attributed to polymer-linking functional groups such as esters and ethers in the bio-crude oils (Adjaye et al., 1992), the authors believe that the much higher M_w for the SD-derived oil is mainly due to the presence of lignin – a more complex and larger molecule in woody biomass, compared with protein, carbohydrates, and lipid in the AB (Nazari et al., 2017).

Table 7-4: Average molecular weight of bio-crude products obtained from co-liquefaction of algal biomass (AB) and sawdust (SD) with different AB/SD mass ratios in ethanol-water (75/25, wt/wt) mixed solvent at 250 °C for 60 min.

	AB/SD mass ratio				
	0/100	25/75	50/50	75/25	100/0
M_n (g/mol)	468	325	316	299	253
M_w (g/mol)	957	707	723	671	536
PDI[a]	2.04	2.18	2.29	2.24	2.12

[a] Calculated by M_w/M_n.

7.4.3.4   FT-IR analysis

FT-IR spectra of the bio-crude oils derived from co-liquefaction of AB/SD with various mass ratios in ethanol-water (75/25, wt/wt) mixed solvents at 250 °C for 60 min are displayed in Fig. 7.7. A broad peak between 3600 and 3000 cm^{-1} corresponding to O-H and N-H stretching vibration was observed in all oil samples. The peaks at 2963 cm^{-1}, 2924 cm^{-1}, and 2856 cm^{-1} may be related to the symmetrical and asymmetrical C-H stretching vibration. Another peak at 1709 and 1670 cm^{-1} can be ascribed to C=O stretching vibration. Besides, the peak at 1655 cm^{-1} can be related to C=O stretching vibration arising from primary amides. The peaks at 1608 cm^{-1} and 1515 cm^{-1} can be attributed to the aryl groups in aromatic compounds. The adsorption peaks at 1203 cm^{-1}, 1112 cm^{-1}, and 1047 cm^{-1} can be assigned to C-O stretching vibrations from tertiary, secondary, and primary alcohols, respectively. Finally, the peak at 760 cm^{-1} can be ascribed to C-H vibration from aromatics. Obviously, there are some distinct differences among the IR spectra of the bio-crude samples. A strong peak at 1709 cm^{-1} representing carbonyl C=O group from carboxylic acid can be only observed in the bio-crude obtained from SD, which combines with the existence of O-H group might indicate the presence of carboxylic acids in the bio-crude. Acids are reported to be one of the most common compounds in the bio-crude obtained from woody biomass (Adjaye et al., 1992). Besides, the peak at 1655 cm^{-1} corresponding to C=O vibration from amides was not detected in

the bio-crude obtained from liquefaction of SD alone, which is expected as the SD used contains negligible N (Table 7.1). The peaks at 1608 cm^{-1} and 1515 cm^{-1} relating to C=C aromatic ring vibration are less intensive in the bio-crude obtained from AB alone or the mixed feedstocks, whereas, an intensive peak 760 cm^{-1} representing C-H vibration from aromatic compounds can only be observed in the oil from SD due to the presence of lignin (phenolic polymer) in the woody biomass sample.
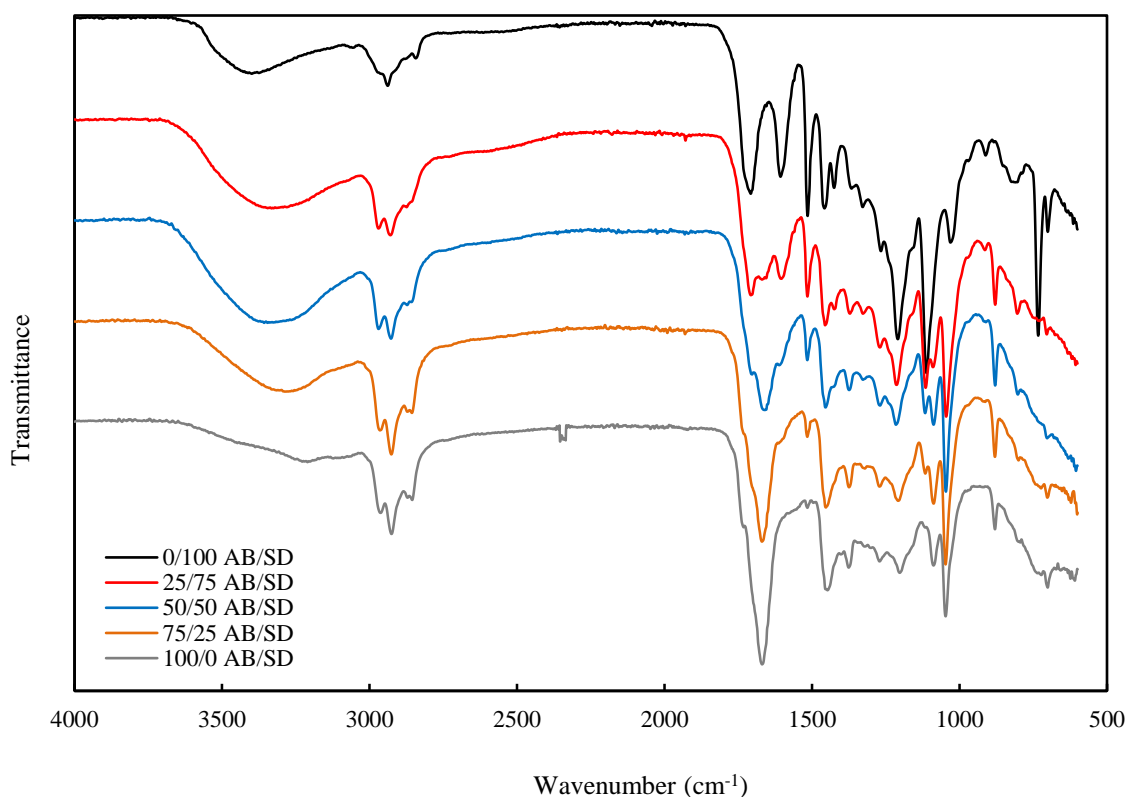
Figure 7-7: FT-IR spectra of bio-crude oils obtained using pure algal biomass (AB), AB/SD (50/50, wt/wt), or pure sawdust (SD) in ethanol-water (75/25, wt/wt) mixed solvents at 250 °C for 60 min.

7.4.4 Characterization of solid residue

The elemental compositions and HHVs of solid residues from co-liquefaction of mixed feedstocks with varying AB/SD mass ratios in ethanol-water (75/25, wt/wt) mixed solvent at 250 °C for 60 min are presented in Table 7.5. The C and H contents in the solid

residue gradually decrease with increasing mass percentage of AB in the mixed feedstocks, so does the HHVs, while the O and N contents in the solid residue exhibit an opposite trend. The solid residue obtained from SD alone has the highest HHV of 16.6 MJ/kg, close to that of the raw material (18.2 MJ/kg, Table 7.1).

Table 7-5: Elemental compositions and HHVs of solid residues obtained using pure algal biomass (AB), AB/SD (50/50, wt/wt), or pure sawdust (SD) as feedstock in ethanol-water (75/25, wt/wt) mixed solvents at 250 °C for 60 min.

Elemental composition (%)[a]	AB/SD mass ratio				
	0/100	25/75	50/50	75/25	100/0
C	46.55	47.41	45.96	44.79	35.00
H	6.48	6.39	5.40	5.51	3.83
O[b]	46.88	45.65	46.97	46.46	56.21
N	0.09	0.55	1.67	3.04	4.81
S	0.00	0.00	0.00	0.20	0.15
H/C	1.67	1.62	1.41	1.48	1.31
O/C	0.76	0.72	0.77	0.78	1.20
N/C	0.00	0.01	0.03	0.06	0.12
HHV (MJ/kg)[c]	16.62	17.00	14.86	14.73	7.28

[a] On dry basis; [b] Determined by difference; [c] Calculated by DuLong equation.

7.4.5 Aqueous phase recirculation studies

Recycling and reuse of aqueous phase (or process water) as liquefaction medium was investigated for co-liquefaction of AB/SD (50/50, wt/wt) at 250 °C for 60 min. As shown in Table 7.6, co-liquefaction in the recycled aqueous phase resulted in a bio-crude yield of 9.2 wt.% and solid residue yield of 38.9 wt.%, both comparable to those of the operation in water medium (11.1 wt.% and 31.3 wt.%, respectively).

Table 7-6: The products distribution and elemental compositions obtained from co-liquefaction of AB and SD (50/50, wt/wt) in recycled aqueous phase at 250 °C for 60 min.

Liquefaction yields (wt.%)	Recycled aqueous phase	Pure water		
Bio-crude	9.16 ± 2.17	11.13 ± 0.17		
Solid residue	38.93 ± 2.24	31.29 ± 3.56		
Aqueous phase & Gas[a]	51.90 ± 0.07	57.58 ± 3.39		
Elemental composition (wt.%)[b]	Recycled aqueous phase		Ethanol-water (75/25, wt/wt) mixed solvents	
	Bio-crude	Solid residue	Bio-crude	Solid residue
C	70.28	62.25	64.23	45.96
H	9.63	6.61	9.17	5.40
O[a]	15.46	26.95	22.10	46.97
N	4.57	4.12	4.50	1.67
S	0.06	0.07	0.00	0.00
H/C	1.64	1.27	1.71	1.41
O/C	0.16	0.32	0.26	0.77
HHV (MJ/kg)[c]	34.75	25.68	30.86	14.86

[a] Determined by difference; [b] On dry basis; [c] Calculated by DuLong equation.

The elemental compositions and HHV of bio-crude and solid residue from co-liquefaction of AB/SD (50/50, wt/wt) in both recycled aqueous phase and ethanol-water (75/25, wt/wt) mixed solvent at 250 °C for 60 min are compared in Table 7.6. Interestingly, HHV (34.8 MJ/kg) of bio-crude obtained using the recycled aqueous phase as liquefaction medium is higher than that (30.9 MJ/kg) of bio-crude obtained in ethanol-water (75/25, wt/wt) mixed solvent. The bio-crude obtained with recycled aqueous phase liquefaction medium has higher C and H contents and lower O content when compared with those of bio-crude obtained in ethanol-water mixed solvent (75/25, wt/wt), while there are not much differences in the N and S contents for the two bio-crude oils. As also shown in Table 7.6, the solid residue obtained from co-liquefaction in the recycled aqueous phase medium has higher C, H, and N contents and a lower O content, hence a greater HHV (25.7 MJ/kg), compared with the solid residue obtained in ethanol-water mixed solvent (75/25, wt/wt). The above results suggest that the aqueous by-product from the co-liquefaction can be potentially recycled and reused as an effective reaction medium for the co-liquefaction process to minimize the waste generation from the process.

The major chemical compounds (i.e., relative peak area>0.5% in the total peak area) of aqueous phase were identified using GC-MS analysis, as shown in Appendix-H. It should be noted that only a fraction of chemical compounds in the aqueous phase can be identified by the GC-MS since some high molecular weight compounds cannot be eluted into GC column. Some organic acids can be observed in the water phase. Acetic acid (RT. 3.73) is the dominant specie with a 11.33% of the total area. In literature, acetic acid is normally identified in the aqueous phase produced from HTL of lignocellulose (Zhu et al., 2015) or algal biomass (Hu et al., 2018). Besides, it can be found that the polyols are present in the aqueous phase, such as glycerol (RT. 9.76) and 1,2,3,4-butanetetrol, [S-(R*,R*)]- (RT. 9.84), which is possibly attributed to the polyol structure of cellulose and hemicellulose in the sawdust. Another reason could be due to the hydrolysis of lipid fraction in the algal biomass into glycerol (RT. 9.84). As expectedly, N-containing compounds are detected as the major compounds in the aqueous phase, possibly caused

by the degradation of protein in the co-liquefaction process. Among them, small amine compounds [e.g., 2-butanamine, (S)- (RT. 18.53)] can be observed in the aqueous phase, which could be resulted from the decarboxylation of amino acid.

7.5   Conclusions

In this study, co-liquefaction of algal biomass (AB) and sawdust (SD) in ethanol-water mixed solvent was investigated. The highest bio-crude yield of 57.8 wt.% was obtained from co-liquefaction of AB/SD (50/50, wt/wt) in ethanol-water (75/25, wt/wt) mixed solvent at 250 °C for 60 min. This work demonstrated the synergistic interactions between AB/SD feedstocks and ethanol/water mixed solvents in the co-liquefaction process. The co-liquefaction of AB/SD resulted in bio-crude oil containing a higher fraction of light oil components than those obtained from liquefaction of AB or SD alone. In addition, this work demonstrated that the aqueous by-product could be recycled and reused as reaction medium for the co-liquefaction process to minimize the waste generation from the process.

7.6   References

Andrade LA, Batista FRX, Lira TS, Barrozo MAS, Vieira LGM. Characterization and product formation during the catalytic and non-catalytic pyrolysis of the green microalgae *Chlamydomonas reinhardtii*. Renew Energ 2018; 119: 731-740.

Akhtar J, Amin NAS. A review on process conditions for optimum bio-oil yield in hydrothermal liquefaction of biomass. Renew Sustainable Energy Rev 2011; 15:1615-1624.

Azizi K, Moraveji MK, Najafabadi HA. Characteristics and kinetics study of simultaneous pyrolysis of microalgae Chlorella vulgaris, wood and polypropylene through TGA. Bioresour Technol 2017; 243: 481-491.

Adjaye JD, Sharma RK, Bakhshi NN. Characterization and stability analysis of wood-derived bio-oil. Fuel Process Technol 1992; 31:241-256.

Biller P, Madsen RB, Klemmer M, Becker J, Iversen BB, Glasius M. Effect of hydrothermal liquefaction aqueous phase recycling on bio-crude yields and composition. Bioresour Technol 2016; 220: 190-199.

Chen WT, Zhang YH, Zhang JX, Schideman L, Yu G, Zhang P, Minarick M. Co-liquefaction of swine manure and mixed-culture algal biomass from a wastewater treatment system to produce bio-crude oil. Appl Energy 2014; 128: 209-216.

Chen Y, Wu YL, Zhang PL, Hua DR, Yang MD, Li C, Chen Z, Liu J. Direct liquefaction of *Dunaliella tertiolecta* for bio-oil in sub/supercritical ethanol-water. Bioresour Technol 2012; 124: 190-198.

Cheng S, Dcruz I, Wang M, Leitch M, Xu C. Highly Efficient Liquefaction of Woody Biomass in Hot-compressed Alcohol-Water Co-solvents. Energy Fuels 2010; 24: 4659–4667.

Duan PG, Jin BB, Xu YP, Yang Y, Bai XJ, Wang F, Zhang L, Miao J. Thermo-chemical conversion of *Chlorella pyrenoidosa* to liquid biofuels. Bioresour Technol 2013; 133: 197-205.

Dimitriadis A, Bezergianni S. Hydrothermal liquefaction of various biomass and waste feedstocks for biocrude production: a state of the art review. Renew Sustainable Energy Rev 2017; 68: 113-125.

Guo Y, Yeh T, Song WH, Xu DH, Wang SZ. A review of bio-oil production from hydrothermal liquefaction of algae. Renew Sustainable Energy Rev 2015; 48: 776-790.

Gai C, Li Y, Peng NN, Fan A, Liu ZG. Co-liquefaction of microalgae and lignocellulosic biomass in subcritical water. Bioresour Technol 2015; 185: 240-245.

Hu YL, Feng SH, Yuan ZS, Xu CB, Bassi A. Investigation of aqueous phase recycling for improving bio-crude oil yield in hydrothermal liquefaction of algae. Bioresour Technol 2017; 239: 151-159.

Jena U, Das KC, Kastner JR. Effect of operating conditions of thermochemical liquefaction on biocrude production from *Spirulina platensis*. Bioresour Technol 2011; 102: 6221-6229.

Jin BB, Duan PG, Zhang CC, Xu YP, Zhang L, Wang F. Non-catalytic liquefaction of microalgae in sub- and supercritical acetone. Chem Eng J 2014; 254: 384-392.

Ji CH, He ZX, Wang Q, Xu GS, Wang S, Xu ZX, Ji HS. Effect of operating conditions on direct liquefaction of low-lipid microalgae in ethanol-water co-solvent for bio-oil production. Energy Convers Manag 2017; 141: 155-162.

López EN, Medina AR, Moreno PAG, Cerdán LE, Valverde LM, Grima EM. Biodiesel production from *Nannochloropsis gaditana* lipids through transesterification catalyzed *Rhizopus oryzae* lipase. Bioresour Technol 2016; 203: 236-244.

Nazari L, Yuan ZS, Ray MB, Xu CB. Co-conversion of waste activated sludge and sawdust through hydrothermal liquefaction: optimization of reaction parameters using response surface methodology. Appl Energy 2017; 203: 1-10.

Peng XW, Ma XQ, Lin YS, Wang XS, Zhang XS, Yang C. Effect of process parameters on solvolysis liquefaction of *Chlorella pyrenoidosa* in ethanol-water system and energy evaluation. Energy Convers Manag 2016; 117: 43-53.

Ramos-Tercero EA, Bertucco A, Brilman DWF. Process water recycle in hydrothermal liquefaction of microalgae to enhance bio-oil yield. Energy Fuels 2015; 29: 2422-2430.

Ross AB, Jones JM, Kubacki ML, Bridgeman T. Classification of macroalgae as fuel and its thermochemical behvaviour. Bioresour Technol 2008; 99:6494-6504.

Toor SS, Rosendahl L, Rudolf A. Hydrothermal liquefaction of biomass: a review of subcritical water technologies. Energy 2011; 36: 2328-2342.

TranVan L, Legrand V, Jacquemin F. Thermal decomposition kinetics of balsa wood: kinetics and degradation mechanism comparison between dry and moisturized materials. Polym Degrad Stab 2014; 110: 208-215.

Tian CY, Li BM, Liu ZD, Zhang YH, Lu HF. Hydrothermal liquefaction for algal biorefinery: a critical review. Renew Sustainable Energy Rev 2014; 38: 933-950.

Vardon DR, Sharma BK, Scott J, Yu G, Wang ZC, Schideman L, Zhang YH, Strathmann TJ. Chemical properties of biocrude oil from the hydrothermal liquefaction of Spirulina algae, swine manure, and digested anaerobic sludge. Bioresour Technol 2011; 102:8295-8303.

Yang YF, Feng CP, Inamori Y, Maekawa T. Analysis of energy conversion characteristics in liquefaction of algae. Resour Conserv Recycl 2004; 43: 21-33.

Yuan XZ, Wang JY, Zeng GM, Huang HJ, Pei XK, Li H, Liu ZF, Cong MH. Comparative studies of thermochemical liquefaction characteristics of microalgae using different organic solvents. Energy 2011; 36: 6406-6412.

Zhu Z, Rosendahl L, Toor SS, Yu DH, Chen GY. Hydrothermal liquefaction of barley straw to bio-crude oil: effects of reaction temperature and aqueous phase recirculation. Appl Energy 2015; 137: 183-192.

Chapter 8

8 Conclusions and future work

8.1 Conclusions

The aim of this work was to develop hydrothermal process for the cost-effective production of bio-crude oil from microalgae without the requirement of de-watering/drying. Initially, an alternative pre-treatment using a pre-cooled NaOH/urea solution was investigated in order to maximize energy recovery from microalgae. Based on this microalgal pre-treatment, a two-step HTL treatment was investigated for *C. vulgaris* with aims for producing a high-quality bio-crude oil. This project also demonstrated effectiveness of reusing the water phase from HTL of microalgae as a liquefaction medium for producing bio-crude oil, which yields great significance for the industrial-scale HTL applications. In addition, the effects of solvent, catalyst, residence time, biomass/solvent ratio, reaction temperature, and reaction medium composition on the direct liquefaction of microalgal biomass were explored. Finally, co-conversion of microalgae and lignocellulosic biomass was carried out in ethanol-water mixed solvents under various reaction conditions, and synergistic interaction between the two feedstocks and ethanol/water in the co-liquefaction were proved.

The following detailed conclusions could be drawn from this research:

- **In Chapter 3**, an alternative pre-treatment by cold NaOH/urea solvent was identified as an effective cell-disruption approach for microalgae.

- **In Chapter 4**, the pre-treated microalgae from NaOH/urea solvent pre-treatment resulted in a higher yield of bio-crude oil with a better quality.

- **In Chapter 5**, two catalysts including Na_2CO_3 and HCOOH did not exhibit positive effects on the bio-crude oil yield from *C. vulgaris*. Recycled aqueous phase from catalytic/non-catalytic HTL led to an increase in the bio-crude oil yield without affecting oil quality (i.e., heating value).

- **In Chapter 6**, methanol was determined as the most effective reaction medium for converting microalgae into bio-crude oil. A high bio-crude oil yield of 85.49 wt.% can be obtained from direct liquefaction of microalgal biomass in methanol at mild reaction conditions (i.e., 225 °C; 60 min).

- **In Chapter 7**, the synergistic interactions between microalgae/sawdust and ethanol/water can be observed in the co-liquefaction process. The aqueous by-product could be potentially reused as the reaction medium for bio-crude oil production.

8.2   Future work

- Cell wall structure and composition of microalgae are believed to have great effects on the cell disintegration rate during microalgae pre-treatment, but the relevant literature is still lacking (Scholz et al., 2014). As such, extensive research is required to obtain a deeper understanding of the relationships between cell wall characteristics and disruption efficiency.

- Although HTL has demonstrated to be a promising and cost-effective route for microalgae-to-fuels conversion, no large-scale production facility has been demonstrated due to some technical challenges, of which the most important are: (i) continuous pumping of solid-liquid mixtures to a high-pressure HTL rector in continuous operation mode can be difficult and energy-demanding, (ii) a high content of heteroatoms such as nitrogen and oxygen in microalgae-derived bio-crude oils requires additional upgrading treatment (such as hydro-processing) before they can be sued as a liquid transportation fuel.

- More value-added applications of microalgae-derived bio-crude oils for bio-based chemicals and polymer materials need to be explored. For example, a promising high-value utilization of microalgae-derived bio-crude oils can be as a carbon feedstock for Polyhydroxyalkanoates (PHAs) production via bio-conversion. PHAs are polyesters that are suitable for the production of bio-based and

biodegradable polymer (Andin et al., 2017). PHAs can be accumulated as intracellular carbon and energy reserve in a variety of microorganisms. PHAs can be categorized into two groups, namely, (i) short-chain length PHAs (scl-PHAs) consist of 3-hydroxy fatty acids of 3-5 carbon units, and (ii) medium-chain length PHAs (mcl-PHAs) are composed by 6-14 carbon units (Cruz et al., 2016). Previous studies have used vegetable oils mainly consisting of fatty acids as carbon substrate for mcl-PHA production using *Pseudomonas putida* (Andin et al., 2017; Cruz et al., 2016; Follonier et al., 2015). Long-chain fatty acids such as palmitic acid and linoleic acid are commonly identified in the microalgae-derived bio-crude oil. Hence, fatty acid-containing microalgal bio-crude oil was employed as feedstock for accumulating mcl-PHA by *Pseudomonas putida* KT2440 (ATCC 47054). In fact, we employed similar experiment procedure as reported by Andin et al. (2017), Cruz et al., (2016), and Brandl et al. (1998) and performed some preliminary work on bioconversion of microalgae-derived bio-crude oils for the production of PHAs, while the results are too preliminary to report in this thesis.

8.3   Contributions

- **In Chapter 3**, an alternative pre-treatment by cold NaOH/urea solvent was developed for microalgae.

- **In Chapter 4**, a two-step HTL technology combining with a cold NaOH/urea solvent pre-treatment demonstrated positive effects on the quantity and quality of bio-crude oil.

- **In Chapter 5**, the feasibility for improving the overall economy of catalytic HTL can be achieved through recycling the water phase as the reaction medium for producing bio-crude oil.

- **In Chapter 6**, the use of methanol as the reaction medium exhibits the beneficial effects on the bio-crude oil production from microalgae.

- **In Chapter 7**, very first study on investigating the co-liquefaction of microalgae and other lignocellulosic biomass in ethanol-water mixed solvents under various reaction conditions.

8.4   References

Andin N, Longieras A, Veronese T, Marcato F, Molina-Jouve C, Uribelarrea JL Improving carbon and energy distribution by coupling growth and medium chain length polyhydroxyalkanoate production from fatty acids by *Pseudomonas putida* KT2440. Biotechnol Bioprocess Eng 2017; 22: 308-318.

Brandl H, Gross RA, Lenz RW, Fuller RC. *Pseudomonas oleovorans* as a source of poly(β-hydroxyalkanoates) for potential applications as biodegradable polyesters. Appl Environ Microbiol 1988; 54: 1977-1982.

Cruz MV, Freitas F, Paiva A, Mano F, Dionisio M, Ramos AM, Reis MAM. Valorization of fatty acids-containing wastes and byproducts into short- and medium-chain length polyhydroxyalkanoates. N Biotechnol 2016; 33: 206-215.

Follonier S, Riesen R, Zinn M. Pilot-scale production of functionalized mcl-PHA from grape pomace supplemented with fatty acids. Chem Biochem Eng Q 2015; 29: 113-121.

Scholz MJ, Weiss TL, Jinkerson RE, Jing J, Roth R, Goodenough U, Posewitz MC, Gerken HG. Ultrastructure and composition of the *Nannochloropsis gaditana* cell wall. Eukaryot Cell 2014; 13: 1450-1464.

Appendices

Appendix-A: Major chemical compounds in the bio-crude oil obtained from pre-treated microalgae at 250 °C for 30 min using GC-MS.

RT[a]	Area (%)	Compounds
2.66	2.32	Pyrazine
3.54	2.03	Pyrazine, methyl-
8.40	1.13	Indole
10.07	1.05	3,7,11,15-Tetramethyl-2-hexadecene
10.12	1.55	1,11-Tridecadiene
10.39	1.70	1,4-Eicosadiene
10.53	1.02	6,6-Dimethyl-2-azaspiro[4.4]non-1-ene
10.86	1.73	Cyclohexanol, 2,6-dimethyl-
11.20	1.05	Cyclo(valylvalyl)
11.32	1.86	Isobutyraldehyde, propylhydrazone
11.42	2.41	l-Alanine, N-valeryl-, pentyl ester
11.53	1.59	3-Ethoxy-4-methoxyphenol
11.67	6.32	1-Butylimidazolidine-2,4-dione
11.87	5.38	l-Proline, N-allyloxycarbonyl-, hexyl ester
12.07	3.41	Phenol, 3,5-dimethoxy-
12.20	1.48	di-n-Decylamine
12.31	3.76	3-Nitroso-3-azabicyclo[3.2.2]nonane
12.37	6.59	Pyrrolo[1,2-a]pyrazine-1,4-dione, hexahydro-3-(2-methylpropyl)-
12.52	1.91	Methyl N-(cyclopropylcarbonyl)-L-leucinate
13.72	1.38	9,10-Ethanoanthracene-9(10H)-methylamine, N-methyl-, 9,10-dihydro
14.08	1.89	3-Benzyl-6-isopropyl-2,5-piperazinedione

14.55	1.07	Phenol, 2,2'-methylenebis[6-(1,1-dimethylethyl)-4-ethyl-

[a] Represents retention time (min).

Appendix-B: Major chemical compounds detected by GC-MS in the bio-crude oils obtained from HTL of raw and pre-treated microalgae (pre-treatment by pre-cooled NaOH/urea solution) at 250 ºC for 10 min.

RT[a]	Compounds	Area (%)	
		Oil from raw microalgae	Oil from the pre-treated microalgae
2.69	1,3,5-Hexatriene, (E)-		0.46
3.44	Pyrazine, methyl-		0.58
8.03	3,7,11,15-Tetramethyl-2-hexadecene		0.24
8.08	3-Eicosyne	1.12	
8.25	cis-Pinane		0.90
8.26	6,6-Dimethyl-2-azaspiro[4.4]non-1-ene	1.33	
8.35	1-Ethyl-2-undecylimidazole		0.39
8.36	Pinane	0.56	
8.58	Isophytol	0.74	0.62
8.62	1,3-Dimethyl-3,4,5,6-tetrahydro-2(1H)-pyrimidinone	1.51	0.99
8.89	Palmitic acid	6.92	8.24
8.94	7-Tetradecyne		14.83
8.94	8-Dodecen-1-ol, (Z)-	14.52	
9.01	2-Methoxy-2,3-dihydrofuran-3-carbaldehyde	2.98	2.55
9.10	3-Pyrrolidin-2-yl-propionic acid	1.75	
9.16	5-ethyl-5-pentan-2-yl-1,3-diazinane-2,4,6-trione		7.21
9.17	Cyclo(Valylvalyl)	6.65	
9.24	5,5-Dimethylbarbituric acid	3.25	
9.29	2,6-Dimethylheptane-3,5-dione	3.37	
9.46	Biphenyl		7.48
9.46	l-Proline, N-butoxycarbonyl-, nonyl ester	6.45	
9.55	Glycerol monooleate		2.00
9.59	Linoleic acid	22.19	27.74
9.93	Lauric amide		2.00
9.94	Palmitamide	2.08	
9.98	Z,Z-10,12-Hexadecadien-1-ol acetate		3.57

10.00	5,10-Diethoxy-2,3,7,8-tetrahydro-1H,6H-dipyrrolo[1,2-a:1',2'-d]pyrazine	3.71	
10.84	1,3,12-Nonadecatriene		4.31
10.90	cis-7,cis-11-Hexadecadien-1-yl acetate	1.82	
11.09	2,5-Piperazinedione, 3-methyl-6-(phenylmethyl)-	1.64	1.11
11.25	3-benzyl-6-isopropyl-2,5-Piperazinedione	1.36	1.88
11.65	Phenol, 2,2'-methylenebis[6-(1,1-dimethylethyl)-4-ethyl-	1.27	0.95
11.80	Diethyl itaconate		1.61
12.45	Pyrrolo[1,2-a]pyrazine-1,4-dione, hexahydro-3-(phenylmethyl)-		1.11
12.47	Cyclo-Phe-Pro-diketopiperazine	1.66	
Total		86.88	90.77

[a] Represents retention time (min).

Appendix C: The major compounds in the aqueous phase before and after recycling.

RT (min)[a]	Compounds in aqueous phase	Area (%)	
		Before recycling	After recycling
4.19	Acetic acid	6.96	0.59
5.78	Propanoic acid	0.66	
5.99	N-Ethylidene t-butylamine	0.16	
6.41	Piperidine	0.24	
7.80	Butanoic acid, 3-methyl-	0.76	
7.86	Acetamide, N-methyl-		0.51
8.17	Oxime-, methoxy-phenyl-_	5.39	3.41
8.81	Pentanoic acid, 4-methyl-	1.44	
9.95	Glycerol	8.10	5.49
10.08	1,2,3,4-Butanetetrol, [S-(R*,R*)]-		1.31
10.23	N-Dimethylaminomethyl-N-methylformamide		1.74
10.27	Propanamide, 2-hydroxy-N-methyl-	1.00	
10.66	2-Pyrrolidinone	1.35	1.34
10.80	3-Pyridinol		1.60
10.92	4-Pyridinoe	2.80	
10.99	Methanone, dicyclohexyl-		1.07
11.02	But-3-enyl (E)-2-methylbut-2-enoate	1.37	
11.25	3-Pyridinol, 6-methyl-	2.14	1.63
11.58	1-[2-(2,5-dimethyl-1H-pyrrol-1-yl)ethyl]piperazine	0.11	
11.62	2-Methyl-2,4,5,6-tetrahydrocyclopenta[c]pyrazol-3-amine		0.36
11.78	2-Piperidinone	1.06	1.68
11.87	Spiro-3-(2-butyl-2,4-diazabicyclo[3.3.0]octan-1-one)-cyclohexane		0.73

11.98	2-Piperidinone, 1-methyl-		0.36
12.10	(S)-(+)-2',3'-Dideoxyribonolactone		0.70
12.28	2-Propenoic acid, 3-(2-amino-1H-imidazol-5-yl)-		1.06
12.64	Caprolactam	0.14	
12.92	Indole		0.28
13.14	2,4-Dimethylamphetamine		0.34
13.18	Phenylpropanoic acid	0.35	
13.52	Tenamfetamine		0.13
13.65	2-Propenamide, N-(1-methylethyl)-		0.30
13.70	(3β,20S)-20-Aminopregn-5-en-3-ol		0.11
13.79	Ethanamine, 2-phenoxy-		0.15
13.86	L-Alanine, N-acetyl-		0.43
13.92	2-Heptanamine, 5-methyl-		1.57
13.95	2-(2-Aminopropyl)phenol		0.12
14.04	1-Octadecanamine, N-methyl-		1.09
14.17	N(6)-Methyllysine		0.83
14.43	N-Methyl-2-phenyl-1-propylamine		0.26
14.48	2,3-Dimethoxyamphetamine		0.22
14.49	1,6-Hexanediamine, N,N'-dimethyl-		0.26
14.56	p-Hydroxyamphetamine		0.33
14.71	5,5,8a-Trimethyldecalin-1-one	0.10	
14.73	Metaraminol		4.06
14.75	Arginine		0.22
14.89	Propan-1-one, 2-amino-1-piperidin-1-yl-		0.62
16.04	3,6-Dimethylpiperazine-2,5-dione	2.71	2.24
16.07	3,3-Dimethyl-4-methylamino-butan-2-one		0.45

16.13	N-Acetyl-2-methylamphetamine		0.48
16.18	N,N'-Dimethyl-decane-1,10-diamine		0.26
16.20	Tricyclo[10.2.2.2(5,8)]octadeca-5,7,12,14,15,17-hexaene, 6-nitro-	0.08	
16.41	3,3-Dimethylpiperidine		0.83
16.52	2-Cyclohexen-1-one, 4,4,5-trimethoxy-		1.43
16.58	2,5-Piperazinedione, 3-methyl-6-(1-methylethyl)-	5.41	
16.60	1,3-Dimethyl-3,4,5,6-tetrahydro-2(1H)-pyrimidinone		1.26
16.79	Benzeneethanamine, 4-methoxy-.alpha.-methyl-		1.79
16.83	1-Octanamine, n-octyl-		0.54
17.03	(3S,6S)-3-Butyl-6-methylpiperazine-2,5-dione		1.64
17.07	2,4(1H,3H)-Pyrimidinedione, 5-hydroxy-		1.45
17.09	N-Ethyl-4-methyl-4-octanamine	3.98	
17.13	L-Alanyl-L-Leucine	2.39	
17.21	l-Pyrrolid-2-one, N-carbamoyl-	3.40	1.90
17.24	2-Amino-4-hydroxy-6-methylpyrimidine		2.50
17.28	3-Methoxy-4,4-dimethyl-1-cyclohexene	3.66	
17.33	1-Pyrrolidineethanamine		0.22
17.37	1-Piperidineacetic Acid		0.29
17.46	3H-Pyrrolizin-3-one, hexahydro-	2.71	
17.46	2-Pentanamine, N-(1-methylbutyl)-		0.67
17.53	Cyclo-(glycyl-l-leucyl)	1.66	
17.54	2,4(1H,3H)-Pyrimidinedione, dihydro-		1.21
17.61	L-Threonine, N-glycyl	1.74	
17.61	2-(4-Acetyl-5-methyl-[1,2,3]triazol-1-yl)-acetamide		0.97
17.77	Pyrrolo[1,2-a]pyrazine-1,4-dione, hexahydro-	3.36	2.90

17.86	Phenol, 3,5-dimethoxy-	1.11	
17.99	Duloxetine	0.19	
18.05	3-Azabicyclo[3.2.2]nonane		1.15
18.28	Pyrrolo[1,2-a]pyrazine-1,4-dione, hexahydro-3-(2-methylpropyl)-	0.45	
18.70	Phenethylamine, 3,4,5-trimethoxy-.alpha.-methyl-		2.91
18.98	Propanamide, 3-(3,4-dimethylphenylsulfonyl)-	0.41	
19.66	2,5-Piperazinedione, 3-methyl-6-(phenylmethyl)-	1.41	
19.74	Benzaldehyde, 2-nitro-, diaminomethylidenhydrazone		0.12
19.77	Methylpent-4-enylamine		0.50
19.85	dl-Alanyl-l-phenylalanine		0.82
19.92	Trimethoxyamphetamine		0.18
19.97	Methoxyamphetamine		0.31
20.06	Haliclorensin		0.22
20.08	2-Amino-1-(o-hydroxyphenyl)propane		1.00
20.20	1-Pentanamine, N-methyl-		0.30
20.22	Amphetamine		0.23
20.27	Sarcosine, N-valeryl-, undecyl ester	0.03	
20.41	2,5-Piperazinedione, 3-(phenylmethyl)-	0.63	
20.41	Northiaden		0.20
20.62	Desmethyldoxepin		0.29
20.82	3-Ethoxyamphetamine		1.40
21.41	2-pentanamine		0.26

[a] Represents retention time (min).

Appendix D: The color of aqueous phase obtained from baseline experiment and the subsequent water phase recycling studies at 275 °C for 50 min.
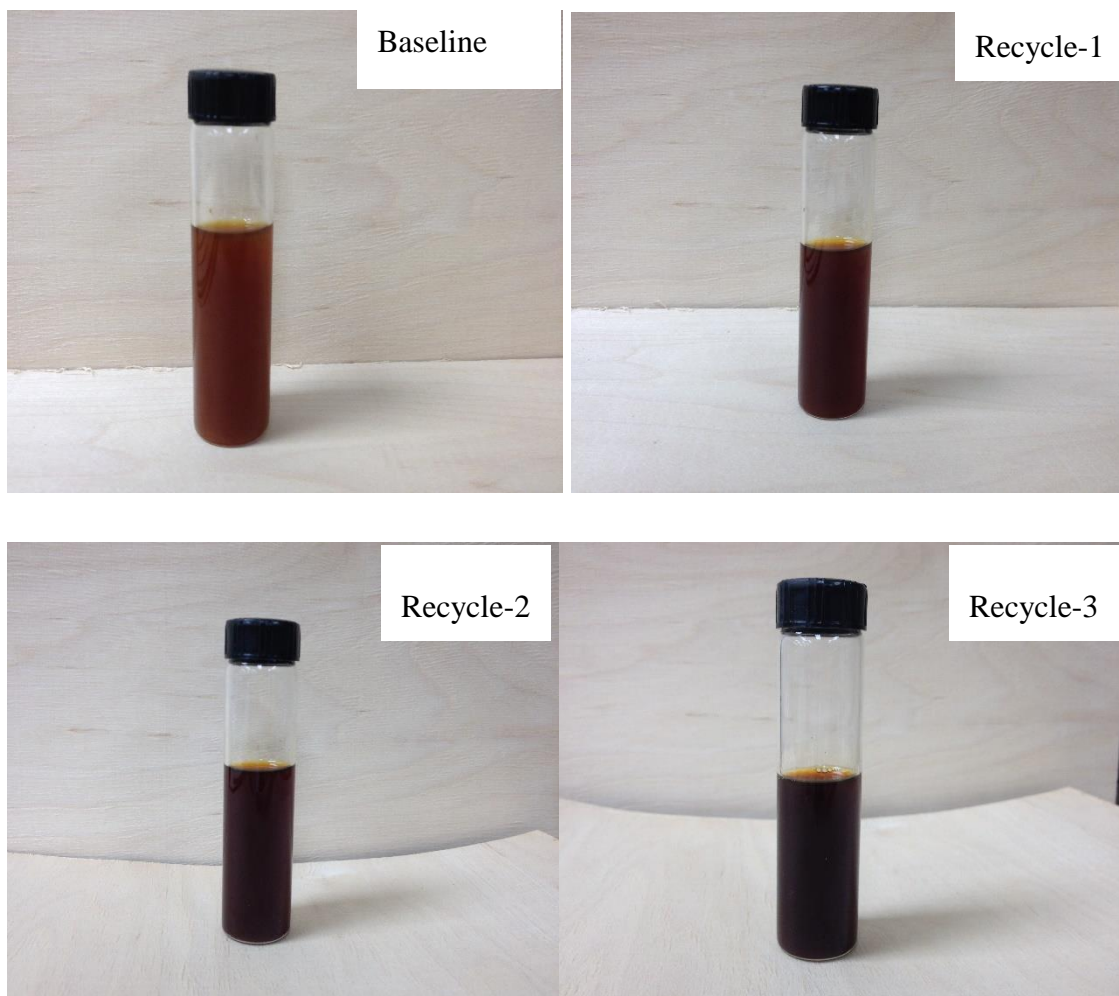
Appendix-E: The major compounds in the bio-crude oil obtained with and without recycled aqueous phase.

RT (min)[a]	Compounds in bio-crude oil	Area (%)			
		Baseline experiment	Recycle rounds		
			1	2	3
2.66	Pyrazine	0.10	0.08	0.09	0.14
2.70	Cyclobutane, 1,2-bis(methylene)-	0.09		0.07	
2.70	Pyridine		0.08		0.21
3.24	1H-Pyrrole, 3-ethyl-		0.02		0.03
3.24	1H-Pyrrole, 1-ethyl-			0.02	
3.33	Pyridine, 2-methyl-	0.17	0.13	0.11	0.23
3.54	Pyrazine, methyl-	0.56	0.58		1.02
3.54	3-Aminopyridine			0.59	
3.91	Acetic acid 6-methoxy-8-methyl-8-azabicyclo[3.2.1]octan-3-yl ester		0.02		
3.91	1H-Pyrrole, 2,5-dimethyl-			0.02	
3.94	Pyridine, 3-methyl-				0.13
3.95	Pyridine, 2,6-dimethyl-		0.04		
3.97	Styrene			0.07	
3.97	Bicyclo[4.2.0]octa-1,3,5-triene				0.12
4.21	Pyridine, 2-ethyl-			0.04	0.07
4.41	Pyrazine, 2,5-dimethyl-	0.37	0.36	0.36	0.64
4.45	Phenol, 2-methyl-	0.54	0.19		0.96
4.45	2-Pyridinamine, 5-methyl-			0.57	
4.53	Pyridine, 2,5-dimethyl-	0.18		0.19	
4.59	2-Methyl-2-cyclopenten-1-one	0.39	0.26	0.23	0.57
5.25	Pyrazine, 2-ethyl-5-methyl-	1.24	1.26	0.50	0.80
5.30	Pyrazine, trimethyl-	0.20	0.26	0.29	0.48

5.44	Pyridine, 5-ethyl-2-methyl-			0.72	1.11
5.52	1H-Pyrrole, 2,3,5-trimethyl-			0.07	0.08
5.60	Phenol	0.26	0.26	0.28	0.33
5.89	Pyrazine, 3-ethyl-2,5-dimethyl-		0.06	0.08	0.10
5.91	4-Nonyne	0.12			
5.91	2-Cyclopenten-1-one, 2,3-dimethyl-			0.07	
5.91	Spiro[2.4]heptan-4-one				0.12
5.94	N-Ethyl-p-toluidine	0.29	0.30		
5.94	Benzenamine, N-ethyl-2-methyl-			0.31	
5.94	Benzenamine, 2-ethyl-6-methyl-				0.43
6.14	2-Ethyl-3,5-dimethylpyridine				6.21
6.15	Pyridine, 2-ethyl-4,6-dimethyl-			0.10	
6.19	1H-Pyrrole, 3-ethyl-2,4-dimethyl-		0.13	0.14	
6.22	Pyridine, 3-methyl-5-propyl-	0.05			0.06
6.25	Phenol, 2-methoxy-	0.11		0.20	
6.25	1-Acetylcyclohexene		0.13		
6.25	Ethanone, 1-(1-cyclohexen-1-yl)-				0.23
6.35	4-methylphenol	0.29	0.28	0.27	0.39
6.35	1-Methyl-1H-imidazole-2-carbonitrile				0.35
6.44	Pyrrole, 2,3,4,5-tetramethyl-		0.26	0.33	
6.55	Benzenamine, N-ethyl-3-methyl-		0.19		
6.55	3-Isopropylaniline			0.19	0.23
6.60	Acetamide, N-(4-methylphenyl)-			0.21	0.26
6.90	2-ethyl-3,4,5-trimethyl-1H-pyrrole	0.16	0.21		
6.90	1H-Pyrrole, 3-ethyl-2,4,5-trimethyl-				0.26
6.95	2,5-Pyrrolidinedione, 1-methyl-	0.93	1.15	1.17	1.40
7.12	2,5-Pyrrolidinedione, 1-ethyl-	0.50	0.44	0.46	0.64

7.29	Pyrrolidine, 1-acetyl-	1.38	1.45	1.63	2.40
7.44	2-Methyl-5-(3-methylbutyl)pyridine	0.58	0.69	0.70	0.90
7.58	Benzenamine,2,6-bis(1-methylethyl)-	0.13	0.25	0.16	0.27
7.65	2-Piperidinone	0.65	0.82	0.86	1.40
8.06	Naphthalene	0.25			0.24
8.16	Caprolactam	0.63	0.64	0.32	
8.16	Piperidine-2,5-dione				0.79
8.32	1-Naphthalenol, 5,6,7,8-tetrahydro	0.37			
8.38	Indole	0.66	0.56	0.50	
8.38	5H-1-Pyrindine				0.57
8.66	Phenylmalonic acid				0.25
8.95	1H-Indole, 3-methyl-	0.45		0.58	
8.95	1H-Indole, 4-methyl-		0.25		
9.00	1H-Indole, 7-methyl-	0.26			
9.22	N6-Methyl-L-lysine		0.28		
9.53	Benzenamine N-(1-methyl-2-propenyl)-			0.50	
9.62	2,5-Dimethylindolizine	0.16			
9.62	Indolizine, 2,8-dimethyl-		0.29		
9.62	2-Methyl-5-(1-butyn-1-yl)pyridine			0.33	
9.72	[1,1'-Biphenyl]-3-amine	0.40			
9.72	[1,1'-Biphenyl]-4-amine		0.44		0.32
9.72	Pyridine, 2-methyl-5-phenyl-			0.36	
9.81	Acetamide, N-(2-phenylethyl)-	0.60	0.72	2.81	0.81
9.90	1H-2-Indenone,2,4,5,6,7,7a-hexahydro-3-(1-methylethyl)-7a-methyl	0.36			
9.90	Dihydroactinidiolide			0.33	
9.90	4,4,7a-Trimethyl-5,6,7,7a-tetrahydrobenzofuran-2(4H)-one				0.29

9.98	3,7,11,15-Tetramethyl-2-hexadecene	1.25	0.60	0.60	
9.98	2,6,10,14-Tetramethyl-2-hexadecene				0.44
10.06	Acetic acid, 3,7,11,15-tetramethyl-hexadecyl ester		0.68		
10.06	Cyclohexane, 2-ethyl-1,3-dimethyl-				0.53
10.07	7-Tetradecene			0.66	
10.11	Citronellyl acetate			0.65	
10.11	6-Octen-1-ol, 3,7-dimethyl-, formate				0.58
10.38	2-Cyclohexen-1-one, 4,4-dimethyl-		1.05		
10.38	6,6-Dimethyl-2-azaspiro[4.4]non-1-ene				0.94
10.50	1,7-Trimethylene-2,3-dimethylindole	0.18	0.19	0.21	0.16
10.53	(2Z,4E)-3,7,11-Trimethyl-2,4-dodecadiene	0.83		1.12	
10.72	Ethyl 1-methyl-2-oxocyclohexanecarboxylate		0.22		
10.72	Sarcosine, N-(3-cyclopentylpropionyl)-, butyl ester				0.14
10.81	1,7-Trimethylene-2,3,5-trimethylindole		0.26	0.30	
10.86	Glycylsarcosine		0.70		
10.92	(3S,6S)-3-Butyl-6-methylpiperazine-2,5-dione	0.50		0.58	
11.07	Hexadecanenitrile			0.44	
11.20	Cyclo(valylvalyl)	1.15	4.76	0.98	1.29
11.33	n-Hexadecanoic acid	2.37	2.40	3.20	2.07
11.37	Cyclooctanone Oxime	3.56			
11.37	3,3-Diacetyl-2,3,4,5-tetrahydro-2-oxofuran				3.35
11.44	1-Heptanamine, N-heptyl-	2.00	1.90		
11.44	1,3-Dimethyl-3,4,5,6-tetrahydro-2(1H)-pyrimidinone				1.89
11.52	3-Ethoxy-4-methoxyphenol	1.10	1.22		
11.52	3-Acetyl-1H-benzo[e]indole-1,2(3H)-dione 1-oxime			1.16	
11.52	Hexahydropyrrolizin-3-one				1.38
11.68	Probarbital	4.22		3.55	

11.77	4-Dibutylaminobut-2-en-1-ol				1.87
11.78	1-Butylhydantoin	1.86	1.61	1.36	4.92
11.86	1,4-Dioxaspiro[4.5]decane				2.38
11.87	2,2,4,4-Tetramethyl-6-oxabicyclo[3.1.0]hexan-3-one	2.44			
11.87	l-Norvalyl-l-norvaline, n-propargyloxycarbonyl-, pentyl ester		2.16		
11.88	6-oxabicyclo[3.1.0]hexan-3-one, 2, 2,4,4-tetramethyl-		2.08		
11.98	Pyrrolo[1,2-a]pyrazine-1,4-dione, hexahydro-	0.65	0.87		0.74
12.07	Phenol, 3,5-dimethoxy-	2.01	1.70	1.54	
12.07	3-Hydroxy-4-methoxybenzyl alcohol				2.20
12.11	2,5-Piperazinedione, 3,6-bis(2-methylpropyl)-	2.86			
12.11	d-Proline, N-isobutoxycarbonyl-, isobutyl ester		2.26		
12.11	l-Proline, N-isobutoxycarbonyl-, undec-10-enyl ester			2.07	
12.11	l-Leucine, N-allyloxycarbonyl-N-methyl-, heptyl ester				2.58
12.21	5-Acetyl-2,4,6(1H,3H,5H)-pyrimidinetrione	1.24			
12.21	1-Pentanamine, N,N-dipentyl-		1.03		
12.22	p-Hydroxybiphenyl			0.92	1.10
12.26	Formamide, N,N-dioctyl-	0.47			
12.31	9,12-Octadecadienoic acid (Z,Z)-	2.21	9.25	8.25	1.50
12.37	5-Nitroso-2,4,6-triaminopyrimidine	2.32			
12.37	L-Proline, N-valeryl-, undecyl ester		2.20		
12.37	Methyl N-(cyclopropylcarbonyl)-L-leucinate				2.39
12.43	Methyl (9Z,12Z)-9,12-heptadecadienoate		0.38		
12.44	9-Eicosyne			0.46	
12.47	2-Amino-5-nitrophenol	2.37			
12.47	Sebacic acid, butyl 2,6-dimethoxyphenyl ester		2.06		
12.47	3,3,5,5-Tetramethyl-1,2-cyclopentanedione			1.96	

RT	Compound				
12.47	Phenol, 2-amino-5-nitro-				2.48
12.52	Pyrrolo[1,2-a]pyrazine-1,4-dione, hexahydro-3-(2-methylpropyl)-	1.53		2.54	
12.52	L-Proline, N-valeryl-, heptadecylester		1.45		
12.52	d-Proline, N-allyloxycarbonyl-, heptadecyl ester			1.36	
12.53	d-Proline, N-allyloxycarbonyl-, pentadecyl ester				1.57
12.59	3-Azabicyclo[3.2.2]nonane, 3-nitroso-	1.00			
12.59	Methyl (9Z,12Z)-9,12-heptadecadienoate			1.09	
12.67	Varenicline				0.34
12.68	1,3,12-Nonadecatriene			0.43	
12.75	5,10-Diethoxy-2,3,7,8-tetrahydro-1H,6H-dipyrrolo[1,2-a:1',2'-d]pyrazine	2.61			2.47
12.75	5-Hydroxy-2,2,6,6-tetramethyl-4-cyclohexene-1,3-dione		2.63		
12.75	2,3-Dimethyl-1-hexene			2.36	
12.79	N-Methyldodecanamide			1.65	
12.80	1-Hexadecanamine	1.67			
12.80	1-Octadecanamine		1.77		
12.88	1-Octadecanamine, N-methyl-	1.41			
12.89	N,N-Dimethylhexanamide		1.41		
12.89	N-(4-Aminobutyl)guanidine			1.30	
12.96	Phenylephrine	1.23			
12.96	1-Isoquinolinecarbonitrile, 3-methyl-				0.48
13.07	N-Decyl-N-methylbutanamide		0.44		
13.08	Metaraminol	0.52	0.74		
13.08	Pterin-6-carboxylic acid			0.42	
13.12	L-Aspartic acid, N-(2,4-dinitrophenyl)-			0.24	
13.14	10-Hydroxydesmethylimipramine			0.34	
13.19	o-Veratramide		0.77		

13.20	1-(3,5-Dinitro-2-pyridinyl)proline	0.62			
13.27	Benzonitrile, 2-[1-(3-methylphenyl)-2-pyrrolidinylideneamino]-			1.09	
13.28	Alanine, 3-anthraniloyl-, methyl ester, dl-		1.03		
13.43	2-[(3,5-dinitropyridin-2-yl)amino]butanedioic acid	0.95			
13.43	Sarcosine, N-valeryl-, pentyl ester		1.31		
13.43	p-Aminobenzoyl-dl-aspartic acid			1.09	
13.64	Pregn-5-ene-3.beta.,20.alpha.-diamine	0.16	0.14	0.39	
13.64	N,N'-Dimethyl-decane-1,10-diamine		0.37		
13.64	Metanephrine			0.23	
13.71	Cyanoacetylurea	1.33			
13.71	Histidine, 1,N-dimethyl-4-nitro-		2.44		
13.71	Methyl 9,12-heptadecadienoate			1.29	
13.71	2,5-Piperazinedione, 3-methyl-6-(phenylmethyl)-				1.17
13.77	L-Alanine, N-acetyl-	1.22			1.13
13.77	8,11-Octadecadienoic acid, methyl ester		1.31		
13.77	9,12-Octadecadienoic acid, methyl ester, (E,E)-			1.20	
13.86	1-(4,5-Diphenyl-oxazol-2-yl)-ethylamine	0.36			
13.99	1-[8-(2-Hexylcyclopropyl)octanoyl]pyrrolidine		1.01		
14.00	l-Alanine, N-octanoyl-, octyl ester	1.12			
14.08	2 5-piperazinedione 3-benzyl-6-isopropyl-	3.11	2.98	1.03	1.49
14.08	3-Benzyl-6-isopropyl-2,5-piperazinedione			1.50	
14.08	Isocarboxazid				0.91
14.21	Sarcosine, N-valeryl-, propyl ester			0.64	
14.46	Nortriptyline		0.47		
14.46	N-[3,5-Dinitropyridin-2-yl]proline			0.52	
14.54	Phenol, 2,2'-methylenebis[6-(1,1-dimethylethyl)-4-ethyl-		0.71		0.54

14.54	2-Amino-1-(o-methoxyphenyl)propane			0.37	
14.55	p-Benzenediacetohydroxamic acid	0.28			
14.64	1-Benzylpiperidin-4-onoxim		1.13		
14.65	12-(4,4-Dimethyl-4,5-dihydro-oxazol-2-yl)-dodecan-1-ol	1.54			
14.65	2-Piperidinone, 1-methyl-			1.12	
14.82	Cyclo(L-leucyl-L-phenylalanyl)	1.04		0.72	0.19
14.82	Pyrrolidine, 1-(1-oxopentadecyl)-		1.14		
14.82	Pyrrolidine, 1-(12-methyl-1-oxotetradecyl)-			0.89	
15.28	Pyrrolo[1,2-a]pyrazine-1,4-dione, hexahydro-3-(phenylmethyl)-	2.71	2.61	1.06	1.43
15.41	(3β,20S)-20-Aminopregn-5-en-3-ol				0.02
15.50	Spermidine			0.77	

[a] Represents retention time

Appendix-F: Major chemical compounds, determined by GC-MS, in the bio-crude oil samples obtained with various methanol contents (in methanol-water mixed solvents) at 225 °C for 60 min, with a solid/solvent mass ratio of 1/5.

RT (min)[a]	Compounds	Methanol content (wt.%, in methanol-water mixed solvents)		
		0	50	100
	N-containing compounds			
3.54	Pyrazine, methyl-	1.02		
11.16	2,4(1H,3H)-Pyrimidinedione, 1,3-dimethyl-			1.26
12.32	(S)-6,6-Dimethyl-2-azaspiro[4.4]non-1-ene	1.07		
13.17	3,6-Diisopropylpiperazin-2,5-dione	11.54	5.78	
13.28	1,3-Dimethyl-3,4,5,6-tetrahydro-2(1H)-pyrimidinone		5.59	
13.31	dl-Alanyl-l-leucine		1.17	
13.32	2,4,5-Trihydroxypyrimidine	8.2		
13.40	Hydrouracil, 1-methyl-	3.08		
13.75	N,3-Diethyl-3-octanamine	3.85		
14.04	3-Isobutylhexahydropyrrolo[1,2-a]pyrazine-1,4-dione	4.23		
14.05	Caffeine			4.19
14.08	2,5-Piperazinedione, 3,6-bis(2-methylpropyl)-	9.92	2.99	
14.29	2-Butenamide, N,N-diisopropyl-, (E)-	1.56		
14.34	Pyrrolo[1,2-a]pyrazine-1,4-dione, hexahydro-3-(2-methylpropyl)-	9.33	1.82	2.43
14.72	5,10-Diethoxy-2,3,7,8-tetrahydro-1H,6H-dipyrrolo[1,2-a:1',2'-d]pyrazine	5.5		
14.72	2-Hydroxyimino-N-(4-methoxy-phenyl)-acetamide		1.19	
15.67	2,5-Piperazinedione, 3-methyl-6-(phenylmethyl)-	2.95	1.04	
15.97	dl-Alanyl-l-phenylalanine	1.64		

16.04	2,5-Piperazinedione, 3-benzyl-6-isopropyl-	4.34	1.08	
16.61	2-Piperidinone, 1-methyl-	3.86		
16.78	Glyoxime, 1-cyano-	1.56		
17.24	Pyrrolo[1,2-a]pyrazine-1,4-dione, hexahydro-3-(phenylmethyl)-	2.39		
	Esters			
10.89	DL-Proline, 5-oxo-, methyl ester			3.18
12.87	Hexadecanoic acid, methyl ester	2.44	19.61	27.04
13.63	l-Proline, N-propoxycarbonyl-, isobutyl ester			2.08
13.74	l-Norvaline, N-allyloxycarbonyl-, nonyl ester		1.2	
13.82	8-Octadecenoic acid, methyl ester			2.76
13.83	9-Octadecenoic acid (Z)-, methyl ester		2.19	
13.88	9,12-Octadecadienoic acid (Z,Z)-, methyl ester	2.22	22.1	30.01
13.98	9,12,15-Octadecatrienoic acid, methyl ester, (Z,Z,Z)-		1.14	
13.98	6,9-Octadecadienoic acid, methyl ester			1.24
14.50	L-Leucine, N-cyclopropylcarbonyl-, methyl ester	4.5	1.01	
	Other O-containing compounds			
12.04	Phytol		2.58	
12.32	2-hexadecen-1-ol, 3,7,11,15-tetramethyl		2.83	
13.36	Cyclohexane, ethoxy-			1.98
13.55	4-Methyl-2-pentanone	1.18		
	Cyclic oxygenates			
13.49	3-Ethoxy-4-methoxyphenol	1.59		
13.84	6-Methylene-1,4-dioxaspiro[4.5]decane	3.52		

14.49	Phenol, 3,5-dimethoxy-		1.73	
Total		91.49	75.05	76.17

[a] Retention time (min).

Appendix-G: Major chemical compounds, determined by GC-MS, in the aqueous phase samples obtained in methanol-water mixed solvents with various methanol contents at 225 °C for 60 min, with a solid/solvent mass ratio of 1/5.

RT (min)[a]	Compound	Area (%)			
		Methanol content in reaction medium (wt.%)			
		0	25	50	75
	Organic acid, alcohols, and esters				
3.61	Acetic acid	4.06			
9.86	Glycerol	10.77	15.24	12.79	6.25
10.80	Octyl 2-furoate				1.01
14.19	DL-Proline, 5-oxo-, methyl ester		1.76	5.45	16.93
17.14	l-Alanine, N-allyloxycarbonyl-, pentyl ester		2.77		
17.23	L-Proline, N-(hexanoyl)-, hexyl ester				4.87
17.23	L-Proline, N-(hexanoyl)-, butyl ester		5.04		
	N-containing compounds				
10.61	2-Pyrrolidinone		1.33		
10.77	3-Pyridinol	2.50	1.97		
10.98	3-Aminopyrazole	1.00		1.93	
10.99	Pyridine, 2,3,4,5-tetrahydro-		1.63		
11.10	3-Pyridinol, 6-methyl-	2.89	1.15	2.34	
15.98	3,6-Dimethylpiperazine-2,5-dione	7.39		7.27	13.86
16.42	2,5-Piperazinedione, 3-methyl-	3.79	4.64	4.53	4.45
16.53	Hydrouracil, 1-methyl-	15.20		3.11	2.42
16.61	2,5-Piperazinedione, 3-methyl-6-(1-methylethyl)-	3.89	10.18	11.80	7.40
17.08	(3S,6S)-3-Butyl-6-methylpiperazine-2,5-dione	6.43	14.42	15.71	12.51

17.23	1,7-Diazabicyclo[2.2.0]heptane			3.79	
17.24	1H-Pyrimidine-2,4-dione, 5-(2-hydroxy-1,1-dimethylethylamino)-	5.51			
17.41	3-Methyl-1,4-diazabicyclo[4.3.0]nonan-2,5-dione, N-acetyl-		5.03	4.84	3.66
17.46	Cyclo-(glycyl-l-leucyl)		5.28	4.58	
17.48	1H-1,2,4-Triazole-3-methanol, 5-amino-	5.21			4.81
17.54	N-Ethyl-4-methyl-4-octanamine		3.57	3.12	2.65
17.56	2,4(1H,3H)-Pyrimidinedione, dihydro-	3.37			
17.61	Adenine	2.73	2.39		2.28
17.72	Pyrrolo[1,2-a]pyrazine-1,4-dione,hexahydro-	6.45	7.90	6.47	5.80
19.61	2,5-Piperazinedione, 3-methyl-6-(phenylmethyl)-	2.77		2.92	2.80
19.61	Piperazine, 2,6-dimethyl-		1.29		
20.35	2,5-Piperazinedione, 3-(phenylmethyl)-	1.76	1.51	2.69	2.51
19.04	d-Ribitol, 1-deoxy-1-heptylamino-	1.67			
	Cyclic oxygenates				
17.82	Phenol, 3,5-dimethoxy-	2.86	2.91	2.80	1.53

[a] Retention time (min).

Appendix-H: The major compounds of aqueous by-product obtained from co-liquefaction of algal biomass (AB) and sawdust (SD) in ethanol-water (75/25 wt/wt) mixed solvent at 250 °C for 60 min.

RT (min)[a]	Area (%)	Compound	Formula
3.73	11.33	Acetic acid	CH_3COOH
6.80	0.57	3,3'-Iminobispropylamine	$C_6H_{17}N_3$
6.86	0.57	Pyrazine, methyl-	$C_5H_6N_2$
8.27	0.51	2-Hexynoic acid	$C_6H_8O_2$
8.93	0.56	Tetrahydro-4H-pyran-4-ol	$C_5H_{10}O_2$
9.41	1.52	Phenol	C_6H_5OH
9.76	3.07	Glycerol	$C_3H_8O_3$
9.84	2.39	1,2,3,4-Butanetetrol, [S-(R*,R*)]-	$C_4H_{10}O_4$
10.15	1.83	2-Pyrrolidinone, 1-methyl-	C_5H_9NO
10.62	2.63	2-Pyrrolidinone	C_4H_7NO
10.78	9.02	3-Pyridinol	C_5H_5NO
10.99	1.88	4-Pyridone	C_5H_5NO
11.12	6.48	3-Pyridinol, 6-methyl-	C_6H_7NO
11.30	0.56	Hexahydroindole	$C_8H_{13}N$
11.75	1.20	2-Propenoic acid, ethenyl ester	$C_5H_6O_2$
12.09	1.59	2,7-Octadien-4-ol, 2-methyl-6-methylene-, (S)-	$C_{10}H_{16}O$
16.50	0.71	3,3-Dimethyl-4-methylamino-butan-2-one	$C_7H_{15}NO$
16.58	0.91	2,5-Piperazinedione, 3-methyl-6-(1-methylethyl)-	$C_8H_{14}N_2O_2$

17.01	0.75	2-Butenediamide, (E)-	$C_4H_6N_2O_2$
17.05	2.58	dl-Alanyl-l-leucine	$C_9H_{18}N_2O_3$
17.24	1.58	3-Azabicyclo[3.2.2]nonane	$C_8H_{15}N$
17.52	1.54	1,2,5-Oxadiazole-3,4-dicarboxamide	$C_4H_4N_4O_3$
17.71	1.64	Pyrrolo[1,2-a]pyrazine-1,4-dione, hexahydro-	$C_7H_{10}N_2O_2$
17.81	2.04	3-Azahexan-1-ol, 6-cyclohexyl-	$C_{11}H_{23}NO$
18.53	0.79	2-Butanamine, (S)-	$C_4H_{11}N$
Area	58.25		

[a] Represents retention time (min).

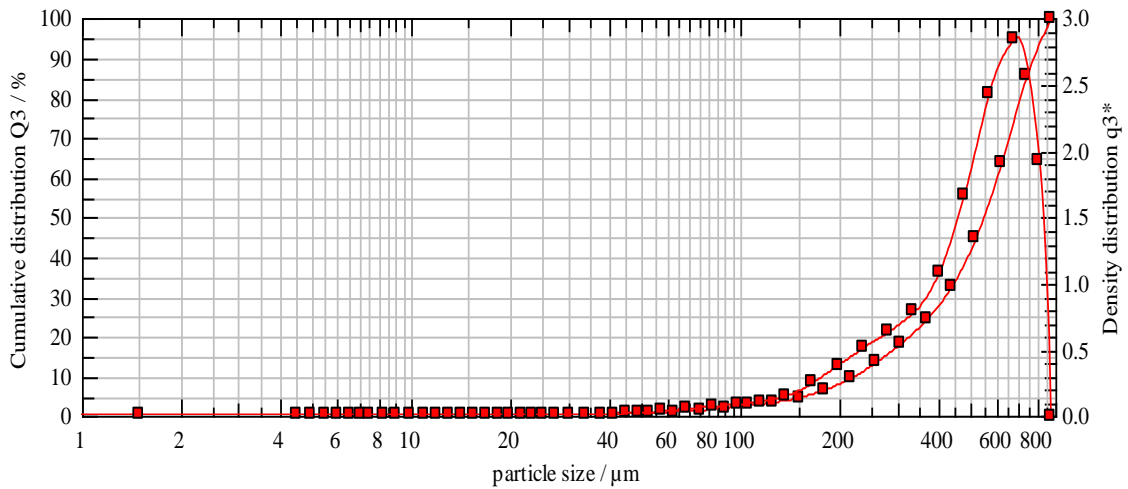**Appendix-I:** Measurement of the particle size of aspen sawdust.

HELOS (H2316) & CUVETTE, R5: 0.5/4.5...875µm   2018-03-12, 14:51:32,453

Saw Dust

WARNING: Coarse particles probably exceeding the measuring range.

x_{10} = 220.55 µm x_{50} = 543.27 µm x_{90} = 778.98 µm   SMD = 314.86 µm   VMD = 518.86 µm

x_{16} = 282.80 µm x_{84} = 727.27 µm x_{99} = 865.40 µm S_V = 0.02 m²/cm³ S_m = 381.12 cm²/g

cumulative distribution

x_0/µm Q_3/%	Q_3/%	x_0/µm	Q_3/%	x_0/µm	Q_3/%	x_0/µm
4.50 18.18	0.07	18.50	0.35	75.00	1.41	305.00
5.50 24.27	0.10	21.50	0.37	90.00	1.97	365.00
6.50 32.55	0.12	25.00	0.39	105.00	2.55	435.00
7.50 44.72	0.15	30.00	0.42	125.00	3.35	515.00
9.00 63.39	0.18	37.50	0.48	150.00	4.55	615.00
11.00 85.42	0.23	45.00	0.58	180.00	6.52	735.00

13.00	0.27	52.50	0.72	215.00	9.47	875.00
100.00						
15.50	0.31	62.50	0.99	255.00	13.27	

density distribution (log.)

$x_m/\mu m$ $q_3 lg$	$q_3 lg$	$x_m/\mu m$	$q_3 lg$	$x_m/\mu m$	$q_3 lg$	$x_m/\mu m$
1.50 0.63	0.00	16.93	0.00	68.47	0.05	278.88
4.97 0.78	0.00	19.94	0.00	82.16	0.07	333.65
5.98 1.09	0.00	23.18	0.00	97.21	0.09	398.47
6.98 1.66	0.00	27.39	0.00	114.56	0.11	473.31
8.22 2.42	0.00	33.54	0.01	136.93	0.15	562.78
9.95 2.85	0.01	41.08	0.01	164.32	0.25	672.33
11.96 1.93	0.01	48.61	0.02	196.72	0.38	801.95
14.20	0.01	57.28	0.03	234.15	0.51	

evaluation: WINDOX 5.4.2.0, *LD*

revalidation:

reference measurement: 03-12 14:50:13
contamination: 0.00 %

product: Saw Dust

density: 0.50 g/cm³, shape factor: 1.00

disp. meth.: 1500rpm
C_{opt}= 23.36 %

trigger condition: 10S

time base: 500.00 ms

start: button
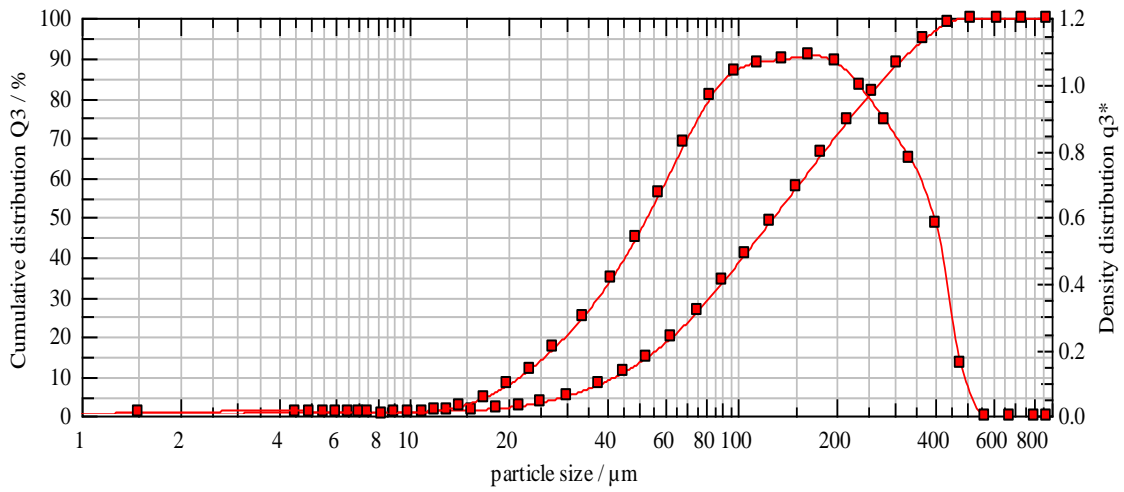
user parameters:

: Josh

:

Appendix-J: Measurement of the particle size of algal biomass.

HELOS (H2316) & CUVETTE, R5: 0.5/4.5...875μm   **2018-03-12, 14:34:28**,281

Unknown

x_{10} = 42.58 μm x_{50} = 128.37 μm x_{90} = 320.53 μm   SMD = 71.40 μm   VMD = 156.65 μm

x_{16} = 55.17 μm x_{84} = 272.87 μm x_{99} = 444.27 μm S_v = 0.08 m²/cm³ S_m = 1120.52 cm²/g

cumulative distribution

x_0/μm Q_3/%	Q_3/%	x_0/μm	Q_3/%	x_0/μm	Q_3/%	x_0/μm
4.50 88.44	0.69	18.50	1.75	75.00	26.22	305.00
5.50 94.46	0.79	21.50	2.36	90.00	33.83	365.00
6.50 98.87	0.86	25.00	3.28	105.00	40.78	435.00
7.50	0.91 100.00	30.00	4.89	125.00	48.85	515.00
9.00	0.95 100.00	37.50	7.77	150.00	57.36	615.00
11.00	1.01 100.00	45.00	11.06	180.00	65.95	735.00

13.00	1.11	52.50	14.65	215.00	74.18	875.00
	100.00					
15.50	1.33	62.50	19.71	255.00	81.53	

density distribution (log.)

$x_m/\mu m$	$q_3 lg$	$x_m/\mu m$	$q_3 lg$	$x_m/\mu m$	$q_3 lg$	$x_m/\mu m$
$q_3 lg$						
1.50	0.01	16.93	0.05	68.47	0.82	278.88
0.89						
4.97	0.01	19.94	0.09	82.16	0.96	333.65
0.77						
5.98	0.01	23.18	0.14	97.21	1.04	398.47
0.58						
6.98	0.01	27.39	0.20	114.56	1.07	473.31
0.15						
8.22	0.01	33.54	0.30	136.93	1.07	562.78
0.00						
9.95	0.01	41.08	0.42	164.32	1.08	672.33
0.00						
11.96	0.01	48.61	0.54	196.72	1.07	801.95
0.00						
14.20	0.03	57.28	0.67	234.15	0.99	

evaluation: WINDOX 5.4.2.0, *LD*

revalidation:

reference measurement: 03-12 14:31:32
contamination: 0.00 %

product: Unknown

density: 0.75 g/cm³, shape factor: 1.00

disp. meth.: 1500rpm
C_{opt}= 21.52 %

trigger condition: 10S

time base: 500.00 ms

start: button :

user parameters:

: Josh

Curriculum Vitae

Name: Yulin Hu
Post-secondary   Jilin Business and Technology College
Education and   Changchun, Jilin, China
Degrees: 2009-2013 B.Sc.

                     McGill University
                     Montreal, Quebec, Canada
                     2013-2015 M.Sc.

                     The University of Western Ontario
                     London, Ontario, Canada
                     2015-2018 Ph.D.

Related Work   Teaching Assistant
Experience   The University of Western Ontario
                     2016-2017

Publications:
Yulin Hu, Shanghuan Feng, Chunbao Xu, Amarjeet Bassi. 2017. Production of low-nitrogen bio-crude oils from microalgae pre-treated with pre-cooled NaOH/urea solution. *Fuel*, 206, 300-306.
Yulin Hu, Shanghuan Feng, Zhongshun Yuan, Chunbao, Amarjeet Bassi. 2017. Investigation of aqueous phase recycling for improving bio-crude oil yield in hydrothermal liquefaction of algae. *Bioresource Technology*, 239, 151-159.
Yulin Hu, Mengyue Gong, Chunbao Xu, Amarjeet Bassi. 2017. Investigation of an alternative cell disruption approach for improving hydrothermal liquefaction of microalgae. *Fuel*, 197, 138-144.

Book chapters:
Mengyue Gong, **Yulin Hu**, Shreyas Yadahalli, Amarjeet Bassi. 2016. Oil extraction processes in microalgae. In: Microalgae as a source of bioenergy: products, processes and Economics.

Conferences:

Yulin Hu, Laleh Nazari, Amarjeet Bassi, Chunbao (Charles) Xu. A novel two-step hydrothermal liquefaction of microalgae for the production of bio-crude oils: effects of

pre-treatment. The 6th International Conference on Algal Biomass and Biofuels and Bioproducts. 2016, San Diego, USA, *Oral Presentation*.

Yulin Hu, Amarjeet Bassi, Chunbao (Charles) Xu. Two step hydrothermal liquefaction (HTL) of microalgae into bio-oil. 66th Canadian Chemical Engineering Conference. 2016, Quebec City, Canada, *Oral Presentation*.

Yulin Hu, Chunbao (Charles) Xu, Amarjeet Bassi. Two-step hydrothermal liquefaction of Chlorella vulgaris using low-temperature NaOH/urea solution. Advanced Biofuels Symposium, 2016, Vancouver, Canada, *Poster Presentation*.